HIGHLY ACCURATE POTENTIAL ENERGY SURFACES FOR THE He–H_2 INTERACTING SYSTEM

By

Janelle A. Bradley

A DISSERTATION

Submitted to
Michigan State University
in partial fulfillment of the requirements
for the degree of

Chemistry–Doctor of Philosophy

2018

ABSTRACT

HIGHLY ACCURATE POTENTIAL ENERGY SURFACES FOR THE He–H_2 INTERACTING SYSTEM

By

Janelle A. Bradley

In this thesis numerical values are presented for the energies of the ground state of the He–H_2 system, obtained with coupled-cluster[1] (CC) methods at ~ 20,000 nuclear geometries. Approximately 68,000 *ab initio* calculations have been performed for the ground and first excited singlet state of He–H_2. In these calculations, the H–H bond lengths range from 0.942 to 5.70 a_0 (at 14 different values), the intermolecular separations R range from 0.25 to 20.0 a_0 (usually at 74 different R values), and the angle θ between r and R ranges from 0° to 90° in steps of 5 degrees. Characteristics of the potentials, the bound vibrational state, and the intersection between the states are investigated.

The CCSD(T)[2] method is known to yield unreliable results when internuclear separations are far from their equilibrium values, whereas the CR-CC(2,3)[3] method has been shown to treat stretched bonds more accurately, the CR-CC(2,3) method was chosen for this work, because regions of the H_2–He potential energy surface having stretched H–H bonds are desired with greater accuracy than in the earlier work. The calculations performed in this work also test the CR-CC(2,3) method for van der Waals molecules. The CR-CC(2,3) results in this work are compared with CCSD(T) results obtained in this work, and with CCSD(T) results in the scientific literature (where available). The parts of the potential surface corresponding to H_2–He, H–H–He, H–He–H, HHe–H, H–HHe, HeH^+–H^- and the conical intersection between the ground and excited state have been calculated.

[1] F. Coester, *Nucl. Phys*. **7**, 421 (1958); F. Coester and H. Kümmel, *Nucl. Phys*. **17**, 477 (1960); J. Čížek, *J. Chem. Phys*. **45**, 4256 (1966); J. Čížek, *Adv. Chem. Phys*. **14**, 35 (1969).

[2] K. Raghavachari, G. W. Trucks, J. A. Pople, and M. Head-Gordon, *Chem. Phys. Lett*. **157**, 479 (1989).

[3] K. Kowalski and P. Piecuch, *J. Chem. Phys*. **113**, 18 (2000); *ibid*. **122**, 074107 (2005); *ibid.* **115**, 643 (2001); K. Kowalski and P. Piecuch, *Chem. Phys. Lett*. **347**, 237 (2001).

To my family

ACKNOWLEDGMENTS

I would like to sincerely thank my advisor Dr. Katharine Hunt for the guidance, knowledge, and enduring patience she has offered throughout the course of my graduate research at MSU. I would like to express my sincere gratitude for her encouragement, support, teaching, and assistance during my time as a graduate student at MSU.

I am indebted to the members of my guidance committee, Dr. Benjamin Levine, Dr. Robert Cukier, and Dr. James McCusker, for the guidance and knowledge each of them has bestowed upon me. I would like to take this opportunity to also thank Dr. James Harrison for an immense amount of invaluable knowledge and for his support and guidance during my graduate research and teaching experiences.

The other members of the Dr. Hunt group were pivotal to my success, so I would like to take this opportunity to thank them. Thank you to all present and past graduate students in the graduate program at MSU that assisted me in both my graduate studies and research, as well as in my personal life. A special thanks is in order for past group members Dr. Evangelos Miliordos, Dr. Anirban Mandal, and Dr. Sasha North, who contributed tremendously to my overall success.

My parents, Sue and David Bradley, and my sister, Emily, have helped me in more ways than I can say, and for this, I sincerely thank you. I also would like to give thanks to my friends and family members who have always been there for me and who helped make this accomplishment possible.

TABLE OF CONTENTS

LIST OF TABLES

LIST OF FIGURES

CHAPTER 1: Introduction

1.1 Overview

In this thesis numerical values are presented for the energies of the ground state and the first excited singlet state of the He–H_2 system, obtained with coupled-cluster (CC) methods[1] at ~20,000 nuclear geometries. Approximately 68,000 *ab initio* calculations have been performed for these two states of He–H_2. In these calculations, the H–H bond lengths range from 0.942 to 5.70 a_0 (at 14 different values), the intermolecular separations R range from 0.25 to 20.0 a_0 (usually at 74 different R values), and the angle θ between r and R ranges from 0° to 90° in steps of 5 degrees. The ground state was treated with the CR-CC(2,3)[2] method and the excited state was treated with the CR-EOMCCSD(T)[3] method. All calculations employed one of the aug-cc-pVXZ basis sets of Dunning and co-workers.[4] Characteristics of the potentials, the bound vibrational state, and the intersection between the states have been investigated.

The CCSD(T)[5] method employs an exponential operator to generate all single and double excitations from a reference state (typically the Hartree-Fock ground state) and then adds a non-iterative, perturbative correction for triple excitations. The CR-CC(2,3) method is based on the method of moments of coupled-cluster equations (MMCC).[6] The CR-CC(2,3) method is one of a class of completely renormalized methods that are denoted generally by CR-CC(m_A, m_B), where m_A gives the excitation level of the results that we wish to correct, and m_B gives the excitation level for the correction. The CCSD(T) method is known to yield unreliable results when internuclear separations are far from their equilibrium values, or bonds are breaking in diatomics such as HF and N_2. The CCST(T) energy may even diverge when the internuclear separations are far from equilibrium. The CR-CC(2,3) method has been shown to treat stretched bonds more accurately. The CR-CC(2,3) methods were chosen for this thesis, because regions of the H_2–He potential energy surface having stretched H–H bonds are desired with greater accuracy than in the previous work. The calculations also test the CR-CC(2,3) method for van der Waals molecules. The CR-CC(2,3) results in this work are compared with CCSD(T) results obtained in this work, and with CCSD(T) results in the scientific literature (where available). For regions of the potential

energy surface where the bond length of the H_2 molecule is not too far from the equilibrium, the CCSD(T) and CR-CC(2,3) results are expected to be comparable. As the distance between the H atoms is increased, the difference between results obtained with the two methods is expected to increase. For selected geometries, full configuration-interaction (FCI) calculations have been performed with the same basis set as in the CR-CC(2,3) and CCSD(T) work, to allow for further comparisons. The CR-CC(2,3) and CCSD(T) energy values are also compared with highly accurate calculations of the H_2–He potential energy surface by the Patkowski group.[7] However, Patkowski *et al*. did not carry out calculations for bond lengths greater than 1.75 a_0. Parts of the potential surface corresponding to H_2–He, H–H–He, H–He–H, HHe–H, H–HHe, HeH^+–H^- and the conical intersection between the ground and excited state have been calculated.

Since hydrogen and helium are the most abundant chemical species in the Universe, detailed information about their interactions is desirable. An accurate understanding of the system is attainable with existing *ab initio* electronic structure methods. The calculations in this thesis cover parts of the H_2–He potential surfaces that have not been treated in previous work and should be useful in modeling spectra at higher temperatures than previously accessible. For example, *ab initio* results are provided that can be used to study transitions up to vibrational quantum number n = 8. The results are needed in order to model the radiative profiles of cool white dwarf stars, with temperatures between 3500 K and 7000 K.[8]

1.2 Review of Experimental Results for H_2–He Interactions Obtained From Molecular Beam Studies

Experimental data on interactions in the H_2–He system comes primarily from molecular beam studies. In a molecular beam study of this system in 1962, Harrison[9] estimated the overall cross section as σ = 58-62 Å^2. In 1967, Moore, Datz, and van der Valk[10] measured the total collision cross section for collisions of H_2 with ^{3}He and ^{4}He and for D_2 with ^{3}He. The hydrogen and deuterium beams were scattered into helium at temperatures from 77 K to 600 K, with the helium at 77 K. The relative velocities ranged from $1.3 \cdot 10^5$ cm s^{-1} to $2.6 \cdot 10^5$ cm s^{-1}. They found an overall cross section for H_2^{4}He collisions of $\sigma = 43 \pm 1$ Å^2. Both Harrison and Moore *et al*. used beams produced by effusion. Harrison used a tungsten-foil furnace with a small hole as the beam source, and Moore used a copper block with a hole for the beam. Later Skofronick[11] introduced a supersonic nozzle source that gave beams 100 to 1000 times more intense than beams produced by effusion, with a smaller velocity range as well. His measured cross section was 49.4 ± 5 Å^2. Cantini, Cavallini, Dondi, and Scoles[12] found a cross section of 46.6 Å^2 in beam studies at room temperature.

In 1971 Gengenbach, Strunck, and Toennies[13] determined absolute integral cross sections for H_2 scattering from helium gas, for relative velocities in the range from 2000 to 20000 m s^{-1}. Relative velocities of this magnitude are too high, however, to probe anything but the repulsive region of the potential. They compared their results with predictions based on a potential obtained by Slater, a composite Born-Mayer-Morse-Lennard-Jones potential, and three other *ab initio* potentials available at that time. Two of the *ab initio* potentials were derived from self-consistent field calculations and the third came from configuration interaction calculations by Gordon and Secrest[14] who fit the short-range exponential repulsion. In order to study the potential well, Gengenbach and Hahn[15] determined absolute effective cross sections for lower relative velocities, namely, from 140 to 1200 m s^{-1}. In contrast to the earlier experiments by Gengenbach, Strunck, and Toennies, Gengenbach and Hahn scattered the helium atoms from H_2 at a temperature of 15

K. The best fit of their isotropic potential to a Morse potential suggested that there was one bound state for ^{3}He or ^{4}He interacting with any of the H_2 isotopic pairs (i.e., H_2, D_2, and T_2).

Grace and Skofronick[16] fit available beam data for relative velocities between 2000 and 3000 m s^{-1}. Their results were sensitive primarily to the region of the potential between 2.7 and 3.3 Å. Within that range, these authors found a good fit to a Lennard-Jones potential, obtaining a potential minimum of $\varepsilon = 0.7$ meV located at $R_e = 3.5$ Å. Lilenfeld, Kinsey, Lang, and Parks[17] measured the total scattering cross section for ^{4}He-D_2 for relative velocities from 760 to 2600 m s^{-1}. In order to fit their data, they used a piecewise potential constructed from *ab initio* data at short range joined to the form $C_6 R^{-6}$ at long range. From this fit, these authors also obtained good values for diffusion coefficients.

In 2004, the Toennies research group found the first experimental evidence for a bound state of the H_2–He van der Waals molecule in a molecular beam study using free-jet expansion of a He/H_2 mixture at $T_0 = 24.7$ K and a total pressure of 7 bar.[18] They used a small percentage of H_2 relative to He to differentiate the $^4HeH_2$ complex from the more strongly bound $(H_2)_2$ dimer. The beam velocity was ~500 m s^{-1}, with a variation of about 1%. The beam was collimated by two slits and then diffracted by a transmission grating, according to Bragg's law. The beam components that diffracted at different angles passed through a collimator, and then were analyzed with an electron-impact ionization mass spectrometer, as shown in Figure 1.1.

The diffraction angle is normally given by Bragg's law, $n\lambda = 2d \sin\theta$, where n is the diffraction order, d is the lattice spacing, and λ is the deBroglie wavelength of the molecules. This standard version describes the diffraction when the angle of the incident beam relative to the surface is θ and the angle of the diffracted beam relative to the surface is also θ. Since the Toennies group used a transmission diffract grating, they determined the deflection of the beam relative to the direction of the incident beam. The measured deflection angle is effective 2θ, relative to the Bragg angle. For small angles θ, $\sin\theta \approx \theta$. So, the Toennies group used the equation $\theta = n\lambda/d$ to relate the deflection angle to the deBroglie wavelength λ of the species in the beam. The deBroglie

wavelength is $\lambda = h/mv$, where h is Planck's constant, m is the mass of the molecule or complex, and v is its velocity.

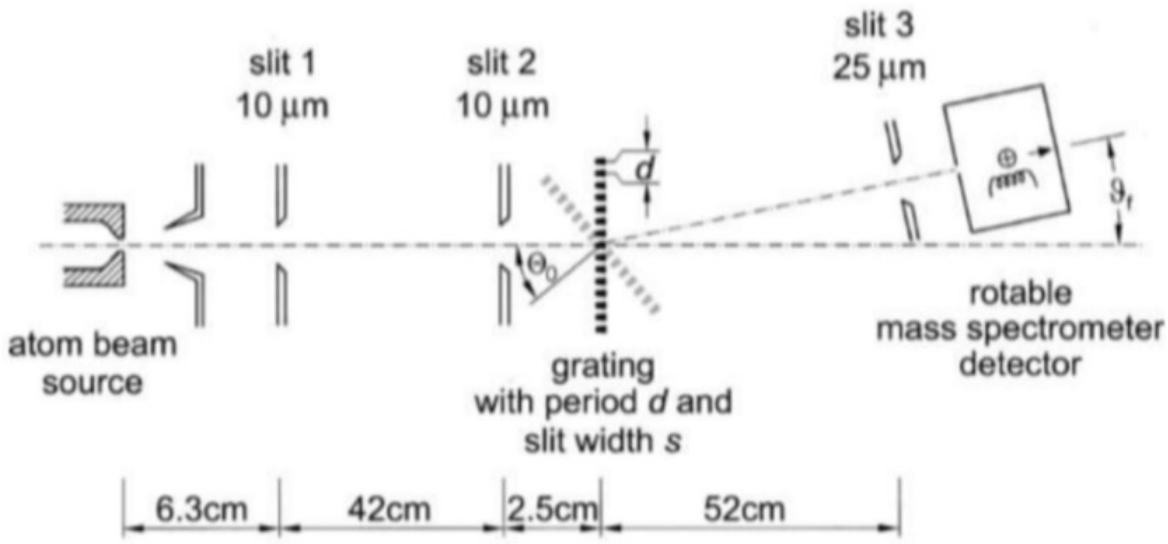

Figure 1.1. From R. E. Grisenti, W. Schöllkopf, J. P. Toennies, J. R. Manson, T. A. Savas, and H. I. Smith, "He-atom diffraction from nanostructure transmission gratings: The role of imperfections," *Phys. Rev. A* **61**, 1345033608 (2000). This figure shows the general set-up of the experiment used to detect bound H_2–He. The beam passes through two collimators to reach the transmission grating, which has a spacing of d = 100 nm. The diffracted beam is detected with a mass spectrometer that can be positioned at a precise angle relative to the incident beam.

In the experiment, the deflection angle is determined by the diffraction of the neutral species. The angular resolution of the experiment was reported as 55 μrad, and the mass spectrometer detector could be positioned to 10^{-3} rad. The peaks detected by the mass spectrometer are determined by the masses of the ion fragments formed from the neutral. The resolution of the mass spectrometer is $m/\Delta m \approx 40$. The first-order peak due to diffraction of the He atoms occurs at $-2.0 \cdot 10^{-3}$ rad, or 0.115°. The peak locations are shown as a function of deflection angle in Figure 1.2, with separate plots for ion masses of 4 amu, 3 amu, 5 amu, and 6 amu.

The deBroglie wavelengths for each of the species observed by the Toennies group were calculated in this thesis research, using the velocity $v = 500.0$ m s^{-1}, given in the paper by the Toennies group. In Table 1.1, the deBroglie wavelengths are listed, and the calculated deflection angles are compared with the observed deflection angles, showing excellent agreement.

Three signals corresponding to H_2–He were observed, all at the correct deflection angle for H_2–He, as shown in Figure 1.2. These appear at ion masses 4 amu, 5 amu, and 6 amu. The peak at 4 amu and a deflection angle of $1.33 \cdot 10^{-3}$ rad comes from He^+ formed from H_2–He. The peak at 5 amu and $1.33 \cdot 10^{-3}$ rad comes from HeH^+ formed from H_2–He, and the peak at mass 6 amu and a deflection angle of $1.33 \cdot 10^{-3}$ rad comes from HeH_2^+ that did not fragment.

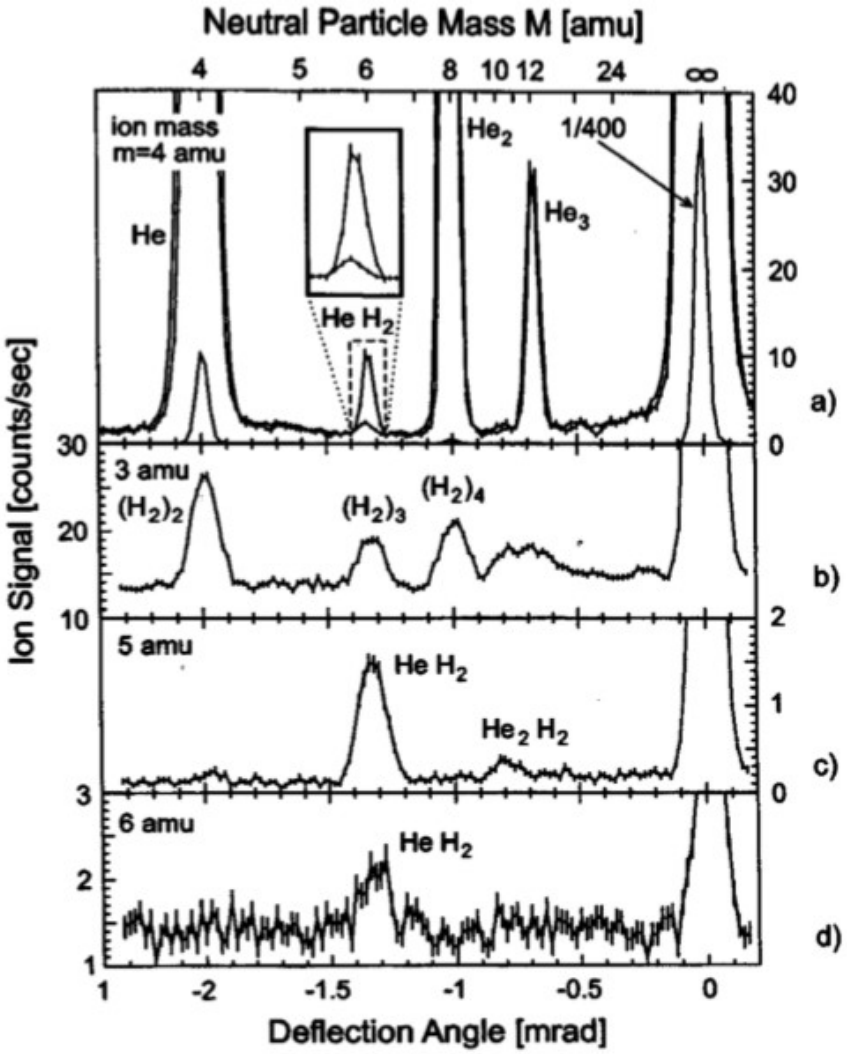

Figure 1.2. From A. Kalinin, O. Kornilov, L. Y. Rusin, and J. P. Toennies, "Evidence for a bound HeH_2 halo molecule by diffraction from a transmission grating," *J. Chem. Phys*. **121**, 625 (2004). The figure shows the ion signal detected by the mass spectrometer as a function of the deflection angle in mrad, for four different masses of the fragment ions: a) 4 amu, b) 3 amu, c) 5 amu, and d) 6 amu. Peaks due to fragments from H_2He are found at a deflection angle near 1.33 mrad (as predicted by calculations based on the deBroglie wavelength of the neutral species and the spacing of the diffraction grating (d = 100 nm). The experiments were run with gas mixtures containing 1% H_2 and 99% He to minimize interferences from H_2 clusters that are more strongly bound than H_2He. The large, bold peaks in the 4 amu plot come from pure He.

Table 1.1. Species detected by the Toennies group. The isotopic masses are listed in amu and kg. The deBroglie wavelengths λ have been calculated based on a particle velocity of 500.0 m/s. The diffraction angles θ_{calc} were determined from $\lambda = d \sin\theta$, with a diffraction grating spacing of d = 100.0 nm. Observed diffraction angles θ_{obs} were read approximately from the figure in the Toennies group paper.

Species	m (amu)	m (kg)	λ (Å)	θ_{calc} (10^{-3} rad)	θ_{obs} (10^{-3} rad)
He	4.00260325	$6.64647897 \cdot 10^{-27}$	1.9939	1.9939	2.00
He_2	8.00520650	$1.32929579 \cdot 10^{-26}$	0.9969	0.9969	1.00
He_3	12.00780976	$1.99264685 \cdot 10^{-26}$	0.6646	0.6646	0.67
HeH_2	6.01825332	$9.99354459 \cdot 10^{-27}$	1.3301	1.3301	1.33
He_2H_2	10.02085657	$1.66400236 \cdot 10^{-26}$	0.7964	0.7964	0.79
$(H_2)_2$	4.03130012	$6.69413125 \cdot 10^{-27}$	1.9797	1.9797	1.98
$(H_2)_3$	6.04695019	$1.00411969 \cdot 10^{-26}$	1.3198	1.3198	1.32
$(H_2)_4$	8.06260026	$1.33882625 \cdot 10^{-26}$	0.9898	0.9898	0.98

In order to provide additional evidence that the He^+ detected at $1.33 \cdot 10^{-3}$ rad was formed by ionization and fragmentation of H_2–He, the same experiment was run with helium alone. Peaks corresponding to neutral masses 4, 8, and 12 amu were essentially the same as the peaks from the H_2/He gas mixture, with one exception: A small peak at $1.33 \cdot 10^{-3}$ rad was seen in the experiments with pure He and attributed to second-order diffraction of $^4He_3$. This peak was higher by ~7.5 counts per second for the H_2/He mixture than for He alone.

The experiment was also run with H_2 alone. In this case, relatively intense signals were seen at 3 amu, due to H_3^+, at deflection angles for $(H_2)_2$, $(H_2)_3$, and $(H_2)_4$, but no signals at 4, 5, or 6 amu were observed in the experiments with pure H_2. A deflection angle of $1.33 \cdot 10^{-3}$ rad might possibly be produced by $(H_2)_3$, but since pure H_2 gas gives no peaks at 5 or 6 amu, this supports the claim that these peaks in the experiments with H_2/He mixtures are due to H_2–He^+. One additional peak at mass 5 amu in the experiments with H_2/He mixtures has the right deflection angle for a neutral mass of 10 amu. This suggests that the peak is due to HeH^+ formed by fragmentation of the neutral He_2H_2.

In 2008, Tejeda, Thibault, Fernández, and Montero[19] determined the rate constants for rotational transitions of J = 2 to J = 0 in collisions of para-H_2 with He, and for J = 3 to J = 1 in collisions of ortho-H_2 with He. They measured the intensities of the vibrational Raman lines in supersonic jets of He/H_2 mixtures at temperatures from 22 K to 180 K, and analyzed the results for the state populations. This is the most recent molecular beam study of H_2–He that cited the 2004 paper from the Toennies group.

1.3 Other Sources of Experimental Data on H_2–He Interactions

In addition to molecular beam scattering studies, measurements of thermal conductivities, NMR relaxation rates, stimulated Raman scattering, and shock wave phenomena have also provided information on the H_2–He potential. Clifford, Colling, Dickinson, and Gray[20] determined the thermal conductivities of mixtures of He with each of the three hydrogen isotopes, as functions of the composition of the mixtures, at temperatures of 77.6 K and 283.2 K. They examined fits to Lennard-Jones potentials, and empirical potential derived from molecular beam studies, and an *ab*

initio potential. Later, Clifford, Fleeter, Kestin, and Wakeham[21] measured thermal conductivities of He/H_2 mixtures as a function of pressure in the range from 2 to 14 MPa have been reported, at 27.C°.

Audibert, Joffrin, and Ducuing[22] used Raman techniques to look at changes in the translational energy of molecules when H_2 collided with ^3He or ^4He and lost vibrational energy. They found large discrepancies from theoretical predictions, but the predictions were based on collinear semi classical scattering calculations and an early *ab initio* potential calculated by Krauss and Mies.[23] Dove, Jones, and Teitelbaum[24] studied the vibrational relaxation of H_2 in shock waves occurring in H_2/He mixtures, for temperatures in the range from 1350 to 3000 K.

NMR studies that measure the T_1 relaxation rates yield information on the anisotropy of the potential because this relaxation time is governed by the torques at play on the interacting systems. The T_1 relaxation rates are determined by two contributions: The first contribution comes from spin-rotation interactions. A magnetic field is generated by the moving charges in the rotating molecule; this field acts on the nuclear spins. When a pulse is applied, the spins can transfer some of their energy into rotation via the spin-rotation coupling. The second contribution to T_1 relaxation comes from magnetic-dipole-magnetic dipole interactions.

Riehl, Kinsey, Waugh, and Rugheimer[25] measured the T_1 relaxation time of He/H_2 mixtures at temperatures from 77 to 300 K. Computing cross sections from their measured relaxation times as a function of temperature and comparing with theoretical values allowed these authors to report approximate anisotropic parameters for the $He–H_2$ potential. In a later study, Riehl, Fisher, Baloga, and Kinsey[26] measured the spin relaxation times in the temperature range from 15.7 to 136 K. They assumed a potential of the form $V = V_0(R) + V_2(R)\, P_2(\cos\theta)$, where R is the distance from the center of mass of H_2 to He, $V_0(R)$ is the isotropic term in the potential, and $V_2(R)$ gives the anisotropy that goes as the second Legendre polynomial of the cosine of the angle between the H_2 bond vector and the vector from the center of mass of H_2 to He. They also assumed that the exponential repulsions in $V_2(R)$ and $V_0(R)$ would fall off at the same rate, when R increases. They looked at four different possible fitting potentials and concluded that a piecewise

potential was the best. They could not find a single potential that fit both their measured T_1 relaxation times and the rotational relaxation rates.

The most recent NMR experiment of relevance to the H_2–He potential was done by Wagner, Armstrong, Bissonnette, and McCourt,[27] who studied the relaxation of hydrogen and deuteron nuclear spin magnetizations in He–HD mixtures at temperatures from 90 to 300 K. These authors compared their results for the temperature dependence with predictions based on *ab initio* potential surface calculations by Schaefer and Köhler[28] and by Meyer, Hariharan, and Kutzelnigg.[29] They found quantitative agreement between the experimental and theoretical results for the H nucleus, but only semi-quantitative agreement for the D nucleus.

Riehl, Kinsey, Waugh, and Rugheimer also noted that the anisotropic part of the potential can be probed in experiments on sound absorption in gases, spectroscopic line broadening, molecular libration in solids, and the dependence of transport coefficients on magnetic fields.

REFERENCES

REFERENCES

1. F. Coester, *Nucl. Phys*. **7**, 421 (1958); F. Coester and H. Kümmel, *Nucl. Phys*. **17**, 477 (1960); J. Čížek, *J. Chem. Phys*. **45**, 4256 (1966); *ibid*. *Adv. Chem. Phys*. **14**, 35 (1969).

2. K. Kowalski and P. Piecuch, *J. Chem. Phys*. **113**, 18 (2000); *ibid*. **122**, 074107 (2005); *ibid.* **115**, 643 (2001); K. Kowalski and P. Piecuch, *Chem. Phys. Lett*. **347**, 237 (2001).

3. K. Kowalski and P. Piecuch, *J. Chem. Phys*. **115**, 2966 (2001); *ibid*. **116**, 7411 (2002); *ibid*. **120**, 1715 (2004); M. Włoch, J.R. Gour, K. Kowalski, and P. Piecuch, *J. Chem. Phys*. **122**, 214107 (2005).

4. T. H. Dunning Jr., *J. Chem. Phys*. **90**, 1007 (1989); R. A. Kendall, T. H. Dunning Jr., and R. J. Harrison, *J. Chem. Phys*. **96**, 6769 (1992); D. E. Woon and T. H. Dunning, Jr., *J. Chem. Phys.* **100**, 2975 (1994).

5. K. Raghavachari, G. W. Trucks, J. A. Pople, and M. Head-Gordon, *Chem. Phys. Lett*. **157**, 479 (1989).

6. P. Piecuch and M. Włoch, *J. Chem. Phys*. **123**, 224105 (2005); P. Piecuch, M. Włoch, J. R. Gour, and A. Kinal, *Chem. Phys. Lett*. **418**, 467 (2006).

7. B. W. Bakr, D. G. A. Smith, and K. Patkowski, *J. Chem. Phys.* **139**, 144305 (2013).

8. L. Frommhold, personal communication.

9. H. Harrison, *J. Chem. Phys*. **37**, 1164 (1962).

10. G. E. Moore, S. Datz, and F. van der Valk, *J. Chem. Phys*. **46**, 2012 (1967).

11. J. G. Skofronick, *Rev. Sci. Instr.* **38**, 1628 (1967).

12. P. Cantini, M. Cavallini, M. G. Dondi, and G. Scoles, *Phys. Lett*. **27A**, 284 (1968).

13. R. Gengenbach, J. Strunck, and J. P. Toennies, *J. Chem. Phys.* **54**, 1830 (1971).

14. M. D. Gordon and D. Secrest, *J. Chem. Phys*. **52**, 120 (1970).

15. R. Gengenbach and Ch. Hahn, *Chem. Phys. Lett*. **15**, 604 (1972).

16. R. S. Grace and J. G. Skofronick, *J. Chem. Phys.* **56**, 3403 (1972).

17. H. V. Lilenfeld, J. L. Kinsey, N. C. Lang, and E. K. Parks, *J. Chem. Phys*. **57**, 4593 (1972).

18. A. Kalinin, O. Kornilov, L. Y. Rusin, and J. P. Toennies, *J. Chem. Phys*. **121**, 625 (2004).

19. G. Tejeda, F. Thibault, J. M. Fernández, and S. Montero, *J. Chem. Phys*. **128**, 224308 (2008).

20. A. A. Clifford, L. Colling, E. Dickinson, and P. Gray, *J. Chem. Soc. Faraday Trans*. **71**, 1962 (1975)

21. A. A. Clifford, R. D. Fleeter, J. Kestin, and W. A. Wakeham, *Berichte der Bunsen-Gesellschaft- Phys. Chem. Chem. Phys*. **84**, 18 (1980).

22. M. M. Audibert, C. Joffrin, and J. Ducuing, *Chem. Phys. Lett*. **19**, 26 (1973); M. M. Audibert, C. Joffrin, and J. Ducuing, *J. Chem. Phys*. **61**, 4357 (1974).

23. M. Krauss and F. H. Mies, *J. Chem. Phys*. **42**, 2703 (1965).

24. J. E. Dove, D. G. Jones, and H. Teitelbaum, Proceedings of the Fourteenth International Symposium on Combustion (The Combustion Institute, Pittsburgh, 1973), p. 177; J. E. Dove and H. Teitelbaum, *Chem. Phys*. **6**, 431 (1974).

25. J. W. Riehl, J. L. Kinsey, J. S. Waugh, and J. H. Rugheimer, *J. Chem. Phys.* **49**, 5276 (1968).

26. J. W. Riehl, C. J. Fisher, J. D. Baloga, and J. L. Kinsey, *J. Chem. Phys.* **58**, 4571 (1973).

27. R. S. Wagner, R. L. Armstrong, E. C. Bissonnette, and F. R. W. McCourt, *J. Chem. Phys*. **92**, 5907 (1990).

28. J. Schaefer and W. E. Köhler, *Physica A* **129**, 469 (1985).

29. W. Meyer, P. C. Hariharan, and W. Kutzelnigg, *J. Chem. Phys*. **73**, 1880 (1980).

CHAPTER 2: Methodology

In this chapter, the methodologies used for the ground-state calculations in this thesis are described. These include traditional coupled-cluster methods that include triple excitations approximately or exactly, coupled-cluster methods with approximate quadruple excitations, completely renormalized coupled-cluster approaches, and configuration-interaction methods.

2.1 Coupled-Cluster Methods

In the original coupled-cluster (CC) methods,[1] the wave function is written as

$$| \Psi \rangle = e^{T} | \Phi_0 \rangle \tag{2.1}$$

where $| \Phi_0 \rangle$ is an independent-particle model reference determinant, usually the Hartree-Fock determinant. In Eq. (2.1), T is the cluster operator of CC theory, which can be written in terms of its many-body components for an N electron system as

$$T = T_1 + T_2 + T_3 + \ldots T_N, \tag{2.2}$$

where T_1 performs all single excitations from occupied i, j, k, … to unoccupied a, b, c, … orbitals, T_2 performs all double excitations, . . . and T_N performs all N-tuple excitations. If the cluster operator contains up to N-body terms and there are N electrons in the system, then we obtain the exact solution of the Schrodinger equation within the basis set. The series in Eq. (2.2) must terminate because electrons must be moved from occupied to unoccupied orbitals and there are only N occupied orbitals in the reference wave function and a finite number of total orbitals in the basis set. The T_1 operator, which generates all single excitations from the reference determinant, is given by

$$T_1 = \sum_{i \in \{occ\},\, a \in \{unocc\}} t_i^a \; a^\dagger_a \, a_i \,. \tag{2.3}$$

In this equation and below $a^\dagger_a$ is the creation operator that places an electron in the unoccupied orbital a, and a_i is the annihilation operator that removes an electron from occupied orbital i. The coupled-cluster operators that generate all double and triple excitations are given, respectively, by

$$T_2 = \sum_{i > j \in \{occ\},\, a > b \in \{unocc\}} t_{ij}^{ab} \; a^\dagger_a \, a_i \, a^\dagger_b \, a_j \tag{2.4}$$

$$T_3 = \sum_{i<j<k \in \{occ\},\, a<b<c \in \{unocc\}} t_{ijk}^{abc} \; a^\dagger_a \, a_i \, a^\dagger_b \, a_j \, a^\dagger_c \, a_k \tag{2.5}$$

and similarly for the higher-order T_n operators.

In approximate CC methods, excitations relative to $| \Phi_0 \rangle$ are truncated at some level $m_A < N$, so that the cluster operator for an approximate CC method A is given by

$$T^{(A)} = \sum_{i=1}^{m_A} T_i^{(A)} . \tag{2.6}$$

In this equation, the notation $T_i^{(A)}$ reflects the fact that the cluster amplitudes t_i^a, t_{ij}^{ab}, t_{ijk}^{abc} . . . are different for different levels of truncation, but the structure of each excitation operator T_n is the same for all of the approximate CC methods regardless of the truncation level. For $m_A = 2$, we have the CCSD[2] method; for $m_A = 3$, we have the CCSDT[3] method; for $m_A = 4$ we have the CCSDTQ[4] method, which is the highest level currently available. Here we note that the CCSDTQ method, which includes all single, double, triple, and quadruple excitations, is exact for the case of H_2–He.

In more detail, for $m_A = 2$ we have the CCSD method[2] which has the cluster operator

$$T^{(CCSD)} = T_1 + T_2 \tag{2.7}$$

whose amplitudes are determined from the system of CC equations obtained by projecting the equations for the CCSD method onto all singly- and doubly-excited configurations relative to $| \Phi_0 \rangle$. In the CCSDT approach,[3] the cluster operator is truncated at $m_A = 3$ so that we have

$$T^{(CCSDT)} = T_1 + T_2 + T_3. \tag{2.8}$$

Similarly, CCSDTQ[4] arises from truncating at the $m_A = 4$ level of excitation to yield the cluster operator given by

$$T^{(CCSDTQ)} = T_1 + T_2 + T_3 + T_4. \tag{2.9}$$

The CCSD method scales as $n_0^3 n_u^3$ with n_0 the number of occupied orbitals and n_u the number of unoccupied orbitals in the basis set.[7] The CCSDT and CCSDTQ methods have even worse scaling with the size of the basis set.

The Schrödinger equation for the coupled-cluster wave function is

$$H e^T | \Phi_0 \rangle = E | \Phi_0 \rangle . \tag{2.10}$$

Multiplying on the left by the "bra" reference configuration $\langle \Phi_0 |$ and moving the energy to the left hand-side, for the equation involving all single excitations from the reference determinant we have

$$(\Phi_i^a \mid e^{-T} H e^{T} \mid \Phi \rangle - E \langle \Phi \mid \Phi \rangle = 0 \tag{2.11}$$

Thus, the equations that are solved to determine the cluster operator amplitudes t_i are the projections of the equations onto all excited determinants relative to $| \Phi_0 \rangle$. This gives the projection equations of CC theory.[1,11]

From an analysis of the results occurring in the fifth order of perturbation theory and their comparison with the CC expansion in terms of the cluster operators, a missing (connected) triples term to CCSD was determined[5] and it is this connected triples correction which is based on perturbation theory that, when applied to the CCSD result, yields the CCSD(T)[5] one. This connected triples correction arises from T_1 and T_2 and needs only to be computed once (i.e., in a non-iterative fashion) to correct the CCSD energy and arrive at the CCSD(T) result. The triples correction that is computed in the CCSD(T) method can be written as

$$\Delta E_t = (\sum_s^S + \sum_s^D) \sum_t^T \sum_u^D (E_0 - E_t)^{-1} a_s V_{st} V_{tu} a_u \tag{2.12}$$

Thus, the CCSD(T) method involves the calculation of all singles and doubles and accounts for the disconnected triples via Eq. (2.12) which involves only the triples that arise from T_1 and T_2.

2.2 The Method of Moments of Coupled-Cluster Equations Formalism

The methods of moments of coupled-cluster (MMCC) equations, referred to generally as the MMCC(m_A, m_B) methods,[6] are based on a correction that when added to the result of an approximate method A, yields the exact correlation energy, given by

$$\Delta E = E - \langle \Phi \mid H \mid \Phi \rangle . \tag{2.13}$$

The MMCC corrections are given generally by

$$\delta = \Delta E - \Delta E^{(A)} \tag{2.14}$$

where ΔE is the exact correlation energy and $\Delta E^{(A)}$ is the correlation energy of approximate method A. Thus, δ represents the error between the correlation energy obtained with approximate method A and the exact value.

In the biorthogonal MMCC formalism,[7] the corrections δ are given by

$$\delta_0^{(A)} = \sum_{n=m_A+1}^{N_A} \sum_{\substack{i_1<\cdots<i_n \\ a_1<\cdots<a_n}}^{n} \ell_{i_1\cdots i_n}^{a_1\cdots a_n} \mathcal{M}_{a_1\cdots a_n}^{i_1\cdots i_n}(m_A) \tag{2.15}$$

where the $\mathcal{M}_{a_1\cdots a_n}^{i_1\cdots i_n}(m_A)$ are the generalized moments of CC equations and the coefficients,

$$\ell_{i_1\cdots i_n}^{a_1\cdots a_n} = \left\langle \Psi \left| e^{T^{(A)}} \right| \Phi_{i_1\cdots i_n}^{a_1\cdots a_n} \right\rangle \tag{2.16}$$

are those of the de-excitation operator $\mathcal{L}$ of CC theory[7] which gives the exact $\langle\Psi|$, i.e.,

$$\langle \Psi | = \langle \Phi | \mathcal{L}\, e^{-T^{(A)}} \tag{2.17}$$

In order for the correction $\delta_0^{(A)}$ to correspond to the difference between the correlation energy computed with approximate CC method A, $\Delta E^{(A)}$, and the exact result, ΔE, the wavefunction $\langle \Psi |$ must be normalized such that

$$\langle \Psi | \Psi^{(A)} \rangle = \left\langle \Psi \left| e^{T^{(A)}} \right| \Phi \right\rangle = 1, \tag{2.18}$$

where $e^{T^{(A)}} | \Phi \rangle$ is the CC wavefunction for approximate CC method A. Then, the cluster operator $T^{(A)}$ is determined by solving the CC equations

$$\left\langle \Phi_{i_1\cdots i_n}^{a_1\cdots a_n} \left| \overline{H}^{(A)} \right| \Phi \right\rangle = 0, \tag{2.19}$$

projected on all singly, doubly, …, up to n-tuply excited configurations with $n = 1, \ldots, m_A$ and

$$\overline{H}^{(A)} = e^{-T^{(A)}} H\, e^{T^{(A)}} = \left(H\, e^{T^{(A)}} \right)_C, \tag{2.20}$$

where the subscript C means only connected diagrams contribute to this operator product, is the similarity transformed Hamiltonian of CC method A. The similarity transformed Hamiltonian $\overline{H}^{(A)}$ includes only connected contributions by the connected cluster theorem.[1,11]

The generalized moments $\mathcal{M}_{a_1\cdots a_n}^{i_1\cdots i_n}(m_A)$ appearing in Eqn. (2.15) are the projections of the CC equations for method A onto all the excited determinants that are ignored in CC method A,[7] i.e.,

$$\mathcal{M}_{a_1\cdots a_j}^{i_1\cdots i_j}(m_A) = \sum \left\langle \Phi_{i_1\cdots i_j}^{a_1\cdots a_j} \left| \overline{H}^{(A)} \right| \Phi \right\rangle, \tag{2.21}$$

where $j \geq m_A + 1$. Thus, all generalized moments that are net set to zero when solving the CC equations for method A are considered within the biorthogonal MMCC formalism.[7]

In the completely-renormalized CC methods based on the biorthogonal MMCC formalism [CR-CC(m_A , m_B)[8]], the energy is computed via the equation

$$E(m_A, m_B)_{\mathcal{L}} = E^{(A)} + \delta(m_A, m_B)_{\mathcal{L}} \tag{2.22}$$

where the correction $\delta(\mathrm{m_A}, \mathrm{m_B})_{\mathcal{L}}$ is given by

$$\delta(\mathrm{m_A}, \mathrm{m_B})_{\mathcal{L}} = \sum_{\mathrm{n}=\mathrm{m_A}+1}^{\mathrm{m_B}} \sum_{\substack{\mathrm{i_1}<\cdots<\mathrm{i_n} \\ \mathrm{a_1}<\cdots<\mathrm{a_n}}} \tilde{l}_{\mathrm{i_1}\cdots\mathrm{i_n}}^{\mathrm{a_1}\cdots\mathrm{a_n}} \mathcal{M}_{\mathrm{a_1}\cdots\mathrm{a_n}}^{\mathrm{i_1}\cdots\mathrm{i_n}}(\mathrm{m_A}). \tag{2.23}$$

For example, in the CR-CC(2,3) approach,[8] $\mathrm{m_A} = 2$ and $\mathrm{m_B} = 3$, and one must find $\mathcal{M}_3(2)$ in order to compute the correction to the CCSD result given by

$$\delta(2,3)_{\mathcal{L}} = \sum_{\substack{\mathrm{i}<\mathrm{j}<\mathrm{k} \\ \mathrm{a}<\mathrm{b}<\mathrm{c}}} \tilde{\ell}_{\mathrm{ijk}}^{\mathrm{abc}}(\mathrm{CCSD})\ \mathcal{M}_{\mathrm{abc}}^{\mathrm{ijk}}(2) \tag{2.24}$$

where

$$\mathcal{M}_3(2) = \mathcal{M}_{\mathrm{abc}}^{\mathrm{ijk}}(2) = \left\langle \Phi_{\mathrm{ijk}}^{\mathrm{abc}} \middle| \left(\mathrm{H}\, \mathrm{e}^{\mathrm{T}^{(\mathrm{A})}}\right)_{\mathrm{C}} \middle| \Phi \right\rangle, \tag{2.25}$$

is the generalized moment of the CCSD equations corresponding to projections on to all triply excited configurations (this moment is not considered in the CCSD calculation where it is set to zero) and the coefficients, $\tilde{\ell}_{\mathrm{ijk}}^{\mathrm{abc}}$, are amplitudes of the many-body Λ operator of the analytic gradient CCSD theory,[9] often expressed as

$$\tilde{\ell}_{\mathrm{ijk}}^{\mathrm{abc}}\,(\mathrm{CCSD}) = \frac{\left\langle \Phi \middle| \Lambda^{(\mathrm{CCSD})}\, \overline{\mathrm{H}}^{(\mathrm{CCSD})} \middle| \Phi_{\mathrm{ijk}}^{\mathrm{abc}} \right\rangle}{\mathrm{D}_{\mathrm{abc}}^{\mathrm{ijk}}\,(\mathrm{CCSD})}. \tag{2.26}$$

In the case of the CCSD method, the Λ operator is given as

$$\Lambda^{(\mathrm{CCSD})} = \Lambda_1{}^{(\mathrm{CCSD})} + \Lambda_2{}^{(\mathrm{CCSD})}. \tag{2.27}$$

(The amplitudes $\tilde{\ell}_{\mathrm{ijk}}^{\mathrm{abc}}$ contain both connected and disconnected contributions). The denominator in Eqn. (2.26) is given by

$$\mathrm{D}_{\mathrm{abc}}^{\mathrm{ijk}}(\mathrm{CCSD}) = \mathrm{E}^{(\mathrm{CCSD})} - \left\langle \Phi_{\mathrm{ijk}}^{\mathrm{abc}} \middle| \overline{\mathrm{H}} \middle| \Phi_{\mathrm{ijk}}^{\mathrm{abc}} \right\rangle. \tag{2.28}$$

The expression above involves all n-body components of the similarity transformed Hamiltonian up to three-body, so we have for the generalized moment characterizing the CR-CC(2,3) method[8]

$$\mathcal{M}_{\mathrm{abc}}^{\mathrm{ijk}}(2) = \left\langle \Phi_{\mathrm{ijk}}^{\mathrm{abc}} \middle| \mathrm{H}\left(\mathrm{T_2} + \mathrm{T_1}\,\mathrm{T_2} + \tfrac{1}{2}\,\mathrm{T_2}^2 + \tfrac{1}{2}\,\mathrm{T_1}^2\,\mathrm{T_2} + \tfrac{1}{2}\,\mathrm{T_1}\,\mathrm{T_2}^2 + \tfrac{1}{6}\,\mathrm{T_1}^6\,\mathrm{T_2}\right)_{\mathrm{C}} \middle| \Phi \right\rangle. \tag{2.29}$$

The CR-CC(2,3) energy can then be computed as follows:

$$\mathrm{E}^{(\mathrm{CR\text{-}CC(2,3)})} = \mathrm{E}^{(\mathrm{CCSD})} + \sum_{\substack{\mathrm{i}<\mathrm{j}<\mathrm{k} \\ \mathrm{a}<\mathrm{b}<\mathrm{c}}} \tilde{\ell}_{\mathrm{ijk}}^{\mathrm{abc}}(\mathrm{CCSD})\, \mathcal{M}_{\mathrm{abc}}^{\mathrm{ijk}}(2)\,. \tag{2.30}$$

There have been various variants of the CR-CC(2,3) approach, labeled as variants A, B, C, and D,[8] developed based on the form of the denominator $\mathrm{D}_{\mathrm{abc}}^{\mathrm{ijk}}(\mathrm{CCSD})$ employed. The variant CR-

CC(2,3), A involves replacing the D_{abc}^{ijk} denominator (approximated only by its 1-body contribution) by the orbital energy difference $\varepsilon_i + \varepsilon_j + \varepsilon_k - \varepsilon_a - \varepsilon_b - \varepsilon_c$. The CR-CC(2,3), B approach is obtained when the denominator D_{abc}^{ijk} includes only the one-body contribution. If the three-body term is not included in D_{abc}^{ijk}, variant C results. The most complete form of the D_{abc}^{ijk} denominator is that given by Eqn. (2.28) and is termed the CR-CC(2,3), D approach. In this thesis, the results presented for HeH_2 were obtained with the most complete variant of the CR-CC(2,3) method, i.e., the CR-CC(2,3), D method. The CR-CC(2,3), D variant keeps the entire triples-triples section of the matrix representing the similarity transformed Hamiltonian whereas variants A – C involve setting parts of the triples block to zero.

2.3 Configuration Interaction and its Relation to Coupled Cluster Theory

One of the most widely used methods in computational chemistry is the configuration-interaction (CI)[10] method. In CI, the wave function for an N-electron system is written as

$$| \Psi \rangle = (1 + C) | \Phi_0 \rangle \tag{2.31}$$

where the excitation operator of CI theory C is composed of a sum of its many-body components ranging from the 1-body term (all single excitations) up to the N-body term (all N-tuple excitations), i.e.,

$$C = \sum_{j=1}^{j=N} C_j \tag{2.32}$$

Thus, the wave function is written as a linear combination of Slater determinants within the CI formalism. The CI excitation operators C_j are related to the coupled-cluster excitation operators T_i by the following relations:

$$C_1 = T_1,$$

$$C_2 = T_2 + 1/2\ (T_1)^2,$$

$$C_3 = T_3 + T_1 T_2 + 1/6\ (T_1)^2,$$

$$C_4 = T_4 + 1/2\ (T_2)^2 + 1/2\ (T_1)^2\ T_2 + 1/24\ (T_1)^4 + T_1\ T_3,$$

etc.[11] In practical implementations, the sum in Eq. (2.32) must be truncated at some (usually low) level of excitation. For example, truncating the series at j = 2 gives the CISD[10] (configuration-interaction with all single and double excitations) method characterized by the wave function

$$| \Psi^{\,CISD} \rangle = (1 + C_1 + C_2) \, | \Phi_0 \rangle \tag{2.33}$$

If the sum in Eq. (2.32) is not truncated so that it includes all terms up to j = N, then the full configuration interaction[10] (FCI) method is obtained. FCI calculations yield the exact solution to the Schrödinger equation for a given basis set.

REFERENCES

REFERENCES

1. F. Coester, *Nucl. Phys*. **7**, 421 (1958); F. Coester and H. Kümmel, *Nucl. Phys*. **17**, 477 (1960); J. Čížek, *J. Chem. Phys*. **45**, 4256 (1966); *ibid*. *Adv. Chem. Phys*. **14**, 35 (1969).

2. G. D. Purvis III and R. J. Bartlett, *J. Chem. Phys*. **76**, 1910 (1982).

3. J. Noga and R. J. Bartlett, *J. Chem. Phys*. **86**, 7041 (1987); *ibid*. **89**, 3401 (1988) (erratum); G. E. Scuseria and H. F. Schaefer III, *Chem. Phys. Lett*. **152**, 382 (1988).

4. S. A. Kucharski and R. J. Bartlett, *Theor. Chim. Acta* **80**, 387 (1991); S. A. Kucharski and R. J. Bartlett, *J. Chem. Phys*. **97**, 4282 (1992); N. Oliphant and L. Adamowicz, *J. Chem. Phys*. **95**, 6645 (1991); P. Piecuch and L. Adamowicz, *J. Chem. Phys*. **100**, 5792 (1994).

5. K. Raghavachari, G. W. Trucks, J. A. Pople, and M. Head-Gordon, *Chem. Phys. Lett*. **157**, 479 (1989).

6. P. Piecuch, K. Kowalski, I. S. O. Pimienta, P. D. Fan, M. Lodriguito, M. J. McGuire, S. A. Kucharski, T. Kus, and M. Musial, *Theor. Chem. Acc*. **112**, 349 (2004); P. Piecuch, K. Kowalski, I. S. O. Pimienta, and M. J. McGuire, *Int. Rev. Phys. Chem*. **21**, 527 (2002); K. Kowalski and P. Piecuch, *J. Chem. Phys*. **113**, 18 (2000); P. Piecuch and K. Kowalski, in *Computational Chemistry: Reviews of Current Trends*, edited by J. Leszczyński (World Scientific, Singapore, 2000), Vol. 5, p. 1.

7. P. Piecuch and M. Włoch, *J. Chem. Phys*. **123**, 224105 (2005); P. Piecuch, M. Włoch, J. R. Gour, and A. Kinal, *Chem. Phys. Lett*. **418**, 467 (2006).

8. K. Kowalski and P. Piecuch, *J. Chem. Phys*. **113**, 18 (2000); *ibid*. **122**, 074107 (2005); *ibid.* **115**, 643 (2001); K. Kowalski and P. Piecuch, *Chem. Phys. Lett*. **347**, 237 (2001).

9. E. A. Salter, G. W. Trucks, and R. J. Bartlett, *J. Chem. Phys*. **90**, 1752 (1989).

10. O. Sïnanoğlu, *J. Chem. Phys.* **36**, 706 (1962); I. Shavitt, The method of configuration interaction, in Methods of Electronic Structure Theory, edited by H. F. Schaefer (Plenum Press, New York, 1977), pp. 189-275; R. J. Harrison and N. C. Handy, *Chem. Phys. Lett*. **95**, 386 (1983); R. McWeeny, Methods of Molecular Quantum Mechanics (Academic Press, New York, 2nd edition, 1992).

11. T. D. Crawford and H. F. Shaefer III, An Introduction to Coupled Cluster Theory for Computational Chemists, in *Reviews in Computational Chemistry*, Volume 14, edited by Kenny B. Lipkowitz and Donald B. Boyd, (Wiley-VCH, John Wiley and Sons, Inc., New York, 2000).

CHAPTER 3: Earlier Theoretical Studies of H_2–He in the Ground Electronic State

The He–H_2 system in the ground electronic state has been studied by numerous authors using various self-consistent field and configuration interaction (CI) methods. The potential energy surfaces available for the ground state prior to the current work (reported in this thesis) covered a much smaller region of the nuclear configuration space. A few earlier studies have employed the CCSD(T) method; these are discussed briefly below. When this work was initiated, the CR-CC(2,3) method had not been used in any study of weakly bound van der Waals complexes, to the best of our knowledge. The results obtained here allow an assessment of the applicability of this method to van der Waals molecules. They should also make it possible to determine whether the CR-CC(2,3) method is superior to CCSD(T) for weakly interacting systems, particularly when the bond in one of the interacting molecules is stretched away from equilibrium.

The geometry of the He–H_2 system is specified by three variables: the H_2 bond length r, the distance from the center of mass of the H_2 molecule R to the helium nucleus, and the angle θ between the bond vector r and the vector R from the H_2 center of mass to the helium nucleus, as shown in Figure 3.1. The system is planar, so we can set $\phi = 0$. Thus, each point on the potential energy surface is characterized by an ordered set of three coordinates, (R, r, θ). The distances R and r are given in atomic units of length (bohr, 1 $a_0 = 5.2917721092 \cdot 10^{-11}$ m = 0.52917721092 Å), the angle θ is given in degrees, and energies are given in the atomic unit of energy, the Hartree (1 $E_h = 4.359744417 \cdot 10^{-18}$ J = 27.211385 eV, corresponding to 627.509 kcal mol^{-1}), unless otherwise noted.

The energy of the ground-state of the H_2 molecule as a function of the bond length r is used with the energy of an isolated helium atom to locate the dissociation limit for the H_2–He system. Table 3.1 shows the computed CCSD energy of the hydrogen molecule ground-state, H_2 ($X\,^1\Sigma_g^+$), obtained with the aug-cc-pVXZ (X = 4, 5)[1,2] basis sets at several values of the internuclear distance.

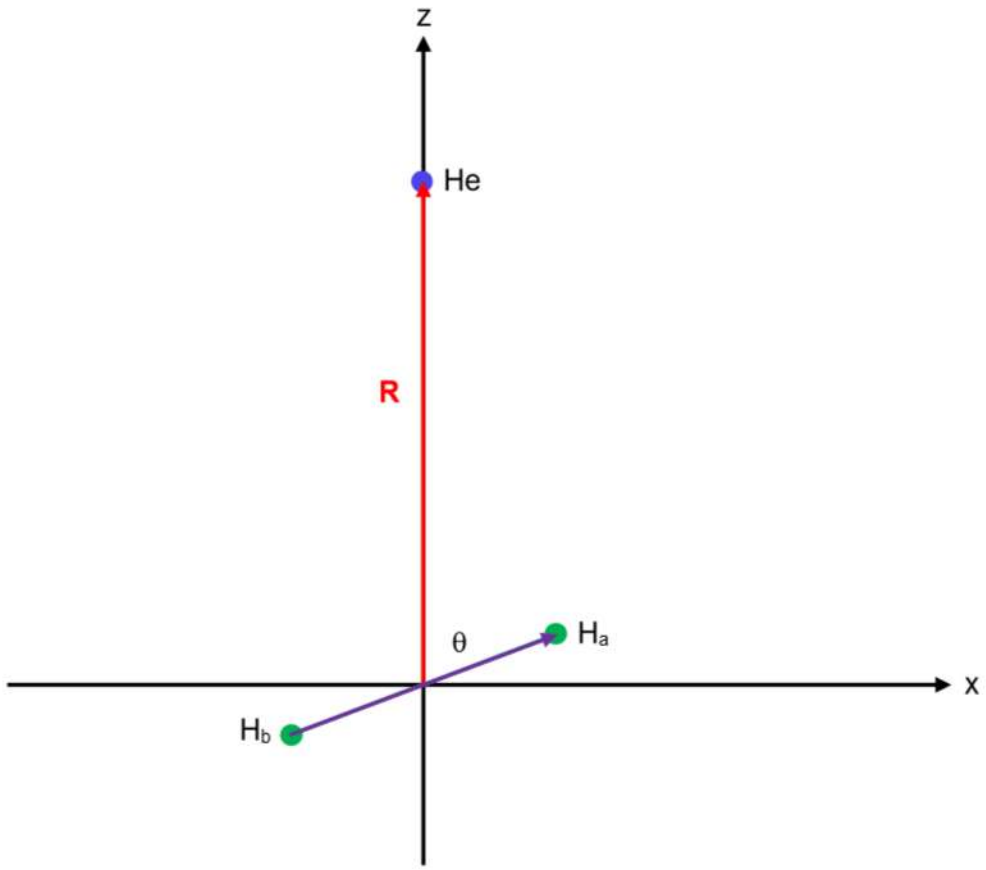

Figure 3.1. Geometry employed for the He–H_2 system. The separation R is between the center of mass of the two H nuclei and the He nucleus, and the angle θ is between the H–H vector and the z axis. The He atom is located along the z axis.

Table 3.1. Energy (in E_h) of the H_2 ground state, $H_2(X\,^1\Sigma_g^+)$, at the CCSD level of theory using the aug-cc-pVQZ and aug-ccpV5Z basis sets; energy as a function of the internuclear distance r.

r / a_0	a4Z	a5Z
0.250	1.242905583	1.241313672
0.942	-1.102220329	-1.102784494
1.000	-1.123720026	-1.124249917
1.111	-1.151398415	-1.151878442
1.280	-1.170684971	-1.171105802
1.4011	-1.173867240	-1.174252185
1.448736	-1.173487648	-1.173859947
1.449	-1.173483443	-1.173855674
1.750	-1.158391415	-1.158701456
1.787	-1.155592725	-1.155896785
2.125	-1.126477641	-1.126737393
2.430	-1.099459044	-1.099693080
2.463	-1.095816970	-1.096048215
2.801	-1.070268826	-1.070481645
3.250	-1.042913536	-1.043100800
3.730	-1.023431609	-1.023587436
5.000	-1.003647699	-1.003755860
5.700	-1.001189292	-1.001290600
8.000	-0.999949717	-1.000043272
10.00	-0.999905028	-0.999997971
20.00	-0.999896751	-0.999989668

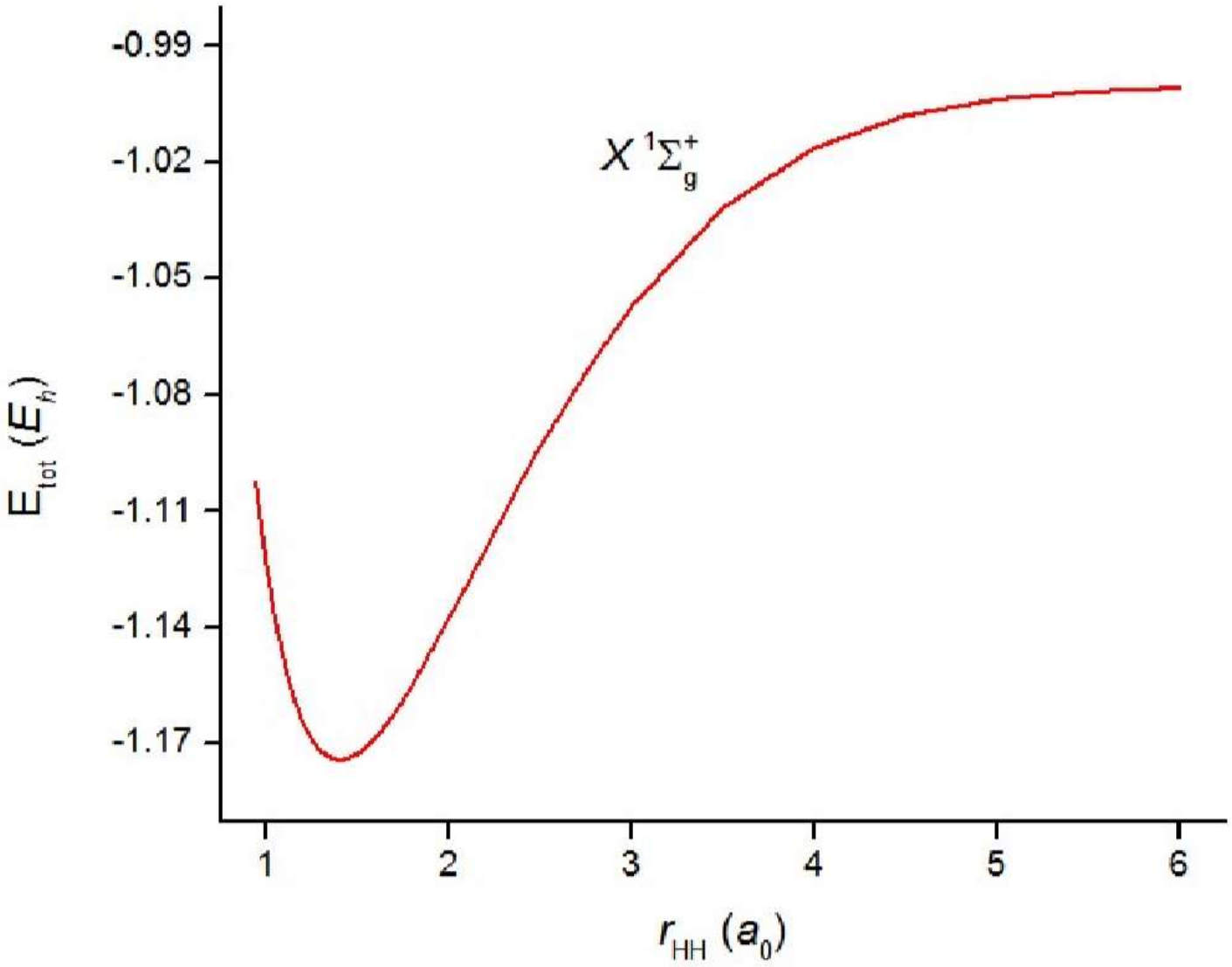

Figure 3.2. Ground state energy curve of H_2 computed with the CCSD method and the aug-cc-pV5Z basis set.

3.1 Early Theoretical Studies of the Ground State Potential Energy Surface

The first theoretical study of the H_2−He ground state was carried out in 1963 by Roberts,[3] using a valence bond approach, with the H–H bond length r = 1.406 a_0, R in the range from 3.8 to 5.2 a_0, and θ between 0 and 90°. In addition, Roberts reported energies for the bond length r = 1.486 a_0. As in other early calculations on this system,[4-8] only a small number of H_2 bond lengths were investigated, all fairly close to the equilibrium bond length. Gordon and Secrest[9] performed the first approximate configuration interaction calculations on H_2−He in 1970.

The ground-state van der Waals minimum was first obtained in 1973 by Tsapline and Kutzelnigg[10] who used the IEPA-PNO (i.e., independent electron pair approximation using pair natural orbitals) approach. The energy was calculated for three r values, three angles, and for R from 3 to 20 a_0. Tsapline and Kutzelnigg obtained a ground-state van der Waals minimum of depth ~ 66.5 μE_h located near R = 6.5 a_0 for the linear (θ = 0°) geometry, and for the T-shaped (θ = 90°) arrangement, a minimum of ~ 44.3 μE_h near R ~ 6.29 a_0. The surface of Tsapline and Kutzelnigg was later extended by Raczkowski and Lester[11] to include geometries within the repulsive region of the potential energy surface.

In the late 1970's, Römelt, Peyerimhoff, and Buenker[12] (RPB) performed calculations for the ground-state and the six lowest-lying excited-states of H_2−He using standard SCF and Buenker's MRD-CI[13] (multiple reference single- and double-excitation configuration interaction) methods. They found the van der Waals well to be slightly deeper for the linear geometry than for the T-shaped arrangement, i.e., $\varepsilon(C_{\infty v}) > \varepsilon(C_{2v})$, where ε denotes the well-depth as a positive number. A few years later, Meyer, Hariharan, and Kutzelnigg[14] (MHK) reported *ab initio* results from CI calculations for geometries having intermolecular separations R = 1.5 a_0 to R = ∞ and H_2 bond lengths between r = 0.9 a_0 and 2.0 a_0, for three angles. For r = 1.449 a_0, the ground-state minimum for the linear structure was found at R = 6.50 a_0 with a depth of ε = 45.6 μE_h, while the minimum for the T-shaped geometry was determined to be at R = 6.35 a_0 with a depth ε = 41.2 μE_h.

3.2 More Recent Theoretical Studies for Comparison

The previous theoretical studies of the H_2–He ground-state of primary interest for comparisons with the results presented in this thesis are those by Tao,[15] Lee,[16] Boothroyd, Martin, and Peterson[17] (BMP), and Bakr, Smith, and Patkowski[18] (BSP). In 1994 Tao[15] published 69 ground-state energies calculated with the complete fourth-order Møller-Plesset perturbation theory[19] (MP4) for the linear, bent, and T-shaped nuclear arrangements (θ = 0°, 45°, and 90°, respectively) for r = 1.449 a_0 at 15 values of R ranging from 2.0 to 15.0 a_0. For R = 3.0, 5.0, 6.5, and 8.0 a_0, calculations were also reported for H–H separations of r = 1.128 and 1.618 a_0. (Note that both of these additional r values are far from the vibrationally averaged H_2 bond length, r = 1.449 a_0*).* For r = 1.449 a_0, a ground-state van der Waals minimum of depth ε = 47.19 μE_h at R = 6.5 a_0 and θ = 0° was reported by Tao. These results cover much less of the nuclear configuration space than the current work.

In 2001 Lee[16] computed the CCSD(T) ground-state interaction energy at the complete basis set limit, with a correction to bring the result closer to that which would be obtained in an FCI calculation. Lee performed calculations only for ground-state van der Waals minimum, using the aug-cc-pV5Z and aug-ccpV6Z basis sets.[1,2] A two-point $1/ (X - 1)^3$ extrapolation scheme[20] was used to determine the CCSD(T) energy values at the complete basis set limit. Lee obtained an estimated FCI/complete basis set limit value for the CCSD(T) interaction energy at the ground-state van der Waals minimum of – 49.8 μE_h.

In the 2003 study by Boothroyd, Martin, and Peterson[17] (BMP), energies of the ground and first two excited singlet states were determined using Buenker's MRD-CI method.[13] In total, 23,703 energies were considered for "He–H_2 geometries where the interaction energy was expected to be non-negligible." A ground-state van der Waals minimum of depth $\varepsilon \sim 47$ μE_h located near R ~ 6.50 a_0 for r = 1.449 a_0 and linear H_2−He may be inferred from the results reported by BMP. For the ground state with the three nuclei in the T-shaped arrangement, a minimum was located at R ~ 6.35 a_0 for r = 1.449 a_0, and an interaction energy of approximately – 41.50 μE_h may be inferred from the BMP results.

The most recent *ab initio* potential energy surface study for the ground-state He–H_2 system was carried out in 2013 by Bakr, Smith, and Patkowski[18] (BSP). These authors found the energies for 1,900 ground-state geometrical points, specifically, those having r between 1.1 and 1.75 a_0, R from 3.5 to 15.0 a_0, and θ from 0° to 90° in ten-degree increments. This work is highly accurate, because it starts with the CCSD(T) method, but includes corrections for quadruple excitations, relativistic effects, and diagonal Born-Oppenheimer effects.

The calculations that we have carried out cover a greatly enlarged range of H–H bond lengths compared to both the BMP[17] and BSP[18] studies, ranging from r = 0.942 to 5.70 a_0, as well as an enlarged range of the separation R between the center of mass of the two H nuclei and the He nucleus, down to R = 0.25 a_0 out to 20.0 a_0 for most of the 14 r values studied. Having results for large r values is important in astrophysical applications, where transitions up to the H_2 vibrational quantum number v = 8 need to be included. Our angular step size ($\Delta\theta = 5°$) was smaller than that of both BMP (usually $\Delta\theta = 15°$) and BSP ($\Delta\theta = 10°$). This allows us to determine high-order anisotropies in the H_2–He potential. Bakr, Smith, and Patkowski provided results only for the isotropic potential $V_0(R)$ and the leading anisotropy $V_2(R)$.

We define two characteristic points as (R, r, θ) = (6.40 a_0, 1.448736 a_0, 0°) and (R, r, θ) = (6.30 a_0, 1.448736 a_0, 90°), the same points considered by BSP.[18] These two points are the linear (L) and T-shaped (T) arrangements, respectively. Table 3.2 gives the interaction energies obtained for these two characteristic points with the CCSD(T) and CR-CC(2,3) methods and the aug-cc-pVXZ (X = 4, 5)[1,2] basis sets. From Table 3.2 we see that the extension of the basis set has an opposite effect on the calculated interaction energies of these two points, for both the CCSD(T) and CR-CC(2,3). In both the L and T geometries the CR-CC(2,3) energies are lower than the CCSD(T) energies (i.e., they have larger negative values).

Table 3.2. Interaction energies obtained with the a4Z and a5Z bases for the two characteristic points (both r = 1.448736 a_0). Distances in a_0; energies in μE_h.

	Near-Minimum (6.40 a.u., 1.448736 a.u., 0°)		Near-Saddle Point (6.30 a.u., 1.448736 a.u., 90°)	
	X = Q	X = 5	X = Q	X = 5
CCSD(T)	-50.5735	-49.1594	-42.0256	-42.3840
CR-CC(2,3)	-51.3046	-49.7810	-42.6021	-42.8444

Tables 3.3 and 3.4 summarize results obtained for the ground-state minima occurring for the $C_{\infty v}$ (the van der Waals minimum) and the C_{2v} (i.e., T-shaped) nuclear geometries computed with the CR-CC(2,3) method and the aug-cc-pVXZ (X = 4, 5) basis sets. All results presented here were obtained with codes available in GAMESS.[21] Also included in Tables 3.3 and 3.4 are previously reported values from the literature for these two geometrical arrangements of H_2–He to allow comparisons with the results obtained in the current work. From Tables 3.3 and 3.4, it is evident that the linear geometry is favored over the T-shaped one near the van der Waals minimum of the ground-state, i.e., $\varepsilon(C_{\infty v}) > \varepsilon(C_{2v})$. Whether the linear or the T-shaped nuclear geometry is the one of lower energy at and near the minimum has been a subject of dispute in the past.

Table 3.3. Depth, ε_{vdW}, and location of the van der Waals well for the linear ($\theta = 0°$) case. (Results obtained in this thesis are printed in bold-faced type).

Reference	r / a_0	R / a_0	$\varepsilon_{vdW1} / \mu E_h$
Experimental			
Gengenbach and Hahn [1]	1.400	6.33	47.88
Riehl *et al*. [2]	1.400	6.40	72
Shafer and Gordon [3]	1.400	6.39	48.93
Theoretical			
Tsapline and Kutzelnigg [4]	1.406	6.50	66.50
Guerts *et al.* [5]	1.400	6.58	44.00
Römelt *et al*. [6]	1.4	6.4	66
Meyer *et al*. [7]	1.449	6.50	45.60
Senff and Burton [8]	1.449	6.50	43.18
Tao [9]	1.449	6.50	47.19
Lee [10]	1.449	6.50	47.4
Lee [11]	1.449	6.50	48.1
Lee [12]	1.449	6.50	46.7
Boothroyd *et al*. [13]	1.449	6.50	47.0
CR-CC(2,3) / a4Z	1.449	6.50	**51.018**
CR-CC(2.3) / a5Z	1.449	6.50	**48.933**
Bakr *et al.* [14]	1.448736	6.40	50.238
Bakr *et al.* [15]	1. 448736	6.40	50.257
CR-CC(2,3) / a4Z	1.448736	6.40	**51.305**
CR-CC(2,3) / a5Z	1.448736	6.40	**49.781**

[1] Empirical minimum of the spherically averaged potential of Ref. 22.
[2] Ref. [23].
[3] From an empirical potential that fir the experimental and theoretical data available at that time, Ref. [24].
[4] IEPA-PNO method of Ref. [10].
[5] Ref. [6].
[6] MRD-CI of Ref. [12].
[7] CI method of Ref. [14].
[8] SCF-(PNOCI-CEPA2) method of Ref. [25]
[9] MP4 of Ref. [15].
[10] CCSD(T) with a6Z basis. Counterpoise corrected. Uncorrected value: 48 μE_h. Ref. [16].
[11] Estimated CBS limit CCSD(T) interaction energy. Counterpoise corrected. Uncorrected value: 47 μE_h. Ref. [16].
[12] CCSD(T) with a5Z basis. Counterpoise corrected. Uncorrected value: 49 μE_h. Ref. [16].
[13] Estimated from the MRD-CI results presented in Ref. [17].
[14] 2-Body IE obtained with the "best" basis set combination used in Ref. [18].
[15] Obtained with the "production level" basis of Ref. [18].

Table 3.4. Location of the potential minimum for the T-shaped (θ = 0°) nuclear arrangement. (Our results are in bold).

Reference	r / a_0	R / a_0	$E_{int} / \mu E_h$
Experimental			
Gengenbach and Hahn [1]	1.400	6.25	50.50
Riehl *et al.* [2]		6.33	60.00
Theoretical			
Tsapline and Kutzelnigg [3]	1.406	6.29	44.33
Guerts *et al.* [4]	1.400	6.42	40.20
Guerts *et al.*	1.400	6.50	40.00
Römelt *et al.* [5]	1.400	6.50	45.00
Meyer *et al.* [6]	1.449	6.35	41.20
Senff and Burton [7]	1.449	6.40	38.34
Tao [8]	1.449	6.25	42.48
CR-CC(2,3) / a4Z	**1.449**	**6.25**	**41.881**
CR-CC(2,3) / a5Z	**1.449**	**6.25**	**42.263**
Boothroyd *et al.* [9]	1.449	6.35	41.50
CR-CC(2,3) / a4Z	**1.449**	**6.35**	**41.974**
CR-CC(2,3) / a5Z	**1.449**	**6.35**	**42.311**
Bakr *et al.* [10]	1.448736	6.30	45.022
Bakr *et al.* [11]	1.448736	6.30	45.038
CR-CC(2,3) / a5Z	**1.448736**	**6.30**	**42.844**

[1] Ref. [22].
[2] Ref. [23].
[3] IEPA-PNO method of Ref.[10].
[4] Ref. [6].
[5] MRD-CI result of Ref. [12].
[6] Ref. [14].
[7] SCF-(PNOCI-CEPA2) result of Ref. [25].
[8] MP4 result of Ref. [15].
[9] Estimated from the MRD-CI results presented in Ref. [17].
[10] 2-Body IE obtained with the "best" basis used in Ref. [18].
[11] Obtained with the "production level" basis set of Ref. [18].

REFERENCES

REFERENCES

1. T. H. Dunning Jr., *J. Chem. Phys*. **90**, 1007 (1989); D. E. Woon and T. H. Dunning Jr., *J. Chem. Phys*. **98**, 1358 (1993); *ibid*. **100**, 2975 (1994); K. A. Peterson, D. E. Woon, and T. H. Dunning Jr., *J. Chem. Phys*. **100**, 7410 (1994); A. Wilson, T. van Mourik, and T. H. Dunning Jr., *J. Mol. Struct*. (*Theochem*.) **388**, 339 (1997); A. Wilson, D. E. Woon, K. A. Peterson, and T. H. Dunning Jr., *J. Chem. Phys*. **110**, 7667 (1999).

2. Basis sets were obtained from the Extensible Computational Chemistry Environment Basis Set Database, as developed and distributed by the Molecular Science Computing Facility, Environmental and Molecular Sciences Laboratory which is part of the Pacific Northwest Laboratory, P.O. Box 999, Richland, WA 99352, USA, and funded by the US DOE.

3. C. S. Roberts, *Phys. Rev*. **131**, 209 (1963).

4. M. Karplus and H. J. Kolker, *J. Chem. Phys*. **41**, 3955 (1964).

5. M. Krauss and F. H. Mies, *J. Chem. Phys*. **42**, 2703 (1965).

6. P. J. M. Guerts, P. E. S. Wormer, and A. van der Avoird, *Chem. Phys. Lett*. **35**, 444 (1975).

7. K. T. Tang and J. P. Toennies, *J. Chem. Phys*. **66**, 1496 (1977).

8. K. T. Tang and J. P. Toennies, *J. Chem. Phys*. **68**, 5501 (1978).

9. M. D. Gordon and D. Secrest, *J. Chem. Phys*. **52**, 120 (1970).

10. B. Tsapline and W. Kutzelnigg*, Chem. Phys. Lett*. **23**, 173 (1973).

11. A. W. Raczkowski and W. A. Lester, Jr., *Chem. Phys. Lett*. **47**, 45 (1977).

12. J. Römelt, S. D. Peyerimhoff, and R. J. Buenker, *Chem. Phys*. **34**, 403 (1978).

13. R. J. Buenker and S. D. Peyerimhoff, *Theoret. Chim. Acta* **35**, 33 (1974); *ibid*. **39**, 217 (1975); R. J. Buenker, S. D. Peyerimhoff and W. Butscher, *Mol. Phys*. **35**, 771 (1978).

14. W. Meyer, P. C. Hariharan, and W. Kutzelnigg, *J. Chem. Phys*. **73**, 1880 (1980).

15. F.-M. Tao, *J. Chem. Phys*. **100**, 4947 (1994).

16. J. S. Lee, *Chem. Phys. Lett*. **339**, 133 (2001).

17. A. I. Boothroyd, P. G. Martin, and M. R. Peterson, *J. Chem. Phys*. **119**, 3187 (2003).

18. B. W. Bakr, D. G. A. Smith, and K. Patkowski, *J. Chem. Phys*. **139**, 144305 (2013).

19. C. Møller and M. S. Plesset, *Phys. Rev*. **46**, 618 (1934); J. A. Pople, P. Krishnan, H. B. Schlegel, and J. S. Binkley, *Int. J. Quant. Chem. Symp*. **13**, 325 (1979).

20. C. Schwartz, *Phys. Rev*. **126**, 1015 (1962); R. N. Hill, *J. Chem. Phys*. **83**, 1173 (1985); W. Kutzelnigg and J. D. Morgan III, *J. Chem. Phys*. **96**, 4484 (1992).

21. M. W. Schmidt, K. K. Baldridge, J. A. Boatz, S. T. Elbert, M. S. Gordon, J. H. Jensen, S. Koseki, N. Matsunaga, K. A. Nguyen, S. Su, T. L. Windus, M. Dupuis, and J. A. Montgomery, *J. Comput. Chem*. **14**, 1347 (1993); M. S. Gordon and M. W. Schmidt, pp. 1167-1189, in "*Theory and Applications of Computational Chemistry: the first forty years*," C. E. Dykstra, G. Frenking, K. S. Kim, G. E. Scuseria (editors), Elsevier, Amsterdam, 2005.

22. R. Gengenbach and Ch. Hahn, *Chem. Phys. Lett*. **15**, 604 (1972).

23. J. W. Riehl, J. L. Kinsey, J. S. Waugh, and J. H. Rugheimer, *J. Chem. Phys*. **49**, 5269 (1968); *ibid*. 5276 (1968); J. W. Riehl, C. J. Fisher, J. D. Baloga, and J. L. Kinsey, *J. Chem. Phys*. **58**, 4571 (1973).

24. R. Shafer and R. G. Gordon, *J. Chem. Phys*. **58**, 5422 (1973).

25. U. E. Senff and P. G. Burton, *J. Phys. Chem*. **86**, 1053 (1982).

CHAPTER 4: Electronic Ground-State Potential of H_2−He for $r_{H–H}$ = 1.449 a.u.

In this chapter, the CR-CC(2,3)[1] results for the ground-state potential energy of H_2–He are presented and analyzed for r = 1.449 a.u., the average H–H separation in the ground vibrational state. The results presented here have been obtained with an aug-cc-pV5Z basis,[2] although results have also been obtained with an aug-cc-pvQZ[2] basis to permit an extrapolation to the full basis set limit in the future.

The geometry used in the calculations on the H_2−He system has been specified in Figure 3.1. The vector R between the center of mass of the H_2 molecule and the He nucleus defines the z axis of the system. Points on the potential surface are identified by three variables: the H_2 bond length r (which is fixed at 1.449 a.u. in this chapter) the distance R from the center of mass of the H_2 molecule to the helium nucleus, and the angle θ between R and a vector r along the H_2 bond vector. Thus, a point on the potential energy surface can be characterized by an ordered set of three coordinates, (R, r, θ), and we will use this notation henceforth. The distances R and r are given in atomic units of length (bohr, $a_0 = 5.2917721067 \cdot 10^{-11}$ m = 0.52917721067 Å), the angle θ in degrees, and the energies in atomic units (Hartree, $E_h = 4.35974417 \cdot 10^{-18}$ J = 27.211385 eV). An energy of one Hartree corresponds to 627.509 kcal mol^{-1}.

The computed energies for 49 values of R, ranging from 2.20 a.u. to 20.0 a.u. are listed in Table 4.1, as a function of θ from 0º to 90º in intervals of 5º. The R values start when the distance between the He nucleus and the nearest H nucleus exceeds the H–H distance of 1.449 a.u. The energies have also been computed for smaller R values, which corresponds to H−HHe, and at R values such that the helium nucleus lands between the H nuclei. In the course of analyzing the potential, additional sets of energy values were determined as a function of θ for R = 13.0 a.u., 15.0 a.u.,16.0 a.u., 30.0 a.u., and 60.0 a.u.

Table 4.1. CR-CC(2,3) energies of H_2–He for r_{H-H} = 1.449 a_0 obtained with an aug-cc-pV5Z basis, as a function of the separation R between the center of mass of the two H nuclei and the He nucleus, and the angle θ between the H–H vector and the z axis. The He atom is located along the z axis. Entries in blue denote the maximum and entries in bold black denote the minimum of the potential, as a function of the angle θ for each R value.

	R (in a.u.)				
θ (degs)	2.20	2.40	2.60	2.80	3.00
0	**-3.9334506334**	**-3.9770441326**	**-4.0073917582**	**-4.0287260484**	**-4.0437347782**
5	-3.9339558651	-3.9773543934	-4.0075951206	-4.0288639232	-4.0438293187
10	-3.9354295745	-3.9782650891	-4.0081942439	-4.0292709833	-4.0441096150
15	-3.9377490106	-3.9797143949	-4.0091538097	-4.0299257651	-4.0445616941
20	-3.9407360744	-3.9816088601	-4.0104202131	-4.0307944802	-4.0451635525
25	-3.9441884219	-3.9838381250	-4.0119273936	-4.0318352431	-4.0458873460
30	-3.9479072646	-3.9862883598	-4.0136044712	-4.0330019026	-4.0467019975
35	-3.9517164750	-3.9888517735	-4.0153809838	-4.0342466926	-4.0475747941
40	-3.9554721915	-3.9914322191	-4.0171913720	-4.0355238534	-4.0484738993
45	-3.9590646271	-3.9939491693	-4.0189768680	-4.0367914897	-4.0493692521
50	-3.9624128416	-3.9963362482	-4.0206869701	-4.0380122322	-4.0502340131
55	-3.9654589192	-3.9985406517	-4.0222793310	-4.0391540048	-4.0510447147
60	-3.9681610047	-4.0005205862	-4.0237189909	-4.0401898919	-4.0517816185
65	-3.9704888982	-4.0022433873	-4.0249782369	-4.0410983544	-4.0524289302
70	-3.9724201196	-4.0036834349	-4.0260350383	-4.0418623603	-4.0529738474
75	-3.9739382336	-4.0048217767	-4.0268728211	-4.0424689682	-4.0534069231
80	-3.9750312580	-4.0056445248	-4.0274795198	-4.0429087776	-4.0537211832
85	-3.9756906610	-4.0061423428	-4.0278471176	-4.0431754265	-4.0539117659
90	**-3.9759114803**	**-4.0063091379**	**-4.0279709112**	**-4.0432653625**	**-4.0539760072**

Table 4.1 (cont'd).

	R (in a.u.)				
θ (degs)	3.50	4.00	4.50	5.00	5.50
0	**-4.0643558208**	**-4.0725129297**	**-4.0755772672**	**-4.0766559620**	**-4.0770016802**
5	-4.0643930441	-4.0725267216	-4.0755822328	-4.0766574704	-4.0770019803
10	-4.0645033600	-4.0725683157	-4.0755966016	-4.0766618773	-4.0770029813
15	-4.0646818047	-4.0726354571	-4.0756199134	-4.0766690295	-4.0770046279
20	-4.0649202721	-4.0727252846	-4.0756510663	-4.0766786753	-4.0770068834
25	-4.0652082566	-4.0728337935	-4.0756887927	-4.0766903725	-4.0770096430
30	-4.0655337045	-4.0729566198	-4.0757316246	-4.0767036683	-4.0770128130
35	-4.0658837589	-4.0730887774	-4.0757777178	-4.0767178757	-4.0770161735
40	-4.0662456094	-4.0732255131	-4.0758253136	-4.0767325578	-4.0770196876
45	-4.0666070967	-4.0733623149	-4.0758729318	-4.0767472967	-4.0770231776
50	-4.0669571172	-4.0734947026	-4.0759190491	-4.0767614860	-4.0770265357
55	-4.0672859765	-4.0736190201	-4.0759624278	-4.0767748336	-4.0770296487
60	-4.0675853830	-4.0737322583	-4.0760018613	-4.0767870021	-4.0770325434
65	-4.0678486110	-4.0738316738	-4.0760364958	-4.0767976688	-4.0770350584
70	-4.0680705473	-4.0739155506	-4.0760656193	-4.0768066307	-4.0770371361
75	-4.0682469216	-4.0739820686	-4.0760887423	-4.0768137388	-4.0770387532
80	-4.0683749361	-4.0740302796	-4.0761055105	-4.0768188896	-4.0770399159
85	-4.0684527878	-4.0740596571	-4.0761156528	-4.0768219956	-4.0770406162
90	**-4.0684788907**	**-4.0740695984**	**-4.0761191555**	**-4.0768231121**	**-4.0770409224**

Table 4.1 (cont'd).

	R (in a.u.)				
θ (degs)	6.00	6.05	6.10	6.15	6.20
0	-4.0770937320	**-4.0770970105**	**-4.0770996521**	**-4.0771017389**	**-4.0771033324**
5	-4.0770936944	-4.0770969582	-4.0770995815	-4.0771016530	-4.0771032405
10	-4.0770936101	-4.0770968368	-4.0770994364	-4.0771014790	-4.0771030433
15	-4.0770935723	-4.0770967194	-4.0770992466	-4.0771012185	-4.0771027484
20	**-4.0770935418**	-4.0770965969	-4.0770990549	-4.0771009837	-4.0771024497
25	-4.0770936087	-4.0770965444	-4.0770988963	-4.0771007247	-4.0771021328
30	-4.0770937139	-4.0770964900	-4.0770987382	-4.0771004893	-4.0771018044
35	-4.0770938005	-4.0770964687	-4.0770985876	-4.0771002307	-4.0771014582
40	-4.0770939212	-4.0770964338	-4.0770984279	-4.0770999677	-4.0771011087
45	-4.0770940308	-4.0770963994	-4.0770982693	-4.0770997028	-4.0771007560
50	-4.0770941409	-4.0770963703	-4.0770981233	-4.0770994531	-4.0771004195
55	-4.0770942216	-4.0770963194	-4.0770979565	-4.0770991913	-4.0771000785
60	-4.0770942932	-4.0770962636	-4.0770977935	-4.0770989373	-4.0770997438
65	-4.0770943275	-4.0770961897	-4.0770976262	-4.0770986899	-4.0770994286
70	**-4.0770943393**	-4.0770961113	-4.0770974695	-4.0770984657	-4.0770991461
75	-4.0770943274	-4.0770960281	-4.0770973221	-4.0770982608	-4.0770988944
80	-4.0770942943	-4.0770959497	-4.0770971944	-4.0770981163	-4.0770987309
85	-4.0770942993	**-4.0770959175**	**-4.0770971514**	**-4.0770980398**	-4.0770986297
90	-4.0770943350	-4.0770959444	-4.0770971643	-4.0770980432	**-4.0770986248**

Table 4.1 (cont'd).

	R (in a.u.)				
θ (degs)	6.25	6.30	6.35	6.40	6.45
0	**-4.0771045048**	**-4.0771053050**	**-4.0771057835**	**-4.0771059843**	**-4.0771059435**
5	-4.0771044053	-4.0771052018	-4.0771056768	-4.0771058748	-4.0771058324
10	-4.0771041869	-4.0771049571	-4.0771054280	-4.0771056159	-4.0771055657
15	-4.0771038669	-4.0771046228	-4.0771050660	-4.0771052380	-4.0771051759
20	-4.0771035118	-4.0771042224	-4.0771046344	-4.0771047890	-4.0771047143
25	-4.0771031429	-4.0771038100	-4.0771041816	-4.0771042980	-4.0771041956
30	-4.0771027438	-4.0771033540	-4.0771036806	-4.0771037622	-4.0771036331
35	-4.0771023282	-4.0771028837	-4.0771031615	-4.0771032041	-4.0771030454
40	-4.0771019039	-4.0771023980	-4.0771026307	-4.0771026369	-4.0771024478
45	-4.0771014781	-4.0771019112	-4.0771020937	-4.0771020596	-4.0771018392
50	-4.0771010671	-4.0771014377	-4.0771015681	-4.0771014908	-4.0771012350
55	-4.0771006381	-4.0771009637	-4.0771010489	-4.0771009351	-4.0771006509
60	-4.0771002568	-4.0771005152	-4.0771005525	-4.0771004019	-4.0771000887
65	-4.0770998848	-4.0771000962	-4.0771000957	-4.0770999132	-4.0770995738
70	-4.0770995526	-4.0770997218	-4.0770996869	-4.0770994763	-4.0770991148
75	-4.0770992663	-4.0770994107	-4.0770993570	-4.0770991312	-4.0770987573
80	-4.0770990809	-4.0770992027	-4.0770991278	-4.0770988840	-4.0770984953
85	-4.0770989603	-4.0770990673	-4.0770989820	-4.0770987303	-4.0770983347
90	**-4.0770989479**	**-4.0770990470**	**-4.0770989529**	**-4.0770986929**	**-4.0770982913**

Table 4.1 (cont'd).

	R (in a.u.)				
θ (degs)	6.50	6.55	6.60	6.65	6.70
0	**-4.0771056960**	**-4.0771052729**	**-4.0771047021**	**-4.0771040086**	**-4.0771032131**
5	-4.0771055841	-4.0771051614	-4.0771045920	-4.0771038996	-4.0771031043
10	-4.0771053125	-4.0771048871	-4.0771043156	-4.0771036213	-4.0771028248
15	-4.0771049133	-4.0771044804	-4.0771039074	-4.0771032175	-4.0771024251
20	-4.0771044403	-4.0771040008	-4.0771034222	-4.0771027265	-4.0771019324
25	-4.0771039053	-4.0771034551	-4.0771028697	-4.0771021706	-4.0771013781
30	-4.0771033232	-4.0771028598	-4.0771022665	-4.0771015642	-4.0771007712
35	-4.0771027139	-4.0771022357	-4.0771016332	-4.0771009270	-4.0771001348
40	-4.0771020922	-4.0771015960	-4.0771009812	-4.0771002669	-4.0770994703
45	-4.0771014596	-4.0771009447	-4.0771003162	-4.0770995933	-4.0770987924
50	-4.0771008265	-4.0771002910	-4.0770996534	-4.0770989260	-4.0770981203
55	-4.0771002216	-4.0770996693	-4.0770990135	-4.0770982715	-4.0770974585
60	-4.0770996370	-4.0770990679	-4.0770984001	-4.0770976498	-4.0770968320
65	-4.0770991006	-4.0770985167	-4.0770978388	-4.0770970820	-4.0770962567
70	-4.0770986256	-4.0770980327	-4.0770973499	-4.0770965897	-4.0770957676
75	-4.0770982575	-4.0770976517	-4.0770969579	-4.0770961913	-4.0770953640
80	-4.0770979838	-4.0770973687	-4.0770966676	-4.0770958962	-4.0770950678
85	-4.0770978166	-4.0770971961	-4.0770964908	-4.0770957160	-4.0770948859
90	**-4.0770977696**	**-4.0770971470**	**-4.0770964402**	**-4.0770956644**	**-4.0770948324**

Table 4.1 (cont'd).

	R (in a.u.)				
θ (degs)	6.75	6.80	6.90	7.00	7.10
0	**-4.0771023333**	**-4.0771013850**	**-4.0770993371**	**-4.0770971608**	**-4.0770949263**
5	-4.0771022237	-4.0771012778	-4.0770992332	-4.0770970587	-4.0770948192
10	-4.0771019429	-4.0771010013	-4.0770989621	-4.0770967933	-4.0770945730
15	-4.0771015443	-4.0771006034	-4.0770985729	-4.0770964261	-4.0770942247
20	-4.0771010583	-4.0771001204	-4.0770981038	-4.0770959710	-4.0770937928
25	-4.0771005087	-4.0770995773	-4.0770975755	-4.0770954632	-4.0770933029
30	-4.0770999055	-4.0770989811	-4.0770970020	-4.0770949163	-4.0770927776
35	-4.0770992718	-4.0770983520	-4.0770963876	-4.0770943150	-4.0770921887
40	-4.0770986071	-4.0770976897	-4.0770957337	-4.0770936737	-4.0770915739
45	-4.0770979283	-4.0770970123	-4.0770950636	-4.0770930224	-4.0770909544
50	-4.0770972514	-4.0770963334	-4.0770943941	-4.0770923771	-4.0770903374
55	-4.0770965876	-4.0770956719	-4.0770937465	-4.0770917497	-4.0770897343
60	-4.0770959594	-4.0770950441	-4.0770931297	-4.0770911533	-4.0770891605
65	-4.0770953887	-4.0770944776	-4.0770925712	-4.0770906065	-4.0770886318
70	-4.0770948950	-4.0770939824	-4.0770920784	-4.0770901242	-4.0770881652
75	-4.0770944908	-4.0770935753	-4.0770916725	-4.0770897283	-4.0770877822
80	-4.0770941907	-4.0770932718	-4.0770913762	-4.0770894394	-4.0770875012
85	-4.0770940056	-4.0770930954	-4.0770912045	-4.0770892698	-4.0770873351
90	**-4.0770939559**	**-4.0770930451**	**-4.0770911553**	**-4.0770892216**	**-4.0770872888**

Table 4.1 (cont'd).

	R (in a.u.)				
θ (degs)	7.20	7.30	7.40	7.50	7.60
0	**-4.0770926832**	**-4.0770904654**	**-4.0770883054**	**-4.0770862209**	**-4.0770842276**
5	-4.0770925766	-4.0770903819	-4.0770882307	-4.0770861500	-4.0770841604
10	-4.0770923515	-4.0770901647	-4.0770880251	-4.0770859558	-4.0770839798
15	-4.0770920226	-4.0770898499	-4.0770877264	-4.0770856741	-4.0770837188
20	-4.0770916132	-4.0770894601	-4.0770873522	-4.0770853277	-4.0770833947
25	-4.0770911388	-4.0770890099	-4.0770869288	-4.0770849306	-4.0770830230
30	-4.0770906254	-4.0770885128	-4.0770864660	-4.0770844980	-4.0770826173
35	-4.0770900654	-4.0770879909	-4.0770859782	-4.0770840392	-4.0770821847
40	-4.0770894892	-4.0770874484	-4.0770854684	-4.0770835609	-4.0770817315
45	-4.0770889017	-4.0770868909	-4.0770849421	-4.0770830689	-4.0770812661
50	-4.0770883129	-4.0770863306	-4.0770844115	-4.0770825704	-4.0770807994
55	-4.0770877365	-4.0770857832	-4.0770838944	-4.0770820842	-4.0770803439
60	-4.0770871880	-4.0770852626	-4.0770834031	-4.0770816223	-4.0770799106
65	-4.0770866815	-4.0770847811	-4.0770829488	-4.0770811939	-4.0770795105
70	-4.0770862340	-4.0770843549	-4.0770825456	-4.0770808140	-4.0770791594
75	-4.0770858656	-4.0770840024	-4.0770822091	-4.0770804877	-4.0770788759
80	-4.0770855942	-4.0770837417	-4.0770819572	-4.0770802539	-4.0770786599
85	-4.0770854332	-4.0770835871	-4.0770818108	-4.0770801104	-4.0770785167
90	**-4.0770853892**	**-4.0770835446**	**-4.0770817736**	**-4.0770800855**	**-4.0770784884**

Table 4.1 (cont'd).

	R (in a.u.)				
θ (degs)	7.70	7.80	7.90	8.00	8.50
0	**-4.0770823363**	**-4.0770805497**	**-4.0770788698**	**-4.0770772966**	**-4.0770709414**
5	-4.0770822740	-4.0770804928	-4.0770788168	-4.0770772472	-4.0770709085
10	-4.0770821065	-4.0770803362	-4.0770786710	-4.0770771119	-4.0770708180
15	-4.0770818626	-4.0770801082	-4.0770784593	-4.0770769165	-4.0770706830
20	-4.0770815592	-4.0770798260	-4.0770781975	-4.0770766738	-4.0770705149
25	-4.0770812122	-4.0770795026	-4.0770778972	-4.0770763953	-4.0770703221
30	-4.0770808323	-4.0770791491	-4.0770775693	-4.0770760915	-4.0770701109
35	-4.0770804271	-4.0770787734	-4.0770772214	-4.0770757690	-4.0770698839
40	-4.0770800059	-4.0770783836	-4.0770768593	-4.0770754320	-4.0770696472
45	-4.0770795778	-4.0770779842	-4.0770764866	-4.0770750849	-4.0770694067
50	-4.0770791446	-4.0770775796	-4.0770761099	-4.0770747351	-4.0770691672
55	-4.0770787167	-4.0770771817	-4.0770757405	-4.0770743926	-4.0770689350
60	-4.0770783107	-4.0770768042	-4.0770753904	-4.0770740686	-4.0770687178
65	-4.0770779387	-4.0770764586	-4.0770750704	-4.0770737727	-4.0770685202
70	-4.0770776119	-4.0770761543	-4.0770747879	-4.0770735114	-4.0770683469
75	-4.0770773435	-4.0770759036	-4.0770745554	-4.0770732965	-4.0770682051
80	-4.0770771421	-4.0770757163	-4.0770743816	-4.0770731358	-4.0770681003
85	-4.0770770153	-4.0770756001	-4.0770742751	-4.0770730384	-4.0770680382
90	**-4.0770769831**	**-4.0770755695**	**-4.0770730115**	**-4.0770730115**	**-4.0770680210**

Table 4.1 (cont'd).

	R (in a.u.)				
θ (degs)	9.00	9.50	10.0	10.5	11.0
0	**-4.0770666327**	**-4.0770637000**	**-4.0770616711**	**-4.0770602498**	**-4.0770592485**
5	-4.0770666084	-4.0770636829	-4.0770616570	-4.0770602388	-4.0770592403
10	-4.0770665441	-4.0770636398	-4.0770616257	-4.0770602164	-4.0770592219
15	-4.0770664488	-4.0770635693	-4.0770615775	-4.0770601809	-4.0770591938
20	-4.0770663289	-4.0770634862	-4.0770615154	-4.0770601349	-4.0770591576
25	-4.0770661896	-4.0770633843	-4.0770614420	-4.0770600805	-4.0770591154
30	-4.0770660355	-4.0770632713	-4.0770613601	-4.0770600203	-4.0770590691
35	-4.0770658715	-4.0770631511	-4.0770612726	-4.0770599559	-4.0770590204
40	-4.0770657024	-4.0770630276	-4.0770611821	-4.0770598894	-4.0770589705
45	-4.0770655326	-4.0770629044	-4.0770610914	-4.0770598220	-4.0770589201
50	-4.0770653663	-4.0770627842	-4.0770610024	-4.0770597554	-4.0770588700
55	-4.0770652075	-4.0770626697	-4.0770609173	-4.0770596910	-4.0770588213
60	-4.0770650601	-4.0770625636	-4.0770608383	-4.0770596306	-4.0770587751
65	-4.0770649263	-4.0770624680	-4.0770607668	-4.0770595757	-4.0770587327
70	-4.0770648093	-4.0770623845	-4.0770607047	-4.0770595280	-4.0770586957
75	-4.0770647135	-4.0770623161	-4.0770606537	-4.0770594891	-4.0770586651
80	-4.0770646430	-4.0770622657	-4.0770606157	-4.0770594606	-4.0770586426
85	-4.0770646013	-4.0770622358	-4.0770605930	-4.0770594431	-4.0770586287
90	**-4.0770645894**	**-4.0770622271**	**-4.0770605862**	**-4.0770594377**	**-4.0770586244**

Table 4.1 (cont'd).

	R (in a.u.)			
θ (degs)	12.0	14.0	17.0	20.0
0	**-4.0770579976**	**-4.0770568779**	**-4.0770564003**	**-4.0770562747**
5	-4.0770579928	-4.0770568766	-4.0770564000	**-4.0770562747**
10	-4.0770579803	-4.0770568732	-4.0770563992	-4.0770562744
15	-4.0770579611	-4.0770568678	-4.0770563980	-4.0770562740
20	-4.0770579369	-4.0770568607	-4.0770563964	-4.0770562735
25	-4.0770579093	-4.0770568523	-4.0770563944	-4.0770562729
30	-4.0770578798	-4.0770568428	-4.0770563920	-4.0770562722
35	-4.0770578498	-4.0770568326	-4.0770563894	-4.0770562714
40	-4.0770578196	-4.0770568220	-4.0770563867	-4.0770562705
45	-4.0770577898	-4.0770568107	-4.0770563839	-4.0770562696
50	-4.0770577608	-4.0770567997	-4.0770563810	-4.0770562687
55	-4.0770577327	-4.0770567892	-4.0770563783	-4.0770562679
60	-4.0770577057	-4.0770567791	-4.0770563757	-4.0770562670
65	-4.0770576810	-4.0770567701	-4.0770563734	-4.0770562663
70	-4.0770576588	-4.0770567621	-4.0770563714	-4.0770562657
75	-4.0770576401	-4.0770567557	-4.0770563698	-4.0770562652
80	-4.0770576260	-4.0770567509	-4.0770563686	-4.0770562648
85	-4.0770576172	-4.0770567479	-4.0770563679	-4.0770562646
90	**-4.0770576144**	**-4.0770567469**	**-4.0770563676**	**-4.0770562645**

The Patkowski group[3] has previously computed the energies at 10º intervals and determined the isotropic potential $V_0(R)$ and the leading term in the anisotropy $V_2(R)$. The inclusion of more angles in the current study permits us to obtain higher anisotropies in the potential.

From the results in Table 4.1, we determined the isotropic potential and the anisotropies of the potential, as characterized by their dependence on the Legendre polynomials of the cosine of the angle θ. We expressed the potential as a series in the spherical harmonics of the orientation angles of H_2 and the orientation angles of the intermolecular vector R, which is fixed along the z axis in the current case. There are two potential sources of angular momentum that need to be coupled at the current stage of the calculation: rotation of the H_2 molecule about its center of mass and rotation of the vector R. The Clebsch-Gordan coefficient $\langle j_1\ m_1\ j_2\ m_2 \mid j_3\ m_3 \rangle$ accomplishes the coupling of the systems 1 and 2 with angular momentum quantum numbers j_1 and j_2, and projections m_1 and m_2 of the angular momentum on the z axis, to give the net angular momentum quantum number j_3 and projection m_3. The two angular momenta must be coupled to give a scalar, since the energy is a scalar. Therefore, $j_3 = m_3 = 0$, and the potential can be cast in the form

$$V(R, \theta) = \sum_{\substack{j_1\ ,\ j_2, \\ m_1,\ m_2 = 0}}^{\infty} \langle j_1\ m_1\ j_2\ m_2 \mid 0\ 0 \rangle\ c_j(R)\ Y_{j_1}^{m_1}(\theta, \varphi)\ Y_{j_2}^{m_2}(\theta_R, \varphi_R)\ . \tag{4.1}$$

The complex is planar, so $\varphi = \varphi_R = 0$. The vector R runs along the z axis, so θ_R is also zero for the spherical harmonic of the angles of R. The spherical harmonic $Y_{j_2}^{m_2}(\theta_R, \varphi_R)$ is non-zero only if $m_2 = 0$. Since (j_1, m_1) and (j_2, m_2) couple to give (0, 0), we must have $m_1 = -m_2$. Therefore, $m_1 = 0$ also. Additionally, we must have $j_1 = j_2$. This simplifies the series in the spherical harmonics to the form

$$V(R, \theta) = \sum_{j\ =\ 0}^{\infty} \langle j\ 0\ j\ 0 \mid 0\ 0 \rangle\ c_j(R)\ Y_j^0(\theta, \varphi)\ Y_j^0\ (0, 0)\ . \tag{4.2}$$

In Eq. (4.2), θ, φ refer to the orientation angles of H_2 relative to the z axis in the complex. Additionally, because of the symmetry of H_2, the angular momentum quantum numbers j must be

even. The coefficient $c_0(R)$ characterizes the isotropic potential, $c_2(R)$ gives the leading anisotropy, and $c_4(R)$, $c_6(R)$, $c_8(R)$ . . . give the higher-order anisotropies. In this work we have truncated the series at $j = 10$ and determined the c_j coefficients using a Mathematica[4] fitting routine. A sample program is provided in the Appendix.

The results for the c_j coefficients for $r = 1.449$ a.u. are listed as functions of R in Table 4.2. As expected, the isotropic coefficients c_0 are the largest, and the c_2 coefficients are the next largest. The coefficients c_{10} are the smallest, also as expected.

First, we analyzed the isotropic potential $V_0(R)$, which is derived from the spherical expansion coefficients $c_0(R)$. The Clebsch-Gordan coefficient $\langle\, 0\,0\,0\,0 \mid 0\,0 \,\rangle = 1$, and the spherical harmonics $Y_0^0(\theta, \varphi)$ are both equal to $1/(4\pi)^{1/2}$. Therefore, the isotropic potential is given by $V_0(R) = c_0(R)/(4\pi)$. We used the Mathematica[4] command Interpolation to generate the isotropic potential $V_0(R)$ from the values of $c_0(R)/(4\pi)$, for each intermolecular separation R. The isotropic potential $V_0(R)$ is plotted in Figure 4.1, along with the original *ab initio* points.

We tested the use of a Lennard-Jones potential as an approximation for $V_0(R)$. It is worth emphasizing that this potential has no arbitrary adjustable parameters. The Lennard-Jones potential is given by

$$V_{LJ}(R) = 4\varepsilon \left[(\sigma/R)^{12} - (\sigma/R)^{6} \right] , \tag{4.3}$$

where ε is the well depth (with a positive sign) and σ is the R value of the intermolecular separation where the potential is equal to zero.

Table 4.2. Spherical harmonic coefficients from the Mathematica fit to the ground-state potential of H_2–He with an H–H separation r = 1.449 a_0.

R	2.20	2.40	2.60	2.80	3.00
c_0	1.42021E+00	9.90896E-01	6.94498E-01	4.80278E-01	3.29536E-01
c_2	1.46845E-01	1.05961E-01	7.38189E-02	5.25309E-02	3.71505E-02
c_4	1.53753E-02	1.15773E-02	4.71380E-03	2.93397E-03	1.91222E-03
c_6	2.32752E-03	-5.36661E-03	4.26080E-04	2.01090E-04	1.03026E-04
c_8	3.20953E-04	2.95848E-03	4.23680E-05	1.51607E-05	4.11595E-06
c_{10}	4.18042E-05	7.22939E-04	4.51034E-06	2.13185E-06	8.00173E-07

R	3.50	4.00	4.50	5.00	5.50
c_0	1.23800E-01	4.35812E-02	1.38815E-02	3.57881E-03	3.44861E-04
c_2	1.50129E-02	5.67227E-03	1.97508E-03	6.09104E-04	1.43443E-04
c_4	7.13982E-04	2.68914E-04	9.39776E-05	2.95798E-05	7.54115E-06
c_6	2.60932E-05	7.28731E-06	1.84683E-06	6.45085E-07	-2.14177E-07
c_8	-1.11223E-06	-6.62775E-07	-2.24047E-07	-1.34522E-07	-8.34376E-08
c_{10}	-2.11308E-07	2.92011E-08	-1.36093E-07	-2.16046E-07	-2.05854E-07

Table 4.2 (cont'd).

R	6.00	6.05	6.10	6.15	6.20
c_0	-4.75829E-04	-5.02533E-04	-5.23405E-04	-5.39167E-04	-5.50487E-04
c_2	3.16338E-06	-2.91429E-06	-8.13605E-06	-1.25333E-05	-1.62801E-05
c_4	6.29629E-07	3.48045E-07	1.23002E-07	-5.66960E-08	-2.10985E-07
c_6	-5.93734E-07	-6.17210E-07	-6.14661E-07	-5.99059E-07	-5.93615E-07
c_8	-2.03646E-07	-2.28910E-07	-2.41889E-07	-2.62471E-07	-2.70187E-07
c_{10}	-1.70977E-07	-1.49668E-07	-1.26952E-07	-1.32703E-07	-1.01331E-07

R	6.25	6.30	6.35	6.40	6.45
c_0	-5.57907E-04	-5.61982E-04	-5.63133E-04	-5.61768E-04	-5.58240E-04
c_2	-1.94155E-05	-2.20059E-05	-2.41317E-05	-2.58477E-05	-2.72071E-05
c_4	-3.46687E-07	-4.13355E-07	-4.77550E-07	-5.19206E-07	-5.38664E-07
c_6	-5.67044E-07	-5.61950E-07	-5.56741E-07	-5.49652E-07	-5.38307E-07
c_8	-2.66292E-07	-2.78843E-07	-2.84369E-07	-2.82499E-07	-2.77282E-07
c_{10}	-1.04568E-07	-9.24473E-08	-8.15795E-08	-7.32766E-08	-6.97266E-08

Table 4.2 (cont'd).

R	6.50	6.55	6.60	6.65	6.70
c_0	-5.52864E-04	-5.45935E-04	-5.37705E-04	-5.28384E-04	-5.18158E-04
c_2	-2.82533E-05	-2.90277E-05	-2.95728E-05	-2.99208E-05	-3.00964E-05
c_4	-5.38167E-07	-5.21197E-07	-4.89638E-07	-4.53407E-07	-4.17505E-07
c_6	-5.24425E-07	-5.13471E-07	-5.03756E-07	-4.89763E-07	-4.64975E-07
c_8	-2.70700E-07	-2.57766E-07	-2.49266E-07	-2.46220E-07	-2.47424E-07
c_{10}	-7.27061E-08	-8.10507E-08	-8.56318E-08	-8.82705E-08	-9.49223E-08

R	6.75	6.80	6.90	7.00	7.10
c_0	-5.07207E-04	-4.95673E-04	-4.71405E-04	-4.46240E-04	-4.20823E-04
c_2	-3.01230E-05	-3.00400E-05	-2.95378E-05	-2.86974E-05	-2.76136E-05
c_4	-3.68002E-07	-3.24299E-07	-2.45967E-07	-1.91291E-07	-1.46011E-07
c_6	-4.46435E-07	-4.26885E-07	-3.93468E-07	-3.81922E-07	-4.00944E-07
c_8	-2.35282E-07	-2.35989E-07	-2.27585E-07	-1.94153E-07	-1.71244E-07
c_{10}	-1.14064E-07	-1.18411E-07	-1.28292E-07	-1.28366E-07	-9.81986E-08

Table 4.2 (cont'd).

R	7.20	7.30	7.40	7.50	7.60
c_0	-3.95638E-04	-3.71044E-04	-3.47263E-04	-3.24454E-04	-3.02718E-04
c_2	-2.63768E-05	-2.50552E-05	-2.36546E-05	-2.22477E-05	-2.07941E-05
c_4	-1.02947E-07	-6.33427E-08	-9.67331E-09	3.82740E-08	-5.30647E-08
c_6	-4.23439E-07	-4.27658E-07	-4.17420E-07	-4.04157E-07	-3.30036E-07
c_8	-1.64358E-07	-1.57371E-07	-1.51836E-07	-1.43912E-07	-1.17777E-07
c_{10}	-6.29327E-08	-5.28398E-08	-6.33331E-08	-5.69597E-08	-6.70584E-08

R	7.70	7.80	7.90	8.00	8.50
c_0	-2.82243E-04	-2.62955E-04	-2.44861E-04	-2.27946E-04	-1.59501E-04
c_2	-1.93866E-05	-1.80359E-05	-1.67459E-05	-1.55241E-05	-1.05697E-05
c_4	-4.17076E-08	-3.66550E-08	-4.08431E-08	-5.18887E-08	-1.58310E-07
c_6	-3.19002E-07	-2.94795E-07	-2.65510E-07	-2.36573E-07	-1.34387E-07
c_8	-1.22023E-07	-1.17870E-07	-1.09261E-07	-9.89791E-08	-5.65297E-08
c_{10}	-4.97946E-08	-4.83122E-08	-4.86075E-08	-4.70809E-08	-2.76841E-08

Table 4.2 (cont'd).

R	9.00	9.50	10.00	10.50	11.00
c_0	-1.12709E-04	-8.07708E-05	-5.86676E-05	-4.31889E-05	-3.22201E-05
c_2	-7.34582E-06	-5.30564E-06	-3.92023E-06	-2.94542E-06	-2.24887E-06
c_4	-2.14323E-07	-1.74391E-07	-1.04975E-07	-5.43184E-08	-3.30974E-08
c_6	-9.90016E-08	-6.56622E-08	-4.54164E-08	-3.39722E-08	-3.91480E-08
c_8	-2.47925E-08	-9.83497E-09	-6.69095E-09	-9.81004E-09	-9.99995E-09
c_{10}	-1.56287E-08	-7.43671E-09	-6.33739E-09	-2.83975E-09	-1.97875E-09

R	12.00	14.00	17.00	20.00
c_0	-1.85299E-05	-6.65720E-06	-1.48853E-06	-9.93545E-08
c_2	-1.34948E-06	-4.81509E-07	-1.21999E-07	-3.83055E-08
c_4	-3.54446E-08	-3.33185E-09	-2.86470E-10	-3.49874E-11
c_6	-4.18219E-08	-3.76642E-09	1.84539E-11	1.47065E-10
c_8	-4.92215E-09	-7.62657E-10	-5.22600E-11	-6.33996E-12
c_{10}	-1.38374E-09	-7.26420E-10	-4.72979E-11	-1.12104E-10

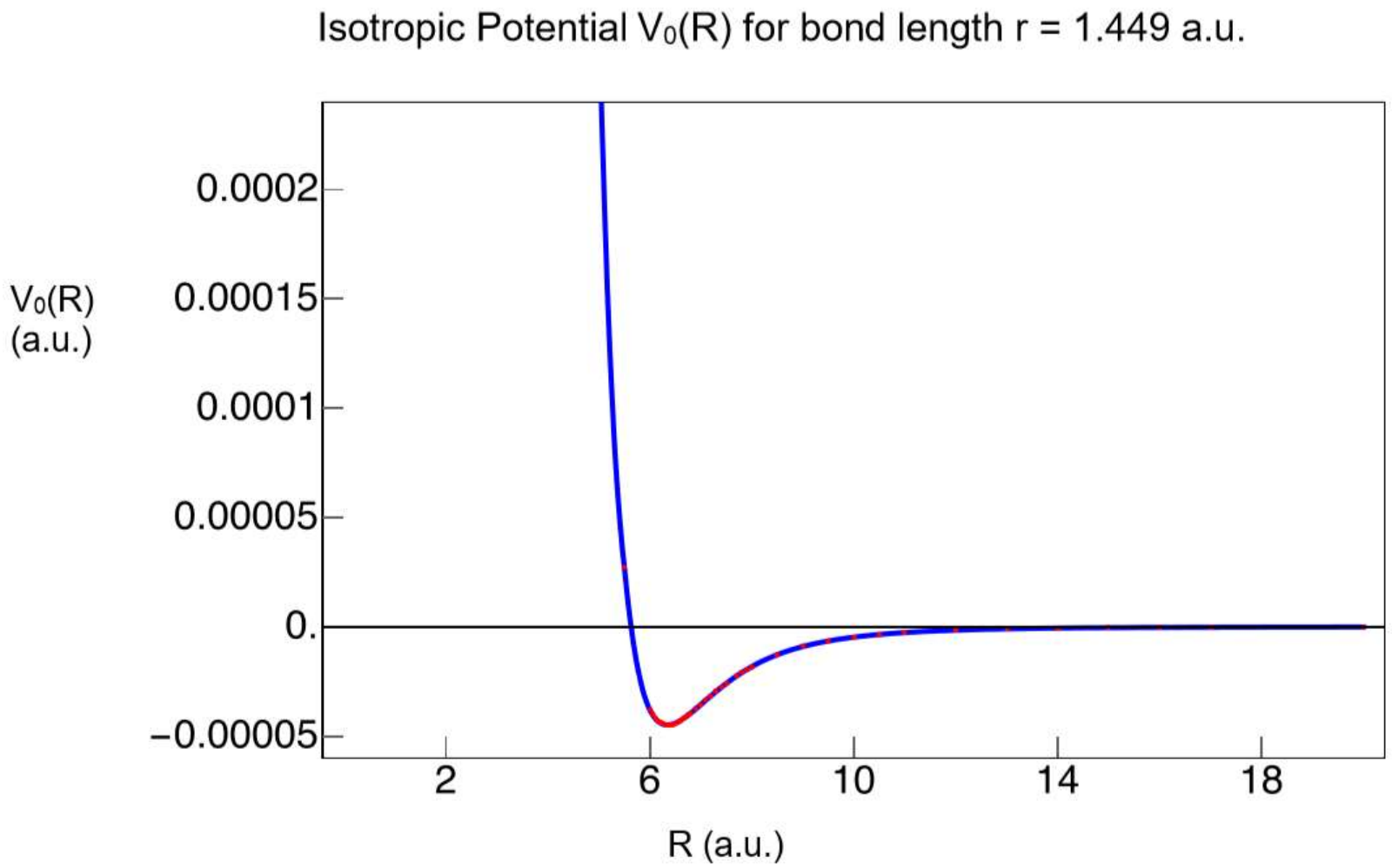

Figure 4.1. Isotropic potential $V_0(R)$ in a.u. vs. the H_2–He separation R in a.u. The values of $c_0(R)/(4\pi)$ are plotted in red. These were derived from *ab initio* calculations at fixed R values, for 19 orientation angles of the H_2 bond axis ranging from 0° to 90° in intervals of 5°. The blue curve is the Mathematica interpolation.

We obtained the values of ε and σ by using the Mathematica[4] command FindMinimum for ε and the FindRoot command to see where the potential crosses zero. Our values are $\varepsilon = 4.48132 \cdot 10^{-5}$ a.u. and $\sigma = 5.6328$ a.u. The Lennard-Jones potential is plotted in Figure 4.2 and compared with the actual isotropic potential in Figure 4.3. The agreement is surprisingly good.

Next, we explored the level of agreement between a Morse potential and the isotropic potential $V_0(R)$. The Morse potential is designed to include the anharmonicity of the vibration of the complex (the relative motion of H_2 and He), and it has the form

$$V_M(R) = D_e \{1 - \exp[-\alpha(R - R_0)]\}^2 , \tag{4.4}$$

where R_0 is the location of the potential minimum, D_e is the well depth, and α is given by

$$\alpha = [k/(2D_e)]^{1/2}. \tag{4.5}$$

In Eq. (4.5), k is the second derivative of the potential at the minimum R_0.

The potential minimum R_0 and the well depth D_e are easily obtained with Mathematica.[4] We found $R_0 = 6.3465$ a.u. and $D_e = 4.48132 \cdot 10^{-5}$ a.u. To determine the second derivative of the potential at the minimum (the harmonic force constant), we first explored a fit of the calculated potential points near the minimum to a quadratic polynomial, but then subsequently used numerical differentiation of the interpolated potential function to find $k = 8.09959 \cdot 10^{-5}$ a.u. The result for our approximate Morse potential based on $V_0(R)$ is plotted in Figure 4.4 and it is compared with the interpolated isotropic potential in Figure 4.5. Again, the agreement is quite good.

Next, we analyzed the anisotropic potential $V_2(R)$, which is given by $5^{1/2}/(4\pi)\, c_2(R)$, since $\langle\, 2\ 0\ 2\ 0 \mid 0\ 0 \,\rangle = 1/5^{1/2}$, $Y_2^0(0, 0) = [5/(4\pi)]^{1/2}$, and $Y_2^0(\theta, \varphi) = [5/(4\pi)]^{1/2} P_2(\cos\theta)$. The function $V_2(R)$ generated by Mathematica interpolation of $5^{1/2}/(4\pi)\, c_2(R)$ is plotted in Figure 4.6. At the minimum of the isotropic potential, $V_2(R)$ is about 10% of $V_0(R)$, $D_e = 4.48132 \cdot 10^{-5}$ a.u. The

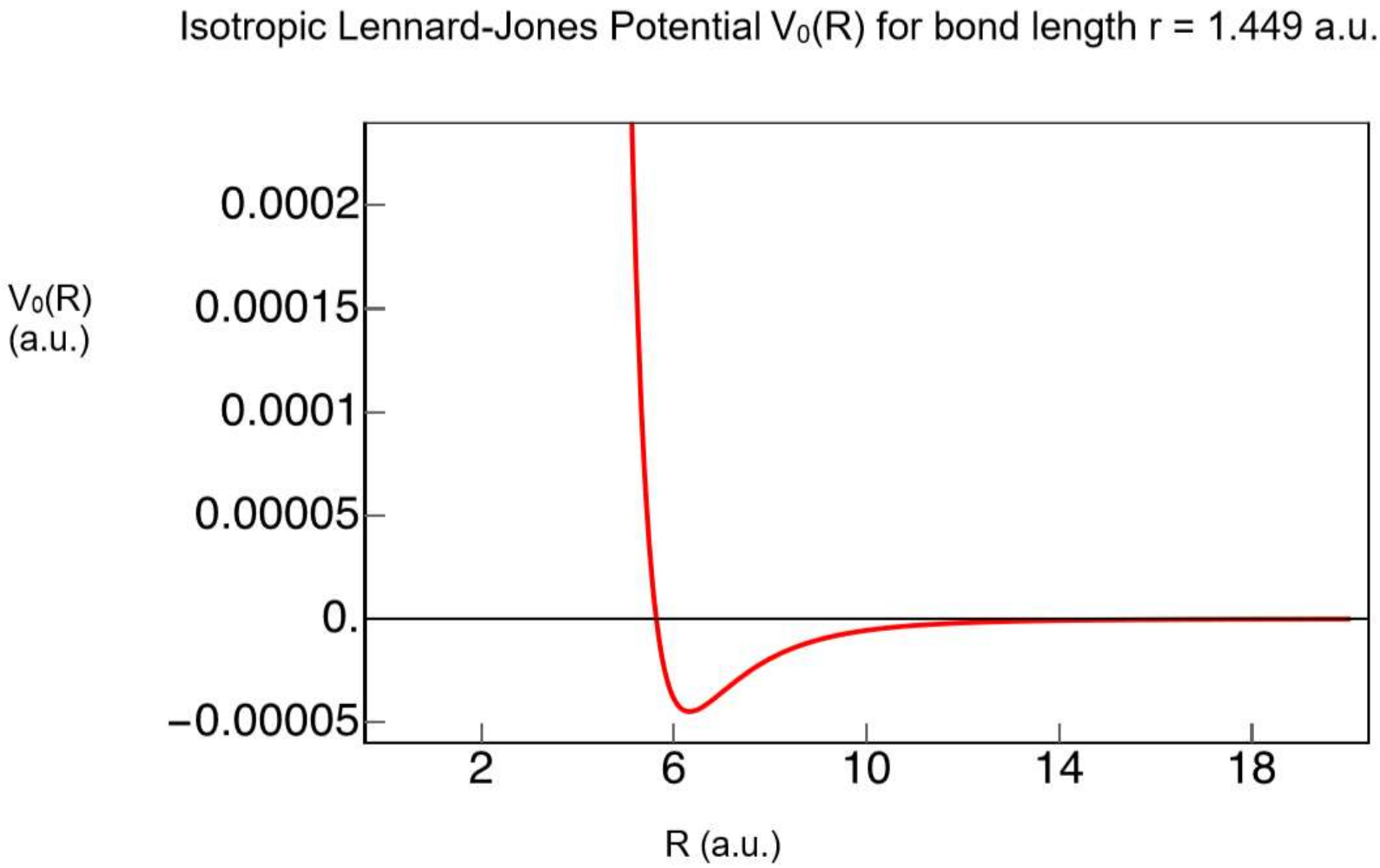

Figure 4.2. Isotropic Lennard-Jones potential $V_0(R)$ in a.u. vs. the H_2–He separation R in a.u. The parameters for the Lennard-Jones potential were obtained from the interpolation function $V_0(R)$ generated by Mathematica from the *ab initio* data. The potential crosses zero at $\sigma = 5.6325$ a.u. and the well depth is $\varepsilon = 4.48132 \cdot 10^{-5}$.

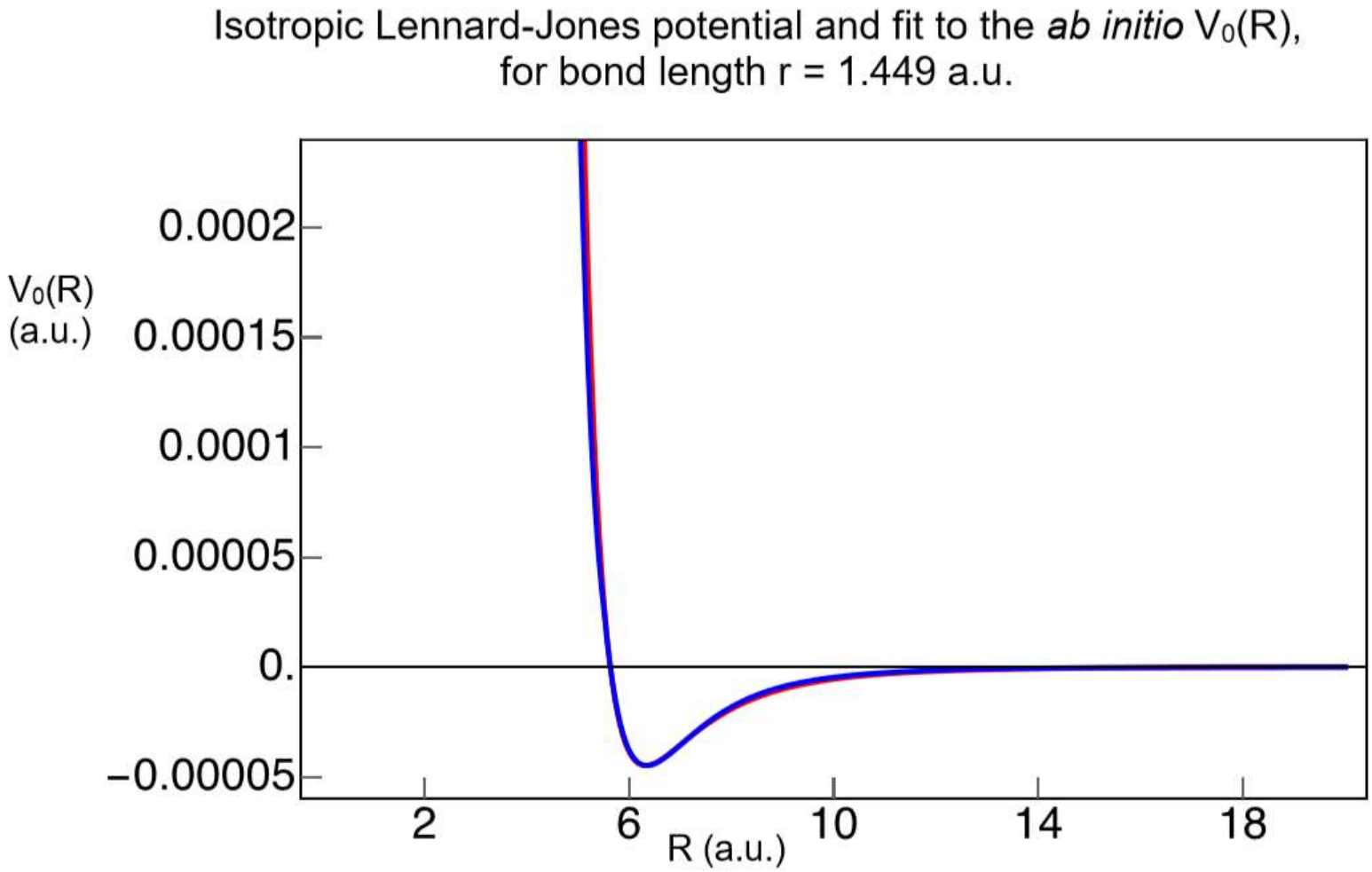

Figure 4.3. Isotropic Lennard-Jones potential in red, for comparison with $V_0(R)$ obtained by interpolating the *ab initio* data directly (in blue). Potentials in a.u. vs. the H_2–He separation R in a.u. The parameters for the Lennard-Jones potential are $\sigma = 5.6325$ a.u. and $\varepsilon = 4.48132 \cdot 10^{-5}$ a.u. The fit is surprisingly good.

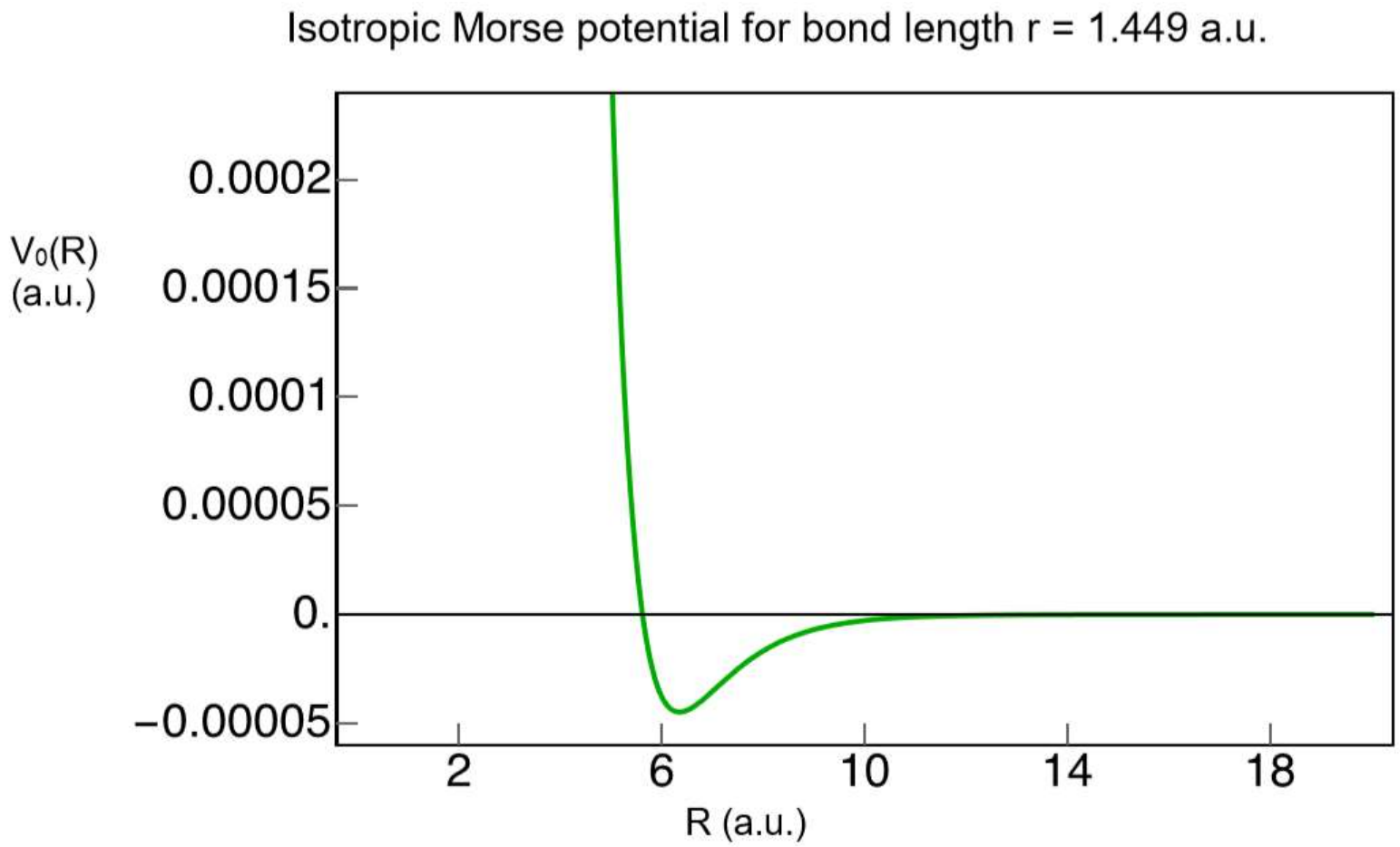

Figure 4.4. Isotropic Morse potential in a.u. vs. the H_2–He separation R in a.u. The parameters for the Morse potential were obtained from the Mathematica interpolation of the *ab initio* $V_0(R)$ data values. The parameters are: the location of the minimum at $R_0 = 6.3465$ a.u., the well depth of $4.48132 \cdot 10^{-5}$ a.u., and the curvature at the potential minimum, found by numerical differentiation of the interpolated function.

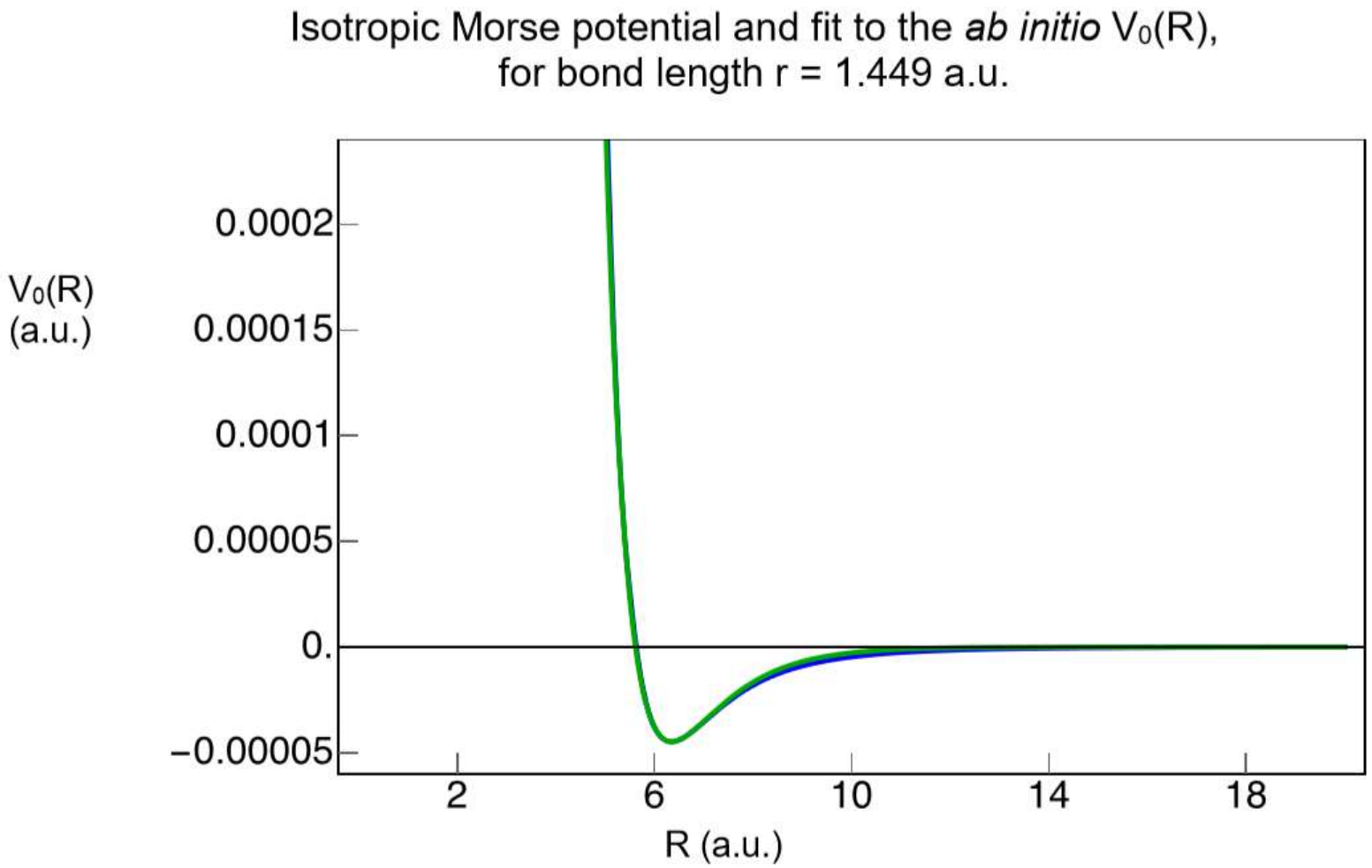

Figure 4.5. Isotropic Morse potential in green, for comparison with $V_0(R)$ obtained by interpolating the *ab initio* data directly (in blue). Potentials in a.u. vs. the H_2–He separation R in a.u. The parameters for the Morse potential are the same as in Figure 4.4. Although the fit is reasonably good, it is not as good as the fit of the isotropic Lennard-Jones potential.

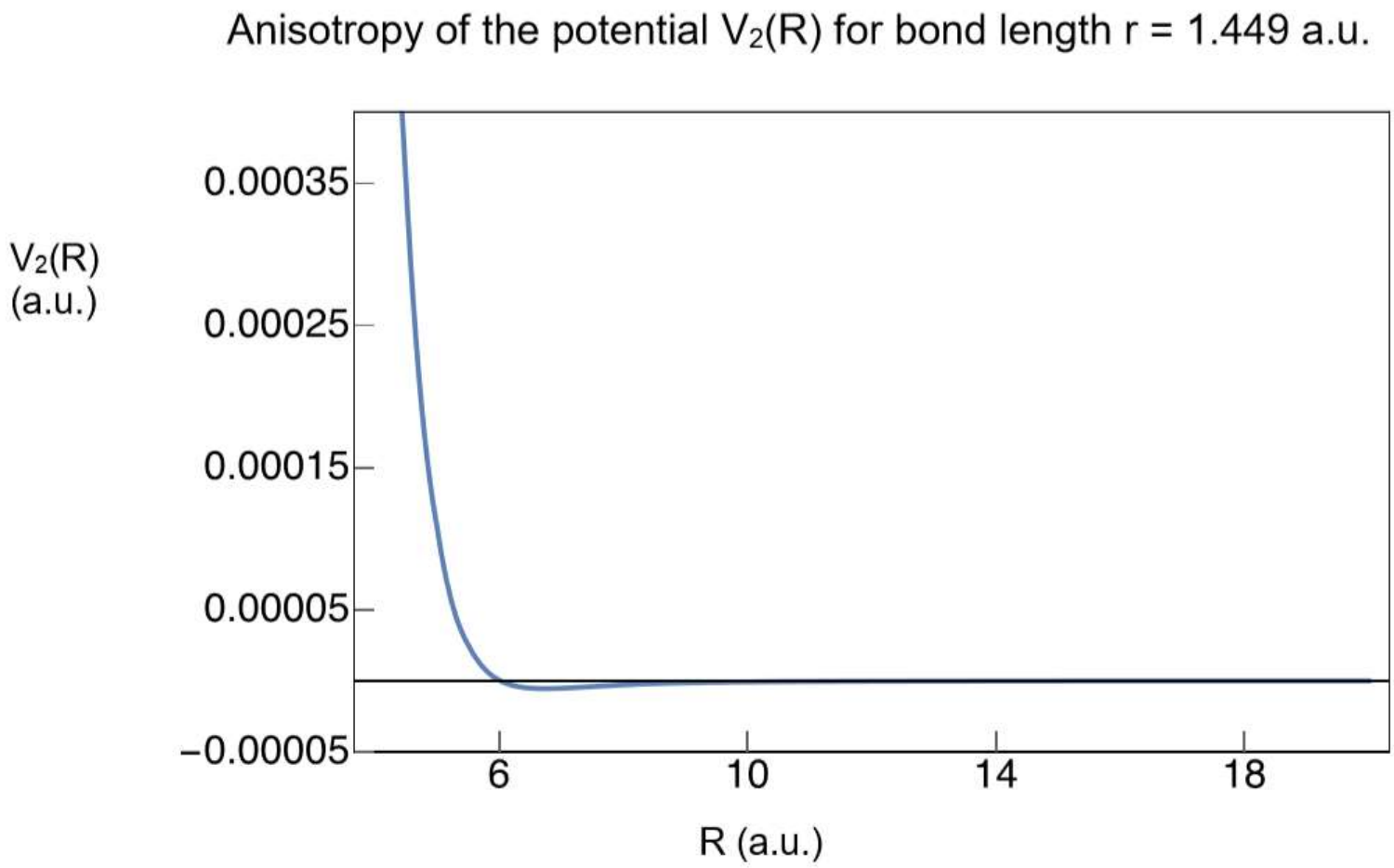

Figure 4.6. Anisotropy of the potential $V_2(R)$ in a.u. vs. the H_2–He separation R in a.u. The $V_2(R)$ anisotropy has been found from an interpolation of the results for the coefficients $c_2(R)$ multiplied by $5^{1/2}/(4\pi)$.

minimum of $V_0(R)$ occurs at $R_0 = 6.3465$ a.u., while the minimum of $V_2(R)$ is a little further out, at $R_2 \sim 6.75$ a.u., with a depth of about $5.5 \cdot 10^{-6}$ a.u. A Lennard-Jones potential is also found to fit $V_2(R)$ surprisingly well. In early work on the potential energy surface of H_2−He, the V_2 component of the potential was approximated as a multiple of V_0. The ratio of $V_2(R)$ to $V_0(R)$ is plotted versus R in Figure 4.7. Over a range of intermediate R values, the ratio is roughly constant. Finally, the anisotropic potential $V_4(R)$ was determined. It is derived from the $c_4(R)$ coefficients multiplied by $3/(4\pi)$, since $\langle\ 4\ 0\ 4\ 0 \mid 0\ 0\ \rangle = 1/3$, $Y_4^0\ (0, 0) = 3/(4\pi)^{1/2}$, and $Y_2^0(\theta, \varphi) = 3/(4\pi)^{1/2}$ $P_4(\cos\theta)$. The anisotropic potential $V_4(R)$ from a Mathematica interpolation is plotted in Figure 4.8.

To see whether H_2 might be viewed as rotating freely within the complex, we found the energy differences between the minima and maxima of the potential at the potential minimum and near the zero-crossing at shorter range. The values are 2.30 K at the minimum, 1.18 K at R = 6.05 a.u., 0.25 K at R = 6.00 a.u., and 12.4 K at 5.50 a.u., smaller than Toennies experimental temperature of 24.7 K. To lowest order, we approximated H_2 as free to rotate within the complex. Then we worked to determine the bound vibrational state energy, based on our isotropic potential $V_0(R)$. The existence of a potential well does not guarantee that it can support a bound state. Previous calculations have given different results for the binding energy of the H_2−He molecule, because it is so small. These earlier theoretical results are listed in Table 4.3.

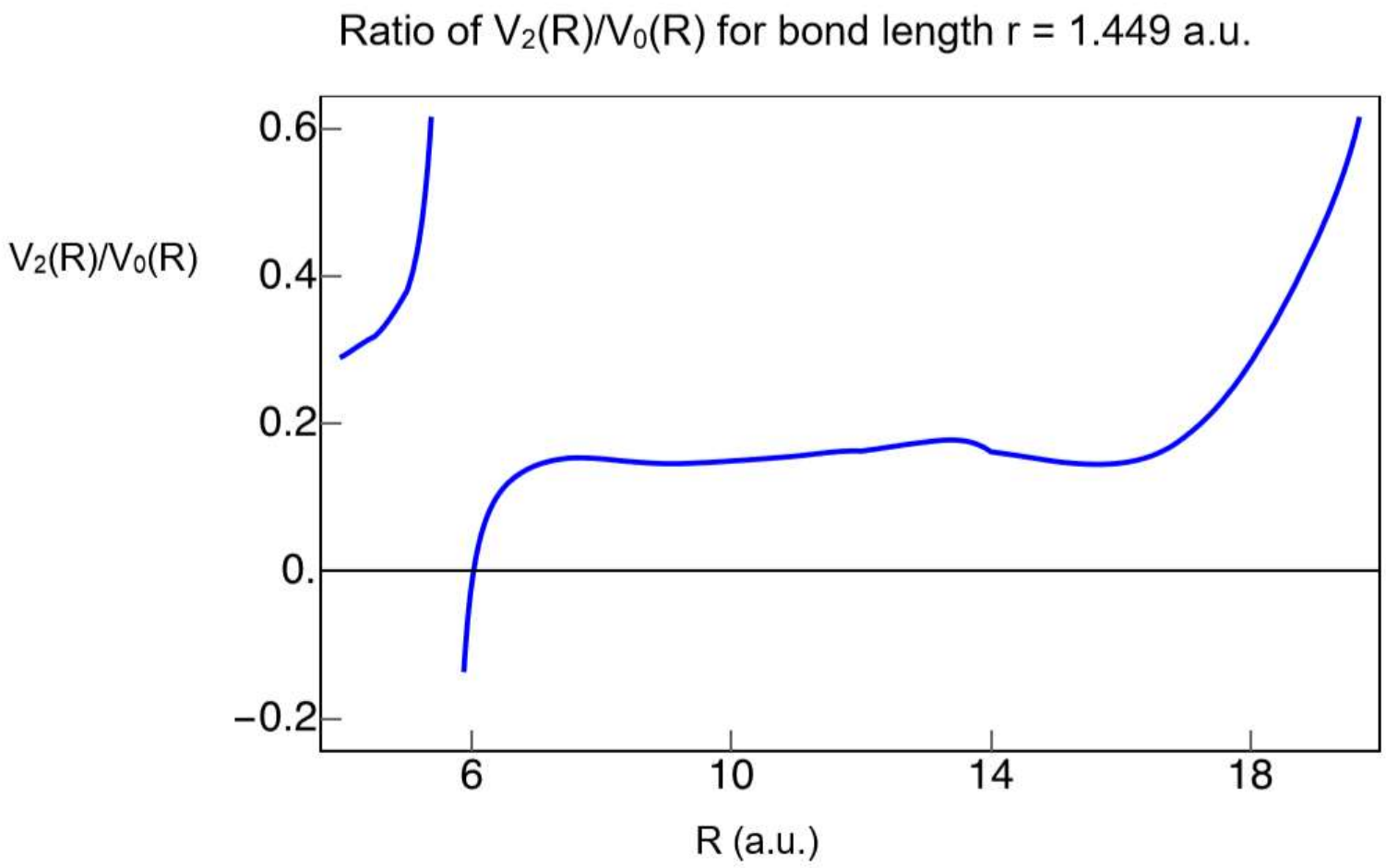

Figure 4.7. Ratio of the anisotropy $V_2(R)$ to $V_0(R)$ vs. the H_2–He separation R in a.u. In early explorations of the H_2–He potential, this ratio had been approximated as constant. The ratio varies considerably because $V_2(R)$ crosses zero at a different R value (6.0251 a.u.) from $V_0(R)$ (5.6328 a.u.). Nevertheless, there is a broad range of R values where the ratio is approximately constant, running from R ~ 7.3 a.u. to 16.3 a.u.

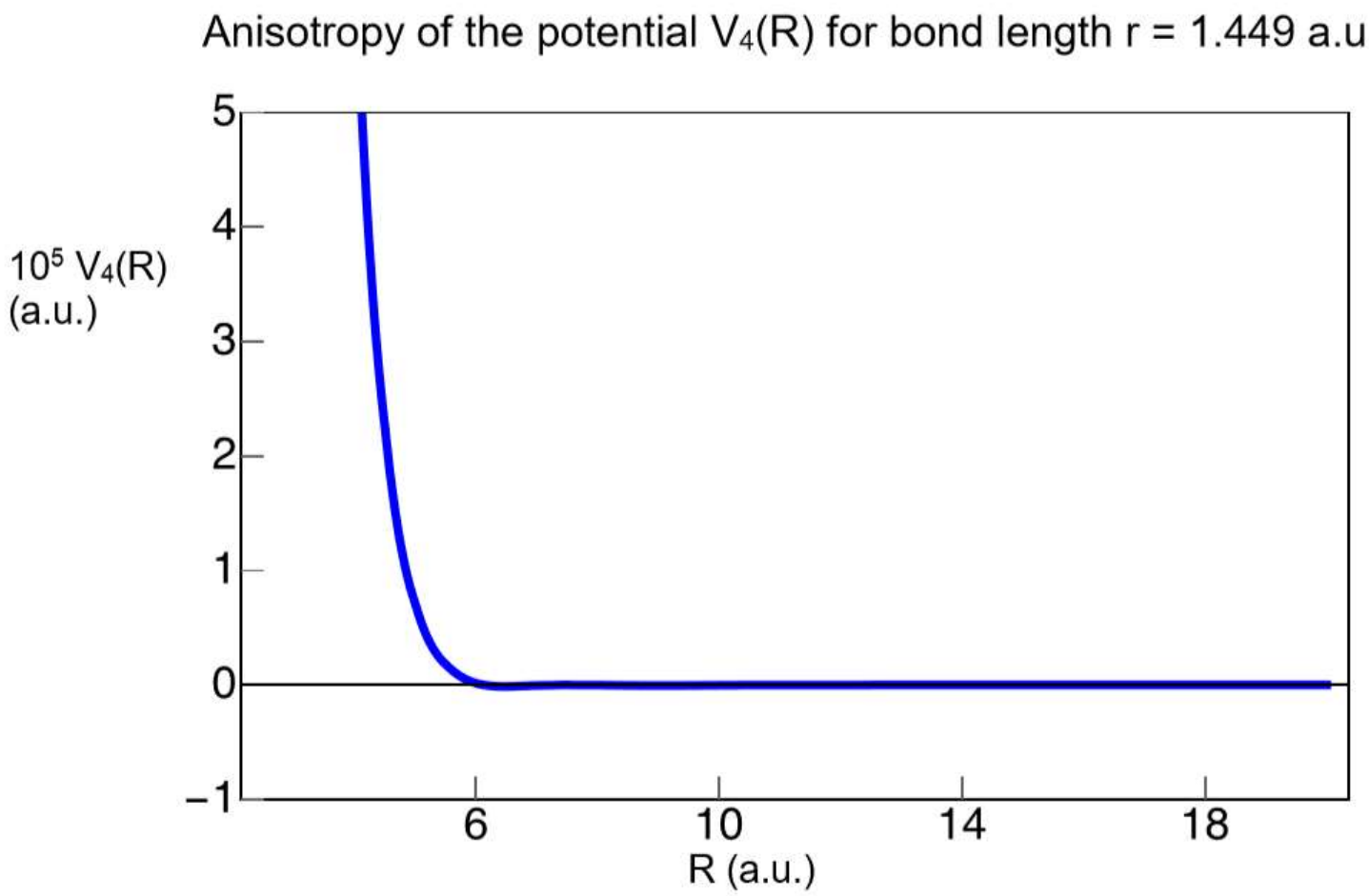

Figure 4.8. Anisotropy of the potential $V_4(R)$, multiplied by 106, in a.u. vs. the H_2–He separation R in a.u. The $V_4(R)$ anisotropy has been found from an interpolation of the results for the coefficients $c_4(R)$ multiplied by $3/(4\pi)$.

Table 4.3. Earlier theoretical results for the bound-state energy of H_2–He and the average intermolecular distance $\langle R \rangle$ in the bound state.

Reference	**E (in a.u.)**	**$\langle R \rangle$ (in a.u.)**
Forrey, Kharchenko, Balakrishnan, and Dalgarno[5]	$-1.36 \cdot 10^{-7}$	27.4
Barnett and Whaley[6]	$-7.79 \cdot 10^{-8}$	34.2
Gianturco, González-Lezana, Delgado-Barrio, and Villarreal[7]	$-1.66 \cdot 10^{-7}$	25.3

We have tried four different approaches to locate a bound state and to determine its energy. First, we used the Numerov method, in an attempt to solve the Schrödinger equation numerically. Initially, $V_0(R)$ had been determined in these calculations out to R = 20.0 a.u.; but H_2−He appears to be a "halo" molecule, with a ground state vibrational wave function that extends to intermolecular separations well beyond 20.0 a.u., and the attempt did not work. The Numerov method would work with a potential that is about 10 times deeper than $V_0(R)$ in the well region. Second, we employed the WKB (Wentzel-Kramers-Brillouin) approximation. The condition that determines the energy of the ground vibrational state of the complex in the WKB approximation is

$$\pi/2 = \int_{t_1}^{t_2} p(E)\, dR\ . \tag{4.6}$$

In Eq. (4.6), t_1 is the R value at the inner classical turning point and t_2 is the R value at the outer classical turning point. Both are functions of E for a known potential V(R). The integrand is the classical momentum, determined by the energy E, the reduced mass m of the complex, and the isotropic potential $V_0(R)$ as

$$p(E) = \{2\mu\, [E - V_0(R)]\}^{1/2}\ . \tag{4.7}$$

The WKB method was implemented by first checking that the integral in Eq. (4.7) with E = 0 is greater than π/2, which guarantees the existence of a bound state in the WKB approximation. Then we selected a trial energy, determined the inner and outer turning points at that energy and evaluated the integral numerically. Successive estimates of the energy were based on the values of the integral, to bring it closer to π/2, which is approximately 1.5708. Using the WKB method, we found an energy of $-7.4 \cdot 10^{-7}$ a.u. for the vibrational ground state. Values of the inner and outer turning points as functions of E, the integral in Eq. (4.7) for several different E values, and the final bound-state energy from the WKB approximation are listed in Table 4.4.

Table 4.4. WKB study of the potential $V_0(R)$ for bond length r = 1.449 a_0.

Trial Energy	Inner Turning Point	Outer Turning Point	WKB Integral
0	5.6327997	[20.0]	1.87845
-0.0000007	5.636850165	13.593127	1.58018
-0.00000072	5.636966605	13.541465	1.57553
-0.00000073	5.637024840	13.515443	1.57287
-0.00000074	**5.637083077**	**13.489320**	**1.57091**
-0.00000075	5.63714133	13.463110	1.56861
-0.00000077	5.63725786	13.410505	1.56406
-0.000001	5.6386006	12.831060	1.51560
-0.000003	5.6504880	10.728365	1.26629
-0.00001	5.6954995	8.840885	0.85786
-0.00005	5.8753800	7.275550	0.28457

Next, we investigated the bound-state energy of the Morse potential that we fit to $V_0(R)$. The bound-state energies of the Morse oscillator are known, and they take the for

$$E(n) = h\nu_0 (n + 1/2) - [h\nu_0 (n + 1/2)]^2/(4D_e) - D_e, \tag{4.8}$$

for vibrational quantum number n, which is zero for the lowest vibrational state, and the frequency ν_0 is given by

$$\nu_0 = (\alpha/2\pi) (2D_e/\mu)^{1/2}, \tag{4.9}$$

and we have taken μ as the reduced mass of the H_2–He complex, just based on the masses of H_2 and He. The result for the energy of the bound state is $E = -1.0968 \cdot 10^{-8}$ a.u., which is higher than the result from the WKB approximation. This may be due to the omission of dispersion effects from the Morse potential, which means that the Morse potential rises too fast at long range.

The exact solution of the Schrödinger equation for the Lennard-Jones potential was derived by Sesma[8] in 2013. This offers another possible means of determining the bound-state energy for H_2–He, based on the Lennard-Jones fit of the isotropic potential. Sesma has cast the Lennard-Jones potential for two-body interactions in terms of an intensity parameter λ as

$$V(R) = \hbar^2\lambda/(2\mu R_e^2) [(R_e/R)^{12} - 2 (R_e/R)^6]. \tag{4.10}$$

In this equation μ is the reduced mass of the interacting species, and R_e is the separation at the minimum of the potential. The solution of the Schrödinger equation for the complex has the form $\Psi(R, \theta, \varphi) = \psi(R)\, Y_L^M(\theta, \varphi)$, where $Y_L^M(\theta, \varphi)$ is a spherical harmonic with angular momentum quantum number L for the rotation of the entire complex, and $\psi(R)$ is the solution of the radial equation,

$$-(\hbar^2/2\mu) (d^2\, \psi(R)/dR^2 - L (L + 1)\, \psi(R)/R^2 + V(R)\, \psi(R) = E\, \psi(R). \tag{4.11}$$

Sesma has provided the critical values of the intensity parameter λ that determine how many bound states are found for the potential V(R) and how high the angular momentum L can become before a bound state can no longer be found.

Sesma remarked that the Schrödinger equation for the Lennard-Jones potential has two irregular singular points, “one of rank 5 at the origin, and another of rank 1 at infinity.” He

expressed the condition for a continuous solution that is regular at both singular points in terms of a connection formula,

$$T_{1,4}\,T_{2,6} - T_{2,4}\,T_{1,6} = 0 \ . \tag{4.12}$$

The quantity $T_{1,4}T_{2,6} - T_{2,4}T_{1,6}$ is a function of E, and the roots of Eq. (4.12) give the energies of the bound states. $T_{1,4}$, $T_{2,4}$, $T_{1,6}$, and $T_{2,6}$ have expressions in terms of ratios of the Wronskians of the two solutions of the Schrödinger equation as $z \rightarrow \infty$ and the two solutions as $z \rightarrow 0$. The Wronskian of two functions is given by

$$W[f(z), g(z)] = f(z)\, dg(z)/dz - g(z)\, df(z)/dz \ . \tag{4.13}$$

All together, we need six Wronskians to find $T_{1,4}T_{2,6} - T_{2,4}T_{1,6} = 0$ as a function of E, in order to determine the bound-state energies. Two of the Wronskians are simple, with values of $-2\,\lambda^{1/2}$ and $2(2\mu R_e^2 E/\hbar^2)^{1/2}$. The other four Wronskians are more challenging to compute. Their evaluation requires an integration in the complex plane around the unit circle centered on R = 0. Work to determine the Wronskians for our version of the Lennard-Jones potential is still in progress. However, we can use the results in the Sesma paper to gain information on the number of bound state solutions and the maximum possible angular momentum quantum number L for the Lennard Jones potential that we have fit to $V_0(R)$ with Mathematica.

We have worked with a Lennard-Jones potential in the form $V(R) = 4\varepsilon\,[(\sigma/r)^{12} - (\sigma/r)^6]$. The point σ where the potential crosses zero is related to R_e by $R_e = 2^{1/6}\,\sigma$, if the Lennard-Jones potential is accurate. The Mathematica[4] interpolation of the isotropic potential $V_0(R)$ for the bond length r = 1.449 a.u. gives σ = 5.6328 a.u. and R_e = 6.3465 a.u. Their ratio is 1.12670 versus $2^{1/6}$ = 1.12246, the ratio for an exact Lennard-Jones potential. The difference is less than half a percent. We have used our value of ε and the location of the actual minimum at R_e = 6.3465 a.u. in order to determine the values of Sesma's intensity parameter λ. The relationship is $\lambda = 2\varepsilon\mu R_e^2 / \hbar^2$. In place of μR_e^2, we plan to use the moment of inertia of the complex, obtained as an isotropic average over the orientations of the H_2 in the complex. For the current work, we have calculated μ for various isotopic forms of H_2–He and H_2 isotopes by simply taking the reduced mass of the pair and converting to atomic units by dividing by the mass of the electron. The well depth ε and the

location of the minimum are already in atomic units. The intensity parameter λ is dimensionless. The reduced masses and the resulting numerical values of λ are listed in Table 4.5.

Sesma has tabulated the lowest values of λ for which a new bound state of angular momentum L appears in the solution of the Schrödinger equation for the Lennard-Jones potential. A bound state with angular momentum quantum number L = 0 exists, provided that $\lambda \geq 7.04314$. All of the He–H_2 isotopic species meet the condition for the existence of at least one bound state. The lowest value of λ for a second bound state with L = 0 to exist (a vibrationally excited state of the complex, in effect) is 46.61703; and none of the pairs have sufficiently high λ to have a second L = 0 level. A bound state of the complex in the lowest vibrational state, but with L = 1 exists if $\lambda \geq 13.29573$. Our Lennard-Jones potential (as treated above) gives an L = 1 bound state for DT–^{4}He and T_2–^{4}He, but not for the other species. The asterisks in Table 4.5 indicate species where λ is close to the cut-off for the existence of a state with L = 1.

Table 4.5. Values of the reduced mass, intensity parameter λ, and the number of bound states of the Lennard-Jones potential for various isotopes of H_2–He.

Isotopic form	μ (amu)	λ	Number of bound states
H_2–^{3}He	1.208197	7.95064	1
HD–^{3}He	1.509488	9.93331	1
HT–^{3}He	1.723905	11.34430	1
D_2–^{3}He	1.724699	11.34952	1
DT–^{3}He	1.885501	12.40769	1
T_2–^{3}He	2.010691	13.23151	1*
H_2–^{4}He	1.340563	8.82168	1
HD–^{4}He	1.721905	11.33114	1
HT–^{4}He	2.006605	13.20463	1*
D_2–^{4}He	2.007681	13.21171	1*
DT–^{4}He	2.228966	14.66789	2
T_2–^{4}He	2.406060	15.83328	2

Modification of the isotropic potential based on a perturbative treatment of the effect of the anisotropies may show that bound states with L = 1 exist for T_2–^{3}He, HT–^{4}He, and D_2–^{4}He. This will be investigated in the future. A bound state with L = 2 exists if $\lambda \geq 21.48500$, but none of the H_2–He isotopes have a sufficiently large value of λ for an L = 2 state. All other states require even higher values of λ to exist.

Since we have determined the anisotropy of the potential, we can estimate its effects on the energy of the J = 0 state of H_2 in the complex, using perturbation theory. In this approximation, the unperturbed energy at any R is given by $V_0(R)$. The first-order correction to the energy vanishes, and the second-order correction is determined by a sum over excited rotational states of H_2. The energies of the rotational states of H_2 are approximated as $B_e J (J + 1)$ in atomic units. The second-order perturbation result for H_2 in the rotational state $Y_0^0(\theta, \varphi)$ takes the form

$$\Delta E^{(2)} = - \sum_{J, M} \langle Y_0^0(\theta, \varphi) \mid V_a \mid Y_J^M(\theta, \varphi) \rangle \langle Y_J^M(\theta, \varphi) \mid V_a \mid Y_0^0(\theta, \varphi) \rangle / (E_J - E_0) \qquad (4.14)$$

At this stage, of the work, $\Delta E^{(2)}$ has been evaluated only at the minimum of the isotropic potential. The value of is comparatively small, but because the ground-state energy is so close to zero, the effect may be significant. This will be explored in future work.

We have also analyzed the long-range behavior of the potentials $V_0(R)$, $V_2(R)$, and $V_4(R)$ for r = 1.449 a.u. Results are given in the next chapter, where they are compared with the long-range forms of the potential found for r = 1.111 a.u. and r = 2.463 a.u.

APPENDIX

APPENDIX

Sample Mathematica program of the fitting routine used to determine the spherical expansion coefficients $c_j(R)$:

```
In[ ]:=
        f0[theta_] :=
        Chop[N[(ClebschGordan[{0, 0}, {0, 0}, {0, 0}]
                SphericalHarmonicY[0, 0, theta, 0] SphericalHarmonicY[0, 0, 0, 0])]]
In[ ]:=
        f2[theta_] :=
        Chop[N[(ClebschGordan[{2, 0}, {2, 0}, {0, 0}]
                SphericalHarmonicY[2, 0, theta, 0] SphericalHarmonicY[2, 0, 0, 0])]]
In[ ]:=
        f4[theta_] :=
        Chop[N[(ClebschGordan[{4, 0}, {4, 0}, {0, 0}]
                SphericalHarmonicY[4, 0, theta, 0] SphericalHarmonicY[4, 0, 0, 0])]]
In[ ]:=
        f6[theta_] :=
        Chop[N[(ClebschGordan[{6, 0}, {6, 0}, {0, 0}]
                SphericalHarmonicY[6, 0, theta, 0] SphericalHarmonicY[6, 0, 0, 0])]]
In[ ]:=
        f8[theta_] :=
        Chop[N[(ClebschGordan[{8, 0}, {8, 0}, {0, 0}]
                SphericalHarmonicY[8, 0, theta, 0] SphericalHarmonicY[8, 0, 0, 0])]]
In[ ]:=
        f10[theta_] :=
        Chop[N[(ClebschGordan[{10, 0}, {10, 0}, {0, 0}]
                SphericalHarmonicY[10, 0, theta, 0] SphericalHarmonicY[10, 0, 0, 0])]]
In[ ]:=
        energy[theta_, eval_] :=
        {f0[theta], f2[theta], f4[theta], f6[theta], f8[theta], f10[theta], eval}
In[ ]:=
        eval[1]= -4.0770579976
        eval[2]= -4.0770579928
        eval[3]= -4.0770579803
        eval[4]= -4.0770579611
        eval[5]= -4.0770579369
        eval[6]= -4.0770579093
        eval[7]= -4.0770578798
        eval[8]= -4.0770578498
        eval[9]= -4.0770578196
        eval[10]= -4.0770577898
        eval[11]= -4.0770577608
        eval[12]= -4.0770577327
        eval[13]= -4.0770577057
        eval[14]= -4.077057681
        eval[15]= -4.0770576588
        eval[16]= -4.0770576401
        eval[17]= -4.077057626
        eval[18]= -4.0770576172
        eval[19]= -4.0770576144
Out[ ]=  -4.07706
Out[ ]=  -4.07706
```

Out[ ]= -4.07706
Out[ ]= -4.07706
Out[ ]= -4.07706
Out[ ]= -4.07706
Out[ ]= -4.07706
Out[ ]= -4.07706
Out[ ]= -4.07706
Out[ ]= -4.07706
Out[ ]= -4.07706
Out[ ]= -4.07706
Out[ ]= -4.07706
Out[ ]= -4.07706
Out[ ]= -4.07706
Out[ ]= -4.07706
Out[ ]= -4.077060
Out[ ]= -4.07706
In[ ]:= b = 4.0770562645
Out[ ]= 4.07706
In[ ]:= e1 = energy[0, eval[1] + b]
e2 = energy[5 × 2Pi / 360, eval[2] + b]
e3 = energy[10 × 2Pi / 360, eval[3] + b]
e4 = energy[15 × 2Pi / 360, eval[4] + b]
e5 = energy[20 × 2Pi / 360, eval[5] + b]
e6 = energy[25 × 2Pi / 360, eval[6] + b]
e7 = energy[30 × 2Pi / 360, eval[7] + b]
e8 = energy[35 × 2Pi / 360, eval[8] + b]
e9 = energy[40 × 2Pi / 360, eval[9] + b]
e10 = energy[45 × 2Pi / 360, eval[10] + b]
e11 = energy[50 × 2Pi / 360, eval[11] + b]
e12 = energy[55 × 2Pi / 360, eval[12] + b]
e13 = energy[60 × 2Pi / 360, eval[13] + b]
e14 = energy[65 × 2Pi / 360, eval[14] + b]
e15 = energy[70 × 2Pi / 360, eval[15] + b]
e16 = energy[75 × 2Pi / 360, eval[16] + b]
e17 = energy[80 × 2Pi / 360, eval[17] + b]
e18 = energy[85 × 2Pi / 360, eval[18] + b]
e19 = energy[90 × 2Pi / 360, eval[19] + b]
Out[ ]= {0.0795775, 0.177941, 0.238732, 0.286921, 0.328106, 0.36467, -1.7331×10^{-6}}
Out[ ]= {0.0795775, 0.175913, 0.229725, 0.264425, 0.284635, 0.292183, -1.7283×10^{-6}}
Out[ ]= {0.0795775, 0.169892, 0.203689, 0.202127, 0.171221, 0.117218, -1.7158×10^{-6}}
Out[ ]= {0.0795775, 0.160061, 0.163459, 0.114282, 0.0315587, -0.0601909, -1.6966×10^{-6}}
Out[ ]= {0.0795775, 0.146718, 0.113393, 0.0206305, -0.0826301, -0.146331, -1.6724×10^{-6}}
Out[ ]= {0.0795775, 0.130269, 0.0588552, -0.0585267, -0.133286, -0.111311, -1.6448×10^{-6}}
Out[ ]= {0.0795775, 0.111213, 0.00559529, -0.107315, -0.111154, -0.00256659, -1.6153×10^{-6}}
Out[ ]= {0.0795775, 0.0901296, -0.0409245, -0.118053, -0.0378764, 0.0926843, -1.5853×10^{-6}}
Out[ ]= {0.0795775, 0.0676595, -0.0761567, -0.0928391, 0.0454843, 0.108433, -1.5551×10^{-6}}
Out[ ]= {0.0795775, 0.0444852, -0.096985, -0.0425898, 0.0978872, 0.041978, -1.5253×10^{-6}}
Out[ ]= {0.0795775, 0.0213109, -0.102066, 0.0161761, 0.0966871, -0.0503658, -1.4963×10^{-6}}
Out[ ]= {0.0795775, -0.0011593, -0.0919566, 0.0659123, 0.0466458, -0.0981705,
-1.4682×10^{-6}}
Out[ ]= {0.0795775, -0.0222426, -0.0690086, 0.0927449, -0.0241614, -0.0686413,
-1.4412×10^{-6}}
Out[ ]= {0.0795775, -0.0412984, -0.0370537, 0.0900435, -0.0791208, 0.0117871,

-1.4165 × 10^{-6}}

Out[ ]= {0.0795775, -0.0577477, -0.000907193, 0.0599311, -0.0912185, 0.0799688,
-1.3943 × 10^{-6}}

Out[ ]= {0.0795775, -0.0710907, 0.0342413, 0.0123664, -0.0558502, 0.0844685, -1.3756 × 10^{-6}}

Out[ ]= {0.0795775, -0.080922, 0.0634793, -0.0379083, 0.00764745, 0.0235876, -1.3615 × 10^{-6}}

Out[ ]= {0.0795775, -0.0869428, 0.0827845, -0.075684, 0.0661942, -0.0546621, -1.3527 × 10^{-6}}

Out[ ]= {0.0795775, -0.0889703, 0.0895247, -0.0896627, 0.0897166, -0.089743, -1.3499 × 10^{-6}}

In[ ]:= data ={e1, e2, e3, e4, e5, e6, e7, e8,
e9, e10, e11, e12, e13, e14, e15, e16, e17, e18, e19}

Out[ ]={ {0.0795775, 0.177941, 0.238732, 0.286921, 0.328106, 0.36467, -1.7331 × 10^{-6}},
{0.0795775, 0.175913, 0.229725, 0.264425, 0.284635, 0.292183, -1.7283 × 10^{-6}},
{0.0795775, 0.169892, 0.203689, 0.202127, 0.171221, 0.117218, -1.7158 × 10^{-6}},
{0.0795775, 0.160061, 0.163459, 0.114282, 0.0315587, -0.0601909, -1.6966 × 10^{-6}},
{0.0795775, 0.146718, 0.113393, 0.0206305, -0.0826301, -0.146331, -1.6724 × 10^{-6}},
{0.0795775, 0.130269, 0.0588552, -0.0585267, -0.133286, -0.111311, -1.6448 × 10^{-6}},
{0.0795775, 0.111213, 0.00559529, -0.107315, -0.111154, -0.00256659, -1.6153 × 10^{-6}},
{0.0795775, 0.0901296, -0.0409245, -0.118053, -0.0378764, 0.0926843, -1.5853 × 10^{-6}},
{0.0795775, 0.0676595, -0.0761567, -0.0928391, 0.0454843, 0.108433, -1.5551 × 10^{-6}},
{0.0795775, 0.0444852, -0.096985, -0.0425898, 0.0978872, 0.041978, -1.5253 × 10^{-6}},
{0.0795775, 0.0213109, -0.102066, 0.0161761, 0.0966871, -0.0503658, -1.4963 × 10^{-6}},
{0.0795775, -0.0011593, -0.0919566, 0.0659123, 0.0466458, -0.0981705, -1.4682 × 10^{-6}},
{0.0795775, -0.0222426, -0.0690086, 0.0927449, -0.0241614, -0.0686413, -1.4412 × 10^{-6}},
{0.0795775, -0.0412984, -0.0370537, 0.0900435, -0.0791208, 0.0117871, -1.4165 × 10^{-6}},
{0.0795775, -0.0577477, -0.000907193, 0.0599311, -0.0912185, 0.0799688, -1.3943 × 10^{-6}},
{0.0795775, -0.0710907, 0.0342413, 0.0123664, -0.0558502, 0.0844685, -1.3756 × 10^{-6}},
{0.0795775, -0.080922, 0.0634793, -0.0379083, 0.00764745, 0.0235876, -1.3615 × 10^{-6}},
{0.0795775, -0.0869428, 0.0827845, -0.075684, 0.0661942, -0.0546621, -1.3527 × 10^{-6}},
{0.0795775, -0.0889703, 0.0895247, -0.0896627, 0.0897166, -0.089743, -1.3499 × 10^{-6}}}

In[ ]:= Fit [data, {c0, c2, c4, c6, c8, c10}, {c0, c2, c4, c6, c8, c10}]

Out[ ]= - 0.0000184734 c0 - 1.38374 × 10^{-9} c10 - 1.34948 × 10^{-6} c2 -
3.54446 × 10^{-8} c4 - 4.18219 × 10^{-8} c6 - 4.92215 × 10^{-9} c8

REFERENCES

REFERENCES

1. K. Kowalski and P. Piecuch, *J. Chem. Phys*. **113**, 18 (2000); K. Kowalski and P. Piecuch, *J. Chem. Phys.* **115**, 643 (2001); K. Kowalski and P. Piecuch, *Chem. Phys. Lett*. **347**, 237 (2001); K. Kowalski and P. Piecuch, *J. Chem. Phys*. **122**, 074107 (2005).

2. T. H. Dunning, Jr., *J. Chem. Phys*. **90**, 1007 (1989); R. A. Kendall, T. H. Dunning, Jr., and R. J. Harrison, *J. Chem. Phys*. **96**, 6769 (1992); D. E. Woon and T. H. Dunning, Jr., *J. Chem. Phys*. **100**, 2975 (1994).

3. B. W. Bakr, D. G. A. Smith, and K. Patkowski, *J. Chem. Phys*. **139**, 144305 (2013).

4. Mathematica, Wolfram Research, Inc., Version 11.3, Champaign, IL (2018).

5. R. C. Forrey, V. Kharchenko, N. Balakrishnan, and A. Dalgarno, *Phys. Rev. A* **59**, 2146 (1999).

6. R. N. Barnett and K. B. Whaley, *J. Chem. Phys*. **96**, 2953 (1992).

7. F. A. Gianturco, T. González-Lezana, G. Delgado-Barrio, and P. Villarreal, *J. Chem. Phys*. **122**, 084308 (2005).

8. J. Sesma, *J. Math. Chem*. **51**, 1881 (2013).

CHAPTER 5: Comparison of Potentials for Different H_2 Bond Lengths

In this chapter, results are presented for the potential energy of H_2 interacting with He for bond lengths r = 1.111 a.u. and 2.463 a.u., for comparison with the results at r = 1.449 a.u., the expectation value of the bond length in the ground vibrational state of H_2.

For r = 1.111 a.u., points on the potential energy surface for H_2–He were computed for a H_2–He separations R from 2.1 a.u. to 20.0 a.u. and for angles θ of the H_2 bond axis (relative to vector from the center of mass of H_2 to the He nucleus) ranging from 0° to 90° in intervals of 5°. The results are listed in Table 5.1.

The results at r = 1.111 a.u. in Table 5.1 were analyzed as before, to determine the coefficients in the spherical tensor expansion of the potential (Equation 4.1), and then converted to the coefficients for $P_0(\cos\theta)$, $P_2(\cos\theta)$, and $P_4(\cos\theta)$ to permit later comparisons with previous calculations. The $c_j(R)$ coefficients are listed for various R values in Table 5.2. A Lennard-Jones potential was derived from the minimum and zero of the potential $V_0(R)$ for r = 1.111 a.u. The Lennard-Jones potential fits $V_0(R)$ in the potential well, but it rises a little too sharply for R ~ 5.0 a.u. and smaller, as shown in Figure 5.1.

Points on the H_2–He potential energy surface at r = 2.463 a.u. were computed for a range of H_2−He separations R out to 20.0 a.u. and angles θ of the H_2 bond axis from 0° to 90° in intervals of 5°. As before, values were also determined for smaller R (down to 0.25 a.u.), covering points on the H−HHe surface and geometrical configurations with the He nucleus between the two H nuclei. Those results are not included in the current chapter. The numerical values of the energy for R from 4.0 a.u. to 20.0 a.u. and the full θ range are provided in Table 5.3. These results were also analyzed to determine the $c_j(R)$ coefficients, which are listed in Table 5.4. The isotropic potential $V_0(R)$ for r = 2.463 a_0 is reasonably well described by the corresponding Lennard-Jones

Table 5.1. CR-CC(2,3) energies of H_2–He for $r_{H-H} = 1.111\ a_0$ with an aug-cc-pV5Z basis, as a function of the separation R between the center of mass of the two H nuclei and the He nucleus, and the angle θ between the H–H vector and the z axis. The He atom is located along the z axis. Entries in blue denote the maximum and entries in bold black denote the minimum of the potential, as a function of the angle θ for each value of R.

	R (in a.u.)				
θ (degs)	2.10	2.20	2.30	2.40	2.50
0	**-3.9065923646**	**-3.9321206229**	**-3.9533049470**	**-3.9709124704**	**-3.9855551108**
5	-3.9069015973	-3.9323639798	-3.9534993277	-3.9710692253	-3.9856824292
10	-3.9078113150	-3.9330816660	-3.9540729011	-3.9715320946	-3.9860584971
15	-3.9092658244	-3.9342323310	-3.9549947930	-3.9722776563	-3.9866654713
20	-3.9111801403	-3.9357534915	-3.9562179221	-3.9732698615	-3.9874749954
25	-3.9134507546	-3.9375677734	-3.9576834976	-3.9744626228	-3.9884507659
30	-3.9159659163	-3.9395900890	-3.9593253585	-3.9758044749	-3.9895522079
35	-3.9186165423	-3.9417360579	-3.9610766723	-3.9772419051	-3.9907360133
40	-3.9213019426	-3.9439256369	-3.9628739669	-3.9787230951	-3.9919597305
45	-3.9239344310	-3.9460871754	-3.9646576221	-3.9801993189	-3.9931834705
50	-3.9264402222	-3.9481581830	-3.9663753085	-3.9816266258	-3.9943702498
55	-3.9287598577	-3.9500872017	-3.9679828505	-3.9829672793	-3.9954881252
60	-3.9308462191	-3.9518316989	-3.9694427219	-3.9841887072	-3.9965091534
65	-3.9326629405	-3.9533578398	-3.9707244270	-3.9852639573	-3.9974098442
70	-3.9341821563	-3.9546391725	-3.9718035500	-3.9861713633	-3.9981713046
75	-3.9353832324	-3.9556552860	-3.9726614019	-3.9868939524	-3.9987784332
80	-3.9362512456	-3.9563913875	-3.9732840858	-3.9874191243	-3.9992200777
85	-3.9367763364	-3.9568374507	-3.9736619099	-3.9877381115	-3.9994884737
90	**-3.9369525295**	**-3.9569873100**	**-3.9737889875**	**-3.9878458619**	**-3.9995795108**

Table 5.1 (cont'd).

	R (in a.u.)				
θ (degs)	2.60	2.70	2.80	3.00	3.50
0	**-3.9977297920**	**-4.0078456072**	**-4.0162425153**	**-4.0289676392**	**-4.0457573906**
5	-3.9978337123	-4.0079305650	-4.0163121235	-4.0290146084	-4.0457745706
10	-3.9981407028	-4.0081821507	-4.0165184915	-4.0291536375	-4.0458256633
15	-3.9986369123	-4.0085891293	-4.0168528196	-4.0293793909	-4.0459086263
20	-3.9993001278	-4.0091336761	-4.0173004712	-4.0296822058	-4.0460199828
25	-4.0001011166	-4.0097924647	-4.0178429028	-4.0300498042	-4.0461556622
30	-4.0010074560	-4.0105392713	-4.0184587069	-4.0304678643	-4.0463103953
35	-4.0019840613	-4.0113456381	-4.0191245381	-4.0309209814	-4.0464782877
40	-4.0029965190	-4.0121834666	-4.0198175608	-4.0313935640	-4.0466541512
45	-4.0040115074	-4.0130249929	-4.0205147346	-4.0318699595	-4.0468319005
50	-4.0049982352	-4.0138447253	-4.0211947949	-4.0323357252	-4.0470061396
55	-4.0059295952	-4.0146197957	-4.0218386703	-4.0327774877	-4.0471718194
60	-4.0067818246	-4.0153300319	-4.0224293528	-4.0331834655	-4.0473243508
65	-4.0075349428	-4.0159584035	-4.0229524889	-4.0335435311	-4.0474597937
70	-4.0081724350	-4.0164907951	-4.0233960829	-4.0338492669	-4.0475748969
75	-4.0086812585	-4.0169160733	-4.0237506183	-4.0340938769	-4.0476671991
80	-4.0090515747	-4.0172258290	-4.0240089692	-4.0342722482	-4.0477345277
85	-4.0092768903	-4.0174143384	-4.0241662030	-4.0343809727	-4.0477755636
90	**-4.0093533638**	**-4.0174784232**	**-4.0242197807**	**-4.0344178666**	**-4.0477896147**

Table 5.1 (cont'd).

	R (in a.u.)				
θ (degs)	4.00	4.50	5.00	5.50	6.00
0	**-4.0519788689**	**-4.0541633106**	**-4.0548759300**	**-4.0550815958**	**-4.0551252007**
5	-4.0519847654	-4.0541651665	-4.0548764194	-4.0550816436	-4.0551251626
10	-4.0520024276	-4.0541706625	-4.0548778587	-4.0550818516	-4.0551250542
15	-4.0520309280	-4.0541796994	-4.0548802418	-4.0550822207	-4.0551248812
20	-4.0520698799	-4.0541919442	-4.0548834834	-4.0550827247	-4.0551246537
25	-4.0521170304	-4.0542068928	-4.0548874663	-4.0550833408	-4.0551243851
30	-4.0521707972	-4.0542239563	-4.0548920428	-4.0550840322	-4.0551240927
35	-4.0522293997	-4.0542426988	-4.0548970362	-4.0550847598	-4.0551237971
40	-4.0522908041	-4.0542620894	-4.0549021565	-4.0550854916	-4.0551234349
45	-4.0523529205	-4.0542816803	-4.0549073786	-4.0550862430	-4.0551230548
50	-4.0524138273	-4.0543009143	-4.0549125235	-4.0550869984	-4.0551226827
55	-4.0524716801	-4.0543192730	-4.0549174138	-4.0550877098	-4.0551223180
60	-4.0525249033	-4.0543362576	-4.0549219257	-4.0550883657	-4.0551219946
65	-4.0525722739	-4.0543513427	-4.0549259247	-4.0550889467	-4.0551216999
70	-4.0526125386	-4.0543641127	-4.0549293233	-4.0550894343	-4.0551214398
75	-4.0526447969	-4.0543743457	-4.0549320436	-4.0550898161	-4.0551212224
80	-4.0526683098	-4.0543818224	-4.0549340342	-4.0550900913	-4.0551210599
85	-4.0526827610	-4.0543863804	-4.0549352584	-4.0550902707	-4.0551209627
90	**-4.0526876655**	**-4.0543879658**	**-4.0549357216**	**-4.0550903444**	**-4.0551209362**

Table 5.1 (cont'd).

	R (in a.u.)				
θ (degs)	6.05	6.10	6.15	6.20	6.25
0	**-4.0551260866**	**-4.0551266313**	**-4.0551268782**	**-4.0551268722**	**-4.0551266492**
5	-4.0551260457	-4.0551265866	-4.0551268319	-4.0551268234	-4.0551265983
10	-4.0551259265	-4.0551264587	-4.0551266969	-4.0551266828	-4.0551264548
15	-4.0551257350	-4.0551262527	-4.0551264820	-4.0551264653	-4.0551262380
20	-4.0551254836	-4.0551259873	-4.0551262099	-4.0551261869	-4.0551259523
25	-4.0551251954	-4.0551256800	-4.0551258838	-4.0551258461	-4.0551256035
30	-4.0551248702	-4.0551253254	-4.0551255623	-4.0551255099	-4.0551252584
35	-4.0551245409	-4.0551249682	-4.0551251287	-4.0551250625	-4.0551248011
40	-4.0551241374	-4.0551245376	-4.0551246758	-4.0551245920	-4.0551243184
45	-4.0551237225	-4.0551240930	-4.0551242094	-4.0551241086	-4.0551238218
50	-4.0551233116	-4.0551236515	-4.0551237433	-4.0551236230	-4.0551233216
55	-4.0551229093	-4.0551232207	-4.0551232907	-4.0551231541	-4.0551228413
60	-4.0551225479	-4.0551228302	-4.0551228782	-4.0551227248	-4.0551223993
65	-4.0551222253	-4.0551224815	-4.0551225071	-4.0551223360	-4.0551219974
70	-4.0551219394	-4.0551221747	-4.0551221832	-4.0551219983	-4.0551216488
75	-4.0551217009	-4.0551219191	-4.0551219141	-4.0551217184	-4.0551213606
80	-4.0551215227	-4.0551217284	-4.0551217132	-4.0551215094	-4.0551211454
85	-4.0551214157	-4.0551216135	-4.0551215917	-4.0551213826	-4.0551210141
90	**-4.0551213865**	**-4.0551215820**	**-4.0551215586**	**-4.0551213479**	**-4.0551209784**

Table 5.1 (cont'd).

	R (in a.u.)				
θ (degs)	6.30	6.35	6.40	6.45	6.50
0	**-4.0551262430**	**-4.0551256841**	**-4.0551249957**	**-4.0551242020**	**-4.0551233217**
5	-4.0551261894	-4.0551256266	-4.0551249373	-4.0551241463	-4.0551232692
10	-4.0551260472	-4.0551254887	-4.0551248002	-4.0551240094	-4.0551231353
15	-4.0551258305	-4.0551252702	-4.0551245841	-4.0551237959	-4.0551229214
20	-4.0551255383	-4.0551249793	-4.0551242955	-4.0551235071	-4.0551226345
25	-4.0551251887	-4.0551246258	-4.0551239381	-4.0551231389	-4.0551222837
30	-4.0551248360	-4.0551242695	-4.0551235831	-4.0551227977	-4.0551219316
35	-4.0551243719	-4.0551238015	-4.0551231141	-4.0551223307	-4.0551214693
40	-4.0551238815	-4.0551233076	-4.0551226197	-4.0551218383	-4.0551209809
45	-4.0551233763	-4.0551227974	-4.0551221070	-4.0551213273	-4.0551204742
50	-4.0551228669	-4.0551222834	-4.0551215929	-4.0551208145	-4.0551199646
55	-4.0551223792	-4.0551217915	-4.0551210994	-4.0551203216	-4.0551194746
60	-4.0551219286	-4.0551213355	-4.0551206407	-4.0551198624	-4.0551190164
65	-4.0551215173	-4.0551209183	-4.0551202201	-4.0551194405	-4.0551185948
70	-4.0551211606	-4.0551205560	-4.0551198546	-4.0551190734	-4.0551182277
75	-4.0551208660	-4.0551202569	-4.0551195528	-4.0551187705	-4.0551179242
80	-4.0551206458	-4.0551200331	-4.0551193267	-4.0551185434	-4.0551176959
85	-4.0551205110	-4.0551198955	-4.0551191873	-4.0551184026	-4.0551175571
90	**-4.0551204745**	**-4.0551198584**	**-4.0551191491**	**-4.0551183635**	**-4.0551175165**

Table 5.1 (cont'd).

	R (in a.u.)				
θ (degs)	6.55	6.60	6.65	6.70	6.75
0	**-4.0551223732**	**-4.0551213696**	**-4.0551203253**	**-4.0551192499**	**-4.0551181530**
5	-4.0551223226	-4.0551213209	-4.0551202781	-4.0551192040	-4.0551181086
10	-4.0551221898	-4.0551211901	-4.0551201491	-4.0551190765	-4.0551179848
15	-4.0551219784	-4.0551209818	-4.0551199442	-4.0551188749	-4.0551177841
20	-4.0551216925	-4.0551206950	-4.0551196699	-4.0551186085	-4.0551175262
25	-4.0551213496	-4.0551203629	-4.0551193362	-4.0551182815	-4.0551172065
30	-4.0551210013	-4.0551200219	-4.0551190042	-4.0551179576	-4.0551168914
35	-4.0551205457	-4.0551195732	-4.0551185633	-4.0551175257	-4.0551164686
40	-4.0551200628	-4.0551190970	-4.0551180948	-4.0551170669	-4.0551160208
45	-4.0551195615	-4.0551186026	-4.0551176088	-4.0551165901	-4.0551155526
50	-4.0551190580	-4.0551181067	-4.0551171211	-4.0551161121	-4.0551150878
55	-4.0551185724	-4.0551176272	-4.0551166495	-4.0551156486	-4.0551146319
60	-4.0551181168	-4.0551171749	-4.0551162039	-4.0551152101	-4.0551142012
65	-4.0551176970	-4.0551167589	-4.0551157908	-4.0551148025	-4.0551138001
70	-4.0551173308	-4.0551163952	-4.0551154302	-4.0551144443	-4.0551134459
75	-4.0551170281	-4.0551160941	-4.0551151316	-4.0551141492	-4.0551131539
80	-4.0551168013	-4.0551158685	-4.0551149076	-4.0551139273	-4.0551129351
85	-4.0551166622	-4.0551157296	-4.0551147698	-4.0551137907	-4.0551128001
90	**-4.0551166208**	**-4.0551156882**	**-4.0551147280**	**-4.0551137489**	**-4.0551127585**

Table 5.1 (cont'd).

	R (in a.u.)				
θ (degs)	6.80	6.90	7.00	7.10	7.20
0	**-4.0551170433**	**-4.0551148114**	**-4.0551125986**	**-4.0551104439**	**-4.0551083574**
5	-4.0551169999	-4.0551147696	-4.0551125583	-4.0551104035	-4.0551083221
10	-4.0551168790	-4.0551146547	-4.0551124482	-4.0551103032	-4.0551082270
15	-4.0551166833	-4.0551144733	-4.0551122803	-4.0551101435	-4.0551080766
20	-4.0551164314	-4.0551142313	-4.0551120531	-4.0551099299	-4.0551078764
25	-4.0551161194	-4.0551139360	-4.0551117758	-4.0551096702	-4.0551076320
30	-4.0551158134	-4.0551136477	-4.0551115059	-4.0551094153	-4.0551073957
35	-4.0551154008	-4.0551132578	-4.0551111390	-4.0551090719	-4.0551070730
40	-4.0551149644	-4.0551128439	-4.0551107500	-4.0551087053	-4.0551067334
45	-4.0551145088	-4.0551124140	-4.0551103430	-4.0551083228	-4.0551063768
50	-4.0551140535	-4.0551119801	-4.0551099331	-4.0551079342	-4.0551060138
55	-4.0551136060	-4.0551115552	-4.0551095284	-4.0551075547	-4.0551056543
60	-4.0551131839	-4.0551111503	-4.0551091420	-4.0551071870	-4.0551053092
65	-4.0551127897	-4.0551107681	-4.0551087759	-4.0551068409	-4.0551049821
70	-4.0551124416	-4.0551104322	-4.0551084540	-4.0551065348	-4.0551046917
75	-4.0551121524	-4.0551101540	-4.0551081878	-4.0551062804	-4.0551044499
80	-4.0551119371	-4.0551099450	-4.0551079882	-4.0551060901	-4.0551042691
85	-4.0551118040	-4.0551098175	-4.0551078654	-4.0551059736	-4.0551041591
90	**-4.0551117629**	**-4.0551097775**	**-4.0551078275**	**-4.0551059376**	**-4.0551041253**

Table 5.1 (cont'd).

	R (in a.u.)				
θ (degs)	7.30	7.40	7.50	8.00	8.50
0	**-4.0551063637**	**-4.0551044702**	**-4.0551026818**	**-4.0550953269**	**-4.0550902881**
5	-4.0551063314	-4.0551044411	-4.0551026551	-4.0550953083	-4.0550902748
10	-4.0551062436	-4.0551043595	-4.0551025795	-4.0550952560	-4.0550902376
15	-4.0551061037	-4.0551042293	-4.0551024586	-4.0550951721	-4.0550901787
20	-4.0551059167	-4.0551040546	-4.0551022965	-4.0550950595	-4.0550901534
25	-4.0551056858	-4.0551038967	-4.0551021494	-4.0550949655	-4.0550900504
30	-4.0551054686	-4.0551036378	-4.0551019093	-4.0550948022	-4.0550899356
35	-4.0551051680	-4.0551033580	-4.0551016494	-4.0550946243	-4.0550898118
40	-4.0551048489	-4.0551030605	-4.0551013727	-4.0550944355	-4.0550896820
45	-4.0551045158	-4.0551027502	-4.0551010839	-4.0550942387	-4.0550895486
50	-4.0551041765	-4.0551024337	-4.0551007895	-4.0550940384	-4.0550894151
55	-4.0551038400	-4.0551021192	-4.0551004966	-4.0550938396	-4.0550892845
60	-4.0551035164	-4.0551018170	-4.0551002149	-4.0550936503	-4.0550891629
65	-4.0551032087	-4.0551015287	-4.0550999456	-4.0550934696	-4.0550890465
70	-4.0551029354	-4.0551012725	-4.0550997061	-4.0550933110	-4.0550889450
75	-4.0551027070	-4.0551010580	-4.0550995078	-4.0550931796	-4.0550888608
80	-4.0551025366	-4.0551008990	-4.0550993599	-4.0550930803	-4.0550887978
85	-4.0551024335	-4.0551008031	-4.0550992703	-4.0550930181	-4.0550887594
90	**-4.0551024014**	**-4.0551007726**	**-4.0550992414**	**-4.0550929997**	**-4.0550887474**

Table 5.1 (cont'd).

	R (in a.u.)				
θ (degs)	9.00	9.50	10.00	10.50	11.00
0	**-4.0550869299**	-4.0550846847	**-4.0550832084**	**-4.0550821160**	**-4.0550813502**
5	-4.0550869204	-4.0550846784	-4.0550832021	-4.0550821112	-4.0550813461
10	-4.0550868938	-4.0550846600	-4.0550831840	-4.0550820974	-4.0550813341
15	-4.0550868522	**-4.0550846972**	-4.0550831564	-4.0550820765	-4.0550813161
20	-4.0550868574	-4.0550846473	-4.0550831209	-4.0550820498	-4.0550812936
25	-4.0550867807	-4.0550845897	-4.0550830792	-4.0550820185	-4.0550812664
30	-4.0550866963	-4.0550845268	-4.0550830331	-4.0550819840	-4.0550812384
35	-4.0550866069	-4.0550844602	-4.0550829839	-4.0550819470	-4.0550812090
40	-4.0550865149	-4.0550843924	-4.0550829332	-4.0550819085	-4.0550811789
45	-4.0550864221	-4.0550843245	-4.0550828817	-4.0550818687	-4.0550811483
50	-4.0550863309	-4.0550842578	-4.0550828309	-4.0550818292	-4.0550811178
55	-4.0550862427	-4.0550841940	-4.0550827816	-4.0550817906	-4.0550810879
60	-4.0550861613	-4.0550841357	-4.0550827371	-4.0550817557	-4.0550810612
65	-4.0550860828	-4.0550840784	-4.0550826921	-4.0550817196	-4.0550810324
70	-4.0550860150	-4.0550840291	-4.0550826541	-4.0550816897	-4.0550810084
75	-4.0550859591	-4.0550839878	-4.0550826222	-4.0550816650	-4.0550809885
80	-4.0550859169	-4.0550839565	-4.0550825981	-4.0550816463	-4.0550809736
85	-4.0550858908	-4.0550839369	-4.0550825831	-4.0550816348	-4.0550809643
90	**-4.0550858827**	**-4.0550839308**	**-4.0550825783**	**-4.0550816313**	**-4.0550809614**

Table 5.1 (cont'd).

	R (in a.u.)			
θ (degs)	12.00	14.00	17.00	20.00
0	**-4.0550803886**	**-4.0550795063**	**-4.0550791276**	**-4.0550790275**
5	-4.0550803852	-4.0550795055	-4.0550791275	-4.0550790274
10	-4.0550803759	-4.0550795032	-4.0550791266	-4.0550790273
15	-4.0550803613	-4.0550794994	-4.0550791251	-4.0550790271
20	-4.0550803438	-4.0550794943	-4.0550791240	-4.0550790268
25	-4.0550803245	-4.0550794886	-4.0550791227	-4.0550790264
30	-4.0550803034	-4.0550794824	-4.0550791218	-4.0550790260
35	-4.0550802835	-4.0550794756	-4.0550791203	-4.0550790255
40	-4.0550802646	-4.0550794685	-4.0550791184	-4.0550790251
45	-4.0550802462	-4.0550794611	-4.0550791172	-4.0550790245
50	-4.0550802292	-4.0550794540	-4.0550791156	-4.0550790240
55	-4.0550802160	-4.0550794470	-4.0550791128	-4.0550790235
60	-4.0550802015	-4.0550794421	-4.0550791132	-4.0550790253
65	-4.0550801845	-4.0550794344	-4.0550791097	-4.0550790226
70	-4.0550801684	-4.0550794291	-4.0550791085	-4.0550790222
75	-4.0550801542	-4.0550794246	-4.0550791076	-4.0550790219
80	-4.0550801399	-4.0550794208	-4.0550791069	-4.0550790217
85	-4.0550801335	-4.0550794187	-4.0550791065	-4.0550790216
90	**-4.0550801312**	**-4.0550794181**	**-4.0550791063**	**-4.0550790215**

Table 5.2. Spherical harmonic coefficients from the Mathematica fit to the ground-state potential of H_2–He with an H–H separation r = 1.111 a_0.

R	2.10	2.20	2.30	2.40	2.50
c_0	1.59739E+00	1.32673E+00	1.10001E+00	9.10401E-01	7.52107E-01
c_2	1.08252E-01	8.93281E-02	7.40065E-02	6.14467E-02	5.10631E-02
c_4	7.85539E-03	5.60112E-03	4.07862E-03	3.02680E-03	2.28436E-03
c_6	7.37945E-04	4.73892E-04	3.09281E-04	2.05688E-04	1.38486E-04
c_8	5.97903E-05	3.45172E-05	1.93151E-05	1.04530E-05	5.47833E-06
c_{10}	5.21734E-06	3.63335E-06	2.41771E-06	1.40546E-06	6.22677E-07

R	2.60	2.70	2.80	3.00	3.50
c_0	6.20191E-01	5.10453E-01	4.19328E-01	2.81292E-01	9.97264E-02
c_2	4.24330E-02	3.52370E-02	2.92270E-02	2.00120E-02	7.48202E-03
c_4	1.74949E-03	1.35635E-03	1.06306E-03	6.67043E-04	2.21608E-04
c_6	9.40285E-05	6.45158E-05	4.53354E-05	2.45361E-05	5.31168E-06
c_8	2.44766E-06	1.18304E-06	2.98888E-07	-5.95675E-07	-4.42788E-07
c_{10}	5.64806E-07	8.29245E-07	4.88682E-07	6.41235E-08	3.12977E-07

Table 5.2 (cont'd).

R	4.00	4.50	5.00	5.50	6.00
c_0	3.28899E-02	9.58521E-03	2.04111E-03	-1.07500E-04	-5.44445E-04
c_2	2.61253E-03	8.28673E-04	2.20576E-04	3.21001E-05	-1.58351E-05
c_4	7.53677E-05	2.33551E-05	6.20139E-06	1.14196E-06	2.43356E-08
c_6	1.09025E-06	5.30495E-07	1.48499E-07	9.60173E-08	-1.04319E-08
c_8	-8.04865E-07	-1.27520E-07	-1.44155E-07	5.85647E-08	-2.66095E-08
c_{10}	5.42129E-08	-5.00455E-07	-1.38949E-07	-7.58031E-08	-9.30476E-08

R	6.05	6.10	6.15	6.20	6.25
c_0	-5.51910E-04	-5.55822E-04	-5.56718E-04	-5.54975E-04	-5.51008E-04
c_2	-1.74687E-05	-1.87757E-05	-1.98467E-05	-2.06339E-05	-2.12099E-05
c_4	1.70803E-08	1.97675E-08	2.73900E-08	5.34525E-08	8.74432E-08
c_6	2.51638E-09	3.29622E-09	4.14234E-08	4.32053E-08	4.70958E-08
c_8	-2.86377E-08	-3.31028E-08	8.44686E-10	1.57419E-09	3.95251E-09
c_{10}	-1.00576E-07	-9.73272E-08	-1.12444E-07	-1.07404E-07	-1.05123E-07

Table 5.2 (cont'd).

R	6.30	6.35	6.40	6.45	6.50
c_0	-5.45157E-04	-5.37723E-04	-5.28972E-04	-5.19136E-04	-5.08434E-04
c_2	-2.16000E-05	-2.18320E-05	-2.19260E-05	-2.19018E-05	-2.18064E-05
c_4	1.24412E-07	1.60055E-07	1.97154E-07	2.39839E-07	2.74776E-07
c_6	4.53245E-08	3.87408E-08	3.06238E-08	1.73204E-08	1.07174E-08
c_8	8.93685E-09	1.45387E-08	1.89585E-08	1.15960E-08	1.66762E-08
c_{10}	-1.02175E-07	-9.71340E-08	-9.29910E-08	-9.25514E-08	-8.43784E-08

R	6.55	6.60	6.65	6.70	6.75
c_0	-4.97028E-04	-4.85081E-04	-4.72732E-04	-4.60090E-04	-4.47256E-04
c_2	-2.16182E-05	-2.13619E-05	-2.10593E-05	-2.07058E-05	-2.03128E-05
c_4	3.17107E-07	3.60376E-07	3.96373E-07	4.37366E-07	4.73463E-07
c_6	1.67082E-09	-6.16299E-09	-1.87583E-08	-2.98631E-08	-4.19412E-08
c_8	1.34198E-08	1.09043E-08	1.33650E-08	1.27199E-08	1.11349E-08
c_{10}	-8.37724E-08	-8.67490E-08	-8.04122E-08	-7.94149E-08	-7.74909E-08

Table 5.2 (cont'd).

R	6.80	6.90	7.00	7.10	7.20
c_0	-4.34318E-04	-4.08422E-04	-3.82880E-04	-3.58032E-04	-3.34124E-04
c_2	-1.98924E-05	-1.89852E-05	-1.80223E-05	-1.70295E-05	-1.60020E-05
c_4	5.07612E-07	5.66385E-07	6.10265E-07	6.17428E-07	6.30429E-07
c_6	-5.04744E-08	-6.83157E-08	-6.79327E-08	-7.47860E-08	-8.80980E-08
c_8	7.71415E-09	-2.23036E-09	-9.91769E-09	-9.38603E-09	-1.73560E-08
c_{10}	-7.57547E-08	-6.33846E-08	-5.86280E-08	-5.47754E-08	-4.72901E-08

R	7.30	7.40	7.50	8.00	8.50
c_0	-3.11321E-04	-2.89739E-04	-2.69372E-04	-1.85940E-04	-1.28928E-04
c_2	-1.49941E-05	-1.40472E-05	-1.30767E-05	-8.83244E-06	-5.86571E-06
c_4	6.18176E-07	5.71402E-07	5.39760E-07	3.32724E-07	1.15250E-07
c_6	-8.86426E-08	-6.99892E-08	-6.27032E-08	-2.73644E-08	-1.86238E-09
c_8	-1.59953E-08	1.84169E-08	1.44463E-08	1.52584E-08	4.42509E-08
c_{10}	-4.28111E-08	-2.31273E-08	-2.01681E-08	-2.66998E-08	1.05834E-08

Table 5.2 (cont'd).

R	9.00	9.50	10.00	10.50	11.00
c_0	-9.07711E-05	-6.50381E-05	-4.72760E-05	-3.47998E-05	-2.59649E-05
c_2	-4.01260E-06	-2.96025E-06	-2.28375E-06	-1.76861E-06	-1.39606E-06
c_4	4.26402E-08	5.86605E-09	-1.68064E-08	2.61081E-09	-4.24859E-09
c_6	1.55800E-08	-3.70056E-09	-4.35711E-08	-2.90859E-08	-3.71358E-08
c_8	5.65461E-08	6.38697E-08	-1.65339E-09	-5.42745E-09	-6.60044E-09
c_{10}	1.43751E-08	6.40840E-08	-2.69443E-09	-1.85791E-09	-9.49251E-11

R	12.00	14.00	17.00	20.00
c_0	-1.49793E-05	-5.35072E-06	-1.15367E-06	-2.75388E-08
c_2	-8.65472E-07	-3.21065E-07	-7.70113E-08	-2.17637E-08
c_4	-1.30559E-08	7.63906E-10	2.75824E-09	1.84501E-09
c_6	-7.13066E-08	-7.54007E-09	-1.30832E-09	-2.53821E-09
c_8	1.03553E-08	6.53633E-10	-2.39307E-09	3.04635E-10
c_{10}	-1.46285E-09	-2.83036E-10	-3.16756E-10	1.02332E-09

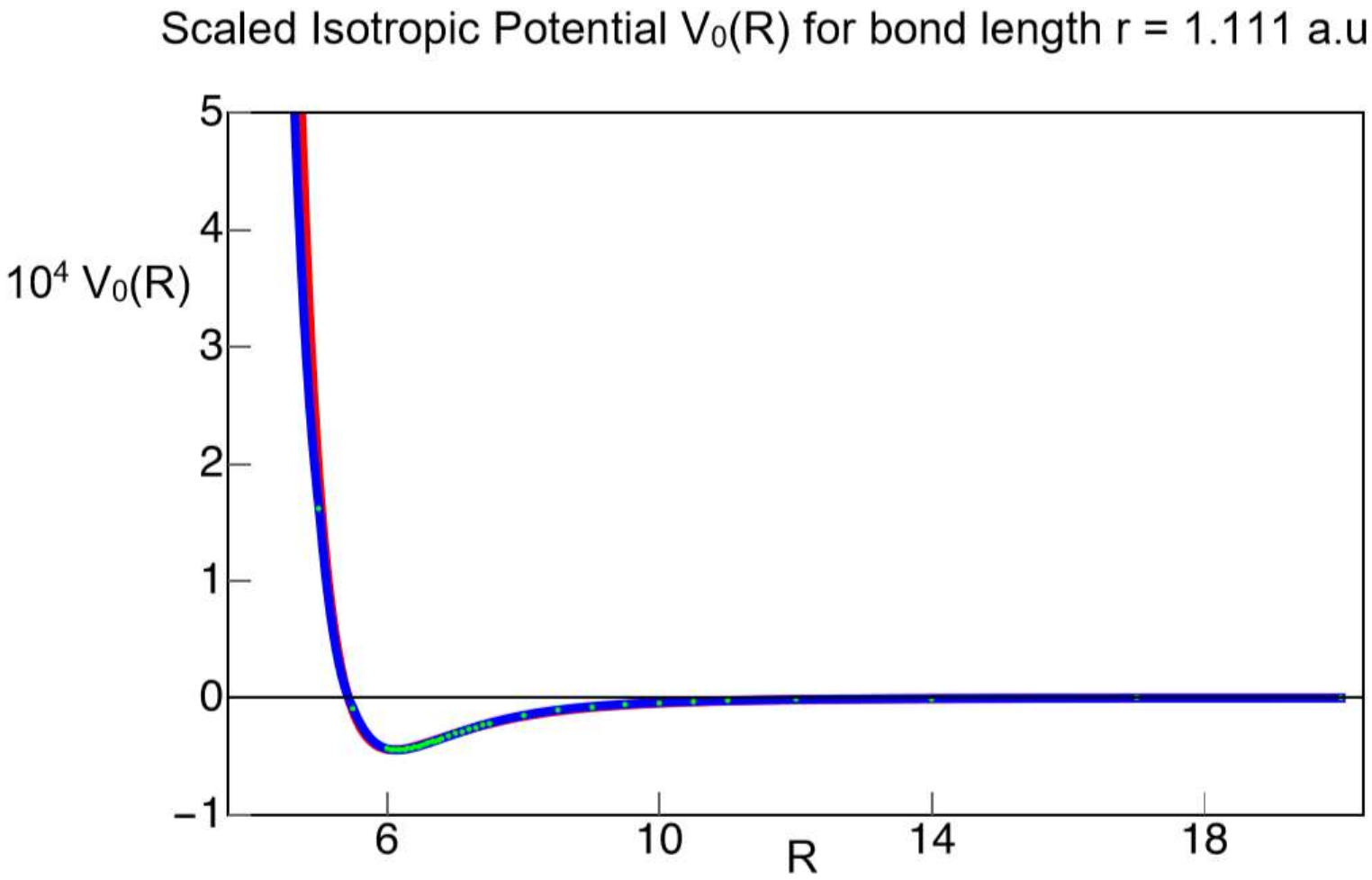

Figure 5.1. Isotropic potential $V_0(R)$ in a.u. multiplied by 104, for H_2–He at an H_2 bond length of r = 1.111 a.u. (in blue), compared with Lennard-Jones potential (in red), and the *ab initio* data points for $V_0(R)$, shown in green. The Lennard-Jones parameters are ε = 0.000443057 a.u. and σ = 5.43316 a.u. The minimum of the isotropic potential is located at r_e = 6.14089 a.u.

Table 5.3. CR-CC(2,3) energies of H_2–He for $r_{H–H}$ = 2.463 a_0 obtained with an aug-cc-pV5Z basis, as a function of the separation R between the center of mass of the two H nuclei and the He nucleus, and the angle θ between the H–H vector and the z axis. The He atom is located along the z axis. Entries in blue denote the maximum and entries in bold black denote the minimum of the potential, as a function of the angle θ for each R value.

	R (in a.u.)				
θ (degs)	2.60	2.70	2.80	2.90	3.00
0	**-3.8777669974**	**-3.8965288367**	**-3.9118555420**	**-3.9246405484**	**-3.9354673141**
5	-3.8790632722	-3.8974968548	-3.9126070417	-3.9252432323	-3.9359629632
10	-3.8827097845	-3.9002490173	-3.9147618537	-3.9269833403	-3.9374014681
15	-3.8881016097	-3.9043911919	-3.9180550670	-3.9296753371	-3.9396464778
20	-3.8944962536	-3.9094327933	-3.9221481314	-3.9330725547	-3.9425116187
25	-3.9012709855	-3.9149285767	-3.9267100362	-3.9369227892	-3.9457969359
30	-3.9080092266	-3.9205509711	-3.9314755822	-3.9410046491	-3.9493154014
35	-3.9144791849	-3.9260804081	-3.9362436854	-3.9451366969	-3.9529043566
40	-3.9205671813	-3.9313759568	-3.9408653050	-3.9491747049	-3.9564301298
45	-3.9262093030	-3.9363413367	-3.9452314606	-3.9530072301	-3.9597863669
50	-3.9313585077	-3.9409012294	-3.9492573440	-3.9565492816	-3.9628911457
55	-3.9359715235	-3.9449978105	-3.9528790254	-3.9597371623	-3.9656855019
60	-3.9400115675	-3.9485876907	-3.9560530871	-3.9625297459	-3.9681314181
65	-3.9434500937	-3.9516417060	-3.9587510061	-3.9649013280	-3.9702064429
70	-3.9462705286	-3.9541438249	-3.9609589087	-3.9668398190	-3.9719003725
75	-3.9484633532	-3.9560866673	-3.9626708850	-3.9683409862	-3.9732108230
80	-3.9500276102	-3.9574708316	-3.9638891405	-3.9694082669	-3.9741418573
85	-3.9509650262	-3.9582997231	-3.9646181779	-3.9700465422	-3.9746980661
90	**-3.9512780138**	**-3.9585769419**	**-3.9648622829**	**-3.9702600229**	**-3.9748838968**

Table 5.3 (cont'd).

	R (in a.u.)				
θ (degs)	3.25	3.50	4.00	4.50	5.00
0	**-3.9562609243**	**-3.9706507832**	**-3.9873877445**	**-3.9949747559**	**-3.9981969195**
5	-3.9565857311	-3.9708716516	-3.9874883094	-3.9950176926	-3.9982140947
10	-3.9575338670	-3.9715179055	-3.9877830343	-3.9951436575	-3.9982641860
15	-3.9590323368	-3.9725425620	-3.9882509767	-3.9953435326	-3.9983435084
20	-3.9609737966	-3.9738760785	-3.9888606995	-3.9956037498	-3.9984464169
25	-3.9632325393	-3.9754344673	-3.9895736756	-3.9959072342	-3.9985665310
30	-3.9656814582	-3.9771303185	-3.9903480269	-3.9962364939	-3.9986965431
35	-3.9682025135	-3.9788789810	-3.9911458054	-3.9965744668	-3.9988295472
40	-3.9706931067	-3.9806070889	-3.9919322178	-3.9969062585	-3.9989597439
45	-3.9730685619	-3.9822550423	-3.9926789886	-3.9972201757	-3.9990823619
50	-3.9752669066	-3.9837766156	-3.9933656404	-3.9975075542	-3.9991940977
55	-3.9772421352	-3.9851411898	-3.9939781340	-3.9977628908	-3.9992928767
60	-3.9789666618	-3.9863291751	-3.9945085952	-3.9979830112	-3.9993776838
65	-3.9804251877	-3.9873311033	-3.9949538041	-3.9981669038	-3.9994482069
70	-3.9816127348	-3.9881445702	-3.9953135802	-3.9983150114	-3.9995047344
75	-3.9825294239	-3.9887712917	-3.9955894762	-3.9984283081	-3.9995477667
80	-3.9831795013	-3.9892150951	-3.9957843146	-3.9985080761	-3.9995779676
85	-3.9835671431	-3.9894796865	-3.9959003365	-3.9985554272	-3.9995959561
90	**-3.9836967008**	**-3.9895680149**	**-3.9959392553**	**-3.9985714221**	**-3.9996020572**

Table 5.3 (cont'd).

	R (in a.u.)				
θ (degs)	5.50	6.00	6.05	6.10	6.15
0	**-3.9994751445**	**-3.9999435513**	**-3.9999681589**	**-3.9999901031**	**-4.0000096334**
5	-3.9994814125	-3.9999455355	-3.9999698989	-3.9999915964	-4.0000109280
10	-3.9994997597	-3.9999515235	-3.9999752085	-3.9999963322	-4.0000151157
15	-3.9995288794	-3.9999610446	-3.9999836515	-4.0000037858	-4.0000216826
20	-3.9995665670	-3.9999733484	-3.9999945263	-4.0000133750	-4.0000301163
25	-3.9996104939	-3.9999875661	-4.0000071034	-4.0000244740	-4.0000398839
30	-3.9996578189	-4.0000028088	-4.0000205775	-4.0000363503	-4.0000503140
35	-3.9997060234	-4.0000181391	-4.0000340853	-4.0000482230	-4.0000607258
40	-3.9997528165	-4.0000329089	-4.0000470924	-4.0000596422	-4.0000707173
45	-3.9997966809	-4.0000465421	-4.0000590809	-4.0000701510	-4.0000798938
50	-3.9998363871	-4.0000587815	-4.0000698081	-4.0000795099	-4.0000880209
55	-3.9998711414	-4.0000692382	-4.0000789348	-4.0000874461	-4.0000948911
60	-3.9999007176	-4.0000779580	-4.0000865276	-4.0000940273	-4.0001005649
65	-3.9999252125	-4.0000850385	-4.0000926703	-4.0000993297	-4.0001051151
70	-3.9999447130	-4.0000905908	-4.0000974717	-4.0001034571	-4.0001086371
75	-3.9999594655	-4.0000947530	-4.0001010602	-4.0001065289	-4.0001112533
80	-3.9999697047	-4.0000975543	-4.0001034642	-4.0001085817	-4.0001129868
85	-3.9999758692	-4.0000992183	**-4.0001048874**	-4.0001098022	-4.0001140222
90	**-3.9999779770**	**-4.0000998910**	**-4.0001054874**	**-4.0001103235**	**-4.0001144769**

Table 5.3 (cont'd).

	R (in a.u.)				
θ (degs)	6.20	6.25	6.30	6.35	6.40
0	**-4.0000269843**	**-4.0000423598**	**-4.0000559551**	**-4.0000679405**	**-4.0000784782**
5	-4.0000281579	-4.0000434014	-4.0000568693	-4.0000687373	-4.0000791638
10	-4.0000317879	-4.0000465518	-4.0000595944	-4.0000710865	-4.0000811831
15	-4.0000375570	-4.0000516049	-4.0000640058	-4.0000749226	-4.0000845035
20	-4.0000449535	-4.0000580719	-4.0000696392	-4.0000798087	-4.0000887196
25	-4.0000535200	-4.0000655533	-4.0000761471	-4.0000854576	-4.0000936061
30	-4.0000626389	-4.0000735029	-4.0000830735	-4.0000914587	-4.0000987674
35	-4.0000717546	-4.0000814549	-4.0000899559	-4.0000973788	-4.0001038317
40	-4.0000804612	-4.0000890060	-4.0000964721	-4.0001029685	-4.0001085958
45	-4.0000884393	-4.0000959066	-4.0001024049	-4.0001080335	-4.0001128820
50	-4.0000954616	-4.0001019403	-4.0001075551	-4.0001123957	-4.0001165427
55	-4.0001013773	-4.0001070020	-4.0001118538	-4.0001160110	-4.0001195520
60	-4.0001062330	-4.0001111347	-4.0001153379	-4.0001189185	-4.0001219430
65	-4.0001101153	-4.0001144103	-4.0001180719	-4.0001211723	-4.0001237722
70	-4.0001130952	-4.0001169073	-4.0001201411	-4.0001228591	-4.0001251171
75	-4.0001153034	-4.0001187502	-4.0001216584	-4.0001240860	-4.0001260858
80	-4.0001167531	-4.0001199531	-4.0001226432	-4.0001248772	-4.0001267024
85	-4.0001176218	-4.0001206686	-4.0001232218	-4.0001253341	-4.0001270536
90	**-4.0001180182**	**-4.0001210120**	**-4.0001235167**	**-4.0001255852**	**-4.0001272654**

Table 5.3 (cont'd).

	R (in a.u.)				
θ (degs)	6.45	6.50	6.55	6.60	6.65
0	**-4.0000877103**	**-4.0000957679**	**-4.0001027750**	**-4.0001088363**	**-4.0001140502**
5	-4.0000882946	-4.0000962618	-4.0001031868	-4.0001091766	-4.0001143286
10	-4.0000900241	-4.0000977356	-4.0001044319	-4.0001102171	-4.0001151856
15	-4.0000928829	-4.0001001827	-4.0001065134	-4.0001119735	-4.0001166493
20	-4.0000964983	-4.0001032590	-4.0001091021	-4.0001141358	-4.0001184615
25	-4.0001007012	-4.0001068500	-4.0001121481	-4.0001166876	-4.0001205520
30	-4.0001051116	-4.0001105923	-4.0001152986	-4.0001193104	-4.0001227024
35	-4.0001094159	-4.0001142210	-4.0001183263	-4.0001218042	-4.0001247223
40	-4.0001134438	-4.0001175899	-4.0001211065	-4.0001240614	-4.0001265178
45	-4.0001170319	-4.0001205578	-4.0001235281	-4.0001260031	-4.0001280355
50	-4.0001200684	-4.0001230427	-4.0001255212	-4.0001275592	-4.0001292054
55	-4.0001225373	-4.0001250284	-4.0001270796	-4.0001287403	-4.0001300537
60	-4.0001244723	-4.0001265566	-4.0001282481	-4.0001295898	-4.0001306209
65	-4.0001259207	-4.0001276691	-4.0001290647	-4.0001301455	-4.0001309486
70	-4.0001269672	-4.0001284537	-4.0001296170	-4.0001304941	-4.0001311185
75	-4.0001277058	-4.0001289898	-4.0001299742	-4.0001306928	-4.0001311772
80	-4.0001281649	-4.0001293081	-4.0001301682	-4.0001307770	-4.0001311648
85	-4.0001284237	-4.0001294829	-4.0001302671	-4.0001308097	-4.0001311402
90	**-4.0001286007**	**-4.0001296305**	**-4.0001303899**	**-4.0001309103**	**-4.0001312205**

Table 5.3 (cont'd).

	R (in a.u.)				
θ (degs)	6.70	6.75	6.80	6.85	6.90
0	**-4.0001185096**	**-4.0001222980**	**-4.0001254821**	**-4.0001281300**	**-4.0001303027**
5	-4.0001187323	-4.0001224684	-4.0001256096	-4.0001282214	-4.0001303614
10	-4.0001194243	-4.0001230147	-4.0001260292	-4.0001285307	-4.0001305751
15	-4.0001206068	-4.0001239724	-4.0001267860	-4.0001291078	-4.0001309934
20	-4.0001221124	-4.0001251819	-4.0001277309	-4.0001298168	-4.0001314930
25	-4.0001238125	-4.0001265337	-4.0001287746	-4.0001305878	-4.0001320202
30	-4.0001255421	-4.0001278903	-4.0001298014	-4.0001313247	-4.0001325047
35	-4.0001271426	-4.0001291190	-4.0001306951	-4.0001319320	-4.0001328635
40	-4.0001285354	-4.0001301608	-4.0001314319	-4.0001323920	-4.0001330790
45	-4.0001296735	-4.0001309614	-4.0001319398	-4.0001326452	**-4.0001331102**
50	-4.0001305042	-4.0001314952	-4.0001322143	**-4.0001326940**	-4.0001329636
55	-4.0001310632	-4.0001317971	**-4.0001322902**	-4.0001325724	-4.0001326702
60	-4.0001313810	**-4.0001318993**	-4.0001322050	-4.0001323227	-4.0001322824
65	-4.0001315069	-4.0001318508	-4.0001320076	-4.0001319982	-4.0001318448
70	**-4.0001315199**	-4.0001317256	-4.0001317602	-4.0001316458	-4.0001314024
75	-4.0001314559	-4.0001315548	-4.0001314970	-4.0001313035	-4.0001309929
80	-4.0001313589	-4.0001313843	-4.0001312635	-4.0001310164	-4.0001306613
85	-4.0001312851	-4.0001312677	-4.0001311090	-4.0001308304	-4.0001304529
90	-4.0001313469	-4.0001313129	-4.0001311396	-4.0001308457	-4.0001304480

Table 5.3 (cont'd).

	R (in a.u.)				
θ (degs)	6.95	7.00	7.05	7.10	7.15
0	-4.0001320515	**-4.0001334250**	-4.0001344681	**-4.0001352201**	**-4.0001357151**
5	-4.0001320832	-4.0001334358	-4.0001344613	-4.0001351961	-4.0001356753
10	-4.0001322140	-4.0001334942	-4.0001344574	-4.0001351398	-4.0001355741
15	-4.0001324925	-4.0001336495	-4.0001345036	-4.0001350895	-4.0001354386
20	-4.0001328076	-4.0001338027	**-4.0001345149**	-4.0001349769	-4.0001352190
25	-4.0001331171	-4.0001339357	-4.0001344949	-4.0001348175	-4.0001349380
30	-4.0001333809	-4.0001339893	-4.0001343664	-4.0001345452	-4.0001345455
35	-4.0001335231	-4.0001339435	-4.0001341541	-4.0001341817	-4.0001340506
40	**-4.0001335254**	-4.0001337605	-4.0001338110	-4.0001337008	-4.0001334514
45	-4.0001333633	-4.0001334306	-4.0001333366	-4.0001331031	-4.0001327492
50	-4.0001330494	-4.0001329728	-4.0001327493	-4.0001324070	-4.0001319626
55	-4.0001326070	-4.0001324038	-4.0001320847	-4.0001316716	-4.0001311511
60	-4.0001321031	-4.0001318018	-4.0001313962	-4.0001309015	-4.0001303280
65	-4.0001315669	-4.0001311818	-4.0001307054	-4.0001301505	-4.0001295286
70	-4.0001310478	-4.0001305979	-4.0001300667	-4.0001294666	-4.0001288132
75	-4.0001305819	-4.0001300850	-4.0001295149	-4.0001288879	-4.0001282035
80	-4.0001302136	-4.0001296915	-4.0001290956	-4.0001284417	-4.0001277403
85	-4.0001299883	-4.0001294486	-4.0001288355	-4.0001281670	-4.0001274542
90	**-4.0001299671**	**-4.0001294060**	**-4.0001287818**	**-4.0001281057**	**-4.0001273872**

Table 5.3 (cont'd).

	R (in a.u.)				
θ (degs)	7.20	7.25	7.30	7.35	7.40
0	**-4.0001359865**	**-4.0001360607**	**-4.0001359640**	**-4.0001357181**	**-4.0001353419**
5	-4.0001359307	-4.0001359891	-4.0001358738	-4.0001356114	-4.0001352371
10	-4.0001357907	-4.0001358161	-4.0001356751	-4.0001353886	-4.0001349765
15	-4.0001355799	-4.0001355402	-4.0001353443	-4.0001350131	-4.0001345654
20	-4.0001352690	-4.0001351518	-4.0001348900	-4.0001345035	-4.0001340103
25	-4.0001348834	-4.0001346774	-4.0001343402	-4.0001338904	-4.0001333441
30	-4.0001343867	-4.0001340903	-4.0001336759	-4.0001331608	-4.0001325603
35	-4.0001337820	-4.0001333950	-4.0001329054	-4.0001323284	-4.0001316772
40	-4.0001330818	-4.0001326093	-4.0001320491	-4.0001314151	-4.0001307189
45	-4.0001322916	-4.0001317450	-4.0001311281	-4.0001304443	-4.0001297080
50	-4.0001314362	-4.0001308292	-4.0001301595	-4.0001294373	-4.0001286718
55	-4.0001305568	-4.0001298997	-4.0001291899	-4.0001284365	-4.0001276480
60	-4.0001296861	-4.0001289890	-4.0001282473	-4.0001274754	-4.0001266703
65	-4.0001288497	-4.0001281294	-4.0001273663	-4.0001265741	-4.0001257597
70	-4.0001281059	-4.0001273591	-4.0001265813	-4.0001257795	-4.0001249604
75	-4.0001274766	-4.0001267157	-4.0001259284	-4.0001251214	-4.0001243004
80	-4.0001270003	-4.0001262303	-4.0001254370	-4.0001246270	-4.0001238054
85	-4.0001267059	-4.0001259299	-4.0001251329	-4.0001243208	-4.0001234988
90	**-4.0001266347**	**-4.0001258557**	**-4.0001250565**	**-4.0001242430**	**-4.0001234202**

Table 5.3 (cont'd).

	R (in a.u.)				
θ (degs)	7.50	7.60	7.75	7.80	7.85
0	**-4.0001342714**	**-4.0001328661**	**-4.0001303556**	**-4.0001294596**	**-4.0001285428**
5	-4.0001341545	-4.0001327465	-4.0001302356	-4.0001293356	-4.0001284161
10	-4.0001338530	-4.0001324251	-4.0001299059	-4.0001290046	-4.0001280848
15	-4.0001333895	-4.0001319241	-4.0001293824	-4.0001284791	-4.0001275595
20	-4.0001327648	-4.0001312592	-4.0001286958	-4.0001277928	-4.0001268763
25	-4.0001320190	-4.0001304642	-4.0001278698	-4.0001269651	-4.0001260504
30	-4.0001311554	-4.0001295531	-4.0001269322	-4.0001260277	-4.0001251165
35	-4.0001302001	-4.0001285574	-4.0001259195	-4.0001250182	-4.0001241190
40	-4.0001291794	-4.0001275039	-4.0001248638	-4.0001239678	-4.0001230721
45	-4.0001281171	-4.0001264194	-4.0001237840	-4.0001228980	-4.0001220150
50	-4.0001270444	-4.0001253398	-4.0001227152	-4.0001218411	-4.0001209730
55	-4.0001260002	-4.0001242866	-4.0001216865	-4.0001208267	-4.0001199751
60	-4.0001250023	-4.0001232934	-4.0001207271	-4.0001198838	-4.0001190504
65	-4.0001240877	-4.0001223909	-4.0001198633	-4.0001190365	-4.0001182211
70	-4.0001232909	-4.0001216086	-4.0001191186	-4.0001183074	-4.0001175087
75	-4.0001226359	-4.0001209678	-4.0001185113	-4.0001177134	-4.0001169288
80	-4.0001221458	-4.0001204894	-4.0001180591	-4.0001172716	-4.0001164980
85	-4.0001218424	-4.0001201934	-4.0001177801	-4.0001169995	-4.0001162332
90	**-4.0001217640**	**-4.0001201167**	**-4.0001177072**	**-4.0001169279**	**-4.0001161629**

Table 5.3 (cont'd).

	R (in a.u.)				
θ (degs)	7.90	8.00	8.50	9.00	9.50
0	**-4.0001276100**	**-4.0001257221**	**-4.0001167447**	**-4.0001095739**	**-4.0001044206**
5	-4.0001274827	-4.0001255953	-4.0001166294	-4.0001095066	-4.0001043764
10	-4.0001271525	-4.0001252700	-4.0001163632	-4.0001093203	-4.0001042480
15	-4.0001266293	-4.0001247562	-4.0001159520	-4.0001090272	-4.0001040442
20	-4.0001259516	-4.0001240945	-4.0001154113	-4.0001086415	-4.0001037766
25	-4.0001251301	-4.0001232943	-4.0001147903	-4.0001081722	-4.0001034570
30	-4.0001242027	-4.0001223852	-4.0001140681	-4.0001076788	-4.0001030996
35	-4.0001232146	-4.0001214229	-4.0001133085	-4.0001071341	-4.0001027177
40	-4.0001221806	-4.0001204214	-4.0001125300	-4.0001065754	-4.0001023285
45	-4.0001211383	-4.0001194142	-4.0001117563	-4.0001060213	-4.0001019374
50	-4.0001201133	-4.0001184282	-4.0001110098	-4.0001054883	-4.0001015557
55	-4.0001191339	-4.0001174905	-4.0001103106	-4.0001049903	-4.0001011978
60	-4.0001182290	-4.0001166278	-4.0001096751	-4.0001045382	-4.0001008753
65	-4.0001174188	-4.0001158585	-4.0001091139	-4.0001041394	-4.0001005905
70	-4.0001167238	-4.0001152002	-4.0001086367	-4.0001038010	-4.0001003474
75	-4.0001161586	-4.0001146654	-4.0001082517	-4.0001035293	-4.0001001509
80	-4.0001157392	-4.0001142695	-4.0001079693	-4.0001033306	-4.0001000064
85	-4.0001154819	-4.0001140278	-4.0001078005	-4.0001032098	-4.0000999180
90	**-4.0001154131**	**-4.0001139620**	**-4.0001077488**	**-4.0001031698**	**-4.0000998887**

Table 5.3 (cont'd).

	R (in a.u.)			
θ (degs)	10.00	10.50	11.00	12.00
0	**-4.0001008020**	**-4.0000982442**	**-4.0000964297**	**-4.0000942106**
5	-4.0001007701	-4.0000982213	-4.0000964135	-4.0000942017
10	-4.0001006786	-4.0000981555	-4.0000963664	-4.0000941756
15	-4.0001005348	-4.0000980525	-4.0000962913	-4.0000941341
20	-4.0001003459	-4.0000979173	-4.0000961928	-4.0000940794
25	-4.0001001215	-4.0000977562	-4.0000960761	-4.0000940144
30	-4.0000998701	-4.0000975760	-4.0000959459	-4.0000939422
35	-4.0000995987	-4.0000973830	-4.0000958073	-4.0000938656
40	-4.0000993183	-4.0000971839	-4.0000956646	-4.0000937871
45	-4.0000990388	-4.0000969849	-4.0000955220	-4.0000937086
50	-4.0000987683	-4.0000967914	-4.0000953828	-4.0000936319
55	-4.0000985134	-4.0000966080	-4.0000952503	-4.0000935585
60	-4.0000982799	-4.0000964393	-4.0000951275	-4.0000934899
65	-4.0000980728	-4.0000962890	-4.0000950174	-4.0000934279
70	-4.0000978961	-4.0000961604	-4.0000949226	-4.0000933740
75	-4.0000977537	-4.0000960562	-4.0000948453	-4.0000933298
80	-4.0000976493	-4.0000959800	-4.0000947883	-4.0000932969
85	-4.0000975857	-4.0000959337	-4.0000947535	-4.0000932768
90	**-4.0000975645**	**-4.0000959183**	**-4.0000947423**	**-4.0000932706**

Table 5.3 (cont'd).

	R (in a.u.)		
θ (degs)	14.00	17.00	20.00
0	**-4.0000923299**	**-4.0000915431**	**-4.0000913355**
5	-4.0000923271	-4.0000915424	-4.0000913353
10	-4.0000923192	-4.0000915404	-4.0000913346
15	-4.0000923063	-4.0000915371	-4.0000913336
20	-4.0000922891	-4.0000915327	-4.0000913322
25	-4.0000922680	-4.0000915271	-4.0000913303
30	-4.0000922442	-4.0000915209	-4.0000913283
35	-4.0000922183	-4.0000915140	-4.0000913260
40	-4.0000921913	-4.0000915068	-4.0000913237
45	-4.0000921637	-4.0000914993	-4.0000913213
50	-4.0000921363	-4.0000914920	-4.0000913188
55	-4.0000921099	-4.0000914849	-4.0000913164
60	-4.0000920853	-4.0000914783	-4.0000913143
65	-4.0000920630	-4.0000914724	-4.0000913124
70	-4.0000920439	-4.0000914675	-4.0000913108
75	-4.0000920282	-4.0000914633	-4.0000913094
80	-4.0000920168	-4.0000914603	-4.0000913084
85	-4.0000920101	-4.0000914585	-4.0000913077
90	**-4.0000920080**	**-4.0000914580**	**-4.0000913076**

Table 5.4. Spherical harmonic coefficients from the Mathematica fit to the ground-state potential of H_2–He with an H–H separation r = 2.463 a_0.

R	4.00	4.50	5.00	5.50	6.00
c_0	8.13128E-02	3.12249E-02	1.08323E-02	3.07049E-03	3.84460E-04
c_2	2.95318E-02	1.23686E-02	4.81100E-03	1.70939E-03	5.23826E-04
c_4	3.72746E-03	1.64008E-03	6.70492E-04	2.57016E-04	9.13392E-05
c_6	2.87544E-04	1.29935E-04	5.36972E-05	2.14747E-05	7.62439E-06
c_8	1.57112E-05	6.31516E-06	2.18147E-06	5.77883E-07	3.43265E-08
c_{10}	1.77440E-06	2.63776E-07	1.60988E-07	-1.13916E-07	1.33766E-08

R	6.05	6.10	6.15	6.20	6.25
c_0	2.51402E-04	1.34282E-04	3.15367E-05	-5.82574E-05	-1.36427E-04
c_2	4.58984E-04	4.00688E-04	3.48332E-04	3.01356E-04	2.59276E-04
c_4	8.19317E-05	7.33982E-05	6.56777E-05	5.86860E-05	5.23833E-05
c_6	6.83418E-06	6.14041E-06	5.50593E-06	4.91501E-06	4.38738E-06
c_8	2.24516E-09	-3.39398E-08	-6.97704E-08	-1.30585E-07	-1.74191E-07
c_{10}	2.56389E-08	4.57032E-08	4.46566E-08	1.57065E-08	-4.47061E-09

Table 5.4 (cont'd).

R	6.30	6.35	6.40	6.45	6.50
c_0	-2.04157E-04	-2.62523E-04	-3.12493E-04	-3.54945E-04	-3.90682E-04
c_2	2.21599E-04	1.87916E-04	1.57858E-04	1.31081E-04	1.07271E-04
c_4	4.66906E-05	4.15541E-05	3.69349E-05	3.27817E-05	2.90520E-05
c_6	3.94020E-06	3.54581E-06	3.18173E-06	2.85368E-06	2.55729E-06
c_8	-1.96023E-07	-1.95060E-07	-1.88718E-07	-1.79042E-07	-1.68940E-07
c_{10}	-3.47380E-08	-6.10671E-08	-7.77138E-08	-9.44404E-08	-1.09531E-07

R	6.55	6.60	6.65	6.70	6.75
c_0	-4.20425E-04	-4.44831E-04	-4.64500E-04	-4.79960E-04	-4.91706E-04
c_2	8.61461E-05	6.74306E-05	5.08745E-05	3.63014E-05	2.34709E-05
c_4	2.57088E-05	2.27104E-05	2.00146E-05	1.76311E-05	1.54789E-05
c_6	2.27964E-06	2.02018E-06	1.78103E-06	1.57023E-06	1.36780E-06
c_8	-1.61487E-07	-1.54785E-07	-1.38471E-07	-1.36383E-07	-1.31522E-07
c_{10}	-1.27306E-07	-1.31553E-07	-1.17265E-07	-1.33286E-07	-1.31094E-07

Table 5.4 (cont'd).

R	6.80	6.85	6.90	6.95	7.00
c_0	-5.00160E-04	-5.05727E-04	-5.08770E-04	-5.09604E-04	-5.08513E-04
c_2	1.22314E-05	2.41051E-06	-6.12722E-06	-1.35122E-05	-1.98854E-05
c_4	1.35449E-05	1.18105E-05	1.02559E-05	8.85610E-06	7.59130E-06
c_6	1.16824E-06	9.94788E-07	8.35889E-07	6.91804E-07	5.59255E-07
c_8	-1.26082E-07	-1.22703E-07	-1.24526E-07	-1.32736E-07	-1.22465E-07
c_{10}	-1.18622E-07	-1.12729E-07	-1.04913E-07	-8.86676E-08	-7.07670E-08

R	7.05	7.10	7.15	7.20	7.25
c_0	-5.05731E-04	-5.01512E-04	-4.96025E-04	-4.89465E-04	-4.82002E-04
c_2	-2.53595E-05	-3.00132E-05	-3.39393E-05	-3.72214E-05	-3.99191E-05
c_4	6.46782E-06	5.48159E-06	4.59042E-06	3.80445E-06	3.10210E-06
c_6	4.24911E-07	2.93512E-07	1.90801E-07	1.05538E-07	2.95666E-08
c_8	-9.95905E-08	-8.16037E-08	-5.78795E-08	-5.60463E-08	-4.89624E-08
c_{10}	-5.61682E-08	-4.23098E-08	-4.58150E-08	-4.28180E-08	-4.48545E-08

Table 5.4 (cont'd).

R	7.30	7.35	7.40	7.50	7.60
c_0	-4.73780E-04	-4.64936E-04	-4.55577E-04	-4.35730E-04	-4.14926E-04
c_2	-4.21064E-05	-4.38329E-05	-4.51572E-05	-4.67737E-05	-4.72767E-05
c_4	2.48142E-06	1.93059E-06	1.43391E-06	6.07553E-07	-3.50604E-08
c_6	-2.83176E-08	-8.45356E-08	-1.30999E-07	-2.06508E-07	-2.50934E-07
c_8	-5.32293E-08	-5.45501E-08	-6.03523E-08	-6.85411E-08	-7.07658E-08
c_{10}	-4.44623E-08	-4.30625E-08	-4.98629E-08	-4.67151E-08	-3.86099E-08

R	7.75	7.80	7.85	7.90	8.00
c_0	-3.83059E-04	-3.72458E-04	-3.61935E-04	-3.51514E-04	-1.65546E-04
c_2	-4.65148E-05	-4.59609E-05	-4.52962E-05	-4.45311E-05	-4.27851E-05
c_4	-7.31333E-07	-9.12697E-07	-1.06961E-06	-1.20589E-06	-1.42085E-06
c_6	-2.68229E-07	-2.72754E-07	-2.70190E-07	-2.71685E-07	-2.74414E-07
c_8	-5.96389E-08	-5.63794E-08	-5.17934E-08	-4.88141E-08	-6.03345E-08
c_{10}	-3.04570E-08	-3.20295E-08	-3.76694E-08	-3.73660E-08	-3.61251E-05

Table 5.4 (cont'd).

R	8.50	9.00	9.50	10.00	10.50
c_0	-2.41047E-04	-1.73599E-04	-1.25389E-04	-9.12519E-05	-6.70568E-05
c_2	-3.23099E-05	-2.30304E-05	-1.63740E-05	-1.17271E-05	-8.42751E-06
c_4	-1.67525E-06	-1.23162E-06	-7.78937E-07	-5.03346E-07	-3.26743E-07
c_6	-2.20351E-07	-1.50298E-07	-9.79007E-08	-6.90508E-08	-6.17923E-08
c_8	-2.08336E-08	-1.15361E-08	-9.74339E-10	-1.56127E-09	-6.65185E-09
c_{10}	-5.04310E-08	-2.99992E-08	-1.86189E-08	-1.19641E-08	-5.57333E-09

R	11.00	12.00	14.00	17.00	20.00
c_0	-4.98213E-05	-2.84725E-05	-1.01138E-05	-2.23783E-06	-1.14679E-07
c_2	-6.11145E-06	-3.36871E-06	-1.19020E-06	-3.16529E-07	-1.03987E-07
c_4	-2.07145E-07	-7.20188E-08	-1.67551E-08	-4.52906E-09	-1.25778E-09
c_6	-6.17708E-08	-1.11419E-07	-4.78682E-09	-2.27445E-11	-1.39792E-11
c_8	-5.97155E-09	5.28054E-08	-1.62235E-09	-8.13963E-11	1.82445E-10
c_{10}	-1.90250E-09	-1.51618E-08	7.68912E-10	4.88235E-11	-1.13731E-10

potential, though this fit is probably the most approximate. The Lennard-Jones potential and $V_0(R)$ are plotted in Figure 5.2. Discrepancies are apparent in the range from R = 8.0 a.u. to R = 16.0 a.u. where the Lennard-Jones potential is detectably below the *ab initio* points and the interpolated potential $V_0(R)$.

In Figure 5.3, the isotropic He–H_2 potentials $V_0(R)$ are plotted versus R for r = 1.111 a.u., r = 1.449 a.u., and r = 2.463 a.u. Of these three bond lengths, r = 1.449 a.u. gives the deepest minimum, slightly deeper than the minimum on the curve for r = 1.111 a.u. but significantly deeper than the minimum for r = 2.463 a.u. The R_e value at the minimum is smallest when r = 1.111 and largest when r = 2.463, as expected. When r = 2.463 a.u., the repulsive wall rises at R > 6.0 a.u., where the other potentials are still attractive.

In Figure 5.4, the anisotropic component $V_2(R)$ of the potential is plotted versus R for r = 1.111 a.u., r = 1.449 a.u., and r = 2.463 a.u. The anisotropy $V_2(R)$ has the deepest well for r = 2.463 a.u., and the R_e values at the minima of $V_2(R)$ increase as r increases.

In Figure 5.5, the anisotropic component $V_4(R)$ of the potential is plotted versus R for r = 1.111 a.u., r = 1.449 a.u., and r = 2.463 a.u. The potential $V_4(R)$ shows a clear minimum near R = 7.6 a.u. when r = 2.463 a.u., but the $V_4(R)$ potentials entirely repulsive for r = 1.111 a.u. and r = 1.449 a.u., within the accuracy of the calculations. For the smaller r values, numerical noise becomes apparent in the results for $V_4(R)$ that are near to zero, if the vertical scale is expanded considerably.

At long distances between H_2 and He, exchange-repulsion and orbital overlap effects drop off exponentially. Then the potential is determined by van der Waals dispersion and quadrupolar induction effects. The leading van der Waals dispersion term varies as R^{-6}. The coefficients of this term are given by integrals over imaginary frequencies of the product of the polarizability

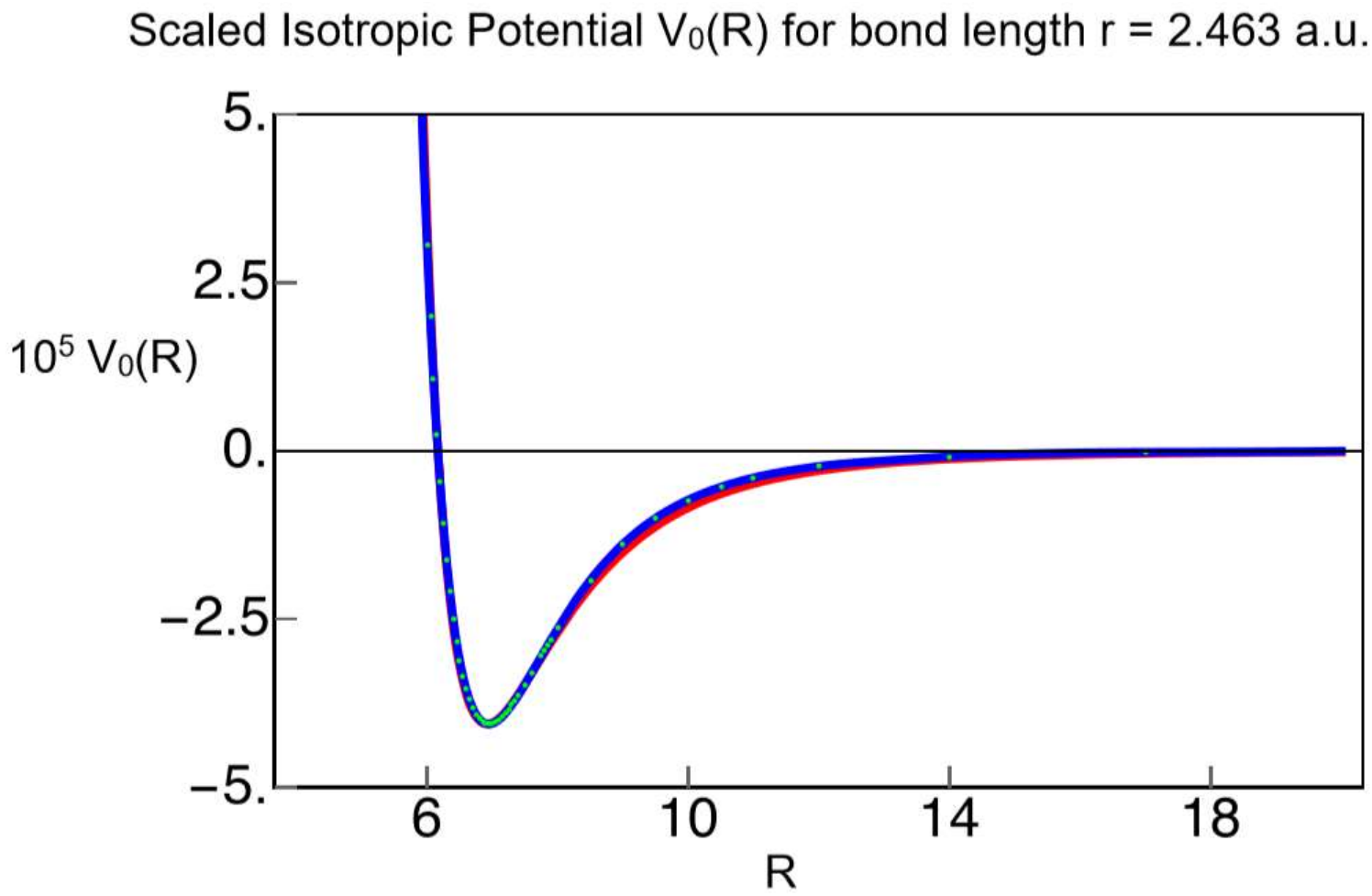

Figure 5.2. Isotropic potential $V_0(R)$ in a.u. multiplied by 105, for H_2–He at an H_2 bond length of r = 2.463 a.u. (in blue), compared with Lennard-Jones potential (in red), and the *ab initio* data points for $V_0(R)$, shown in green. The Lennard-Jones parameters are ε = 0.000405536 a.u. and σ = 6.16679 a.u. The minimum of the isotropic potential is located at r_e = 6.94495 a.u.

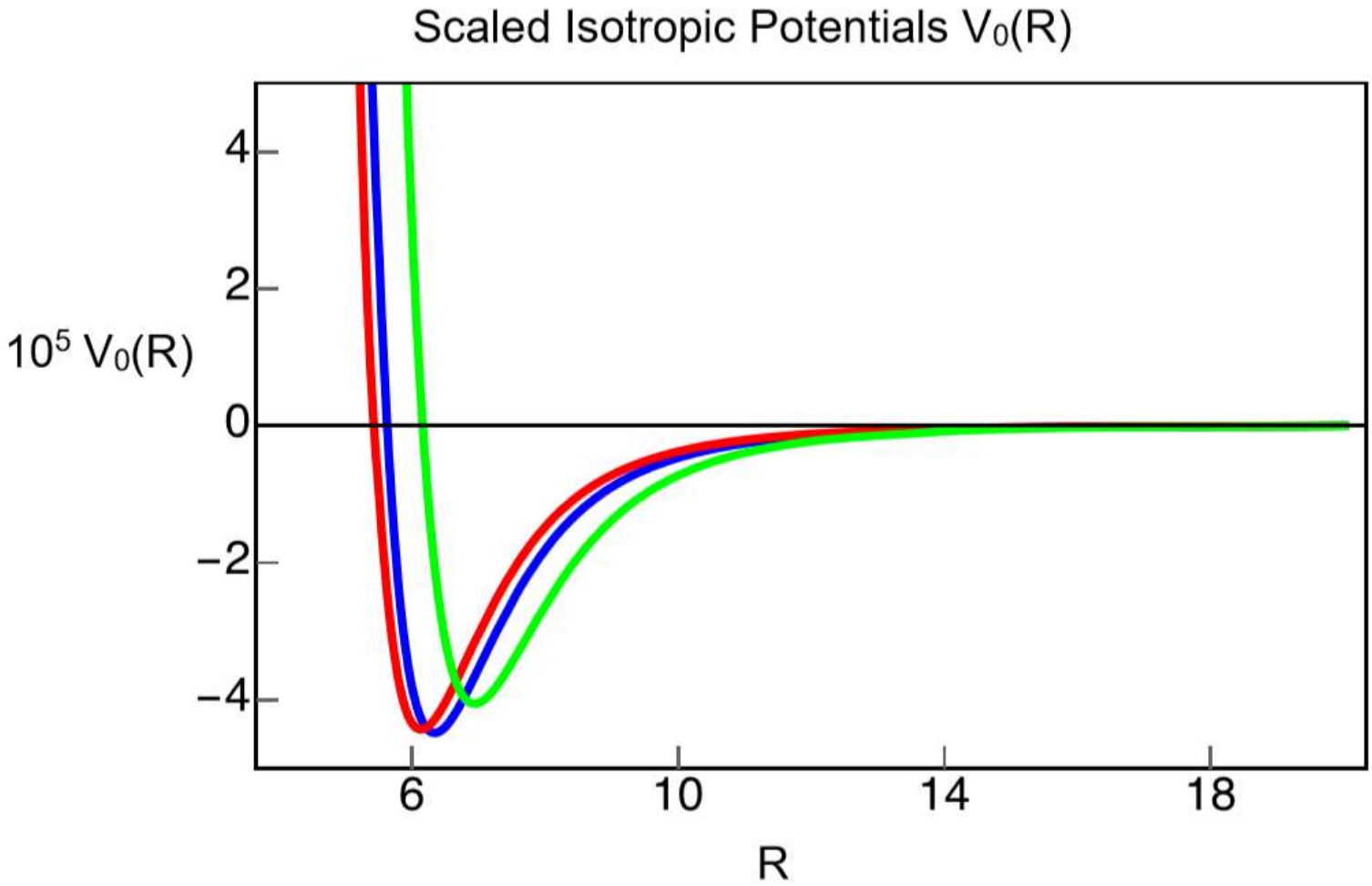

Figure 5.3. Isotropic potentials $V_0(R)$ in a.u. multiplied by 105, for H_2–He at H_2 bond lengths of r = 1.111 a.u. (red), 1.449 a.u. (blue), and 2.463 a.u. (green).

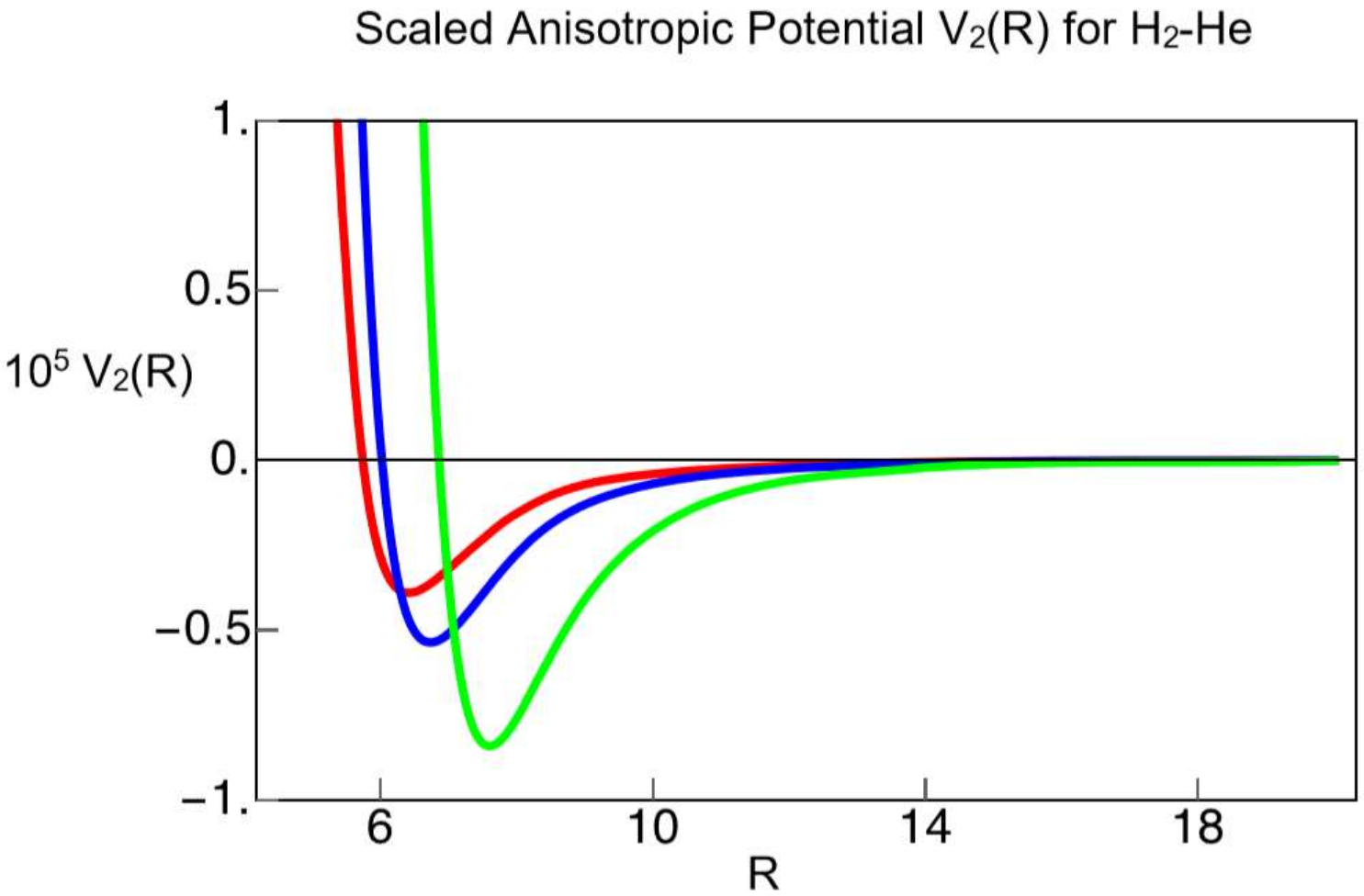

Figure 5.4. Anisotropic potential $V_2(R)$ in a.u. multiplied by 105, for H_2–He at H_2 bond lengths of r = 1.111 a.u. (red), r = 1.449 a.u. (blue), and r = 2.463 a.u. (green).

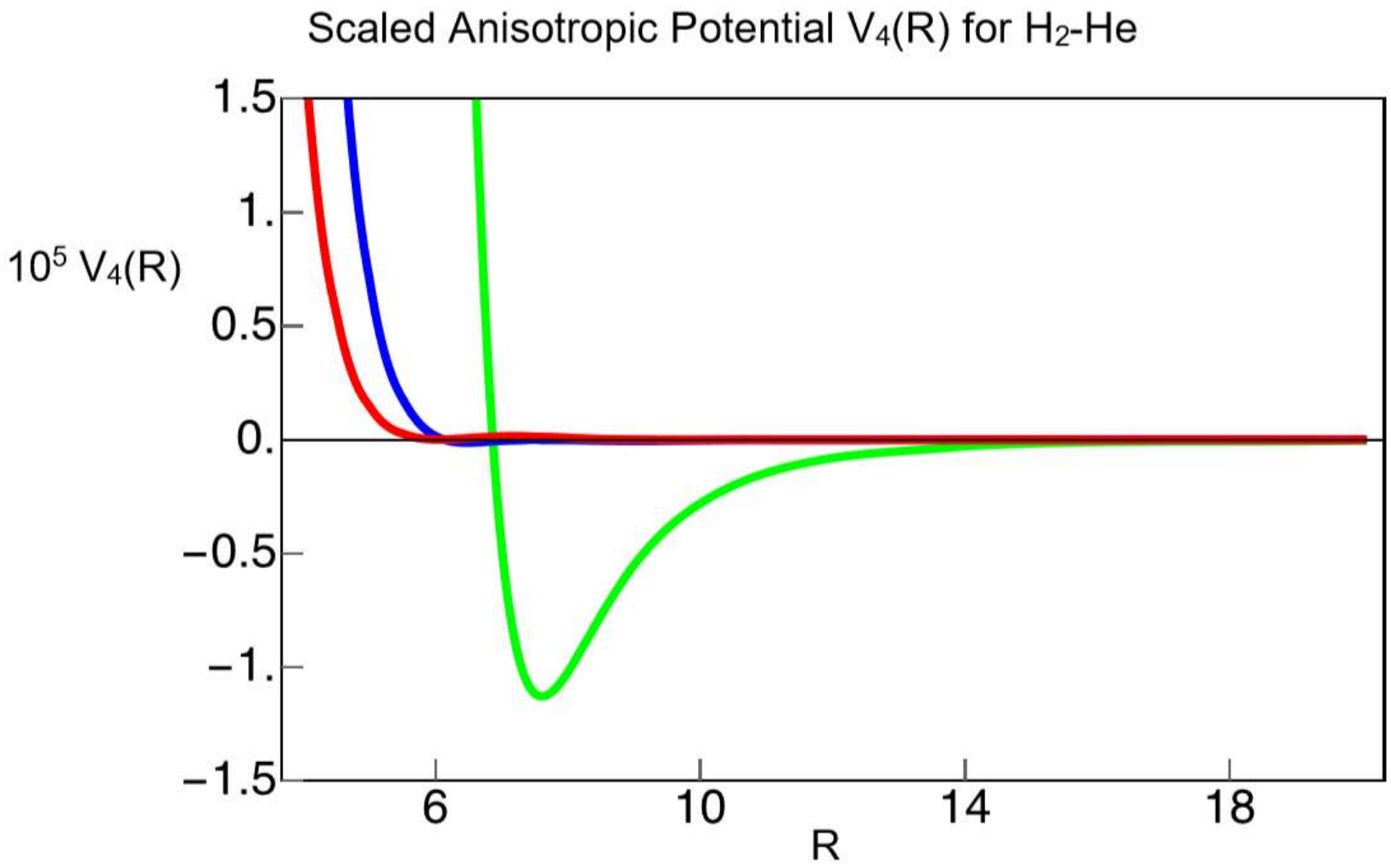

Figure 5.5. Anisotropic potential $V_4(R)$ in a.u. multiplied by 105, for H_2–He at H_2 bond lengths of r = 1.111 a.u. (red), r = 1.449 a.u. (blue), and r = 2.463 a.u. (green).

$\alpha(i\omega)$ of H_2 and $\alpha(i\omega)$ of He. The polarizability $\alpha(i\omega)$ of He is isotropic, and the polarizability $\alpha(i\omega)$ of H_2 is a symmetric Cartesian tensor of rank 2. Therefore, the C_6 dispersion coefficient has an isotropic component $C_6^{(0)}$ and an anisotropic component $C_6^{(2)}$. It has no anisotropic component $C_6^{(4)}$. At order R^{-8}, the H_2–He potential is affected both by van der Waals dispersion and by quadrupolar induction. The van der Waals dispersion coefficient depends on the integral over imaginary frequencies of the product of the quadrupole polarizability $C(i\omega)$ of H_2 with the dipole polarizability $\alpha(i\omega)$ of He, and it also depends on the integral over imaginary frequencies of the product of the dipole polarizability $\alpha(i\omega)$ of H_2 with the quadrupole polarizability $C(i\omega)$ of He. The quadrupole polarizability is a fourth-rank Cartesian tensor. For He, it is isotropic; and for H_2, it has spherical tensor components of ranks 0, 2, and 4. Therefore, the C_8 dispersion coefficient has components $C_8^{(0)}$, $C_8^{(2)}$, and $C_8^{(4)}$.

Quadrupolar induction also affects the long-range energy at order R^{-8}. The permanent quadrupole of H_2 produces an electric field that acts on He, inducing a dipole in He that is proportional to R^{-4}. The induced dipole of He produces a reaction field gradient at H_2 that modifies the energy of the pair, due to its effect on the permanent quadrupole of H_2. Quadrupolar induction contributes to both the isotropic and anisotropic potentials of H_2–He. The contribution to the isotropic potential is $V_{0\Theta} = -3\alpha\Theta^2R^{-8}$, where α is the polarizability of He and Θ is the zz component of the permanent quadrupole of H_2 (where z is the bond axis). We plan to examine the contribution to the anisotropic potential in future work.

The permanent quadrupole of H_2 is known as a function of bond length from calculations by Miliordos and Hunt.[1] The dispersion energy coefficients $C_6^{(0)}$, $C_6^{(2)}$, $C_8^{(0)}$, $C_8^{(2)}$, and $C_8^{(4)}$ for He–H_2 have all been determined with very high accuracy by Bishop and Pipin[3] for r = 1.449 a.u. The *ab initio* results obtained in this work are sufficiently accurate that it seemed worthwhile to fit the values $V_0(R)$, $V_2(R)$, and $V_4(R)$ at long range to $-C_6^{(0)}R^{-6} - C_8^{(0)}R^{-8}$, $-C_6^{(2)}R^{-6} - C_8^{(2)}R^{-8}$, and $-C_8^{(4)}R^{-8} - C_{10}^{(4)}R^{-10}$, respectively. It is possible to fit the long-range values quite well to these forms, but the coefficients obtained from the fit are sensitive to the range of R values included in the fit.

For r = 1.449 a.u., our initial fit to $C_6^{(0)}$ and $C_8^{(0)}$ was based on the *ab initio* results for $V_0(R)$ at R = 9.0 a.u., 9.5 a.u., 10.0 a.u., 10.5 a.u., 11.0 a.u., 12.0 a.u., 14.0 a.u., 17.0 a.u., and 20.0 a.u. We found $C_6^{(0)}$ = 4.07134 a.u. and $C_8^{(0)}$ = 57.3655 a.u., in very good agreement with the dispersion energy coefficients that have been calculated directly by Bishop and Pipin, $C_6^{(0)}$ = 4.0128132 a.u. and $C_8^{(0)}$ = 55.381453 a.u. The error is about 1.5% in $C_6^{(0)}$ and ~ 2% in $C_8^{(0)}$, taking into account the quadrupolar induction term that is not included in the dispersion energy calculations of Bishop and Pipin. Subsequently, additional *ab initio* calculations of the energy as a function of the angle θ were run for R values of 13.0 a.u., 15.0 a.u., and 16.0 a.u. and the additional $c_j(R)$ coefficients were found. The added values improved the smoothness of the $V_0(R)$ interpolation generated by Mathematica. New fits to $-C_6^{(0)} R^{-6} - C_8^{(0)} R^{-8}$ at long range gave $C_6^{(0)}$ = 3.9987 a.u. and $C_8^{(0)}$ = 63.677 a.u., with results shown in Figure 5.6. The error in $C_6^{(0)}$ is about 0.25% in this fit, relative to the values given by Bishop and Pipin. The agreement with $C_8^{(0)}$ (corrected for quadrupolar induction, which contributes approximately −1 a.u. to $C_8^{(0)}$ at r = 1.449 a.u.) is not as good as in the initial fit, which was based on fewer long-range data points. The new error of ~20% is a better estimate of the uncertainty in the $C_8^{(0)}$ coefficient derived in this way. The next term in the series for the isotropic dispersion energy is $C_{10}^{(0)} R^{-10}$. Since the fitted $C_8^{(0)}$ was too large relative to the result given by Bishop and Pipin, we tested whether adding a $C_{10}^{(0)}$ term to the fit would improve the results, allowing all three values $C_6^{(0)}$, $C_8^{(0)}$, and $C_{10}^{(0)}$ to be determined from the fit. The results for the C_{10} coefficient were aphysical (positive in one attempt when it must be negative, and essentially the same negative value as C_6 and C_8 in another).

The bond lengths r = 1.111 a.u. and r = 2.463 a.u. were not covered in the work of Bishop and Pipin (BP). We have calculated the isotropic dispersion coefficients $C_6^{(0)}$ and $C_8^{(0)}$ by fitting $V_0(R)$ at these bond lengths, with the results $C_6^{(0)}$ = 3.2876 a.u. and $C_8^{(0)}$ = 45.4450 a.u. at r = 1.111 a.u., and $C_6^{(0)}$ = 6.43383 a.u. and $C_8^{(0)}$ = 76.3722 a.u. at r = 2.463 a.u.

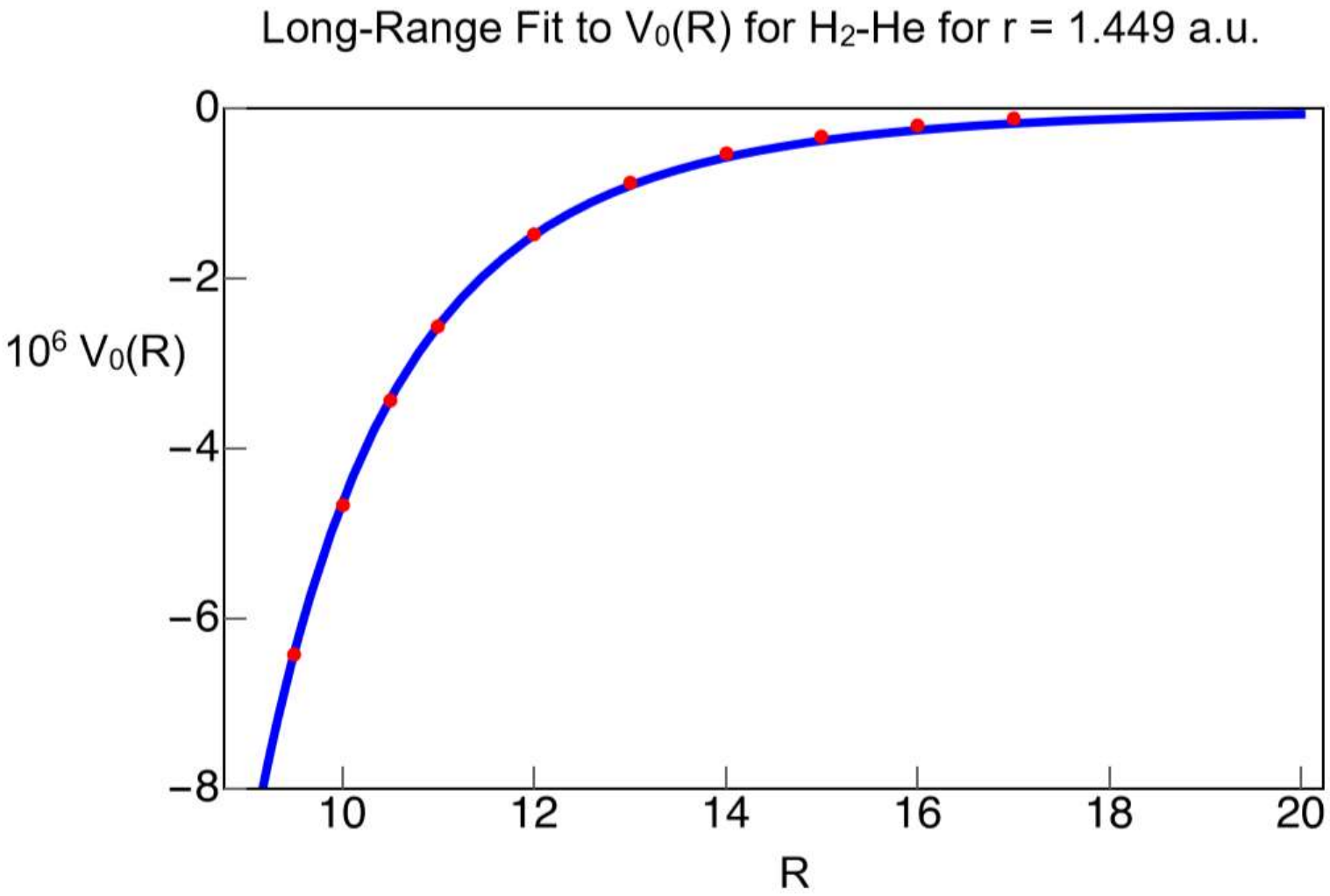

Figure 5.6. *Ab initio* results for $V_0(R)$ at long range (red points) and the Mathematica fit to $V_0(R)$ in the form $-C_6^{(0)} R^{-6} - C_8^{(0)} R^{-8}$, with $C_6^{(0)} = 3.9987$ a.u. and $C_8^{(0)} = 63.677$ a.u. (blue curve).

For the anisotropic coefficients $C_6^{(2)}$ and $C_8^{(2)}$ at r = 1.449 a.u., the agreement between the fit of the *ab initio* results for $V_2(R)$ the direct calculations of BP were not as good. Fitting $V_2(R)$ to $-C_6^{(2)} R^{-6} - C_8^{(2)} R^{-8}$ in the range from 12.0 a.u. to 20.0 a.u. gave $C_6^{(2)} = 0.639204$ a.u. and $C_8^{(2)} = 5.27924$ a.u. *vs*. the values published by BP, values $C_6^{(2)} = 0.37739$ a.u. and $C_8^{(2)} = 17.0588$ a.u. The results for $C_6^{(2)}$ and $C_8^{(2)}$ might be strongly correlated with each other, since $C_6^{(2)}$ from the fit is greater than $C_6^{(2)}$ from BP, but $C_8^{(2)}$ from the fit was less than $C_8^{(2)}$ from BP. An alternative possibility was suggested by the plot of the BP curve (green), the *ab initio* data points (red), and our fit (blue), shown in Figure 5.7. The BP curve falls above the data points, which appear to behave smoothly as a function of R. It is possible that the *ab initio* results are picking up correlation effects beyond $C_8^{(2)} R^{-8}$. To test this possibility, we fit the $-C_6^{(2)} R^{-6} - C_8^{(2)} R^{-8} - C_{10}^{(2)} R^{-10}$ to the *ab initio* results, using the BP values for $C_6^{(2)}$ and $C_8^{(2)}$ and fitting only $C_{10}^{(2)}$. This gave the curve in purple in Figure 5.7, which fits the data much better. (The same strategy has not yet been implemented successfully for the isotropic coefficients.)

The potential $V_4(R)$ was sufficiently stable at long range to fit $C_8^{(4)}$ only for r = 2.463 a.u. A fit based on $- C_8^{(2)} R^{-8} - C_{10}^{(2)} R^{-10}$ is shown in Figure 5.8.

Points on the potential energy surface for H_2–He have also been calculated for other bond lengths r of H_2 (in a.u.) including 0.942, 1.280, 1.787, 2.125, 2.43, 2.463, 2.801, 3.730, and 5.700, plus 1.100, 1.448736, and 1.75 chosen for comparison with the work of the Patkowski group.[4] The results for 0.942, 1.280, 1.787, 2.125, 2.43, 2.801, 3.730, and 5.700 a.u. with the aug-cc-pV5Z basis set are tabulated in the Appendix. The coefficients $c_j(R)$ will be determined for these R values.

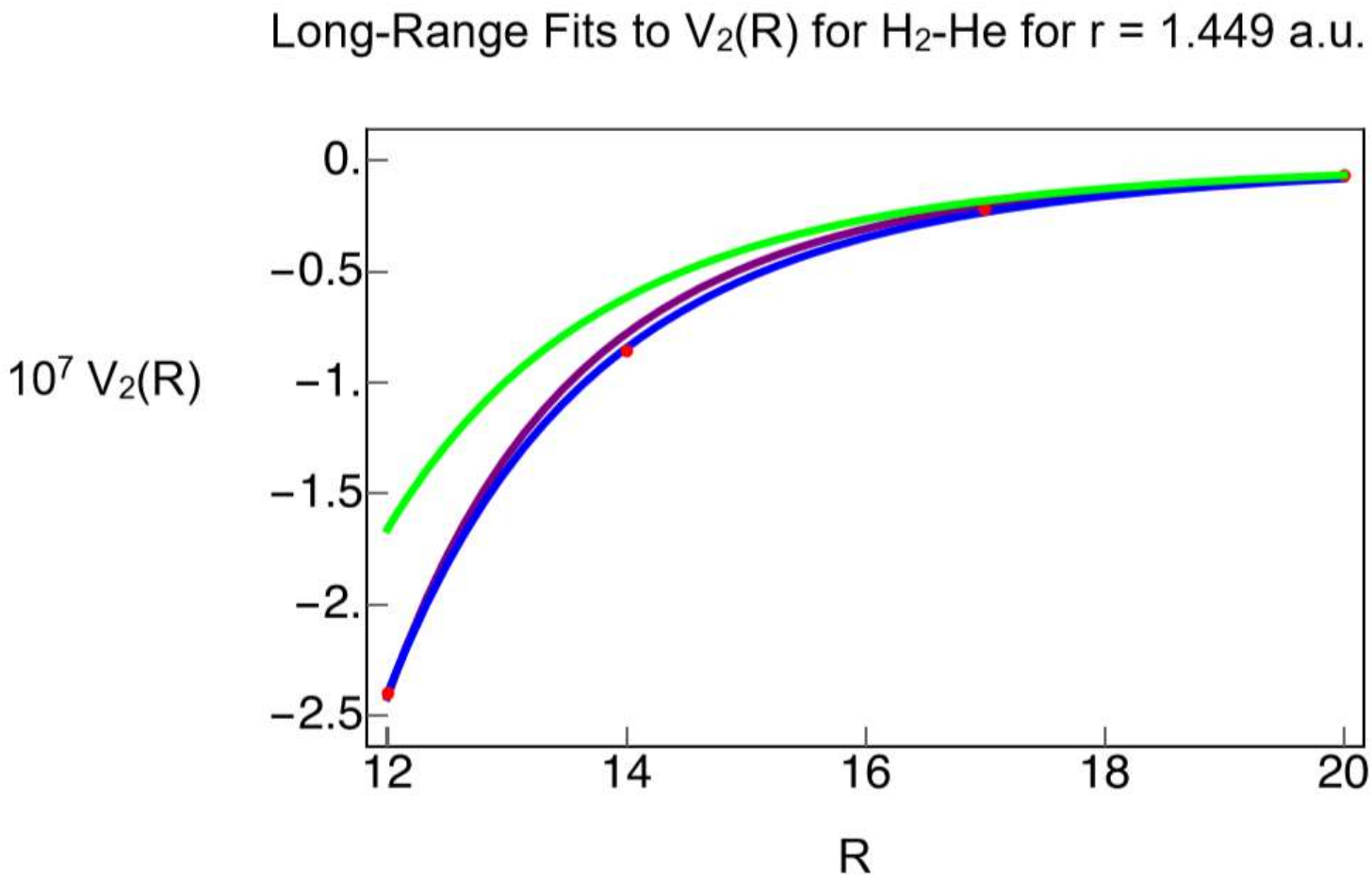

Figure 5.7. *Ab initio* results for $V_2(R)$ at long range (red points), scaled by 107. The blue curve shows the Mathematica fit to $V_2(R)$ based on the form $-C_6^{(2)} R^{-6} - C_8^{(2)} R^{-8}$, with $C_6^{(2)} = 0.639204$ a.u. and $C_8^{(2)} = 5.27924$ a.u. The green curve shows the Bishop and Pipin function, with $C_6^{(2)} = 0.37739$ a.u. and $C_8^{(2)} = 17.0588$ a.u. The purple curve shows the fitted function $-C_6^{(2)} R^{-6} - C_8^{(2)} R^{-8} - C_{10}^{(2)} R^{-10}$ with the BP values for $C_6^{(2)}$ and $C_8^{(2)}$ and the $C_{10}^{(2)}$ value taken from the Mathematica fit, $C_{10}^{(2)} = -4691.54$ a.u. This improves the agreement noticeably.

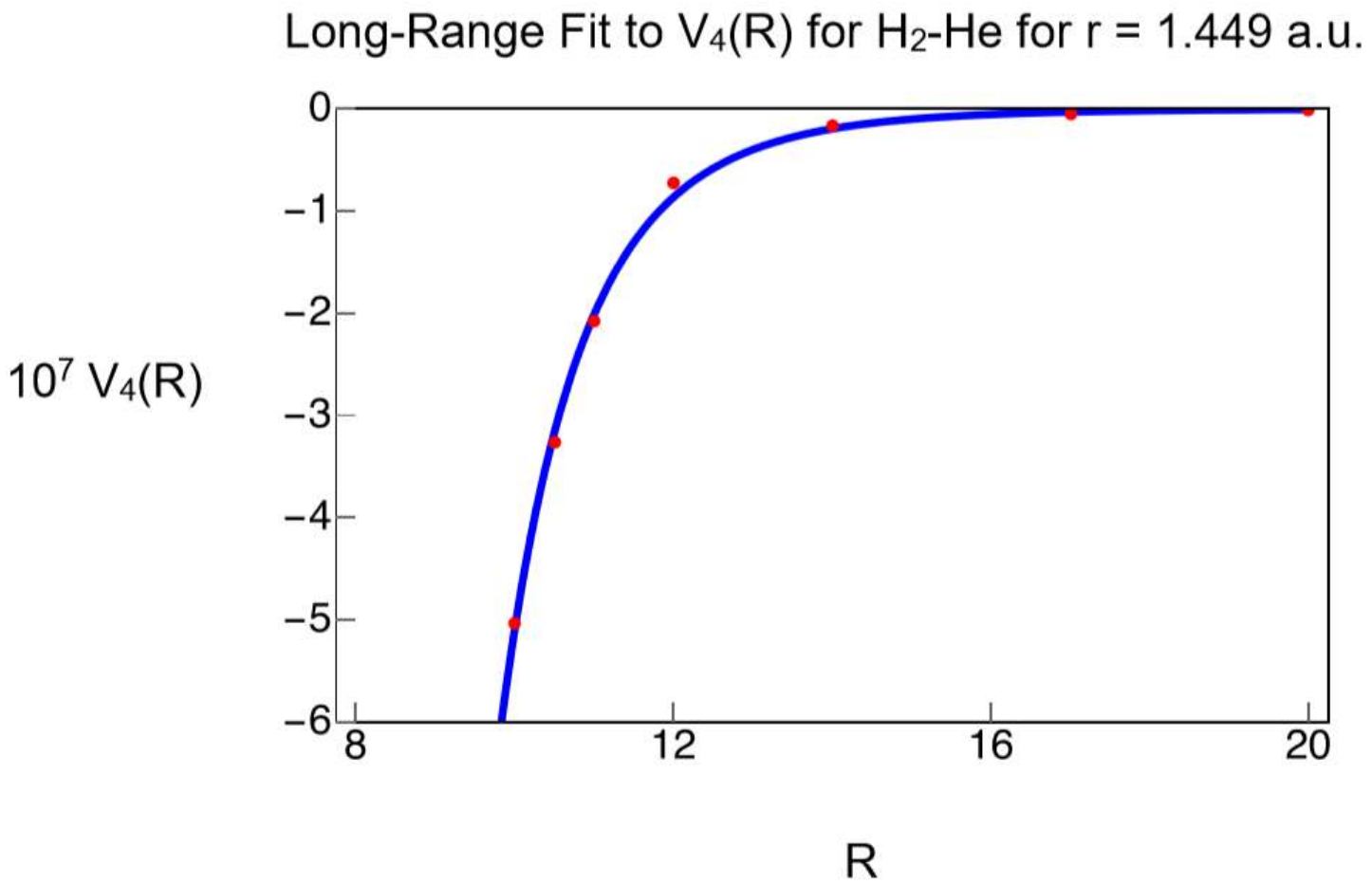

Figure 5.8. *Ab initio* results for $V_4(R)$ at long range (red points) scaled by 10, with r = 1.449 a.u. The blue curve is the Mathematica fit to $V_4(R)$ based on the form $-C_8^{(4)} R^{-8} - C_{10}^{(4)} R^{-8}$.

APPENDIX

Table A.1. CR-CC(2,3) energies of H_2–He for $r_{H-H} = 0.942\ a_0$ with an aug-cc-pV5Z basis, as a function of the separation R between the center of mass of the two H nuclei and the He nucleus, and the angle θ between the H–H vector and the z axis. The He atom is located along the z axis. Entries in blue denote the maximum and entries in bold black denote the minimum of the potential, as a function of the angle θ for each value of R.

	R (in a.u.)					
θ (deg)	1.75	2.00	2.20	2.40	2.60	2.80
0	**-3.7358837055**	**-3.8392806373**	**-3.8926553619**	**-3.9292426366**	**-3.9543114296**	**-3.9714227748**
5	-3.7364064412	-3.8395427457	-3.8928187930	-3.9293486382	-3.9543813414	-3.9714693703
10	-3.7379398852	-3.8403159597	-3.8933024985	-3.9296625571	-3.9545886900	-3.9716072872
15	-3.7403825799	-3.8415580895	-3.8940828188	-3.9301701959	-3.9549249068	-3.9718313520
20	-3.7435800210	-3.8432039352	-3.8951230024	-3.9308498147	-3.9553760704	-3.9721324732
25	-3.7473456943	-3.8451718121	-3.8963765999	-3.9316732279	-3.9559242286	-3.9724991221
30	-3.7514800168	-3.8473716714	-3.8977907790	-3.9326073177	-3.9565484696	-3.9729175309
35	-3.7557916074	-3.8497118220	-3.8993099902	-3.9336173322	-3.9572260242	-3.9733727060
40	-3.7601084237	-3.8521046659	-3.9008796946	-3.9346674788	-3.9579333839	-3.9738491570
45	-3.7642863228	-3.8544710441	-3.9024480233	-3.9357233857	-3.9586475247	-3.9743314865
50	-3.7682105960	-3.8567415063	-3.9039678777	-3.9367528672	-3.9593465600	-3.9748048486
55	-3.7717945369	-3.8588580001	-3.9053981774	-3.9377273102	-3.9600105559	-3.9752554992
60	-3.7749760811	-3.8607730638	-3.9067034812	-3.9386213473	-3.9606217618	-3.9756711377
65	-3.7777126649	-3.8624484202	-3.9078541855	-3.9394130588	-3.9611647087	-3.9760409916
70	-3.7799758804	-3.8638546434	-3.9088263565	-3.9400845449	-3.9616262042	-3.9763558939
75	-3.7817485755	-3.8649695028	-3.9096010612	-3.9406214246	-3.9619959428	-3.9766084513
80	-3.7830206615	-3.8657767199	-3.9101643036	-3.9410127214	-3.9622658499	-3.9767929431
85	-3.7837860022	-3.8662655380	-3.9105062667	-3.9412508206	-3.9624303174	-3.9769053484
90	**-3.7840419283**	**-3.8664299592**	**-3.9106218391**	**-3.9413314631**	**-3.9624858278**	**-3.9769434252**

Table A.1 (cont'd).

	R (in a.u.)					
θ (deg)	3.00	3.50	4.00	4.50	5.00	5.50
0	**-3.9830410051**	**-3.9980632692**	**-4.0034503134**	**-4.0052771983**	**-4.0058488601**	**-4.0060039458**
5	-3.9830720078	-3.9980741727	-4.0034538997	-4.0052782557	-4.0058490937	-4.0060039646
10	-3.9831639067	-3.9981066445	-4.0034646506	-4.0052814202	-4.0058498341	-4.0060040294
15	-3.9833130453	-3.9981594852	-4.0034821405	-4.0052865982	-4.0058510908	-4.0060041373
20	-3.9835139381	-3.9982305743	-4.0035057456	-4.0052936262	-4.0058527906	-4.0060042830
25	-3.9837588175	-3.9983172910	-4.0035346520	-4.0053022255	-4.0058548655	-4.0060044581
30	-3.9840386831	-3.9984167451	-4.0035677830	-4.0053121062	-4.0058572382	-4.0060046494
35	-3.9843436682	-3.9985253018	-4.0036039797	-4.0053230142	-4.0058598142	-4.0060048263
40	-3.9846633549	-3.9986394243	-4.0036422018	-4.0053343886	-4.0058625466	-4.0060049921
45	-3.9849874790	-3.9987554403	-4.0036809209	-4.0053459545	-4.0058652610	-4.0060051534
50	-3.9853060575	-3.9988697369	-4.0037190959	-4.0053573813	-4.0058680085	-4.0060053194
55	-3.9856098029	-3.9989789741	-4.0037555414	-4.0053683265	-4.0058706111	-4.0060054784
60	-3.9858903981	-3.9990800601	-4.0037892874	-4.0053784771	-4.0058730283	-4.0060056247
65	-3.9861403920	-3.9991702655	-4.0038194958	-4.0053875452	-4.0058751762	-4.0060057630
70	-3.9863535192	-3.9992471291	-4.0038452588	-4.0053952555	-4.0058770146	-4.0060058807
75	-3.9865245842	-3.9993089586	-4.0038659485	-4.0054014467	-4.0058784895	-4.0060059713
80	-3.9866495463	-3.9993541872	-4.0038810926	-4.0054059886	-4.0058795780	-4.0060060394
85	-3.9867257669	-3.9993818226	-4.0038903729	-4.0054087774	-4.0058802612	-4.0060060856
90	**-3.9867516189**	**-3.9993912946**	**-4.0038935974**	**-4.0054097305**	**-4.0058805103**	**-4.0060061129**

Table A.1 (cont'd).

	R (in a.u.)					
θ (deg)	6.00	6.05	6.10	6.15	6.20	6.25
0	**-4.0060315664**	**-4.0060317316**	**-4.0060316527**	**-4.0060313674**	**-4.0060309077**	**-4.0060303026**
5	-4.0060315273	-4.0060316936	-4.0060316138	-4.0060313270	-4.0060308651	-4.0060302569
10	-4.0596313741	-4.0060315867	-4.0060315040	-4.0060312150	-4.0060307543	-4.0060301513
15	-4.0060312580	-4.0060314142	-4.0060313300	-4.0060310436	-4.0060305863	-4.0060299849
20	-4.0060310371	-4.0060311899	-4.0060311056	-4.0060308182	-4.0060303594	-4.0060297573
25	-4.0060307784	-4.0060309241	-4.0060308318	-4.0060305384	-4.0060300762	-4.0060294727
30	-4.0060304823	-4.0060306121	-4.0060305086	-4.0060302080	-4.0060297412	-4.0060291344
35	-4.0060301419	-4.0060302554	-4.0060301409	-4.0060298326	-4.0060293592	-4.0060287472
40	-4.0060297626	-4.0060298622	-4.0060297379	-4.0060294212	-4.0060289402	-4.0060283435
45	-4.0060293619	-4.0060294488	-4.0060293150	-4.0060289875	-4.0060285155	-4.0060279212
50	-4.0060289619	-4.0060290359	-4.0060288921	-4.0060285517	-4.0060280899	-4.0060274903
55	-4.0060285749	-4.0060286320	-4.0060284804	-4.0060281356	-4.0060276736	-4.0060270715
60	-4.0060282218	-4.0060282661	-4.0060281036	-4.0060277525	-4.0060272850	-4.0060266806
65	-4.0060279012	-4.0060279339	-4.0060277631	-4.0060274122	-4.0060269328	-4.0060263263
70	-4.0060276249	-4.0060276469	-4.0060274681	-4.0060271186	-4.0060266202	-4.0060260180
75	-4.0060274024	-4.0060274159	-4.0060272304	-4.0060268767	-4.0060263805	-4.0060257613
80	-4.0060272381	-4.0060272469	-4.0060270584	-4.0060267025	-4.0060262055	-4.0060255907
85	-4.0060271350	-4.0060271402	-4.0060269497	-4.0060265935	-4.0060260977	-4.0060254850
90	**-4.0060271048**	**-4.0060271081**	**-4.0060269161**	**-4.0060265589**	**-4.0060260630**	**-4.0060254511**

Table A.1 (cont'd).

	R (in a.u.)					
θ (deg)	6.30	6.35	6.40	6.45	6.50	6.55
0	**-4.0060295766**	**-4.0060287513**	**-4.0060278452**	**-4.0060268795**	**-4.0060258673**	**-4.0060248173**
5	-4.0060295308	-4.0060287091	-4.0060278062	-4.0060268417	-4.0060258308	-4.0060247825
10	-4.0060294294	-4.0060286084	-4.0060277060	-4.0060267402	-4.0060257306	-4.0060246849
15	-4.0060292636	-4.0060284441	-4.0060275446	-4.0060265797	-4.0060255693	-4.0060245274
20	-4.0060290367	-4.0060282191	-4.0060273228	-4.0060263627	-4.0060253494	-4.0060243084
25	-4.0060287522	-4.0060279351	-4.0060270391	-4.0060260823	-4.0060250809	-4.0060240453
30	-4.0060284104	-4.0060275957	-4.0060267143	-4.0060257721	-4.0060247800	-4.0060237508
35	-4.0060280347	-4.0060272340	-4.0060263541	-4.0060254143	-4.0060244284	-4.0060234154
40	-4.0060276370	-4.0060268339	-4.0060259596	-4.0060250244	-4.0060240465	-4.0060230432
45	-4.0060272117	-4.0060264135	-4.0060255419	-4.0060246161	-4.0060236516	-4.0060226524
50	-4.0060267819	-4.0060259865	-4.0060251232	-4.0060242068	-4.0060232476	-4.0060222558
55	-4.0060263649	-4.0060255743	-4.0060247163	-4.0060238044	-4.0060228505	-4.0060218656
60	-4.0060259748	-4.0060251860	-4.0060243306	-4.0060234222	-4.0060224732	-4.0060214940
65	-4.0060256197	-4.0060248317	-4.0060239779	-4.0060230725	-4.0060221272	-4.0060211527
70	-4.0060253108	-4.0060245231	-4.0060236708	-4.0060227676	-4.0060218253	-4.0060208544
75	-4.0060250586	-4.0060242721	-4.0060234210	-4.0060225194	-4.0060215793	-4.0060206110
80	-4.0060248778	-4.0060240852	-4.0060232357	-4.0060223361	-4.0060213978	-4.0060204314
85	-4.0060247742	-4.0060239829	-4.0060231285	-4.0060222254	-4.0060212850	-4.0060203197
90	**-4.0060247420**	**-4.0060239518**	**-4.0060230973**	**-4.0060221946**	**-4.0060212555**	**-4.0060202895**

Table A.1 (cont'd).

	R (in a.u.)					
θ (deg)	6.60	6.65	6.70	6.75	6.80	6.85
0	**-4.0060237413**	**-4.0060226489**	**-4.0060215475**	**-4.0060204445**	**-4.0060193448**	**-4.0060182535**
5	-4.0060237077	-4.0060226160	-4.0060215156	-4.0060204132	-4.0060193145	-4.0060182239
10	-4.0060236124	-4.0060225229	-4.0060214247	-4.0060203244	-4.0060192282	-4.0060181399
15	-4.0060234585	-4.0060223723	-4.0060212747	-4.0060201794	-4.0060190844	-4.0060179990
20	-4.0060232420	-4.0060221598	-4.0060210768	-4.0060199893	-4.0060189041	-4.0060178263
25	-4.0060229927	-4.0060219229	-4.0060208423	-4.0060197593	-4.0060186795	-4.0060176078
30	-4.0060227040	-4.0060216380	-4.0060205637	-4.0060194878	-4.0060184158	-4.0060173520
35	-4.0060223723	-4.0060213141	-4.0060202486	-4.0060191820	-4.0060181194	-4.0060170655
40	-4.0060220099	-4.0060209617	-4.0060199063	-4.0060188501	-4.0060177982	-4.0060167548
45	-4.0060216289	-4.0060205911	-4.0060195463	-4.0060185007	-4.0060174593	-4.0060164262
50	-4.0060212415	-4.0060202133	-4.0060191785	-4.0060181428	-4.0060171113	-4.0060160879
55	-4.0060208592	-4.0060198396	-4.0060188136	-4.0060177869	-4.0060167644	-4.0060157503
60	-4.0060204942	-4.0060194817	-4.0060184631	-4.0060174442	-4.0060164298	-4.0060154239
65	-4.0060201582	-4.0060191513	-4.0060181389	-4.0060171266	-4.0060161191	-4.0060151203
70	-4.0060198639	-4.0060188615	-4.0060178538	-4.0060168466	-4.0060158444	-4.0060148512
75	-4.0060196233	-4.0060186241	-4.0060176199	-4.0060166164	-4.0060156182	-4.0060146292
80	-4.0060194457	-4.0060184485	-4.0060174469	-4.0060164459	-4.0060154502	-4.0060144640
85	-4.0060193361	-4.0060183411	-4.0060173409	-4.0060163415	-4.0060153475	-4.0060143631
90	**-4.0060193051**	**-4.0060183095**	**-4.0060173093**	**-4.0060163100**	**-4.0060153164**	**-4.0060143325**

Table A.1 (cont'd).

	R (in a.u.)					
θ (deg)	6.90	7.00	7.10	7.20	7.30	7.50
0	**-4.0060171742**	**-4.0060150659**	**-4.0060130248**	**-4.0060110888**	**-4.0060092548**	**-4.0060059059**
5	-4.0060171453	-4.0060150370	-4.0060129995	-4.0060110599	-4.0060092313	-4.0060058869
10	-4.0060170634	-4.0060149572	-4.0060129256	-4.0060109971	-4.0060091700	-4.0060058342
15	-4.0060169292	-4.0060148364	-4.0060128154	-4.0060108921	-4.0060090722	-4.0060057497
20	-4.0060167603	-4.0060146752	-4.0060126661	-4.0060107516	-4.0060089412	-4.0060056374
25	-4.0060165480	-4.0060144766	-4.0060124826	-4.0060105797	-4.0060087807	-4.0060054992
30	-4.0060163003	-4.0060142468	-4.0060122685	-4.0060103801	-4.0060085935	-4.0060053387
35	-4.0060160240	-4.0060139887	-4.0060120280	-4.0060101557	-4.0060083858	-4.0060051591
40	-4.0060157234	-4.0060137067	-4.0060117628	-4.0060099111	-4.0060081588	-4.0060049633
45	-4.0060154046	-4.0060134073	-4.0060114843	-4.0060096531	-4.0060079169	-4.0060047549
50	-4.0060150761	-4.0060130964	-4.0060111978	-4.0060093844	-4.0060076661	-4.0060045388
55	-4.0060147476	-4.0060127879	-4.0060109085	-4.0060091135	-4.0060074136	-4.0060043212
60	-4.0060144294	-4.0060124893	-4.0060106258	-4.0060088487	-4.0060071671	-4.0060041075
65	-4.0060141335	-4.0060122065	-4.0060103595	-4.0060085987	-4.0060069354	-4.0060039047
70	-4.0060138704	-4.0060119562	-4.0060101208	-4.0060083746	-4.0060067270	-4.0060037223
75	-4.0060136527	-4.0060117485	-4.0060099230	-4.0060081876	-4.0060065506	-4.0060035696
80	-4.0060134906	-4.0060115933	-4.0060097752	-4.0060080478	-4.0060064186	-4.0060034561
85	-4.0060133918	-4.0060114988	-4.0060096852	-4.0060079622	-4.0060063380	-4.0060033875
90	**-4.0060133617**	**-4.0060114703**	**-4.0060096588**	**-4.0060079383**	**-4.0060063148**	**-4.0060033664**

Table A.1 (cont'd).

	R (in a.u.)					
θ (deg)	8.00	8.50	9.00	9.50	10.00	10.50
0	**-4.0059993295**	**-4.0059948916**	**-4.0059919633**	**-4.0059900180**	**-4.0059886866**	**-4.0059877477**
5	-4.0059993170	-4.0059948827	-4.0059919565	-4.0059900136	-4.0059886833	-4.0059877451
10	-4.0059992811	-4.0059948573	-4.0059919382	-4.0059900011	-4.0059886735	-4.0059877376
15	-4.0059992233	-4.0059948168	-4.0059919097	-4.0059899809	-4.0059886579	-4.0059877257
20	-4.0059991457	-4.0059947630	-4.0059918719	-4.0059899536	-4.0059886369	-4.0059877096
25	-4.0059990504	-4.0059946971	-4.0059918258	-4.0059899198	-4.0059886111	-4.0059876898
30	-4.0059989399	-4.0059946209	-4.0059917726	-4.0059898807	-4.0059885813	-4.0059876667
35	-4.0059988168	-4.0059945363	-4.0059917139	-4.0059898374	-4.0059885483	-4.0059876410
40	-4.0059986836	-4.0059944460	-4.0059916512	-4.0059897910	-4.0059885129	-4.0059876132
45	-4.0059985432	-4.0059943519	-4.0059915863	-4.0059897430	-4.0059884760	-4.0059875840
50	-4.0059983987	-4.0059942567	-4.0059915212	-4.0059896948	-4.0059884387	-4.0059875543
55	-4.0059982540	-4.0059941630	-4.0059914574	-4.0059896475	-4.0059884017	-4.0059875248
60	-4.0059981130	-4.0059940734	-4.0059913969	-4.0059896026	-4.0059883663	-4.0059874964
65	-4.0059979806	-4.0059939907	-4.0059913417	-4.0059895615	-4.0059883335	-4.0059874701
70	-4.0059978619	-4.0059939174	-4.0059912934	-4.0059895255	-4.0059883045	-4.0059874467
75	-4.0059977636	-4.0059938563	-4.0059912538	-4.0059894958	-4.0059882805	-4.0059874274
80	-4.0059976892	-4.0059938104	-4.0059912245	-4.0059894737	-4.0059882625	-4.0059874129
85	-4.0059976422	-4.0059937823	-4.0059912065	-4.0059894601	-4.0059882513	-4.0059874039
90	**-4.0059976276**	**-4.0059937731**	**-4.0059912005**	**-4.0059894555**	**-4.0059882475**	**-4.0059874008**

Table A.1 (cont'd).

	R (in a.u.)				
θ (deg)	11.00	12.00	14.00	17.00	20.00
0	**-4.0059870770**	**-4.0059862315**	**-4.0059854892**	**-4.0059851587**	**-4.0059850719**
5	-4.0059870750	-4.0059862303	-4.0059854887	-4.0059851586	**-4.0059850719**
10	-4.0059870692	-4.0059862268	-4.0059854872	-4.0059851582	-4.0059850718
15	-4.0059870599	-4.0059862210	-4.0059854848	-4.0059851577	-4.0059850716
20	-4.0059870474	-4.0059862132	-4.0059854814	-4.0059851569	-4.0059850714
25	-4.0059870319	-4.0059862035	-4.0059854773	-4.0059851560	-4.0059850712
30	-4.0059870138	-4.0059861921	-4.0059854725	-4.0059851549	-4.0059850709
35	-4.0059869935	-4.0059861794	-4.0059854672	-4.0059851537	-4.0059850705
40	-4.0059869714	-4.0059861655	-4.0059854616	-4.0059851524	-4.0059850702
45	-4.0059869482	-4.0059861509	-4.0059854557	-4.0059851510	-4.0059850698
50	-4.0059869245	-4.0059861360	-4.0059854499	-4.0059851497	-4.0059850695
55	-4.0059869009	-4.0059861212	-4.0059854443	-4.0059851484	-4.0059850691
60	-4.0059868781	-4.0059861069	-4.0059854390	-4.0059851472	-4.0059850688
65	-4.0059868570	-4.0059860938	-4.0059854390	-4.0059851461	-4.0059850685
70	-4.0059868384	-4.0059860822	-4.0059854300	-4.0059851452	-4.0059850683
75	-4.0059868230	-4.0059860727	-4.0059854266	-4.0059851444	-4.0059850680
80	-4.0059868115	-4.0059860656	-4.0059854242	-4.0059851439	-4.0059850679
85	-4.0059868043	-4.0059860612	-4.0059854226	-4.0059851435	-4.0059850678
90	**-4.0059868019**	**-4.0059860597**	**-4.0059854221**	**-4.0059851434**	**-4.0059850677**

Table A.2. CR-CC(2,3) energies of H_2–He for $r_{H-H} = 1.280\ a_0$ with an aug-cc-pV5Z basis, as a function of the separation R between the center of mass of the two H nuclei and the He nucleus, and the angle θ between the H–H vector and the z axis. The He atom is located along the z axis. Entries in blue denote the maximum and entries in bold black denote the minimum of the potential, as a function of the angle θ for each value of R.

	R (in a.u.)					
θ (deg)	0.90	1.00	1.10	1.25	1.50	1.75
0	**0.5236003277**	**-1.3313980570**	**-2.2781675941**	**-3.0092283713**	**-3.5347766262**	**-3.7613569317**
5	0.3133448325	-1.4116208342	-2.3153797171	-3.0235894628	-3.5387167264	-3.7627392823
10	-0.2072567559	-1.6240945566	-2.4171583639	-3.0638405008	-3.5499710238	-3.7667326304
15	-0.8285733279	-1.9057370927	-2.5596234467	-3.1226684717	-3.5670043182	-3.7729102985
20	-1.4042478342	-2.1968874114	-2.7164991510	-3.1910277424	-3.5877411728	-3.7806691406
25	-1.8788080755	-2.4608629013	-2.8677012771	-3.2607298675	-3.6100545855	-3.7893490688
30	-2.2486754876	-2.6826812126	-3.0017197368	-3.3258993605	-3.6321393949	-3.7983375745
35	-2.5290886740	-2.8606203032	-3.1140097198	-3.3831685772	-3.6527010912	-3.8071399802
40	-2.7385233025	-2.9990648182	-3.2044040367	-3.4312035313	-3.6709734408	-3.8154035897
45	-2.8932952813	-3.1043262133	-3.2749423161	-3.4700315726	-3.6866301596	-3.8229108613
50	-3.0063826286	-3.1827113064	-3.3285144541	-3.5004564909	-3.6996595648	-3.8295533993
55	-3.0877165476	-3.2397695642	-3.3681266937	-3.5236353422	-3.7102413126	-3.8352989917
60	-3.1447996591	-3.2801461217	-3.3965716128	-3.5408178049	-3.7186492084	-3.8401619637
65	-3.1833486863	-3.3076727532	-3.4163109969	-3.5531976410	-3.7251833172	-3.8441791934
70	-3.2078712266	-3.3255345393	-3.4294550279	-3.5618348493	-3.7301260086	-3.8473951386
75	-3.2221864642	-3.3364104078	-3.4377696846	-3.5676170820	-3.7337185374	-3.8498511034
80	-3.2297560285	-3.3425161362	-3.4426681727	-3.5712440085	-3.7361504789	-3.8515810390
85	-3.2333806765	-3.3455154173	-3.4451876768	-3.5732193975	-3.7375564894	-3.8526095511
90	**-3.2344890295**	**-3.1625598562**	**-3.4459579882**	**-3.5738452611**	**-3.7380167474**	**-3.8529511057**

Table A.2 (cont'd).

	R (in a.u.)					
θ (deg)	1.90	2.00	2.20	2.40	2.60	2.80
0	**-3.8411928859**	**-3.8814548086**	**-3.9413272824**	**-3.9823993535**	**-4.0109627764**	**-4.0308827117**
5	-3.8420118701	-3.8820567078	3.9416795876	-3.9826222077	-4.0111103135	-4.0309819635
10	-3.8443932908	-3.8838130756	-3.9427137867	-3.9832787783	-4.0115455302	-4.0312766816
15	-3.8481177867	-3.8865772544	-3.9443587097	-3.9843310247	-4.0122463501	-4.0317524156
20	-3.8528704746	-3.8901377632	-3.9465090146	-3.9857203986	-4.0131774721	-4.0323869332
25	-3.8582958355	-3.8942501773	-3.9490390806	-3.9873750409	-4.0142947954	-4.0331517005
30	-3.8640492272	-3.8986715841	-3.9518176947	-3.9892173052	-4.0155495191	-4.0340149114
35	-3.8698355417	-3.9031856619	-3.9547199562	-3.9911700637	-4.0168908074	-4.0349424583
40	-3.8754247534	-3.9076155113	-3.9576359278	-3.9931603773	-4.0182697068	-4.0359009505
45	-3.8806544431	-3.9118269842	-3.9604733112	-3.9951241853	-4.0196416282	-4.0368592281
50	-3.8854202260	-3.9157246201	-3.9631568106	-3.9970055400	-4.0209657615	-4.0377881461
55	-3.8896613472	-3.9192435854	-3.9656278497	-3.9987578415	-4.0222071074	-4.0386622613
60	-3.8933472962	-3.9223416729	-3.9678414818	-4.0003431058	-4.0233362783	-4.0394597915
65	-3.8964651908	-3.9249917084	-3.9697629757	-4.0017304603	-4.0243289742	-4.0401626940
70	-3.8990120537	-3.9271766239	-3.9713660527	-4.0028953807	-4.0251655892	-4.0407562607
75	-3.9009891990	-3.9288853994	-3.9726313835	-4.0038194908	-4.0258310281	-4.0412291264
80	-3.9023992633	-3.9301106774	-3.9735449216	-4.0044890752	-4.0263141615	-4.0415728612
85	-3.9032446189	-3.9308479932	-3.9740971748	-4.0048949564	-4.0266072889	-4.0417815871
90	**-3.9035266072**	**-3.9310943338**	**-3.9742822211**	**-4.0050315484**	**-4.0267065581**	**-4.0418524670**

Table A.2 (cont'd).

	R (in a.u.)					
θ (deg)	3.00	3.50	4.00	4.50	5.00	5.50
0	**-4.0447399109**	**-4.0633980418**	**-4.0705411097**	**-4.0731365925**	**-4.0740169937**	**-4.0742854969**
5	-4.0448075941	-4.0634235667	-4.0705504860	-4.0731397039	-4.0740178455	-4.0742856692
10	-4.0450084030	-4.0634998668	-4.0705781044	-4.0731487756	-4.0740204043	-4.0742861055
15	-4.0453333823	-4.0636237199	-4.0706228197	-4.0731635743	-4.0740245874	-4.0742868500
20	-4.0457678189	-4.0637898191	-4.0706828862	-4.0731834647	-4.0740302814	-4.0742879008
25	-4.0462929779	-4.0639910503	-4.0707557850	-4.0732076640	-4.0740372620	-4.0742892479
30	-4.0468875189	-4.0642198078	-4.0708387314	-4.0732353179	-4.0740452569	-4.0742908221
35	-4.0475284973	-4.0644671597	-4.0709285042	-4.0732651596	-4.0740537898	-4.0742924874
40	-4.0481927878	-4.0647244211	-4.0710220294	-4.0732962502	-4.0740627708	-4.0742942657
45	-4.0488586338	-4.0649829642	-4.0711161906	-4.0733275454	-4.0740718667	-4.0742960630
50	-4.0495057533	-4.0652349595	-4.0712079531	-4.0733580821	-4.0740807005	-4.0742977806
55	-4.0501159757	-4.0654731870	-4.0712947057	-4.0733870123	-4.0740890205	-4.0742994325
60	-4.0506738593	-4.0656913135	-4.0713740833	-4.0734135789	-4.0740966769	-4.0743009496
65	-4.0511662345	-4.0658840386	-4.0714441800	-4.0734370345	-4.0741034561	-4.0743022885
70	-4.0515825693	-4.0660472961	-4.0715035958	-4.0734568344	-4.0741091822	-4.0743034114
75	-4.0519145947	-4.0661776264	-4.0715509414	-4.0734726237	-4.0741137432	-4.0743042961
80	-4.0521561172	-4.0662724197	-4.0715854073	-4.0734841218	-4.0741170645	-4.0743049291
85	-4.0523029673	-4.0663301225	-4.0716064897	-4.0734911108	-4.0741190934	-4.0743053126
90	**-4.0523526377**	**-4.0663496545**	**-4.0716137487**	**-4.0734935226**	**-4.0741197988**	**-4.0743054770**

Table A.2 (cont'd).

	R (in a.u.)					
θ (deg)	6.00	6.05	6.10	6.15	6.20	6.25
0	**-4.0743502005**	**-4.0743520947**	**-4.0743535162**	**-4.0743545259**	**-4.0743551801**	**-4.0743555255**
5	-4.0743501351	-4.0743520195	-4.0743534337	-4.0743544306	-4.0743550870	-4.0743554312
10	-4.0743499597	-4.0743518197	-4.0743532230	-4.0743542183	-4.0743548591	-4.0743551843
15	-4.0743497354	-4.0743515628	-4.0743529263	-4.0743539061	-4.0743545312	-4.0743548546
20	-4.0743494909	-4.0743512773	-4.0743526117	-4.0743535524	-4.0743541509	-4.0743544514
25	-4.0743492690	-4.0743509922	-4.0743522720	-4.0743531656	-4.0743537284	-4.0743540100
30	-4.0743490578	-4.0743506852	-4.0743519318	-4.0743527827	-4.0743533103	-4.0743535593
35	-4.0743488210	-4.0743504026	-4.0743515646	-4.0743523641	-4.0743528496	-4.0743530644
40	-4.0743485930	-4.0743500930	-4.0743511888	-4.0743519332	-4.0743523770	-4.0743525598
45	-4.0743483599	-4.0743497797	-4.0743508162	-4.0743515096	-4.0743519090	-4.0743520502
50	-4.0743481284	-4.0743494748	-4.0743504442	-4.0743510842	-4.0743514348	-4.0743515490
55	-4.0743479056	-4.0743491743	-4.0743500759	-4.0743506603	-4.0743509765	-4.0743510550
60	-4.0743476844	-4.0743488844	-4.0743497291	-4.0743502679	-4.0743505419	-4.0743505874
65	-4.0743474941	-4.0743486245	-4.0743494155	-4.0743499116	-4.0743501506	-4.0743501677
70	-4.0743473169	-4.0743484036	-4.0743491535	-4.0743496121	-4.0743498194	-4.0743498107
75	-4.0743471636	-4.0743482092	-4.0743489258	-4.0743493570	-4.0743495414	-4.0743495136
80	-4.0743470459	-4.0743480611	-4.0743487527	-4.0743491631	-4.0743493308	-4.0743492893
85	-4.0743469796	-4.0743479760	-4.0743486515	-4.0743490488	-4.0743492053	-4.0743491546
90	**-4.0743469756**	**-4.0743479664**	**-4.0743486368**	**-4.0743490293**	**-4.0743491814**	**-4.0743491267**

Table A.2 (cont'd).

	R (in a.u.)					
θ (deg)	6.30	6.35	6.40	6.45	6.50	6.55
0	**-4.0743556060**	**-4.0743554578**	**-4.0743551166**	**-4.0743546118**	**-4.0743539680**	**-4.0743532103**
5	-4.0743555091	-4.0743553539	-4.0743550202	-4.0743545150	-4.0743538726	-4.0743531166
10	-4.0743552681	-4.0743551179	-4.0743547754	-4.0743542711	-4.0743536306	-4.0743528771
15	-4.0743549193	-4.0743547627	-4.0743544175	-4.0743539126	-4.0743532735	-4.0743525221
20	-4.0743544991	-4.0743543304	-4.0743539777	-4.0743534697	-4.0743528321	-4.0743520859
25	-4.0743540465	-4.0743538691	-4.0743535095	-4.0743529967	-4.0743523553	-4.0743516069
30	-4.0743535676	-4.0743533694	-4.0743529957	-4.0743524740	-4.0743518285	-4.0743510803
35	-4.0743530494	-4.0743528321	-4.0743524469	-4.0743519186	-4.0743512700	-4.0743505217
40	-4.0743525179	-4.0743522839	-4.0743518861	-4.0743513494	-4.0743506962	-4.0743499460
45	-4.0743519879	-4.0743517316	-4.0743513168	-4.0743507681	-4.0743501073	-4.0743493532
50	-4.0743514517	-4.0743511734	-4.0743507424	-4.0743501827	-4.0743495153	-4.0743487586
55	-4.0743509292	-4.0743506295	-4.0743501825	-4.0743496119	-4.0743489390	-4.0743481798
60	-4.0743504367	-4.0743501182	-4.0743496564	-4.0743490747	-4.0743483952	-4.0743476348
65	-4.0743499944	-4.0743496590	-4.0743491861	-4.0743485968	-4.0743479088	-4.0743471416
70	-4.0743496168	-4.0743492648	-4.0743487788	-4.0743481803	-4.0743474872	-4.0743467163
75	-4.0743493038	-4.0743489389	-4.0743484425	-4.0743478357	-4.0743471386	-4.0743463647
80	-4.0743490684	-4.0743486948	-4.0743481918	-4.0743475807	-4.0743468788	-4.0743461020
85	-4.0743489269	-4.0743485480	-4.0743480415	-4.0743474267	-4.0743467217	-4.0743459430
90	**-4.0743488947**	**-4.0743485122**	**-4.0743480020**	**-4.0743473842**	**-4.0743466775**	**-4.0743458973**

Table A.2 (cont'd).

	R (in a.u.)					
θ (deg)	6.60	6.65	6.70	6.75	6.80	6.85
0	**-4.0743523585**	**-4.0743514303**	**-4.0743504408**	**-4.0743494041**	**-4.0743483316**	**-4.0743472332**
5	-4.0743522671	-4.0743513408	-4.0743503540	-4.0743493196	-4.0743482489	-4.0743471503
10	-4.0743520303	-4.0743511077	-4.0743501245	-4.0743490936	-4.0743480264	-4.0743469309
15	-4.0743516776	-4.0743507579	-4.0743497786	-4.0743487528	-4.0743476944	-4.0743466125
20	-4.0743512490	-4.0743503383	-4.0743493689	-4.0743483539	-4.0743473035	-4.0743462274
25	-4.0743507710	-4.0743498642	-4.0743489009	-4.0743478925	-4.0743468480	-4.0743457845
30	-4.0743502476	-4.0743493457	-4.0743483882	-4.0743473888	-4.0743463569	-4.0743453013
35	-4.0743496925	-4.0743487961	-4.0743478457	-4.0743468540	-4.0743458311	-4.0743447841
40	-4.0743491160	-4.0743482214	-4.0743472752	-4.0743462897	-4.0743452748	-4.0743442401
45	-4.0743485228	-4.0743476309	-4.0743466907	-4.0743457123	-4.0743447052	-4.0743436791
50	-4.0743479286	-4.0743470392	-4.0743461023	-4.0743451298	-4.0743441325	-4.0743431190
55	-4.0743473493	-4.0743464642	-4.0743455358	-4.0743445727	-4.0743435805	-4.0743425714
60	-4.0743468065	-4.0743459230	-4.0743449961	-4.0743440361	-4.0743430529	-4.0743420545
65	-4.0743463124	-4.0743454287	-4.0743445041	-4.0743435485	-4.0743425703	-4.0743415766
70	-4.0743458830	-4.0743449975	-4.0743440740	-4.0743431205	-4.0743421451	-4.0743411558
75	-4.0743455287	-4.0743446441	-4.0743437209	-4.0743427673	-4.0743417944	-4.0743408095
80	-4.0743452647	-4.0743443797	-4.0743434578	-4.0743425074	-4.0743415370	-4.0743405545
85	-4.0743451047	-4.0743442192	-4.0743432970	-4.0743423475	-4.0743413794	-4.0743403994
90	**-4.0743450580**	**-4.0743441718**	**-4.0743432492**	**-4.0743422999**	**-4.0743413319**	**-4.0743403526**

Table A.2 (cont'd).

	R (in a.u.)					
θ (deg)	6.90	6.95	7.00	7.10	7.20	7.30
0	**-4.0743461183**	**-4.0743449938**	**-4.0743438663**	**-4.0743416159**	**-4.0743393999**	**-4.0743372651**
5	-4.0743460394	-4.0743449162	-4.0743437866	-4.0743415413	-4.0743393329	-4.0743372017
10	-4.0743458201	-4.0743447037	-4.0743435826	-4.0743413464	-4.0743391515	-4.0743370333
15	-4.0743455123	-4.0743444013	-4.0743432893	-4.0743410706	-4.0743388952	-4.0743367914
20	-4.0743451331	-4.0743440338	-4.0743429303	-4.0743407335	-4.0743385768	-4.0743364948
25	-4.0743447025	-4.0743436121	-4.0743425195	-4.0743403483	-4.0743382166	-4.0743361479
30	-4.0743442300	-4.0743431508	-4.0743420694	-4.0743399239	-4.0743378129	-4.0743357698
35	-4.0743437221	-4.0743426565	-4.0743415873	-4.0743394649	-4.0743373782	-4.0743353646
40	-4.0743431919	-4.0743421346	-4.0743410761	-4.0743389769	-4.0743369232	-4.0743349381
45	-4.0743426417	-4.0743416015	-4.0743405567	-4.0743384803	-4.0743364543	-4.0743344975
50	-4.0743420918	-4.0743410586	-4.0743400292	-4.0743379792	-4.0743359810	-4.0743340516
55	-4.0743415541	-4.0743405350	-4.0743395102	-4.0743374870	-4.0743355151	-4.0743336134
60	-4.0743410463	-4.0743400319	-4.0743390183	-4.0743370175	-4.0743350705	-4.0743331943
65	-4.0743405738	-4.0743395679	-4.0743385647	-4.0743365840	-4.0743346588	-4.0743328056
70	-4.0743401591	-4.0743391606	-4.0743381654	-4.0743362019	-4.0743342947	-4.0743324608
75	-4.0743398179	-4.0743388250	-4.0743378362	-4.0743358861	-4.0743339932	-4.0743321748
80	-4.0743395661	-4.0743385771	-4.0743375924	-4.0743356517	-4.0743337690	-4.0743319610
85	-4.0743394137	-4.0743384277	-4.0743374460	-4.0743355112	-4.0743336345	-4.0743318335
90	**-4.0743393679**	**-4.0743383831**	**-4.0743374031**	**-4.0743354716**	**-4.0743335979**	**-4.0743317986**

Table A.2 (cont'd).

	R (in a.u.)					
θ (deg)	7.50	8.00	8.50	9.00	9.50	10.00
0	**-4.0743332550**	**-4.0743250570**	**-4.0743193687**	**-4.0743155524**	**-4.0743129670**	**-4.0743111775**
5	-4.0743332007	-4.0743250209	-4.0743193439	-4.0743155342	-4.0743129541	-4.0743111672
10	-4.0743330546	-4.0743249231	-4.0743192758	-4.0743154837	-4.0743129171	-4.0743111419
15	-4.0743328447	-4.0743247816	-4.0743191747	-4.0743154083	-4.0743128654	-4.0743111036
20	-4.0743325839	-4.0743246042	-4.0743190483	-4.0743153143	-4.0743127967	-4.0743110542
25	-4.0743322839	-4.0743243983	-4.0743189021	-4.0743152061	-4.0743127167	-4.0743109962
30	-4.0743319538	-4.0743241701	-4.0743187406	-4.0743150876	-4.0743126291	-4.0743109321
35	-4.0743316001	-4.0743239244	-4.0743185682	-4.0743149628	-4.0743125370	-4.0743108638
40	-4.0743312272	-4.0743236655	-4.0743183890	-4.0743148353	-4.0743124428	-4.0743107936
45	-4.0743308409	-4.0743233983	-4.0743182058	-4.0743147080	-4.0743123491	-4.0743107231
50	-4.0743304501	-4.0743231286	-4.0743180234	-4.0743145833	-4.0743122576	-4.0743106538
55	-4.0743300657	-4.0743228640	-4.0743178459	-4.0743144635	-4.0743121702	-4.0743105878
60	-4.0743296977	-4.0743226117	-4.0743176790	-4.0743143514	-4.0743120889	-4.0743105263
65	-4.0743293563	-4.0743223774	-4.0743175273	-4.0743142488	-4.0743120151	-4.0743104703
70	-4.0743290516	-4.0743221692	-4.0743173948	-4.0743141585	-4.0743119503	-4.0743104215
75	-4.0743287971	-4.0743219977	-4.0743172855	-4.0743140842	-4.0743118969	-4.0743103811
80	-4.0743286086	-4.0743218731	-4.0743172038	-4.0743140289	-4.0743118568	-4.0743103508
85	-4.0743284965	-4.0743217961	-4.0743171538	-4.0743139947	-4.0743118321	-4.0743103321
90	**-4.0743284647**	**-4.0743217728**	**-4.0743171373**	**-4.0743139839**	**-4.0743118244**	**-4.0743103263**

Table A.2 (cont'd).

	R (in a.u.)					
θ (deg)	10.50	11.00	12.00	14.00	17.00	20.00
0	**-4.0743099231**	**-4.0743090402**	**-4.0743079352**	**-4.0743069346**	**-4.0743065067**	**-4.0743063946**
5	-4.0743099154	-4.0743090331	-4.0743079302	-4.0743069337	-4.0743065065	-4.0743063945
10	-4.0743098964	-4.0743090180	-4.0743079196	-4.0743069309	-4.0743065059	-4.0743063944
15	-4.0743098677	-4.0743089949	-4.0743079028	-4.0743069264	-4.0743065050	-4.0743063941
20	-4.0743098311	-4.0743089653	-4.0743078820	-4.0743069204	-4.0743065037	-4.0743063937
25	-4.0743097880	-4.0743089310	-4.0743078583	-4.0743069134	-4.0743065021	-4.0743063932
30	-4.0743097403	-4.0743088937	-4.0743078335	-4.0743069054	-4.0743065002	-4.0743063926
35	-4.0743096897	-4.0743088546	-4.0743078086	-4.0743068969	-4.0743064980	-4.0743063921
40	-4.0743096372	-4.0743088144	-4.0743077839	-4.0743068880	-4.0743064958	-4.0743063913
45	-4.0743095840	-4.0743087741	-4.0743077600	-4.0743068790	-4.0743064936	-4.0743063907
50	-4.0743095312	-4.0743087341	-4.0743077367	-4.0743068701	-4.0743064915	-4.0743063900
55	-4.0743094802	-4.0743086951	-4.0743077142	-4.0743068614	-4.0743064893	-4.0743063894
60	-4.0743094323	-4.0743086582	-4.0743076936	-4.0743068531	-4.0743064871	-4.0743063887
65	-4.0743093888	-4.0743086242	-4.0743076734	-4.0743068457	-4.0743064852	-4.0743063881
70	-4.0743093507	-4.0743085941	-4.0743076551	-4.0743068390	-4.0743064836	-4.0743063877
75	-4.0743093196	-4.0743085694	-4.0743076393	-4.0743068336	-4.0743064824	-4.0743063872
80	-4.0743092965	-4.0743085510	-4.0743076262	-4.0743068295	-4.0743064814	-4.0743063870
85	-4.0743092823	-4.0743085398	-4.0743076187	-4.0743068271	-4.0743064808	**-4.0743063867**
90	**-4.0743092779**	**-4.0743085361**	**-4.0743076162**	**-4.0743068263**	**-4.0743064806**	-4.0743063868

Table A.3. CR-CC(2,3) energies of H_2–He for $r_{H-H} = 1.787\ a_0$ with an aug-cc-pV5Z basis, as a function of the separation R between the center of mass of the two H nuclei and the He nucleus, and the angle θ between the H–H vector and the z axis. The He atom is located along the z axis. Entries in blue denote the maximum and entries in bold black denote the minimum of the potential, as a function of the angle θ for each value of R.

	R (in a.u.)					
θ (deg)	1.25	1.50	1.75	1.90	2.00	2.20
0	**-1.4634549066**	**-3.1272093801**	**-3.6170582166**	**-3.7507260524**	**-3.8102798064**	**-3.8903723804**
5	-1.6055529777	-3.1518671285	-3.6236046741	-3.7540336014	-3.8124675591	-3.8914349291
10	-1.9514662911	-3.2181090006	-3.6417800472	-3.7633271387	-3.8186593250	-3.8944836106
15	-2.3518120741	-3.3078019600	-3.6678590133	-3.7769630773	-3.8278649285	-3.8991294713
20	-2.7079635962	-3.4021674033	-3.6973717435	-3.7928765591	-3.8388142889	-3.9048541533
25	-2.9877299881	-3.4882574949	-3.7264997204	-3.8091802951	-3.8503024373	-3.9111332124
30	-3.1940780888	-3.5599698091	-3.7527614881	-3.8245218008	-3.8614195822	-3.9175302761
35	-2.9165743564	-3.6161380179	-3.7750162543	-3.8381567794	-3.8716147360	-3.9237350482
40	-3.4432386512	-3.6582487127	-3.7931073137	-3.8498364921	-3.8806484392	-3.9295563171
45	-3.5127999906	-3.6888154140	-3.8074398501	-3.8596277565	-3.8884888442	-3.9348948675
50	-3.5589470768	-3.7104713256	-3.8186463046	-3.8677471760	-3.8952130038	-3.9397066502
55	-3.5885318305	-3.7255522230	-3.8273723319	-3.8744464547	-3.9009331166	-3.9439755878
60	-3.6066411239	-3.7359477256	-3.8341686734	-3.8799490953	-3.9057545165	-3.9476950914
65	-3.6171067488	-3.7430853206	-3.8341686734	-3.8844255300	-3.9097572565	-3.9508608069
70	-3.6228260529	-3.7479754820	-3.7479754820	-3.8879920962	-3.9129945951	-3.9534666958
75	-3.6258777885	-3.7512872797	-3.8465455602	-3.8907204659	-3.9154972089	-3.9555048305
80	-3.6275417046	-3.7534329555	-3.8486515026	-3.8926511209	-3.9172802714	-3.9569675632
85	-3.6284207017	-3.7546453884	-3.8498958034	-3.8938040592	-3.9183494377	-3.9578486522
90	**-3.6287075657**	**-3.8941879547**	**-3.8503084241**	**-3.8941879547**	**-3.9187061950**	**-3.9581430343**

Table A.3 (cont'd).

	R (in a.u.)					
θ (deg)	2.40	2.60	2.80	3.00	3.50	4.00
0	**-3.9410981384**	**-3.9755712865**	**-3.9998788081**	**-4.0172712994**	**-4.0421094232**	**-4.0525948663**
5	-3.9416900053	-3.9759402380	-4.0001259488	-4.0174430026	-4.0421813936	-4.0526239178
10	-3.9434088788	-3.9770208674	-4.0008536318	-4.0179503296	-4.0423939946	-4.0527100225
15	-3.9460842194	-3.9787272720	-4.0020119487	-4.0187620827	-4.0427359869	-4.0528483663
20	-3.9494770902	-3.9809354230	-4.0035295824	-4.0198315175	-4.0431890867	-4.0530320759
25	-3.9533333457	-3.9835045075	-4.0053196891	-4.0211025512	-4.0437306815	-4.0532519026
30	-3.9574189142	-3.9862961963	-4.0072927702	-4.0225143613	-4.0443361832	-4.0534974346
35	-3.9615447318	-3.9891852535	-4.0093631041	-4.0240060697	-4.0449790810	-4.0537584964
40	-3.9655683272	-3.9920671888	-4.0114530465	-4.0255214628	-4.0456351231	-4.0540245198
45	-3.9693882296	-3.9948561153	-4.0134953131	-4.0270094676	-4.0462815627	-4.0542866201
50	-3.9729320999	-3.9974840198	-4.0154352029	-4.0284280706	-4.0468989841	-4.0545368044
55	-3.9761490905	-3.9998974810	-4.0172269745	-4.0297419422	-4.0474713916	-4.0547683433
60	-3.9790002899	-4.0020546628	-4.0188347369	-4.0309226296	-4.0479858599	-4.0549762917
65	-3.9814567959	-4.0039234867	-4.0202310338	-4.0319489035	-4.0484328588	-4.0551566017
70	-3.9834953051	-4.0054800191	-4.0213954975	-4.0328050712	-4.0488059831	-4.0553066104
75	-3.9850983150	-4.0067066918	-4.0223138860	-4.0334802857	-4.0490998403	-4.0554245582
80	-3.9862523159	-4.0075909641	-4.0229762390	-4.0339671244	-4.0493116626	-4.0555094508
85	-3.9869483309	-4.0081246384	-4.0233761303	-4.0342611219	-4.0494395299	-4.0555609017
90	**-3.9871812133**	**-4.0083032088**	**-4.0235100430**	**-4.0343603176**	**-4.0494824969**	**-4.0555782326**

Table A.3 (cont'd).

	R (in a.u.)					
θ (deg)	4.50	5.00	5.50	6.00	6.10	6.20
0	**-4.0567991666**	**-4.0583840979**	**-4.0589368836**	**-4.0591068243**	**-4.0591206715**	**-4.0591306849**
5	-4.0568099454	-4.0583878106	-4.0589379921	-4.0591070182	-4.0591207709	-4.0591307150
10	-4.0568425176	-4.0583989414	-4.0589413121	-4.0591076631	-4.0591211546	-4.0591308895
15	-4.0568946934	-4.0584170002	-4.0589466459	-4.0591086961	-4.0591217836	-4.0591311988
20	-4.0569639023	-4.0584409656	-4.0589538024	-4.0591100918	-4.0591226395	-4.0591316804
25	-4.0570469510	-4.0584696515	-4.0589623180	-4.0591117842	-4.0591237079	-4.0591322717
30	-4.0571396750	-4.0585015715	-4.0589717817	-4.0591136591	-4.0591248918	-4.0591329006
35	-4.0572379674	-4.0585353906	-4.0589818115	-4.0591156120	-4.0591261036	-4.0591335204
40	-4.0573382726	-4.0585698237	-4.0589919069	-4.0591175432	-4.0591272662	-4.0591341407
45	-4.0574368929	-4.0586035805	-4.0590017618	-4.0591193749	-4.0591283939	-4.0591346862
50	-4.0575308806	-4.0586355922	-4.0590110552	-4.0591210815	-4.0591293905	-4.0591351459
55	-4.0576176725	-4.0586650658	-4.0590195797	-4.0591225945	-4.0591302595	-4.0591355229
60	-4.0576954097	-4.0586915100	-4.0590271745	-4.0591239042	-4.0591309978	-4.0591358199
65	-4.0577626993	-4.0587143489	-4.0590337066	-4.0591250090	-4.0591315993	-4.0591360392
70	-4.0578185483	-4.0587332883	-4.0590390999	-4.0591258837	-4.0591320700	-4.0591362032
75	-4.0578624428	-4.0587481383	-4.0590432947	-4.0591265435	-4.0591324131	-4.0591362994
80	-4.0578940190	-4.0587588036	-4.0590462632	-4.0591270045	-4.0591326525	-4.0591363660
85	-4.0579130731	-4.0587652080	-4.0590480675	-4.0591272935	-4.0591327970	-4.0591364014
90	**-4.0579196034**	**-4.0587674208**	**-4.0590487088**	**-4.0591274112**	**-4.0591328698**	**-4.0591364377**

Table A.3 (cont'd).

	R (in a.u.)					
θ (deg)	6.25	6.30	6.35	6.40	6.45	6.50
0	-4.0591345137	-4.0591376732	-4.0591402435	**-4.0591422918**	**-4.0591438813**	**-4.0591450677**
5	**-4.0591345118**	**-4.0591376421**	-4.0591401840	-4.0591422066	-4.0591437721	-4.0591449373
10	-4.0591345989	-4.0591376558	-4.0591401354	-4.0591421176	-4.0591436435	-4.0591447781
15	-4.0591347624	-4.0591377393	-4.0591401339	-4.0591420320	-4.0591434946	-4.0591445748
20	-4.0591351151	-4.0591379310	-4.0591402018	-4.0591419921	-4.0591433604	-4.0591443588
25	-4.0591355240	-4.0591381680	-4.0591402833	-4.0591419402	-4.0591431954	-4.0591440984
30	-4.0591359117	-4.0591383662	-4.0591403292	-4.0591418519	-4.0591429882	-4.0591437875
35	-4.0591363153	-4.0591385678	**-4.0591403510**	-4.0591417215	-4.0591427299	-4.0591434212
40	-4.0591366840	-4.0591387283	-4.0591403330	-4.0591415510	-4.0591424297	-4.0591430117
45	-4.0591370002	-4.0591388455	-4.0591402770	-4.0591413449	-4.0591420966	-4.0591425725
50	-4.0591372432	-4.0591389010	-4.0591401719	-4.0591411030	-4.0591417362	-4.0591421088
55	-4.0591374213	**-4.0591389069**	-4.0591400297	-4.0591408336	-4.0591413590	-4.0591416417
60	-4.0591375386	-4.0591388705	-4.0591398616	-4.0591405518	-4.0591409811	-4.0591411846
65	-4.0591376065	-4.0591388072	-4.0591396847	-4.0591402782	-4.0591406237	-4.0591407532
70	-4.0591376444	-4.0591387352	-4.0591395156	-4.0591400244	-4.0591402963	-4.0591403618
75	-4.0591376359	-4.0591386407	-4.0591393508	-4.0591397940	-4.0591400092	-4.0591400277
80	-4.0591376340	-4.0591385713	-4.0591392189	-4.0591396139	-4.0591397891	-4.0591397741
85	-4.0591376278	-4.0591385306	-4.0591391488	-4.0591395170	-4.0591396672	-4.0591396281
90	**-4.0591376470**	-4.0591385341	**-4.0591391385**	**-4.0591394958**	**-4.0591396377**	**-4.0591395930**

Table A.3 (cont'd).

	R (in a.u.)					
θ (deg)	6.55	6.60	6.65	6.70	6.75	6.80
0	**-4.0591459035**	**-4.0591464293**	**-4.0591466880**	**-4.0591467146**	**-4.0591465403**	**-4.0591461933**
5	-4.0591457534	-4.0591462674	-4.0591465214	-4.0591465541	-4.0591463876	-4.0591460490
10	-4.0591455700	-4.0591460624	-4.0591462943	-4.0591463000	-4.0591461111	-4.0591457561
15	-4.0591453198	-4.0591457719	-4.0591459691	-4.0591459459	-4.0591457327	-4.0591453564
20	-4.0591450342	-4.0591454279	-4.0591455769	-4.0591455140	-4.0591452685	-4.0591448668
25	-4.0591446940	-4.0591450207	-4.0591451134	-4.0591450038	-4.0591447199	-4.0591442869
30	-4.0591442935	-4.0591445441	-4.0591445737	-4.0591444122	-4.0591440865	-4.0591436202
35	-4.0591438356	-4.0591440092	-4.0591439746	-4.0591437605	-4.0591433922	-4.0591428922
40	-4.0591433335	-4.0591434325	-4.0591433350	-4.0591430697	-4.0591426607	-4.0591421285
45	-4.0591428052	-4.0591428267	-4.0591426674	-4.0591423521	-4.0591419033	-4.0591413412
50	-4.0591422569	-4.0591422085	-4.0591419906	-4.0591416274	-4.0591411401	-4.0591405483
55	-4.0591417131	-4.0591416012	-4.0591413307	-4.0591409238	-4.0591404005	-4.0591397796
60	-4.0591411884	-4.0591410186	-4.0591406991	-4.0591402515	-4.0591396954	-4.0591390546
65	-4.0591406947	-4.0591404727	-4.0591401095	-4.0591396264	-4.0591390472	-4.0591383844
70	-4.0591402472	-4.0591399778	-4.0591395808	-4.0591390771	-4.0591384779	-4.0591377949
75	-4.0591398771	-4.0591395813	-4.0591391601	-4.0591386301	-4.0591380077	-4.0591373088
80	-4.0591395946	-4.0591392734	-4.0591388306	-4.0591382836	-4.0591376486	-4.0591369405
85	-4.0591394256	-4.0591390832	-4.0591386251	-4.0591380707	-4.0591374302	-4.0591367169
90	**-4.0591393869**	**-4.0591390422**	**-4.0591385793**	**-4.0591380162**	**-4.0591373689**	**-4.0591366516**

Table A.3 (cont'd).

	R (in a.u.)					
θ (deg)	6.90	7.00	7.10	7.15	7.25	7.30
0	**-4.0591450839**	**-4.0591435536**	**-4.0591417340**	**-4.0591407489**	**-4.0591386802**	**-4.0591376139**
5	-4.0591449463	-4.0591434196	-4.0591416079	-4.0591406262	-4.0591385620	-4.0591374974
10	-4.0591446396	-4.0591431094	-4.0591412978	-4.0591403179	-4.0591382587	-4.0591371968
15	-4.0591442093	-4.0591426678	-4.0591408572	-4.0591398789	-4.0591378279	-4.0591367724
20	-4.0591436855	-4.0591421242	-4.0591402998	-4.0591393211	-4.0591372759	-4.0591362243
25	-4.0591430607	-4.0591414750	-4.0591396385	-4.0591386601	-4.0591366238	-4.0591355834
30	-4.0591423474	-4.0591407368	-4.0591388989	-4.0591379242	-4.0591359031	-4.0591348705
35	-4.0591415747	-4.0591399451	-4.0591381064	-4.0591371343	-4.0591351261	-4.0591341036
40	-4.0591407699	-4.0591391201	-4.0591372773	-4.0591363093	-4.0591343163	-4.0591333053
45	-4.0591399450	-4.0591382763	-4.0591364297	-4.0591354649	-4.0591334904	-4.0591324932
50	-4.0591391199	-4.0591374306	-4.0591355845	-4.0591346258	-4.0591326709	-4.0591316858
55	-4.0591383144	-4.0591366074	-4.0591347663	-4.0591338142	-4.0591318796	-4.0591309072
60	-4.0591375484	-4.0591358323	-4.0591339959	-4.0591330503	-4.0591311354	-4.0591301760
65	-4.0591368471	-4.0591351263	-4.0591332952	-4.0591323563	-4.0591304602	-4.0591295124
70	-4.0591362398	-4.0591345122	-4.0591326843	-4.0591317502	-4.0591298693	-4.0591289313
75	-4.0591357361	-4.0591340028	-4.0591321779	-4.0591312479	-4.0591293794	-4.0591284494
80	-4.0591353567	-4.0591336199	-4.0591317977	-4.0591308711	-4.0591290123	-4.0591280883
85	-4.0591351258	-4.0591333861	-4.0591315644	-4.0591306393	-4.0591287856	-4.0591278652
90	**-4.0591350562**	**-4.0591333139**	**-4.0591314913**	**-4.0591305662**	**-4.0591287136**	**-4.0591277945**

Table A.3 (cont'd).

	R (in a.u.)					
θ (deg)	7.35	7.50	8.00	8.50	9.00	9.50
0	**-4.0591365358**	**-4.0591332866**	**-4.0591233125**	**-4.0591156680**	**-4.0591103268**	**-4.0591066587**
5	-4.0591364214	-4.0591331789	-4.0591232299	-4.0591156156	-4.0591102928	-4.0591066359
10	-4.0591361256	-4.0591329015	-4.0591230195	-4.0591154729	-4.0591101962	-4.0591065723
15	-4.0591357062	-4.0591324931	-4.0591227094	-4.0591152598	-4.0591100502	-4.0591064712
20	-4.0591351629	-4.0591319875	-4.0591223197	-4.0591149895	-4.0591098631	-4.0591063392
25	-4.0591345347	-4.0591313906	-4.0591218682	-4.0591146739	-4.0591096421	-4.0591061798
30	-4.0591338318	-4.0591307266	-4.0591213720	-4.0591143240	-4.0591093946	-4.0591060039
35	-4.0591330770	-4.0591300164	-4.0591208444	-4.0591139523	-4.0591091317	-4.0591058154
40	-4.0591322922	-4.0591292811	-4.0591203002	-4.0591135687	-4.0591088601	-4.0591056204
45	-4.0591314948	-4.0591285343	-4.0591197514	-4.0591131830	-4.0591085881	-4.0591054246
50	-4.0591307021	-4.0591277956	-4.0591192098	-4.0591128040	-4.0591083228	-4.0591052330
55	-4.0591299379	-4.0591270816	-4.0591186878	-4.0591124416	-4.0591080704	-4.0591050515
60	-4.0591292209	-4.0591264123	-4.0591181976	-4.0591121042	-4.0591078368	-4.0591048846
65	-4.0591285700	-4.0591258046	-4.0591177534	-4.0591117990	-4.0591076270	-4.0591047346
70	-4.0591279998	-4.0591252725	-4.0591173650	-4.0591115333	-4.0591074457	-4.0591046046
75	-4.0591275273	-4.0591248319	-4.0591170459	-4.0591113154	-4.0591072968	-4.0591044987
80	-4.0591271734	-4.0591245015	-4.0591168071	-4.0591111536	-4.0591071853	-4.0591044202
85	-4.0591269538	-4.0591242968	-4.0591166601	-4.0591110544	-4.0591071168	-4.0591043726
90	**-4.0591268847**	**-4.0591242347**	**-4.0591166126**	**-4.0591110213**	**-4.0591070938**	**-4.0591043575**

Table A.3 (cont'd).

	R (in a.u.)					
θ (deg)	10.00	11.00	12.00	14.00	17.00	20.00
0	**-4.0591041108**	**-4.0591010669**	**-4.0590995056**	**-4.0590981366**	**-4.0590975561**	**-4.0590974024**
5	-4.0591040944	-4.0591010576	-4.0590995001	-4.0590981350	-4.0590975556	-4.0590974023
10	-4.0591040473	-4.0591010315	-4.0590994844	-4.0590981305	-4.0590975544	-4.0590974019
15	-4.0591039736	-4.0591009911	-4.0590994599	-4.0590981232	-4.0590975526	-4.0590974013
20	-4.0591038786	-4.0591009390	-4.0590994282	-4.0590981134	-4.0590975501	-4.0590974005
25	-4.0591037669	-4.0591008778	-4.0590993912	-4.0590981017	-4.0590975470	-4.0590973996
30	-4.0591036408	-4.0591008098	-4.0590993508	-4.0590980883	-4.0590975435	-4.0590973984
35	-4.0591035057	-4.0591007375	-4.0590993083	-4.0590980737	-4.0590975396	-4.0590973971
40	-4.0591033658	-4.0591006630	-4.0590992650	-4.0590980585	-4.0590975356	-4.0590973958
45	-4.0591032252	-4.0591005879	-4.0590992217	-4.0590980428	-4.0590975314	-4.0590973945
50	-4.0591032252	-4.0591005139	-4.0590991792	-4.0590980272	-4.0590975314	-4.0590973931
55	-4.0591029565	-4.0591004423	-4.0590991382	-4.0590980120	-4.0590975231	-4.0590973918
60	-4.0591028348	-4.0591003747	-4.0590990990	-4.0590979978	-4.0590975194	-4.0590973905
65	-4.0591027252	-4.0591003128	-4.0590990632	-4.0590979848	-4.0590975160	-4.0590973895
70	-4.0591026302	-4.0591002589	-4.0590990318	-4.0590979734	-4.0590975131	-4.0590973884
75	-4.0591025524	-4.0591002148	-4.0590990057	-4.0590979642	-4.0590975107	-4.0590973877
80	-4.0591024947	-4.0591001821	-4.0590989862	-4.0590979573	-4.0590975090	-4.0590973871
85	-4.0591024596	-4.0591001620	-4.0590989741	-4.0590979531	-4.0590975079	-4.0590973868
90	**-4.0591024481**	**-4.0591001554**	**-4.0590989701**	**-4.0590979517**	**-4.0590975076**	**-4.0590973867**

Table A.4. CR-CC(2,3) energies of H_2–He for $r_{H-H} = 2.125\ a_0$ with an aug-cc-pV5Z basis, as a function of the separation R between the center of mass of the two H nuclei and the He nucleus, and the angle θ between the H–H vector and the z axis. The He atom is located along the z axis. Entries in blue denote the maximum and entries in bold black denote the minimum of the potential, as a function of the angle θ for each value of R.

	R (in a.u.)					
θ (deg)	1.75	1.90	2.00	2.10	2.20	2.30
0	**-3.3698825671**	**-3.6100583376**	**-3.7067923365**	**-3.7745443430**	**-3.8236315669**	**-3.8604032346**
5	-3.3902788586	-3.6193753560	-3.7125654325	-3.7782370096	-3.8260710296	-3.8620732244
10	-3.4443078846	-3.6446216986	-3.7283834103	-3.7884540070	-3.8328875236	-3.8667818295
15	-3.5155417810	-3.6792566460	-3.7505271950	-3.8030165204	-3.8427692377	-3.8737243290
20	-3.5878542865	-3.7161861957	-3.7747831073	-3.8193747921	-3.8541455845	-3.8819106192
25	-3.6511315601	-3.7502495063	-3.7978757915	-3.8354409270	-3.8656706290	-3.8904569637
30	-3.7015464559	-3.7788960377	-3.8180057354	-3.8499661026	-3.8764749003	-3.8987499581
35	-3.7393551006	-3.8016376583	-3.8346442704	-3.8624768570	-3.8861609116	-3.9064602882
40	-3.7666881296	-3.8191517984	-3.8480501597	-3.8730145735	-3.8946586058	-3.9134667468
45	-3.7861343162	-3.8325435265	-3.8588068652	-3.8818530917	-3.9020614945	-3.9197600700
50	-3.8000280785	-3.8428965585	-3.8675234893	-3.8893047693	-3.9085041011	-3.9253701052
55	-3.8101777812	-3.8510674248	-3.8746873539	-3.8956264285	-3.9141000637	-3.9303268313
60	-3.8178292433	-3.8576414141	-3.8806300169	-3.9009880235	-3.9189216194	-3.9346443775
65	-3.8237531593	-3.8629712131	-3.8855454454	-3.9054850538	-3.9230039025	-3.9383233051
70	-3.8283721843	-3.8672432660	-3.8895311170	-3.9091596988	-3.9263568956	-3.9413547991
75	-3.8318891946	-3.8705422611	-3.8926271224	-3.9120252655	-3.9289780409	-3.9437278206
80	-3.8343849694	-3.8728975053	-3.8948433167	-3.9140798729	-3.9308595939	-3.9454319438
85	-3.8358829448	-3.8743139837	-3.8961771865	-3.9153176766	-3.9319928937	-3.9464584168
90	**-3.8363882020**	**-3.8747891781**	**-3.8966242616**	**-3.9157321480**	**-3.9323719594**	**-3.9468017914**

Table A.4 (cont'd).

	R (in a.u.)					
θ (deg)	2.40	2.50	2.60	2.70	2.80	2.90
0	**-3.8888319231**	**-3.9114348801**	**-3.9298293695**	**-3.9450714347**	**-3.9578683765**	**-3.9687078200**
5	-3.8900183827	-3.9123118743	-3.9305004835	-3.9456011457	-3.9582967956	-3.9690611227
10	-3.8933940525	-3.9148232137	-3.9324353648	-3.9471365261	-3.9595442520	-3.9700927066
15	-3.8984535195	-3.9186449907	-3.9354166888	-3.9495261609	-3.9615015379	-3.9717210925
20	-3.9045556945	-3.9233477280	-3.9391497184	-3.9525616847	-3.9640138530	-3.9738272156
25	-3.9111060600	-3.9285214745	-3.9433398107	-3.9560216282	-3.9669117474	-3.9762772806
30	-3.9176616006	-3.9338353423	-3.9477336402	-3.9597079988	-3.9700351403	-3.9789395711
35	-3.9239484688	-3.9390608884	-3.9521383605	-3.9634561084	-3.9732430899	-3.9816938561
40	-3.9298268435	-3.9440549304	-3.9564165055	-3.9671390682	-3.9764209834	-3.9844374891
45	-3.9352324253	-3.9487282187	-3.9604700485	-3.9706589875	-3.9794763745	-3.9870856567
50	-3.9401362411	-3.9530208667	-3.9642266169	-3.9739407609	-3.9823363379	-3.9895706703
55	-3.9445214461	-3.9568912104	-3.9676319542	-3.9769266454	-3.9849442671	-3.9918397157
60	-3.9483697878	-3.9603044476	-3.9706444159	-3.9795726539	-3.9872580106	-3.9938539373
65	-3.9516622304	-3.9632321909	-3.9732322334	-3.9818475300	-3.9892473268	-3.9955855966
70	-3.9543806711	-3.9656520882	-3.9753720725	-3.9837284860	-3.9908920257	-3.9970165396
75	-3.9565102240	-3.9675480229	-3.9770485052	-3.9852017912	-3.9921796144	-3.9981362180
80	-3.9580392604	-3.9689092025	-3.9782519783	-3.9862589050	-3.9931029606	-3.9989387899
85	-3.9589605020	-3.9697291392	-3.9789765761	-3.9868954245	-3.9936588757	-3.9994217221
90	**-3.9592686679**	**-3.9700033325**	**-3.9792186578**	**-3.9871080296**	**-3.9938447892**	**-3.9995835079**

Table A.4 (cont'd).

	R (in a.u.)					
θ (deg)	3.00	3.25	3.50	3.75	4.00	4.50
0	**-3.9779408815**	**-3.9955791649**	**-4.0075061849**	**-4.0155038176**	**-4.0207978580**	**-4.0264719538**
5	-3.9782358016	-3.9957732059	-4.0076355950	-4.0155895598	-4.0208538910	-4.0264943740
10	-3.9790995610	-3.9963426968	-4.0080145831	-4.0158406738	-4.0210177800	-4.0265606984
15	-3.9804685958	-3.9972503691	-4.0086207992	-4.0162418429	-4.0212796982	-4.0266662728
20	-3.9822492106	-3.9984404083	-4.0094176548	-4.0167696955	-4.0216240702	-4.0268057996
25	-3.9843329681	-3.9998442129	-4.0103604435	-4.0173945121	-4.0220317318	-4.0269703705
30	-3.9866097147	-4.0013893080	-4.0114008503	-4.0180846497	-4.0224809815	-4.0271515880
35	-3.9889770394	-4.0030051571	-4.0124901267	-4.0188069963	-4.0229521095	-4.0273407654
40	-3.9913440651	-4.0046279802	-4.0135849475	-4.0195326703	-4.0234245718	-4.0275302137
45	-3.9936343310	-4.0062025244	-4.0146474473	-4.0202362076	-4.0238820223	-4.0277130657
50	-3.9957865800	-4.0076839337	-4.0156464718	-4.0208972027	-4.0243110899	-4.0278841237
55	-3.9977533350	-4.0090375452	-4.0165585323	-4.0214996902	-4.0247016462	-4.0280393637
60	-3.9994994468	-4.0102382764	-4.0173663021	-4.0220322557	-4.0250464354	-4.0281760016
65	-4.0010001474	-4.0112692890	-4.0180585941	-4.0224880755	-4.0253411254	-4.0282923274
70	-4.0022395342	-4.0121197278	-4.0186290799	-4.0228631508	-4.0255831286	-4.0283876011
75	-4.0032088945	-4.0127837557	-4.0190739277	-4.0231554591	-4.0257711134	-4.0284614643
80	-4.0039032557	-4.0132590871	-4.0193919765	-4.0233638723	-4.0259052191	-4.0285139700
85	-4.0043208852	-4.0135448230	-4.0195831403	-4.0234889873	-4.0259858849	-4.0285456162
90	**-4.0044610133**	**-4.0136405283**	**-4.0196475039**	**-4.0235311406**	**-4.0260130886**	**-4.0285564214**

Table A.4 (cont'd).

	R (in a.u.)					
θ (deg)	5.00	5.50	6.00	6.05	6.10	6.15
0	**-4.0287491154**	**-4.0296010060**	**-4.0298906390**	**-4.0299048290**	**-4.0299172990**	**-4.0299282189**
5	-4.0287574134	-4.0296038420	-4.0298913708	-4.0299054462	-4.0299178069	-4.0299286204
10	-4.0287821150	-4.0296121598	-4.0298936531	-4.0299074043	-4.0299194811	-4.0299300533
15	-4.0288217075	-4.0296254346	-4.0298973669	-4.0299106116	-4.0299222394	-4.0299324107
20	-4.0288736824	-4.0296429664	-4.0299022594	-4.0299148237	-4.0299258512	-4.0299355226
25	-4.0289351272	-4.0296636780	-4.0299080002	-4.0299198159	-4.0299301649	-4.0299391882
30	-4.0290025914	-4.0296863456	-4.0299143165	-4.0299252457	-4.0299348018	-4.0299431223
35	-4.0290729365	-4.0297099023	-4.0299207421	-4.0299307651	-4.0299395106	-4.0299471137
40	-4.0291431113	-4.0297332664	-4.0299270251	-4.0299361571	-4.0299441056	-4.0299509948
45	-4.0292106064	-4.0297555432	-4.0299328832	-4.0299411520	-4.0299483323	-4.0299545375
50	-4.0292735449	-4.0297761537	-4.0299382132	-4.0299456761	-4.0299521446	-4.0299577210
55	-4.0293303233	-4.0297946312	-4.0299429370	-4.0299496741	-4.0299554933	-4.0299604945
60	-4.0293801935	-4.0298107217	-4.0299469500	-4.0299580344	-4.0299583275	-4.0299661928
65	-4.0294225062	-4.0298242989	-4.0299502582	-4.0299558498	-4.0299606434	-4.0299647241
70	-4.0294570238	-4.0298352833	-4.0299528752	-4.0299580344	-4.0299624465	-4.0299661928
75	-4.0294836912	-4.0298437258	-4.0299548223	-4.0299596606	-4.0299637860	-4.0299672752
80	-4.0295026323	-4.0298497184	-4.0299562044	-4.0299608008	-4.0299647142	-4.0299680163
85	-4.0295140428	-4.0298533375	-4.0299570446	-4.0299614996	-4.0299652852	-4.0299684741
90	**-4.0295180010**	**-4.0298546163**	**-4.0299573834**	**-4.0299617892**	**-4.0299655319**	**-4.0299686833**

Table A.4 (cont'd).

	R (in a.u.)					
θ (deg)	6.20	6.25	6.30	6.35	6.40	6.45
0	**-4.0299377478**	**-4.0299460305**	**-4.0299531964**	**-4.0299593616**	**-4.0299646340**	**-4.0299691094**
5	-4.0299380393	-4.0299462549	-4.0299533731	-4.0299594911	-4.0299647215	-4.0299691625
10	-4.0299392754	-4.0299472869	-4.0299542092	-4.0299601710	-4.0299652619	-4.0299695798
15	-4.0299412681	-4.0299489741	-4.0299556199	-4.0299613264	-4.0299661931	-4.0299703114
20	-4.0299439232	-4.0299511987	-4.0299574685	-4.0299628396	-4.0299674093	-4.0299712648
25	-4.0299470247	-4.0299537960	-4.0299596188	-4.0299645947	-4.0299688152	-4.0299723629
30	-4.0299503352	-4.0299565579	-4.0299618954	-4.0299664427	-4.0299702853	-4.0299735003
35	-4.0299536836	-4.0299593367	-4.0299641691	-4.0299682694	-4.0299717180	-4.0299745880
40	-4.0299569351	-4.0299620239	-4.0299663515	-4.0299700021	-4.0299730528	-4.0299755768
45	-4.0299598704	-4.0299644239	-4.0299682824	-4.0299715235	-4.0299742153	-4.0299764179
50	-4.0299624979	-4.0299665597	-4.0299699867	-4.0299728463	-4.0299751988	-4.0299771017
55	-4.0299647626	-4.0299683849	-4.0299714191	-4.0299739302	-4.0299759765	-4.0299776111
60	-4.0299666500	-4.0299719719	-4.0299725675	-4.0299747782	-4.0299765605	-4.0299779633
65	-4.0299681721	-4.0299710621	-4.0299734594	-4.0299754164	-4.0299769779	-4.0299781859
70	-4.0299693465	-4.0299719719	-4.0299741261	-4.0299758582	-4.0299772284	-4.0299782909
75	-4.0299701984	-4.0299726176	-4.0299745991	-4.0299761805	-4.0299774117	-4.0299783332
80	-4.0299707747	-4.0299730500	-4.0299748964	-4.0299763630	-4.0299774936	-4.0299783298
85	-4.0299711322	-4.0299733208	-4.0299750964	-4.0299765033	-4.0299775791	-4.0299783617
90	**-4.0299713081**	**-4.0299734644**	**-4.0299752050**	**-4.0299765770**	**-4.0299776231**	**-4.0299783820**

Table A.4 (cont'd).

	R (in a.u.)					
θ (deg)	6.50	6.55	6.60	6.65	6.70	6.75
0	-4.0299728770	**-4.0299760145**	-4.0299785938	-4.0299806757	-4.0299823198	**-4.0299835742**
5	-4.0299729009	-4.0299760147	**-4.0299785729**	-4.0299806376	-4.0299822668	-4.0299835109
10	-4.0299732099	-4.0299762272	-4.0299787007	-4.0299806924	-4.0299822585	-4.0299834493
15	-4.0299737635	-4.0299766232	-4.0299789582	-4.0299808288	-4.0299822901	-4.0299833898
20	-4.0299744847	-4.0299771384	-4.0299792963	-4.0299810136	-4.0299823386	-4.0299833188
25	-4.0299753127	-4.0299777341	-4.0299796781	-4.0299812078	**-4.0299823708**	-4.0299832105
30	-4.0299761567	-4.0299783174	-4.0299800382	-4.0299813706	-4.0299823599	-4.0299830559
35	-4.0299769472	-4.0299788379	-4.0299803167	-4.0299814297	-4.0299822468	-4.0299827883
40	-4.0299776290	-4.0299792579	-4.0299805157	**-4.0299814480**	-4.0299820925	-4.0299824839
45	-4.0299781858	-4.0299795693	**-4.0299806136**	-4.0299813594	-4.0299818425	-4.0299820959
50	-4.0299786068	-4.0299797607	-4.0299806052	-4.0299811776	-4.0299815116	-4.0299816379
55	-4.0299788816	**-4.0299798309**	-4.0299804974	-4.0299809156	-4.0299811165	-4.0299811287
60	-4.0299790313	-4.0299798044	-4.0299803189	-4.0299806071	-4.0299806976	-4.0299806086
65	**-4.0282923274**	-4.0299797015	-4.0299800760	-4.0299802426	-4.0299802312	-4.0299800650
70	**-4.0299790329**	-4.0299795333	-4.0299798143	-4.0299799003	-4.0299798124	-4.0299795815
75	-4.0299789808	-4.0299793870	-4.0299795798	-4.0299796020	-4.0299794569	-4.0299791764
80	-4.0299789097	-4.0299792584	-4.0299794020	-4.0299793691	-4.0299791843	-4.0299788689
85	-4.0299788871	-4.0299791877	-4.0299792926	-4.0299792276	-4.0299790158	-4.0299786779
90	-4.0299788883	-4.0299791737	-4.0299792660	**-4.0299791908**	**-4.0299789706**	**-4.0299786258**

Table A.4 (cont'd).

	R (in a.u.)					
θ (deg)	6.80	6.85	6.90	6.95	7.00	7.05
0	**-4.0299845009**	**-4.0299851336**	**-4.0299854981**	**-4.0299856327**	**-4.0299855699**	**-4.0299853348**
5	-4.0299844164	-4.0299850234	-4.0299853802	-4.0299855074	-4.0299854365	-4.0299851944
10	-4.0299843097	-4.0299848802	-4.0299851975	-4.0299852935	-4.0299851982	-4.0299849376
15	-4.0299841721	-4.0299846748	-4.0299849336	-4.0299849801	-4.0299848428	-4.0299845472
20	-4.0299839966	-4.0299844094	-4.0299845912	-4.0299845719	-4.0299843806	-4.0299840395
25	-4.0299837691	-4.0299840829	-4.0299841799	-4.0299840888	-4.0299838269	-4.0299834323
30	-4.0299834859	-4.0299836902	-4.0299836906	-4.0299835164	-4.0299831909	-4.0299827392
35	-4.0299830884	-4.0299831772	-4.0299830812	-4.0299828264	-4.0299824453	-4.0299819522
40	-4.0299826548	-4.0299826349	-4.0299824517	-4.0299821286	-4.0299816834	-4.0299811324
45	-4.0299821499	-4.0299820324	-4.0299817669	-4.0299813728	-4.0299808672	-4.0299802670
50	-4.0299815852	-4.0299813788	-4.0299810380	-4.0299805794	-4.0299800207	-4.0299793782
55	-4.0299809828	-4.0299807016	-4.0299802913	-4.0299797742	-4.0299791698	-4.0299784924
60	-4.0299803644	-4.0299787685	-4.0299795407	-4.0299775889	-4.0299783419	-4.0299761509
65	-4.0299797652	-4.0299793511	-4.0299788384	-4.0299782415	-4.0299775734	-4.0299768463
70	-4.0299792285	-4.0299787685	-4.0299782172	-4.0299775889	-4.0299768963	-4.0299761509
75	-4.0299787791	-4.0299782825	-4.0299777032	-4.0299770529	-4.0299763425	-4.0299755838
80	-4.0299784419	-4.0299779205	-4.0299773199	-4.0299766526	-4.0299759289	-4.0299751591
85	-4.0299782326	-4.0299776961	-4.0299770830	-4.0299764051	-4.0299756712	-4.0299748946
90	**-4.0299781748**	**-4.0299776338**	**-4.0299770169**	**-4.0299763357**	**-4.0299756008**	**-4.0299748227**

Table A.4 (cont'd).

	R (in a.u.)					
θ (deg)	7.10	7.15	7.20	7.25	7.30	7.35
0	**-4.0299849531**	**-4.0299844446**	**-4.0299838300**	**-4.0299831243**	**-4.0299823425**	**-4.0299814986**
5	-4.0299848058	-4.0299842980	-4.0299836899	-4.0299829896	-4.0299822097	-4.0299813650
10	-4.0299845350	-4.0299840126	-4.0299833872	-4.0299826728	-4.0299818849	-4.0299810363
15	-4.0299841161	-4.0299835677	-4.0299829202	-4.0299821909	-4.0299813882	-4.0299805308
20	-4.0299835698	-4.0299829900	-4.0299823170	-4.0299815666	-4.0299807529	-4.0299798881
25	-4.0299829223	-4.0299823113	-4.0299816156	-4.0299808492	-4.0299800232	-4.0299791462
30	-4.0299822010	-4.0299815556	-4.0299808267	-4.0299800324	-4.0299791853	-4.0299782961
35	-4.0299813571	-4.0299806733	-4.0299799204	-4.0299791105	-4.0299782534	-4.0299773588
40	-4.0299804918	-4.0299797764	-4.0299789991	-4.0299781714	-4.0299773029	-4.0299764023
45	-4.0299795876	-4.0299788425	-4.0299780436	-4.0299772011	-4.0299763239	-4.0299754202
50	-4.0299786662	-4.0299778969	-4.0299770808	-4.0299762273	-4.0299753441	-4.0299744391
55	-4.0299777546	-4.0299769672	-4.0299761385	-4.0299752767	-4.0299743906	-4.0299734872
60	-4.0299768784	-4.0299745406	-4.0299752371	-4.0299728255	-4.0299734864	-4.0299710577
65	-4.0299760709	-4.0299752568	-4.0299744125	-4.0299735453	-4.0299726621	-4.0299717685
70	-4.0299753627	-4.0299745406	-4.0299736926	-4.0299728255	-4.0299719454	-4.0299710577
75	-4.0299747867	-4.0299739594	-4.0299731090	-4.0299722402	-4.0299713627	-4.0299704790
80	-4.0299743533	-4.0299735197	-4.0299726662	-4.0299717991	-4.0299709234	-4.0299700436
85	-4.0299740857	-4.0299732511	-4.0299723974	-4.0299715305	-4.0299706554	-4.0299697768
90	**-4.0299740111**	**-4.0299731742**	**-4.0299723190**	**-4.0299714514**	**-4.0299705767**	**-4.0299696993**

Table A.4 (cont'd).

	R (in a.u.)					
θ (deg)	7.40	7.45	7.50	7.55	7.60	7.65
0	**-4.0299806019**	**-4.0299796651**	**-4.0299786940**	**-4.0299776978**	**-4.0299766838**	**-4.0299756604**
5	-4.0299804674	-4.0299795273	-4.0299785547	-4.0299775580	-4.0299765463	-4.0299755266
10	-4.0299801374	-4.0299791985	-4.0299782293	-4.0299772380	-4.0299762317	-4.0299752163
15	-4.0299796295	-4.0299786915	-4.0299777248	-4.0299767369	-4.0299757347	-4.0299747245
20	-4.0299789818	-4.0299780415	-4.0299770749	-4.0299760898	-4.0299750929	-4.0299740899
25	-4.0299782296	-4.0299772835	-4.0299763162	-4.0299753345	-4.0299743442	-4.0299733505
30	-4.0299773740	-4.0299764274	-4.0299754628	-4.0299744858	-4.0299735022	-4.0299725168
35	-4.0299764355	-4.0299754908	-4.0299745315	-4.0299735632	-4.0299725912	-4.0299716198
40	-4.0299754775	-4.0299745353	-4.0299735821	-4.0299726230	-4.0299716627	-4.0299707052
45	-4.0299744968	-4.0299735600	-4.0299726154	-4.0299716678	-4.0299707214	-4.0299697798
50	-4.0299735188	-4.0299725891	-4.0299716548	-4.0299707217	-4.0299697886	-4.0299688640
55	-4.0299725723	-4.0299716510	-4.0299707281	-4.0299698074	-4.0299688921	-4.0299679854
60	-4.0299716802	-4.0299699699	-4.0299698594	-4.0299675153	-4.0299680554	-4.0299657922
65	-4.0299708696	-4.0299692774	-4.0299690731	-4.0299681824	-4.0299673006	-4.0299664301
70	-4.0299701671	-4.0299692774	-4.0299683924	-4.0299675153	-4.0299666480	-4.0299657922
75	-4.0299695967	-4.0299687156	-4.0299678398	-4.0299669743	-4.0299661162	-4.0299652697
80	-4.0299691640	-4.0299682878	-4.0299674177	-4.0299665557	-4.0299657039	-4.0299648648
85	-4.0299688983	-4.0299680233	-4.0299671559	-4.0299662971	-4.0299654481	-4.0299646138
90	**-4.0299688229**	**-4.0299679511**	**-4.0299670864**	**-4.0299662314**	**-4.0299653888**	**-4.0299645615**

Table A.4 (cont'd).

	R (in a.u.)					
θ (deg)	7.70	7.75	7.80	7.85	7.90	7.95
0	**-4.0299746346**	**-4.0299736095**	**-4.0299725890**	**-4.0299715758**	**-4.0299705735**	**-4.0299695846**
5	-4.0299745037	-4.0299734813	-4.0299724630	-4.0299714523	-4.0299704521	-4.0299694652
10	-4.0299741971	-4.0299731787	-4.0299721648	-4.0299711587	-4.0299701629	-4.0299691795
15	-4.0299737115	-4.0299727001	-4.0299716941	-4.0299706967	-4.0299697113	-4.0299687406
20	-4.0299730858	-4.0299720849	-4.0299710909	-4.0299701070	-4.0299691352	-4.0299681777
25	-4.0299723573	-4.0299713682	-4.0299703866	-4.0299694154	-4.0299684574	-4.0299675147
30	-4.0299715338	-4.0299705569	-4.0299695892	-4.0299686334	-4.0299676918	-4.0299667663
35	-4.0299706527	-4.0299696934	-4.0299687447	-4.0299678092	-4.0299668887	-4.0299659853
40	-4.0299697541	-4.0299688123	-4.0299678824	-4.0299669666	-4.0299660669	-4.0299651847
45	-4.0299688463	-4.0299679235	-4.0299670138	-4.0299661191	-4.0299652412	-4.0299643811
50	-4.0299679490	-4.0299670461	-4.0299661572	-4.0299652841	-4.0299644281	-4.0299635903
55	-4.0299670898	-4.0299662072	-4.0299653396	-4.0299644882	-4.0299636542	-4.0299628386
60	-4.0299662910	-4.0299654289	-4.0299645821	-4.0299637518	-4.0299629389	-4.0299621442
65	-4.0299655726	-4.0299647292	-4.0299639009	-4.0299630887	-4.0299622934	-4.0299615165
70	-4.0299649486	-4.0299641190	-4.0299633046	-4.0299625070	-4.0299617277	-4.0299609679
75	-4.0299644365	-4.0299636185	-4.0299628175	-4.0299620348	-4.0299612708	-4.0299605258
80	-4.0299640407	-4.0299632338	-4.0299624451	-4.0299616753	-4.0299609245	-4.0299601930
85	-4.0299637980	-4.0299630010	-4.0299622218	-4.0299614603	-4.0299607167	-4.0299599921
90	**-4.0299637499**	**-4.0299629543**	**-4.0299621754**	**-4.0299614146**	**-4.0299606721**	**-4.0299599483**

Table A.4 (cont'd).

	R (in a.u.)					
θ (deg)	8.00	8.50	9.00	9.50	10.00	10.50
0	**-4.0299686106**	**-4.0299599781**	**-4.0299536265**	**-4.0299492100**	**-4.0299461204**	**-4.0299439438**
5	-4.0299684937	-4.0299598936	-4.0299535676	-4.0299491789	-4.0299460969	-4.0299439259
10	-4.0299682107	-4.0299596907	-4.0299534352	-4.0299490872	-4.0299460293	-4.0299438764
15	-4.0299677862	-4.0299593790	-4.0299532271	-4.0299489387	-4.0299459228	-4.0299437999
20	-4.0299672365	-4.0299589738	-4.0299529497	-4.0299487410	-4.0299457836	-4.0299437003
25	-4.0299665892	-4.0299584994	-4.0299526146	-4.0299485088	-4.0299456193	-4.0299435825
30	-4.0299658587	-4.0299579749	-4.0299522489	-4.0299482506	-4.0299454354	-4.0299434510
35	-4.0299651002	-4.0299574196	-4.0299518561	-4.0299479711	-4.0299452372	-4.0299433101
40	-4.0299643213	-4.0299568499	-4.0299514534	-4.0299476827	-4.0299450324	-4.0299431645
45	-4.0299635401	-4.0299562810	-4.0299510529	-4.0299473945	-4.0299448295	-4.0299430187
50	-4.0299627717	-4.0299557292	-4.0299506640	-4.0299471167	-4.0299446326	-4.0299428766
55	-4.0299620422	-4.0299552077	-4.0299502967	-4.0299468561	-4.0299444428	-4.0299427405
60	-4.0299613685	-4.0299547267	-4.0299499591	-4.0299466146	-4.0299442703	-4.0299426169
65	-4.0299607588	-4.0299542976	-4.0299496602	-4.0299464025	-4.0299441134	-4.0299425031
70	-4.0299602281	-4.0299539299	-4.0299494079	-4.0299462178	-4.0299439789	-4.0299424053
75	-4.0299598006	-4.0299536340	-4.0299491980	-4.0299460679	-4.0299438705	-4.0299423267
80	-4.0299594807	-4.0299534076	-4.0299490409	-4.0299459572	-4.0299437909	-4.0299422687
85	-4.0299592868	-4.0299532650	-4.0299489422	-4.0299458905	-4.0299437434	-4.0299422296
90	**-4.0299592436**	**-4.0299532399**	**-4.0299489234**	**-4.0299458731**	**-4.0299437289**	**-4.0299422178**

Table A.4 (cont'd).

	R (in a.u.)				
θ (deg)	11.00	12.00	14.00	17.00	20.00
0	**-4.0299424077**	**-4.0299405192**	**-4.0299388925**	**-4.0299382068**	**-4.0299380250**
5	-4.0299423930	-4.0299405095	-4.0299388903	-4.0299382062	-4.0299380247
10	-4.0299423566	-4.0299404894	-4.0299388842	-4.0299382046	-4.0299380242
15	-4.0299423009	-4.0299404578	-4.0299388746	-4.0299382022	-4.0299380235
20	-4.0299422279	-4.0299404156	-4.0299388614	-4.0299381987	-4.0299380223
25	-4.0299421416	-4.0299403664	-4.0299388455	-4.0299381945	-4.0299380209
30	-4.0299420455	-4.0299403126	-4.0299388274	-4.0299381896	-4.0299380194
35	-4.0299419427	-4.0299402556	-4.0299388076	-4.0299381842	-4.0299380176
40	-4.0299418378	-4.0299401970	-4.0299387868	-4.0299381786	-4.0299380157
45	-4.0299417339	-4.0299401374	-4.0299387655	-4.0299381728	-4.0299380139
50	-4.0299416325	-4.0299400789	-4.0299387443	-4.0299381670	-4.0299380120
55	-4.0299415344	-4.0299400224	-4.0299387238	-4.0299381615	-4.0299380101
60	-4.0299414411	-4.0299399687	-4.0299387044	-4.0299381563	-4.0299380084
65	-4.0299413563	-4.0299399202	-4.0299386869	-4.0299381517	-4.0299380069
70	-4.0299412827	-4.0299398780	-4.0299386717	-4.0299381477	-4.0299380056
75	-4.0299412227	-4.0299398433	-4.0299386595	-4.0299381446	-4.0299380046
80	-4.0299411780	-4.0299398174	-4.0299386503	-4.0299381421	-4.0299380037
85	-4.0299411506	-4.0299398020	-4.0299386448	-4.0299381407	-4.0299380032
90	**-4.0299411415**	**-4.0299397971**	**-4.0299386430**	**-4.0299381403**	**-4.0299380031**

Table A.5. CR-CC(2,3) energies of H_2–He for $r_{H-H} = 2.801\ a_0$ with an aug-cc-pV5Z basis, as a function of the separation R between the center of mass of the two H nuclei and the He nucleus, and the angle θ between the H–H vector and the z axis. The He atom is located along the z axis. Entries in blue denote the maximum and entries in bold black denote the minimum of the potential, as a function of the angle θ for each value of R.

	R (a.u.)					
θ (deg)	1.75	1.90	2.00	2.10	2.20	2.30
0	**-1.4443239290**	**-2.7299837911**	**-3.1452011488**	**-3.3981535663**	**-3.5583827790**	**-3.6630785724**
5	-1.7576234466	-2.8298795952	-3.1978969909	-3.4276801259	-3.5756519310	-3.6735212240
10	-2.3749779999	-3.0582216269	-3.3247590492	-3.5012318595	-3.6197161007	-3.7006566071
15	-2.9070861949	-3.2960482616	-3.4672408488	-3.5883369105	-3.6740033373	-3.7351708210
20	-3.2643605730	-3.4822727049	-3.5871016422	-3.6657882301	-3.7245093478	-3.7685974441
25	-3.4838078147	-3.6093930289	-3.6737706576	-3.7246787403	-3.7647474774	-3.7965001960
30	-3.6136626106	-3.6900862449	-3.7313847739	-3.7657232640	-3.7942512139	-3.8181252039
35	-3.6888042060	-3.7393831084	-3.7682089783	-3.7933929949	-3.8153875031	-3.8346624678
40	-3.7316798471	-3.7693732956	-3.7919555844	-3.8124720442	-3.8310203626	-3.8477389726
45	-3.7565025307	-3.7885773904	-3.8083399206	-3.8266178904	-3.8433709571	-3.8586205251
50	-3.7722612098	-3.8023644466	-3.8209019641	-3.8380421756	-3.8537445727	-3.8680236703
55	-3.7841703930	-3.8135416355	-3.8313939158	-3.8477881433	-3.8627260483	-3.8762462962
60	-3.7944640439	-3.8231739454	-3.8404457953	-3.8562099752	-3.8704976750	-3.8833665333
65	-3.8035666531	-3.8314655104	-3.8481753105	-3.8633670248	-3.8770804601	-3.8893827163
70	-3.8112824279	-3.8383494119	-3.8545444746	-3.8692350537	-3.8824591534	-3.8942848807
75	-3.8173953657	-3.8437419241	-3.8595100560	-3.8737947489	-3.8866267060	-3.8980739186
80	-3.8217921600	-3.8476019970	-3.8630550404	-3.8770422030	-3.8895893765	-3.9007630911
85	-3.8244354689	-3.8499184852	-3.8651799602	-3.8789863082	-3.8913606282	-3.9023690582
90	**-3.8529511057**	**-3.8506909637**	**-3.8658881595**	**-3.8796344138**	**-3.8919511821**	**-3.9029041837**

Table A.5 (cont'd).

	R (a.u.)					
θ (deg)	2.40	2.50	2.60	2.70	2.80	2.90
0	**-3.7334790550**	**-3.7822628396**	**-3.8172167448**	**-3.8432032377**	**-3.8632705634**	**-3.8793282670**
5	-3.7399816321	-3.7864352456	-3.8199933847	-3.8451315945	-3.8646731784	-3.8803955108
10	-3.7571438671	-3.7976187534	-3.8275454537	-3.8504483251	-3.8685911417	-3.8834152935
15	-3.7796027220	-3.8126647893	-3.8379961166	-3.8580193285	-3.8743216934	-3.8879305913
20	-3.8022164714	-3.8284302290	-3.8494025618	-3.8666161872	-3.8810645721	-3.8934041533
25	-3.8220381382	-3.8429717869	-3.8604712849	-3.8753563896	-3.8881925131	-3.8993672075
30	-3.8383348371	-3.8556564693	-3.8706673103	-3.8837861777	-3.8953161080	-3.9054806333
35	-3.8516313585	-3.8666317439	-3.8799302792	-3.8917357681	-3.9022158867	-3.9115086193
40	-3.8627752179	-3.8762705042	-3.8883535649	-3.8991439021	-3.9087524852	-3.9172811612
45	-3.8724238910	-3.8848572333	-3.8960075550	-3.9059630960	-3.9148185076	-3.9226646483
50	-3.8809277632	-3.8925257304	-3.9028992497	-3.9121355467	-3.9203245151	-3.9275560035
55	-3.8884121093	-3.8993012233	-3.9090010841	-3.9176032174	-3.9252002394	-3.9318837924
60	-3.8948934990	-3.9051657842	-3.9142772943	-3.9223248195	-3.9294043037	-3.9356093527
65	-3.9003580870	-3.9101001366	-3.9187084105	-3.9262828851	-3.9329223156	-3.9387212981
70	-3.9048000379	-3.9141024187	-3.9222946446	-3.9294800015	-3.9357587704	-3.9412262844
75	-3.9082257334	-3.9171831308	-3.9250505650	-3.9319328303	-3.9379313540	-3.9431421899
80	-3.9106534411	-3.9193624832	-3.9269973616	-3.9336631139	-3.9394620690	-3.9444903614
85	-3.9121019920	-3.9206619445	-3.9281565385	-3.9346919599	-3.9403714360	-3.9452909211
90	**-3.9125843334**	**-3.9210945297**	**-3.9285425926**	**-3.9350349018**	**-3.9406741377**	**-3.9455569041**

Table A.5 (cont'd).

	R (a.u.)					
θ (deg)	3.00	3.50	4.00	4.50	5.00	5.50
0	**-3.8925672003**	**-3.9350472411**	**-3.9561408876**	**-3.9662406618**	**-3.9707554637**	**-3.9726391781**
5	-3.8934131161	-3.9354152406	-3.9563157518	-3.9663186893	-3.9707881685	-3.9726520501
10	-3.8958324066	-3.9364855542	-3.9568259563	-3.9665472120	-3.9708834434	-3.9726889863
15	-3.8995126295	-3.9381679691	-3.9576295927	-3.9669066789	-3.9710332615	-3.9727470171
20	-3.9040741402	-3.9403313623	-3.9586650529	-3.9673701192	-3.9712253832	-3.9728212591
25	-3.9091519425	-3.9428237636	-3.9598589471	-3.9679019518	-3.9714456997	-3.9729063905
30	-3.9144490941	-3.9454931254	-3.9611355967	-3.9684683584	-3.9716799002	-3.9729964653
35	-3.9197340500	-3.9481980289	-3.9624247234	-3.9690383846	-3.9719148516	-3.9730865851
40	-3.9248274007	-3.9508199432	-3.9636694134	-3.9695863639	-3.9721397648	-3.9731722059
45	-3.9295898914	-3.9532682948	-3.9648255385	-3.9700926612	-3.9723465434	-3.9732504723
50	-3.9339177861	-3.9554813357	-3.9658638742	-3.9705451891	-3.9725304797	-3.9733196084
55	-3.9377423764	-3.9574233862	-3.9667694641	-3.9709376956	-3.9726890452	-3.9733788593
60	-3.9410291455	-3.9590790759	-3.9675369460	-3.9712682378	-3.9728218266	-3.9734280426
65	-3.9437695607	-3.9604493203	-3.9681676701	-3.9715385611	-3.9729298824	-3.9734676552
70	-3.9459724199	-3.9615427767	-3.9686680605	-3.9717520159	-3.9730147222	-3.9734985161
75	-3.9476547042	-3.9623728260	-3.9690460924	-3.9719125894	-3.9730782087	-3.9735214190
80	-3.9488372900	-3.9629536749	-3.9693097403	-3.9720240732	-3.9731221357	-3.9735371567
85	-3.9495390174	-3.9632973848	-3.9694651400	-3.9720896623	-3.9731479139	-3.9735463790
90	**-3.9497723497**	**-3.9634116407**	**-3.9695169836**	**-3.9721116624**	**-3.9731565953**	**-3.9735495281**

Table A.5 (cont'd).

	R (a.u.)					
θ (deg)	6.00	6.05	6.10	6.15	6.20	6.25
0	**-3.9733710374**	**-3.9734113597**	**-3.9734476477**	**-3.9734802608**	**-3.9735095422**	**-3.9735357862**
5	-3.9733753666	-3.9734152608	-3.9734511465	-3.9734833822	-3.9735122513	-3.9735382551
10	-3.9733885327	-3.9734269957	-3.9734616423	-3.9734927780	-3.9735206981	-3.9735457020
15	-3.9734091469	-3.9734454816	-3.9734781676	-3.9735075239	-3.9735338466	-3.9735574130
20	-3.9734355476	-3.9734691306	-3.9734993078	-3.9735263866	-3.9735506512	-3.9735723626
25	-3.9734656774	-3.9734961096	-3.9735234340	-3.9735479329	-3.9735698628	-3.9735894596
30	-3.9734974180	-3.9735245058	-3.9735487934	-3.9735705377	-3.9735899737	-3.9736073161
35	-3.9735288295	-3.9735525758	-3.9735738371	-3.9735928431	-3.9736098002	-3.9736248999
40	-3.9735584744	-3.9735790425	-3.9735974190	-3.9736138119	-3.9736284049	-3.9736413594
45	-3.9735852412	-3.9736028782	-3.9736186088	-3.9736326102	-3.9736450446	-3.9736560608
50	-3.9736085395	-3.9736235938	-3.9736369870	-3.9736488754	-3.9736594011	-3.9736686954
55	-3.9736281717	-3.9736410011	-3.9736523833	-3.9736624572	-3.9736713435	-3.9736791600
60	-3.9736441853	-3.9736551584	-3.9736648640	-3.9736734248	-3.9736809517	-3.9736875490
65	-3.9736568716	-3.9736663473	-3.9736747021	-3.9736820451	-3.9736884756	-3.9736940838
70	-3.9736665944	-3.9736748976	-3.9736821939	-3.9736885840	-3.9736941576	-3.9736989934
75	-3.9736736647	-3.9736810980	-3.9736876101	-3.9736932977	-3.9736982450	-3.9737025172
80	-3.9736785314	-3.9736853516	-3.9736913140	-3.9736965099	-3.9737010126	-3.9737048901
85	-3.9736813426	-3.9736878146	-3.9736934643	-3.9736983718	-3.9737026090	-3.9737062428
90	**-3.9736823641**	**-3.9736887227**	**-3.9736942685**	**-3.9736990828**	**-3.9737032389**	**-3.9737068024**

Table A.5 (cont'd).

	R (a.u.)					
θ (deg)	6.30	6.35	6.40	6.45	6.50	6.55
0	**-3.9735592757**	**-3.9735802579**	**-3.9735989759**	**-3.9736156415**	**-3.9736304492**	**-3.9736435761**
5	-3.9735614950	-3.9735822372	-3.9736007310	-3.9736171924	-3.9736318150	-3.9736447726
10	-3.9735680642	-3.9735880278	-3.9736058183	-3.9736216728	-3.9736357538	-3.9736482242
15	-3.9735784815	-3.9735972833	-3.9736140314	-3.9736289206	-3.9736421288	-3.9736538187
20	-3.9735917575	-3.9736090517	-3.9736244428	-3.9736381105	-3.9736502185	-3.9736609160
25	-3.9736069398	-3.9736225022	-3.9736363285	-3.9736485837	-3.9736594186	-3.9736689671
30	-3.9736227619	-3.9736364911	-3.9736486649	-3.9736594304	-3.9736689240	-3.9736772709
35	-3.9736383176	-3.9736502189	-3.9736607391	-3.9736700190	-3.9736781825	-3.9736853354
40	-3.9736528541	-3.9736630120	-3.9736719667	-3.9736798362	-3.9736867275	-3.9736927370
45	-3.9736657949	-3.9736743714	-3.9736819037	-3.9736884955	-3.9736942416	-3.9736992278
50	-3.9736768784	-3.9736840593	-3.9736903382	-3.9736958061	-3.9737005439	-3.9737046240
55	-3.9736860174	-3.9736920061	-3.9736972116	-3.9737017175	-3.9737055878	-3.9737088912
60	-3.9736933048	-3.9736983042	-3.9737026236	-3.9737063326	-3.9737094947	-3.9737121672
65	-3.9736989516	-3.9737031536	-3.9737067600	-3.9737098331	-3.9737124265	-3.9737145912
70	-3.9737031717	-3.9737067603	-3.9737098106	-3.9737123892	-3.9737145430	-3.9737163136
75	-3.9737061902	-3.9737093217	-3.9737119657	-3.9737141751	-3.9737159966	-3.9737174725
80	-3.9737082050	-3.9737110151	-3.9737133737	-3.9737153291	-3.9737169247	-3.9737181997
85	-3.9737093475	-3.9737119815	-3.9737141770	-3.9737159841	-3.9737174459	-3.9737186057
90	**-3.9737098266**	**-3.9737124020**	**-3.9737145363**	**-3.9737162904**	**-3.9737177061**	**-3.9737188206**

Table A.5 (cont'd).

	R (a.u.)					
θ (deg)	6.60	6.65	6.70	6.75	6.80	6.85
0	**-3.9736551872**	**-3.9736654235**	**-3.9736744247**	**-3.9736823191**	**-3.9736892234**	**-3.9736952228**
5	-3.9736562304	-3.9736663358	-3.9736752192	-3.9736830099	-3.9736898133	-3.9736957222
10	-3.9736592419	-3.9736689509	-3.9736774815	-3.9736849512	-3.9736914653	-3.9736971189
15	-3.9736641376	-3.9736732197	-3.9736811877	-3.9736881528	-3.9736942115	-3.9736994583
20	-3.9736703400	-3.9736786225	-3.9736858635	-3.9736921777	-3.9736976587	-3.9737023920
25	-3.9736773538	-3.9736847035	-3.9736911201	-3.9736966967	-3.9737015172	-3.9737056598
30	-3.9736845887	-3.9736909790	-3.9736965318	-3.9737013313	-3.9737054546	-3.9737089848
35	-3.9736915763	-3.9736969955	-3.9737016815	-3.9737057164	-3.9737091606	-3.9737120666
40	-3.9736979592	-3.9737024716	-3.9737063456	-3.9737096543	-3.9737124517	-3.9737147857
45	-3.9737035300	-3.9737072170	-3.9737103527	-3.9737129945	-3.9737151941	-3.9737170033
50	-3.9737081133	-3.9737110694	-3.9737135462	-3.9737155998	-3.9737172852	-3.9737186432
55	-3.9737116884	-3.9737140336	-3.9737159752	-3.9737175566	-3.9737188161	-3.9737197888
60	-3.9737144014	-3.9737162453	-3.9737177412	-3.9737189278	-3.9737198391	-3.9737205039
65	-3.9737163750	-3.9737178182	-3.9737189567	-3.9737198243	-3.9737204516	-3.9737208662
70	-3.9737177435	-3.9737188708	-3.9737197297	-3.9737203512	-3.9737207631	**-3.9737209902**
75	-3.9737186412	-3.9737195373	-3.9737201917	-3.9737206328	-3.9737208857	-3.9737209732
80	-3.9737191898	-3.9737199275	-3.9737204418	-3.9737207593	-3.9737209036	-3.9737208930
85	-3.9737194976	-3.9737201454	-3.9737205782	-3.9737208228	-3.9737209026	-3.9737208387
90	**-3.9737196680**	**-3.9737202789**	**-3.9737206811**	**-3.9737208995**	**-3.9737209570**	-3.9737208736

Table A.5 (cont'd).

	R (a.u.)					
θ (deg)	6.90	6.95	7.00	7.05	7.10	7.15
0	**-3.9737004100**	**-3.9737048745**	**-3.9737086885**	**-3.9737119230**	**-3.9737146384**	**-3.9737168956**
5	-3.9737008252	-3.9737052125	-3.9737089699	-3.9737121423	-3.9737148160	-3.9737170357
10	-3.9737019992	-3.9737061892	-3.9737097621	-3.9737127869	-3.9737153234	-3.9737174217
15	-3.9737039778	-3.9737078410	-3.9737111211	-3.9737139024	-3.9737162138	-3.9737181102
20	-3.9737064555	-3.9737099195	-3.9737128474	-3.9737152968	-3.9737173185	-3.9737189589
25	-3.9737091963	-3.9737121921	-3.9737147062	-3.9737167888	-3.9737184851	-3.9737198367
30	-3.9737119678	-3.9737144638	-3.9737165280	-3.9737182147	-3.9737195821	-3.9737206306
35	-3.9737145078	-3.9737165308	-3.9737181754	-3.9737194836	-3.9737204929	-3.9737212373
40	-3.9737167071	-3.9737182626	-3.9737194935	-3.9737204366	-3.9737211267	-3.9737216021
45	-3.9737184621	-3.9737195889	-3.9737204651	-3.9737210933	-3.9737215062	**-3.9737217264**
50	-3.9737197034	-3.9737204977	-3.9737210560	-3.9737214054	**-3.9737215711**	-3.9737215807
55	-3.9737205084	-3.9737210083	**-3.9737213085**	**-3.9737214320**	-3.9737214020	-3.9737212379
60	-3.9737209503	**-3.9737212045**	-3.9737212898	-3.9737212273	-3.9737210366	-3.9737207380
65	**-3.9737210937**	-3.9737211595	-3.9737210830	-3.9737208811	-3.9737205704	-3.9737201662
70	-3.9737210548	-3.9737209771	-3.9737207754	-3.9737204662	-3.9737200644	-3.9737195834
75	-3.9737209163	-3.9737207331	-3.9737204407	-3.9737200540	-3.9737195865	-3.9737190503
80	-3.9737207508	-3.9737204981	-3.9737201448	-3.9737197064	-3.9737191958	-3.9737186240
85	-3.9737206499	-3.9737203531	-3.9737199634	-3.9737194942	-3.9737189579	-3.9737183652
90	-3.9737206678	-3.9737203563	-3.9737199536	-3.9737194730	-3.9737189265	-3.9737183246

Table A.5 (cont'd).

	R (a.u.)					
θ (deg)	7.20	7.25	7.30	7.35	7.40	7.45
0	-3.9737187435	-3.9737202281	-3.9737213869	-3.9737222607	**-3.9737228828**	**-3.9737232815**
5	-3.9737188473	-3.9737202970	-3.9737214257	-3.9737222674	-3.9737228496	-3.9737232374
10	-3.9737191294	-3.9737204894	-3.9737215409	-3.9737223191	-3.9737228550	-3.9737231765
15	-3.9737196381	-3.9737208391	-3.9737217509	-3.9737224084	-3.9737228413	-3.9737230688
20	-3.9737202603	-3.9737212609	-3.9737219961	-3.9737224993	-3.9737227995	-3.9737229093
25	-3.9737208824	-3.9737216570	-3.9737221915	**-3.9737225188**	-3.9737226666	-3.9737226388
30	-3.9737214057	-3.9737219442	**-3.9737222730**	-3.9737224156	-3.9737223820	-3.9737222328
35	-3.9737217459	**-3.9737220556**	-3.9737221832	-3.9737221553	-3.9737219906	-3.9737217069
40	**-3.9737218720**	-3.9737219701	-3.9737219154	-3.9737217281	-3.9737214254	-3.9737210233
45	-3.9737217789	-3.9737216855	-3.9737214657	-3.9737211364	-3.9737207130	-3.9737202088
50	-3.9737214534	-3.9737212045	-3.9737208504	-3.9737204058	-3.9737198840	-3.9737192969
55	-3.9737209594	-3.9737205804	-3.9737201157	-3.9737195781	-3.9737189790	-3.9737183287
60	-3.9737203455	-3.9737198689	-3.9737193213	-3.9737187145	-3.9737180587	-3.9737173625
65	-3.9737196822	-3.9737191305	-3.9737185218	-3.9737178657	-3.9737171707	-3.9737164444
70	-3.9737190350	-3.9737184300	-3.9737177779	-3.9737170872	-3.9737163656	-3.9737156197
75	-3.9737184562	-3.9737178140	-3.9737171323	-3.9737164188	-3.9737156802	-3.9737149227
80	-3.9737171458	-3.9737173361	-3.9737166369	-3.9737159106	-3.9737151632	-3.9737144002
85	-3.9737177256	-3.9737170471	-3.9737163372	-3.9737156024	-3.9737148487	-3.9737140815
90	**-3.9737176767**	**-3.9737169913**	**-3.9737162757**	**-3.9737155364**	**-3.9737147796**	**-3.9737140100**

Table A.5 (cont'd).

	R (a.u.)					
θ (deg)	7.50	7.55	7.60	7.65	7.70	7.75
0	**-3.9737234830**	**-3.9737235111**	**-3.9737233879**	**-3.9737231344**	**-3.9737227669**	**-3.9737223035**
5	-3.9737234349	-3.9737234513	-3.9737233156	-3.9737230498	-3.9737226722	-3.9737221988
10	-3.9737233089	-3.9737232764	-3.9737231010	-3.9737228022	-3.9737223972	-3.9737219012
15	-3.9737231206	-3.9737230190	-3.9737227850	-3.9737224366	-3.9737219899	-3.9737214590
20	-3.9737228567	-3.9737226665	-3.9737223572	-3.9737219457	-3.9737214477	-3.9737208758
25	-3.9737224712	-3.9737221841	-3.9737217967	-3.9737213215	-3.9737207691	-3.9737201506
30	-3.9737219605	-3.9737215810	-3.9737211105	-3.9737205624	-3.9737199491	-3.9737192810
35	-3.9737213198	-3.9737208439	-3.9737202923	-3.9737196767	-3.9737190079	-3.9737182952
40	-3.9737205359	-3.9737199758	-3.9737193544	-3.9737186819	-3.9737179672	-3.9737172185
45	-3.9737196359	-3.9737190051	-3.9737183261	-3.9737176074	-3.9737168568	-3.9737160813
50	-3.9737186550	-3.9737179678	-3.9737172438	-3.9737164903	-3.9737157142	-3.9737149214
55	-3.9737176375	-3.9737169115	-3.9737161566	-3.9737153809	-3.9737145898	-3.9737137886
60	-3.9737166340	-3.9737158799	-3.9737151066	-3.9737143195	-3.9737135231	-3.9737127216
65	-3.9737156936	-3.9737149242	-3.9737141417	-3.9737133506	-3.9737125551	-3.9737117588
70	-3.9737148555	-3.9737140785	-3.9737132930	-3.9737125032	-3.9737117125	-3.9737109239
75	-3.9737141517	-3.9737133718	-3.9737125869	-3.9737118007	-3.9737110160	-3.9737102354
80	-3.9737136266	-3.9737128465	-3.9737120636	-3.9737112811	-3.9737105019	-3.9737097283
85	-3.9737133052	-3.9737125242	-3.9737117422	-3.9737109623	-3.9737101869	-3.9737094182
90	**-3.9737132324**	**-3.9737124507**	**-3.9737116684**	**-3.9737108886**	**-3.9737101136**	**-3.9737093456**

Table A.5 (cont'd).

	R (a.u.)					
θ (deg)	7.80	7.85	7.90	7.95	8.00	8.50
0	**-3.9737217569**	**-3.9737211401**	**-3.9737204645**	**-3.9737197397**	**-3.9737189759**	**-3.9737105217**
5	-3.9737216437	-3.9737210194	-3.9737203372	-3.9737196075	-3.9737188394	-3.9737104123
10	-3.9737213280	-3.9737206896	-3.9737199972	-3.9737192601	-3.9737184873	-3.9737100812
15	-3.9737208572	-3.9737201973	-3.9737194876	-3.9737187372	-3.9737179541	-3.9737095638
20	-3.9737202411	-3.9737195533	-3.9737188215	-3.9737180535	-3.9737172562	-3.9737089087
25	-3.9737194767	-3.9737187570	-3.9737180005	-3.9737172155	-3.9737164091	-3.9737081323
30	-3.9737185680	-3.9737178184	-3.9737170399	-3.9737162392	-3.9737154224	-3.9737072402
35	-3.9737175469	-3.9737167706	-3.9737159727	-3.9737151592	-3.9737143354	-3.9737062917
40	-3.9737164431	-3.9737156474	-3.9737148371	-3.9737140172	-3.9737131922	-3.9737053118
45	-3.9737152871	-3.9737144796	-3.9737136636	-3.9737128435	-3.9737120231	-3.9737043372
50	-3.9737141173	-3.9737133062	-3.9737124922	-3.9737116787	-3.9737108686	-3.9737033991
55	-3.9737129817	-3.9737121728	-3.9737113653	-3.9737105620	-3.9737097654	-3.9737025297
60	-3.9737119189	-3.9737111181	-3.9737103221	-3.9737095334	-3.9737087542	-3.9737017487
65	-3.9737109648	-3.9737101758	-3.9737093941	-3.9737086218	-3.9737078606	-3.9737010607
70	-3.9737101402	-3.9737093634	-3.9737085956	-3.9737078385	-3.9737070934	-3.9737004756
75	-3.9737094611	-3.9737086953	-3.9737079397	-3.9737071959	-3.9737064652	-3.9737000067
80	-3.9737089622	-3.9737082056	-3.9737074600	-3.9737067269	-3.9737060071	-3.9736996650
85	-3.9737086581	-3.9737079082	-3.9737071698	-3.9737064441	-3.9737057318	-3.9736994578
90	**-3.9737085866**	**-3.9737078379**	**-3.9737071009**	**-3.9737063768**	**-3.9737056663**	**-3.9736994123**

Table A.5 (cont'd).

	R (a.u.)					
θ (deg)	9.00	9.50	10.00	10.50	11.00	12.00
0	**-3.9737029147**	**-3.9736971538**	**-3.9736930440**	**-3.9736901274**	**-3.9736880504**	**-3.9736855181**
5	-3.9737028309	-3.9736970967	-3.9736930039	-3.9736900978	-3.9736880299	-3.9736855068
10	-3.9737025851	-3.9736969236	-3.9736928864	-3.9736900112	-3.9736879700	-3.9736854736
15	-3.9737021889	-3.9736966512	-3.9736926963	-3.9736898780	-3.9736878729	-3.9736854206
20	-3.9737016831	-3.9736962957	-3.9736924451	-3.9736897010	-3.9736877448	-3.9736853519
25	-3.9737011005	-3.9736958768	-3.9736921479	-3.9736894897	-3.9736875935	-3.9736852704
30	-3.9737004334	-3.9736954155	-3.9736918179	-3.9736892539	-3.9736874252	-3.9736851798
35	-3.9736997278	-3.9736949124	-3.9736914628	-3.9736890026	-3.9736872456	-3.9736850833
40	-3.9736990057	-3.9736943998	-3.9736910967	-3.9736887429	-3.9736870608	-3.9736849842
45	-3.9736982925	-3.9736938887	-3.9736907334	-3.9736884843	-3.9736868767	-3.9736848854
50	-3.9736976090	-3.9736933985	-3.9736903839	-3.9736882350	-3.9736866984	-3.9736847893
55	-3.9736969752	-3.9736929414	-3.9736900571	-3.9736880009	-3.9736865304	-3.9736846980
60	-3.9736964015	-3.9736925279	-3.9736897599	-3.9736877873	-3.9736863763	-3.9736846136
65	-3.9736958998	-3.9736921659	-3.9736894982	-3.9736875986	-3.9736862393	-3.9736845376
70	-3.9736954798	-3.9736918614	-3.9736892772	-3.9736874387	-3.9736861223	-3.9736844722
75	-3.9736951419	-3.9736916190	-3.9736891006	-3.9736873103	-3.9736860278	-3.9736844189
80	-3.9736948953	-3.9736914432	-3.9736889721	-3.9736872167	-3.9736859586	-3.9736843797
85	-3.9736947479	-3.9736913364	-3.9736888944	-3.9736871602	-3.9736859167	-3.9736843558
90	**-3.9736947022**	**-3.9736913006**	**-3.9736888719**	**-3.9736871428**	**-3.9736859032**	**-3.9736843478**

Table A.5 (cont'd).

	R (a.u.)		
θ (deg)	14.00	17.00	20.00
0	**-3.9736834071**	**-3.9736825312**	**-3.9736823023**
5	-3.9736834036	-3.9736825303	-3.9736823020
10	-3.9736833937	-3.9736825279	-3.9736823012
15	-3.9736833775	-3.9736825238	-3.9736822999
20	-3.9736833559	-3.9736825185	-3.9736822982
25	-3.9736833295	-3.9736825117	-3.9736822960
30	-3.9736832999	-3.9736824958	-3.9736822936
35	-3.9736832678	-3.9736824870	-3.9736822909
40	-3.9736832342	-3.9736824870	-3.9736822880
45	-3.9736832004	-3.9736824780	-3.9736822852
50	-3.9736831669	-3.9736824692	-3.9736822823
55	-3.9736831350	-3.9736824607	-3.9736822796
60	-3.9736831052	-3.9736824529	-3.9736822770
65	-3.9736830784	-3.9736824458	-3.9736822747
70	-3.9736830554	-3.9736824399	-3.9736822727
75	-3.9736830366	-3.9736824349	-3.9736822711
80	-3.9736830229	-3.9736824314	-3.9736822700
85	-3.9736830145	-3.9736824292	-3.9736822692
90	**-3.9736830117**	**-3.9736824285**	**-3.9736822690**

Table A.6. CR-CC(2,3) energies of H_2–He for $r_{H-H} = 3.730\ a_0$ with an aug-cc-pV5Z basis, as a function of the separation R between the center of mass of the two H nuclei and the He nucleus, and the angle θ between the H–H vector and the z axis. The He atom is located along the z axis. Entries in blue denote the maximum and entries in bold black denote the minimum of the potential, as a function of the angle θ for each value of R.

	R (in a.u.)					
θ (deg)	2.20	2.40	2.60	2.80	3.00	3.50
0	**-1.2254743997**	**-2.8814595477**	**-3.4352799772**	**-3.6553328689**	**-3.7525521982**	**-3.8441696033**
5	-1.7803491297	-3.0065829290	-3.4735246091	-3.6689299101	-3.7580347829	-3.8455771659
10	-2.6391341396	-3.2611220039	-3.5606329488	-3.7018551027	-3.7720203889	-3.8495885734
15	-3.1975692143	-3.4834290390	-3.6493988098	-3.7389916031	-3.7894919613	-3.8556416599
20	-3.4941229481	-3.6274956417	-3.7156951626	-3.7705860509	-3.8067909914	-3.8630307969
25	-3.6429611324	-3.7093891214	-3.7588574165	-3.7950149025	-3.8227945277	-3.8711281002
30	-3.7161979775	-3.7545455598	-3.7872392344	-3.8146392130	-3.8376067612	-3.8792584323
35	-3.7540897620	-3.7824965700	-3.8086519453	-3.8316556520	-3.8513295604	-3.8869373274
40	-3.7791209408	-3.8041645857	-3.8269388197	-3.8468208251	-3.8636873068	-3.8938422403
45	-3.8005566943	-3.8229792031	-3.8428902215	-3.8600318370	-3.8744177775	-3.8997974371
50	-3.8193739659	-3.8391149409	-3.8564288255	-3.8711729683	-3.8834336694	-3.9047698751
55	-3.8351055038	-3.8524779285	-3.8675754230	-3.8803113788	-3.8908048318	-3.9088053216
60	-3.8477981724	-3.8632360650	-3.8765262049	-3.8876266491	-3.8966865668	-3.9120004868
65	-3.8577777013	-3.8716884976	-3.8835416701	-3.8933455013	-3.9012715097	-3.9144703412
70	-3.8654068615	-3.8781422731	-3.8888861323	-3.8976914810	-3.9047438649	-3.9163261236
75	-3.8710044585	-3.8828679109	-3.8927963470	-3.9008610238	-3.9072695631	-3.9176660367
80	-3.8748269502	-3.8860905378	-3.8954541593	-3.9030119734	-3.9089776905	-3.9185668058
85	-3.8770555465	-3.8879626909	-3.8969964392	-3.9042567846	-3.9099665352	-3.9190849079
90	**-3.8777907449**	**-3.8885832086**	**-3.8975044380**	**-3.9046660499**	**-3.9102916701**	**-3.9192559440**

Table A.6 (cont'd).

	R (in a.u.)					
θ (deg)	4.00	4.50	5.00	5.50	6.00	6.05
0	**-3.8853705856**	**-3.9073985053**	**-3.9183019358**	**-3.9233186658**	**-3.9254769883**	**-3.9256052163**
5	-3.8860704213	-3.9077334600	-3.9184517677	-3.9233800822	-3.9255018217	-3.9256278423
10	-3.8880824500	-3.9086978667	-3.9188845014	-3.9235628724	-3.9255745125	-3.9256938746
15	-3.8911644962	-3.9101755479	-3.9195470722	-3.9238428717	-3.9256860986	-3.9257953273
20	-3.8949772866	-3.9120029887	-3.9203666748	-3.9241889283	-3.9258240795	-3.9259207380
25	-3.8991469611	-3.9140021586	-3.9212617425	-3.9245664469	-3.9259744649	-3.9260574030
30	-3.9033378679	-3.9160056817	-3.9221594875	-3.9249441377	-3.9261244104	-3.9261935803
35	-3.9072868588	-3.9178883494	-3.9230010841	-3.9252972370	-3.9262640233	-3.9263204097
40	-3.9108216804	-3.9195694060	-3.9237484419	-3.9256109355	-3.9263870588	-3.9264319595
45	-3.9138581592	-3.9210086598	-3.9243863343	-3.9258771481	-3.9264905687	-3.9265257204
50	-3.9163803062	-3.9221973653	-3.9249113257	-3.9260943021	-3.9265741021	-3.9266012690
55	-3.9184135042	-3.9231510810	-3.9253293422	-3.9262656231	-3.9266391527	-3.9266600047
60	-3.9200127643	-3.9238946910	-3.9256526454	-3.9263968695	-3.9266882162	-3.9267041806
65	-3.9212389083	-3.9244609158	-3.9258969408	-3.9264950691	-3.9267241604	-3.9267365013
70	-3.9221524349	-3.9248797596	-3.9260759956	-3.9265663564	-3.9267498434	-3.9267595182
75	-3.9228066154	-3.9251773121	-3.9262024935	-3.9266160689	-3.9267674952	-3.9267753046
80	-3.9232441568	-3.9253749761	-3.9262858526	-3.9266483348	-3.9267787898	-3.9267853864
85	-3.9234950945	-3.9254877314	-3.9263331821	-3.9266664783	-3.9267850939	-3.9267909771
90	**-3.9235766535**	**-3.9255245847**	**-3.9263485095**	**-3.9266725570**	**-3.9267872650**	**-3.9267929285**

Table A.6 (cont'd).

	R (in a.u.)					
θ (deg)	6.10	6.15	6.20	6.25	6.30	6.35
0	**-3.9257222142**	**-3.9258289093**	**-3.9259261228**	**-3.9260146050**	**-3.9260951604**	**-3.9261683578**
5	-3.9257427964	-3.9258475669	-3.9259429696	-3.9260298427	-3.9261089376	-3.9261810083
10	-3.9258027834	-3.9259020911	-3.9259925281	-3.9260748303	-3.9261496635	-3.9262176189
15	-3.9258949178	-3.9259857542	-3.9260684355	-3.9261436439	-3.9262120036	-3.9262741087
20	-3.9260088373	-3.9260890854	-3.9261621458	-3.9262285815	-3.9262889483	-3.9263437618
25	-3.9261329431	-3.9262016943	-3.9262642249	-3.9263210780	-3.9263727039	-3.9264195424
30	-3.9262565377	-3.9263138307	-3.9263659452	-3.9264132426	-3.9264561210	-3.9264949643
35	-3.9263716599	-3.9264182020	-3.9264604259	-3.9264987011	-3.9265333652	-3.9265647273
40	-3.9264727222	-3.9265096793	-3.9265431604	-3.9265734866	-3.9266009453	-3.9266257312
45	-3.9265575784	-3.9265864212	-3.9266125021	-3.9266360530	-3.9266572860	-3.9266764008
50	-3.9266258305	-3.9266480107	-3.9266680138	-3.9266860223	-3.9267022058	-3.9267167271
55	-3.9266787925	-3.9266957044	-3.9267109063	-3.9267245456	-3.9267367598	-3.9267476786
60	-3.9267185172	-3.9267313784	-3.9267429053	-3.9267532141	-3.9267624068	-3.9267705810
65	-3.9267475453	-3.9267574063	-3.9267661918	-3.9267740021	-3.9267809182	-3.9267870265
70	-3.9267681367	-3.9267757953	-3.9267825823	-3.9267885658	-3.9267938252	-3.9267984360
75	-3.9267822202	-3.9267883271	-3.9267937023	-3.9267984139	-3.9268025248	-3.9268060935
80	-3.9267911954	-3.9267962938	-3.9268007510	-3.9268046297	-3.9268079869	-3.9268108741
85	-3.9267961434	-3.9268006616	-3.9268045989	-3.9268080203	-3.9268109788	-3.9268135079
90	**-3.9267978959**	**-3.9268022342**	**-3.9268060041**	**-3.9268092618**	**-3.9268120580**	**-3.9268144396**

Table A.6 (cont'd).

	R (in a.u.)					
θ (deg)	6.40	6.45	6.50	6.55	6.60	6.65
0	**-3.9262348678**	**-3.9262952381**	**-3.9263499833**	**-3.9263995659**	**-3.9264444941**	**-3.9264851218**
5	-3.9262464729	-3.9263057031	-3.9263593948	-3.9264080704	-3.9264521348	-3.9264919980
10	-3.9262793974	-3.9263355352	-3.9263863995	-3.9264324720	-3.9264741667	-3.9265118578
15	-3.9263304886	-3.9263816270	-3.9264279788	-3.9264699647	-3.9265079510	-3.9265422697
20	-3.9263934890	-3.9264385622	-3.9264794194	-3.9265163755	-3.9265497561	-3.9265798846
25	-3.9264620086	-3.9265004681	-3.9265352663	-3.9265667081	-3.9265950772	-3.9266206526
30	-3.9265301198	-3.9265619083	-3.9265906228	-3.9266165317	-3.9266398821	-3.9266609021
35	-3.9265930708	-3.9266186564	-3.9266417229	-3.9266624866	-3.9266811352	-3.9266978963
40	-3.9266480648	-3.9266681677	-3.9266862381	-3.9267024591	-3.9267169980	-3.9267300079
45	-3.9266935852	-3.9267090129	-3.9267228412	-3.9267352146	-3.9267462659	-3.9267561149
50	-3.9267297376	-3.9267413743	-3.9267517610	-3.9267610264	-3.9267692677	-3.9267765754
55	-3.9267574252	-3.9267661019	-3.9267738059	-3.9267806286	-3.9267866529	-3.9267919512
60	-3.9267778256	-3.9267842402	-3.9267898903	-3.9267948536	-3.9267991961	-3.9268029778
65	-3.9267924041	-3.9267971210	-3.9268012408	-3.9268048219	-3.9268079169	-3.9268105735
70	-3.9268024701	-3.9268059673	-3.9268089838	-3.9268115694	-3.9268137657	-3.9268156132
75	-3.9268091735	-3.9268118135	-3.9268140581	-3.9268159476	-3.9268175189	-3.9268188051
80	-3.9268133385	-3.9268154228	-3.9268171677	-3.9268186054	-3.9268197709	-3.9268206938
85	-3.9268156409	-3.9268174202	-3.9268188852	-3.9268200709	-3.9268210088	-3.9268217272
90	**-3.9268164487**	**-3.9268181239**	**-3.9268195005**	**-3.9268206106**	**-3.9268214830**	**-3.9268221438**

Table A.6 (cont'd).

	R (in a.u.)					
θ (deg)	6.70	6.75	6.80	6.85	6.90	6.95
0	**-3.9265218378**	**-3.9265549949**	**-3.9265848919**	**-3.9266118293**	**-3.9266360664**	**-3.9266578482**
5	-3.9265280249	-3.9265605328	-3.9265898032	-3.9266160204	-3.9266398074	-3.9266612453
10	-3.9265458906	-3.9265765933	-3.9266042754	-3.9266291961	-3.9266515749	-3.9266716813
15	-3.9265732408	-3.9266011675	-3.9266263079	-3.9266489579	-3.9266692868	-3.9266875200
20	-3.9266070645	-3.9266315495	-3.9266535713	-3.9266733530	-3.9266910992	-3.9267069964
25	-3.9266436812	-3.9266643906	-3.9266829901	-3.9266996713	-3.9267146099	-3.9267279659
30	-3.9266798001	-3.9266967655	-3.9267119717	-3.9267255787	-3.9267377322	-3.9267485697
35	-3.9267129941	-3.9267264652	-3.9267384977	-3.9267492319	-3.9267587816	-3.9267672567
40	-3.9267416281	-3.9267519831	-3.9267611833	-3.9267693556	-3.9267766153	-3.9267830283
45	-3.9267648890	-3.9267726796	-3.9267795728	-3.9267856547	-3.9267910031	-3.9267956865
50	-3.9267830355	-3.9267887278	-3.9267937251	-3.9267980921	-3.9268019086	-3.9268052074
55	-3.9267965998	-3.9268006553	-3.9268041768	-3.9268072167	-3.9268098226	-3.9268120381
60	-3.9268062532	-3.9268090719	-3.9268114791	-3.9268135163	-3.9268152212	-3.9268166285
65	-3.9268128353	-3.9268147413	-3.9268163286	-3.9268176311	-3.9268186771	-3.9268194948
70	-3.9268171476	-3.9268184015	-3.9268194044	-3.9268201835	-3.9268207633	-3.9268211640
75	-3.9268198361	-3.9268206424	-3.9268212486	-3.9268216720	-3.9268219325	-3.9268220511
80	-3.9268214009	-3.9268219163	-3.9268222622	-3.9268224586	-3.9268225230	-3.9268224707
85	-3.9268222521	-3.9268226059	-3.9268228081	-3.9268228755	-3.9268228238	-3.9268226676
90	**-3.9268226162**	**-3.9268229208**	**-3.9268230765**	**-3.9268231005**	**-3.9268230084**	**-3.9268228150**

Table A.6 (cont'd).

	R (in a.u.)					
θ (deg)	7.00	7.05	7.10	7.15	7.20	7.25
0	**-3.9266773925**	**-3.9266949237**	**-3.9267106045**	**-3.9267245982**	**-3.9267370659**	**-3.9267481590**
5	-3.9266804141	-3.9266975937	-3.9267129647	-3.9267266784	-3.9267388367	-3.9267496533
10	-3.9266897214	-3.9267058732	-3.9267203214	-3.9267332270	-3.9267447327	-3.9267549505
15	-3.9267038757	-3.9267184964	-3.9267315456	-3.9267431779	-3.9267535251	-3.9267627068
20	-3.9267212143	-3.9267339080	-3.9267212143	-3.9267552837	-3.9267642164	-3.9267721216
25	-3.9267398856	-3.9267505036	-3.9267599408	-3.9267683029	-3.9267756610	-3.9267822262
30	-3.9267582080	-3.9267667632	-3.9267743375	-3.9267810236	-3.9267869068	-3.9267920656
35	-3.9267747611	-3.9267813867	-3.9267872185	-3.9267923345	-3.9267968055	-3.9268006959
40	-3.9267886709	-3.9267936200	-3.9267979443	-3.9268017044	-3.9268049571	-3.9268077527
45	-3.9267997690	-3.9268033116	-3.9268063715	-3.9268089947	-3.9268112263	-3.9268131102
50	-3.9268080457	-3.9268104706	-3.9268125238	-3.9268142426	-3.9268156606	-3.9268168082
55	-3.9268139025	-3.9268154518	-3.9268167186	-3.9268177329	-3.9268185222	-3.9268191130
60	-3.9268177692	-3.9268186708	-3.9268193590	-3.9268198591	-3.9268201928	-3.9268203790
65	-3.9268201103	-3.9268205451	-3.9268208192	-3.9268209521	-3.9268209614	**-3.9268208623**
70	-3.9268214066	-3.9268215115	-3.9268214945	-3.9268213718	**-3.9268211569**	-3.9268208619
75	-3.9268220472	-3.9268219357	-3.9268217296	**-3.9268214413**	-3.9268210816	-3.9268206605
80	-3.9268223155	-3.9268220698	-3.9268217449	-3.9268213515	-3.9268208994	-3.9268203980
85	-3.9268224202	-3.9268220936	-3.9268216986	-3.9268212451	-3.9268207417	-3.9268201965
90	**-3.9268225340**	**-3.9268221773**	**-3.9268217560**	-3.9268212794	-3.9268207562	-3.9268201940

Table A.6 (cont'd).

	R (in a.u.)					
θ (deg)	7.30	7.35	7.40	7.45	7.50	7.55
0	**-3.9267580021**	**-3.9267667241**	**-3.9267744267**	**-3.9267812096**	**-3.9267871648**	**-3.9267923774**
5	-3.9267593830	-3.9267680209	-3.9267755973	-3.9267822424	-3.9267880679	-3.9267931578
10	-3.9267640047	-3.9267720089	-3.9267790653	-3.9267852643	-3.9267906972	-3.9267954353
15	-3.9267708319	-3.9267780008	-3.9267843061	-3.9267898337	-3.9267946619	-3.9267988610
20	-3.9267791006	-3.9267852419	-3.9267906218	-3.9267953034	-3.9267994021	-3.9268029730
25	-3.9267879909	-3.9267930290	-3.9267974210	-3.9268012323	-3.9268045229	-3.9268073426
30	-3.9267965717	-3.9268004903	-3.9268038797	-3.9268067932	-3.9268092817	-3.9268113819
35	-3.9268040638	-3.9268069608	-3.9268094346	-3.9268115285	-3.9268132801	-3.9268147334
40	-3.9268101353	-3.9268121553	-3.9268138426	-3.9268152321	-3.9268163625	-3.9268172569
45	-3.9268146823	-3.9268159701	-3.9268169985	-3.9268177970	-3.9268183915	-3.9268188059
50	-3.9268177142	-3.9268184052	-3.9268189062	-3.9268192399	-3.9268194317	-3.9268194990
55	-3.9268195253	-3.9268197812	-3.9268199035	-3.9268199048	**-3.9268198008**	**-3.9268196051**
60	-3.9268204357	-3.9268203794	**-3.9268202242**	**-3.9268199825**	-3.9268196656	-3.9268192840
65	**-3.9268206687**	**-3.9268203928**	-3.9268200457	-3.9268196373	-3.9268191767	-3.9268186720
70	-3.9268204979	-3.9268200755	-3.9268196041	-3.9268190906	-3.9268185406	-3.9268179599
75	-3.9268201869	-3.9268196691	-3.9268191142	-3.9268185288	-3.9268179188	-3.9268172891
80	-3.9268198550	-3.9268192777	-3.9268186727	-3.9268180457	-3.9268174017	-3.9268167449
85	-3.9268196164	-3.9268190094	-3.9268183795	-3.9268177322	-3.9268170719	-3.9268164025
90	-3.9268195999	-3.9268189796	-3.9268183389	-3.9268176824	-3.9268170143	-3.9268163384

Table A.6 (cont'd).

	R (in a.u.)					
θ (deg)	7.60	7.65	7.70	7.75	7.80	7.85
0	**-3.9267969187**	**-3.9268008506**	**-3.9268042504**	**-3.9268071555**	**-3.9268096308**	**-3.9268117138**
5	-3.9267975857	-3.9268014203	-3.9268047227	-3.9268075479	-3.9268099458	-3.9268119616
10	-3.9267995501	-3.9268031053	-3.9268061586	-3.9268087618	-3.9268109597	-3.9268127620
15	-3.9268024936	-3.9268056107	-3.9268082581	-3.9268105535	-3.9268124748	-3.9268140624
20	-3.9268060339	-3.9268086450	-3.9268108591	-3.9268127163	-3.9268142519	-3.9268155065
25	-3.9268097457	-3.9268117811	-3.9268134750	-3.9268148751	-3.9268160077	-3.9268169011
30	-3.9268131435	-3.9268146072	-3.9268157999	-3.9268167486	-3.9268174806	-3.9268180199
35	-3.9268159220	-3.9268168686	-3.9268175997	-3.9268181383	-3.9268185037	-3.9268187132
40	-3.9268179394	-3.9268184301	-3.9268187486	-3.9268189157	**-3.9268189528**	**-3.9268188820**
45	-3.9268190607	-3.9268191716	**-3.9268191642**	**-3.9268190598**	-3.9268188665	-3.9268185939
50	**-3.9268194470**	**-3.9268192976**	-3.9268190633	-3.9268187557	-3.9268183852	-3.9268179602
55	-3.9268193296	-3.9268189848	-3.9268185800	-3.9268181236	-3.9268176233	-3.9268170858
60	-3.9268188466	-3.9268183619	-3.9268178369	-3.9268172767	-3.9268166871	-3.9268160832
65	-3.9268181306	-3.9268175591	-3.9268169608	-3.9268163458	-3.9268157159	-3.9268150748
70	-3.9268173547	-3.9268167303	-3.9268160916	-3.9268154426	-3.9268147869	-3.9268141277
75	-3.9268166446	-3.9268159893	-3.9268153268	-3.9268146603	-3.9268139927	-3.9268133262
80	-3.9268160791	-3.9268154079	-3.9268147340	-3.9268140602	-3.9268133887	-3.9268127215
85	-3.9268157275	-3.9268150497	-3.9268143718	-3.9268136959	-3.9268130240	-3.9268123579
90	-3.9268156579	-3.9268149755	-3.9268142941	-3.9268136155	-3.9268129417	-3.9268122742

Table A.6 (cont'd).

	R (in a.u.)					
θ (deg)	7.90	7.95	8.00	8.50	9.00	9.50
0	**-3.9268116145**	**-3.9268109638**	**-3.9268103230**	**-3.9268179461**	**-3.9268125107**	**-3.9268064155**
5	-3.9268136346	-3.9268150091	-3.9268161117	-3.9268178383	-3.9268123838	-3.9268063136
10	-3.9268143263	-3.9268155695	-3.9268165486	-3.9268176155	-3.9268120461	-3.9268060280
15	-3.9268153560	-3.9268163874	-3.9268171854	-3.9268172500	-3.9268115266	-3.9268055744
20	-3.9268165064	-3.9268172795	-3.9268178510	-3.9268167206	-3.9268108279	-3.9268049972
25	-3.9268175821	-3.9268180741	-3.9268183976	-3.9268160022	-3.9268099661	-3.9268043082
30	-3.9268183867	-3.9268185987	**-3.9268186740**	-3.9268150972	-3.9268089670	-3.9268035093
35	**-3.9268187854**	**-3.9268187396**	-3.9268185936	-3.9268140262	-3.9268079035	-3.9268026773
40	-3.9268187193	-3.9268184709	-3.9268181523	-3.9268128281	-3.9268067893	-3.9268018202
45	-3.9268182513	-3.9268178469	-3.9268174030	-3.9268115571	-3.9268056730	-3.9268009851
50	-3.9268174879	-3.9268169749	-3.9268164285	-3.9268102808	-3.9268046013	-3.9268001869
55	-3.9268165182	-3.9268159293	-3.9268153252	-3.9268090543	-3.9268036096	-3.9267994525
60	-3.9268154671	-3.9268148380	-3.9268141999	-3.9268079311	-3.9268027230	-3.9267987951
65	-3.9268144267	-3.9268137749	-3.9268131221	-3.9268069425	-3.9268019542	-3.9267982262
70	-3.9268134678	-3.9268128096	-3.9268121550	-3.9268061034	-3.9268013133	-3.9267977535
75	-3.9268126632	-3.9268120054	-3.9268113544	-3.9268054292	-3.9268008008	-3.9267973815
80	-3.9268120601	-3.9268114061	-3.9268107604	-3.9268049358	-3.9268004272	-3.9267971164
85	-3.9268116989	-3.9268110483	-3.9268104071	-3.9268046408	-3.9268002126	-3.9267969630
90	-3.9268134487	-3.9268148750	-3.9268160262	**-3.9268045871**	**-3.9268001663**	**-3.9267969148**

Table A.6 (cont'd).

	R (in a.u.)					
θ (deg)	10.00	10.50	11.00	12.00	14.00	17.00
0	**-3.9268014802**	**-3.9267978373**	**-3.9267951940**	**-3.9267919533**	**-3.9267893715**	**-3.9267883576**
5	-3.9268014066	-3.9267977852	-3.9267951572	-3.9267919351	-3.9267893662	-3.9267883565
10	-3.9268011969	-3.9267976366	-3.9267950522	-3.9267918819	-3.9267893507	-3.9267883530
15	-3.9268008548	-3.9267974008	-3.9267948847	-3.9267917967	-3.9267893259	-3.9267883475
20	-3.9268004222	-3.9267970898	-3.9267946647	-3.9267916843	-3.9267892930	-3.9267883401
25	-3.9267999106	-3.9267967232	-3.9267944039	-3.9267915507	-3.9267892537	-3.9267883312
30	-3.9267993555	-3.9267963188	-3.9267941151	-3.9267914023	-3.9267892097	-3.9267883210
35	-3.9267987525	-3.9267958922	-3.9267938105	-3.9267912456	-3.9267891625	-3.9267883100
40	-3.9267981290	-3.9267954498	-3.9267934997	-3.9267910867	-3.9267891139	-3.9267882985
45	-3.9267975238	-3.9267950123	-3.9267931918	-3.9267909305	-3.9267890655	-3.9267882870
50	-3.9267969424	-3.9267946005	-3.9267928986	-3.9267907810	-3.9267890184	-3.9267882757
55	-3.9267964125	-3.9267942198	-3.9267926265	-3.9267906414	-3.9267889740	-3.9267882650
60	-3.9267959348	-3.9267938765	-3.9267923820	-3.9267905147	-3.9267889333	-3.9267882551
65	-3.9267955242	-3.9267935807	-3.9267921702	-3.9267904034	-3.9267888972	-3.9267882464
70	-3.9267951834	-3.9267933351	-3.9267919935	-3.9267903092	-3.9267888664	-3.9267882390
75	-3.9267949160	-3.9267931419	-3.9267918540	-3.9267902337	-3.9267888418	-3.9267882331
80	-3.9267947246	-3.9267930032	-3.9267917535	-3.9267901786	-3.9267888240	-3.9267882289
85	-3.9267946109	-3.9267929202	-3.9267916931	-3.9267901455	-3.9267888134	-3.9267882263
90	**-3.9267945735**	**-3.9267928928**	**-3.9267916730**	**-3.9267901350**	**-3.9267888101**	**-3.9267882254**

Table A.7. CR-CC(2,3) energies of H_2–He for $r_{H-H} = 5.70\ a_0$ with an aug-cc-pV5Z basis, as a function of the separation R between the center of mass of the two H nuclei and the He nucleus, and the angle θ between the H–H vector and the z axis. The He atom is located along the z axis. Entries in blue denote the maximum and entries in bold black denote the minimum of the potential, as a function of the angle θ for each value of R.

	R (in a.u.)					
θ (deg)	3.25	3.50	3.75	4.00	4.50	5.00
0	**-1.9446323530**	**-3.2073043686**	**-3.5691285246**	**-3.6971502644**	**-3.8032811331**	**-3.8556739161**
5	-2.5483790968	-3.3272671445	-3.6007953351	-3.7084808887	-3.8073549605	-3.8574674637
10	-3.2414973154	-3.5256693664	-3.6639605319	-3.7357430629	-3.8183193958	-3.8623721318
15	-3.5575542993	-3.6549151919	-3.7209138336	-3.7687911998	-3.8332151588	-3.8692131557
20	-3.6825523089	-3.7275692368	-3.7675468343	-3.8009786733	-3.8488702452	-3.8766384496
25	-3.7496189970	-3.7784127303	-3.8053123304	-3.8286357156	-3.8630978499	-3.8835988272
30	-3.7961699600	-3.8157878756	-3.8342888529	-3.8505151518	-3.8748314036	-3.8894831729
35	-3.8288649713	-3.8427015591	-3.8556314687	-3.8669423475	-3.8838770615	-3.8940956790
40	-3.8518351037	-3.8617982447	-3.8709277043	-3.8788127148	-3.8905129243	-3.8975101642
45	-3.8679317451	-3.8751791835	-3.8816561000	-3.8871653259	-3.8952014862	-3.8999200315
50	-3.8791423925	-3.8844463838	-3.8890655327	-3.8929191885	-3.8984138188	-3.9015645096
55	-3.8869033642	-3.8908066072	-3.8941161227	-3.8968137485	-3.9005617894	-3.9026503989
60	-3.8922395546	-3.8951331097	-3.8975137085	-3.8994082766	-3.9019719611	-3.9033520829
65	-3.8958757367	-3.8980390884	-3.8997696709	-3.9011156678	-3.9028809826	-3.9037972702
70	-3.8983186276	-3.8999649753	-3.9012486794	-3.9022214576	-3.9034572990	-3.9040742102
75	-3.8999206390	-3.9012139516	-3.9021956041	-3.9029216877	-3.9038163829	-3.9042420021
80	-3.9009711120	-3.9019844529	-3.9027740615	-3.9033456980	-3.9040286152	-3.9043398512
85	-3.9014639803	-3.9024009467	-3.9030849975	-3.9035719076	-3.9041404038	-3.9043905679
90	**-3.9016383005**	**-3.9025334316**	**-3.9031832380**	**-3.9036429925**	**-3.9041756489**	**-3.9044064037**

Table A.7 (cont'd).

	R (in a.u.)					
θ (deg)	5.50	6.00	6.05	6.10	6.15	6.20
0	**-3.8819593547**	**-3.8945964281**	**-3.8954053049**	**-3.8961526704**	**-3.8968432209**	**-3.8974807650**
5	-3.8827467464	-3.8949335676	-3.8957141275	-3.8964357782	-3.8971022028	-3.8977168369
10	-3.8849213590	-3.8958731212	-3.8965766530	-3.8972268377	-3.8978267161	-3.8983815267
15	-3.8880006400	-3.8972155236	-3.8978088933	-3.8983572324	-3.8988641335	-3.8993330522
20	-3.8914079987	-3.8987154122	-3.8991871122	-3.8996229400	-3.9000259118	-3.9003985365
25	-3.8946531381	-3.9001558881	-3.9005117644	-3.9008411286	-3.9011455618	-3.9014269004
30	-3.8974388443	-3.9014007917	-3.9016571076	-3.9018941543	-3.9021132769	-3.9023160883
35	-3.8996372392	-3.9023888856	-3.9025674752	-3.9027293171	-3.9028803415	-3.9030198556
40	-3.9012704882	-3.9031204860	-3.9032389323	-3.9033482832	-3.9034491514	-3.9035421177
45	-3.9024208260	-3.9036347781	-3.9037116525	-3.9037824973	-3.9038477206	-3.9039077277
50	-3.9031995672	-3.9039779811	-3.9040267181	-3.9040715339	-3.9041127062	-3.9041504955
55	-3.9037083537	-3.9041994521	-3.9042295708	-3.9042572993	-3.9042826596	-3.9043058433
60	-3.9040317614	-3.9043371099	-3.9043554481	-3.9043721943	-3.9043874330	-3.9044012816
65	-3.9042324042	-3.9044201706	-3.9044310754	-3.9044409442	-3.9044498718	-3.9044579299
70	-3.9043544447	-3.9044688798	-3.9044752105	-3.9044808887	-3.9044859671	-3.9044904962
75	-3.9044266866	-3.9044966396	-3.9045002297	-3.9045033982	-3.9045061815	-3.9045086130
80	-3.9044675927	-3.9045117495	-3.9045137625	-3.9045154846	-3.9045169441	-3.9045181671
85	-3.9044883303	-3.9045192407	-3.9045204866	-3.9045214734	-3.9045222622	-3.9045228730
90	**-3.9044948914**	**-3.9045217050**	**-3.9045226571**	**-3.9045234058**	**-3.9045239727**	**-3.9045243772**

Table A.7 (cont'd).

	R (in a.u.)					
θ (deg)	6.25	6.30	6.35	6.40	6.45	6.50
0	**-3.8980684323**	**-3.8986099713**	**-3.8991092895**	**-3.8995691113**	**-3.8999923610**	**-3.9003818881**
5	-3.8982845580	-3.8988082554	-3.8992909385	-3.8997354243	-3.9001443528	-3.9005204993
10	-3.8988933008	-3.8993650250	-3.8997999186	-3.9002006771	-3.9005700009	-3.9009100761
15	-3.8997653568	-3.9001638574	-3.9005313122	-3.9008702849	-3.9011826462	-3.9014702215
20	-3.9007428302	-3.9010605806	-3.9013537230	-3.9016239235	-3.9018727088	-3.9021016766
25	-3.9016867054	-3.9019264472	-3.9021475894	-3.9023516889	-3.9025401675	-3.9027113763
30	-3.9025040273	-3.9026746858	-3.9028327649	-3.9029787025	-3.9031131853	-3.9032370541
35	-3.9031485717	-3.9032672112	-3.9033764720	-3.9034770547	-3.9035695417	-3.9036545490
40	-3.9036277356	-3.9037065705	-3.9037791042	-3.9038457933	-3.9039070734	-3.9039633462
45	-3.9039628932	-3.9040135748	-3.9040601023	-3.9041027801	-3.9041418921	-3.9041777043
50	-3.9041851445	-3.9042168884	-3.9042459720	-3.9042725252	-3.9042967839	-3.9043189185
55	-3.9043270171	-3.9043463327	-3.9043639325	-3.9043799516	-3.9043945137	-3.9044077328
60	-3.9044138595	-3.9044252720	-3.9044356134	-3.9044449695	-3.9044534197	-3.9044610352
65	-3.9044651918	-3.9044717218	-3.9044775787	-3.9044828196	-3.9044874969	-3.9044916588
70	-3.9044945226	-3.9044980902	-3.9045012397	-3.9045040088	-3.9045064317	-3.9045085400
75	-3.9045107236	-3.9045125422	-3.9045140955	-3.9045154080	-3.9045165024	-3.9045173995
80	-3.9045191770	-3.9045199953	-3.9045206416	-3.9045211347	-3.9045214881	-3.9045217122
85	-3.9045233217	-3.9045236264	-3.9045238028	-3.9045238622	-3.9045238154	-3.9045236755
90	**-3.9045246371**	**-3.9045247682**	**-3.9045247849**	**-3.9045247006**	**-3.9045245274**	**-3.9045242763**

Table A.7 (cont'd).

	R (in a.u.)					
θ (deg)	6.55	6.60	6.65	6.75	6.80	6.85
0	**-3.9007400510**	**-3.9010691204**	**-3.9013713150**	**-3.9019034343**	**-3.9021363932**	**-3.9023496018**
5	-3.9008668726	-3.9011848503	-3.9014768778	-3.9019907381	-3.9022161917	-3.9024229939
10	-3.9012226678	-3.9015099469	-3.9017737640	-3.9022379646	-3.9024416331	-3.9026284305
15	-3.9017346910	-3.9019777834	-3.9022011681	-3.9025946170	-3.9027674688	-3.9029263454
20	-3.9023123196	-3.9025059669	-3.9026839096	-3.9029971831	-3.9031346821	-3.9032607697
25	-3.9028690767	-3.9030146901	-3.9031487541	-3.9033847943	-3.9034882944	-3.9035830585
30	-3.9033509080	-3.9034554440	-3.9035513781	-3.9037200955	-3.9037940394	-3.9038616768
35	-3.9037326268	-3.9038042871	-3.9038700011	-3.9039853312	-3.9040357448	-3.9040818265
40	-3.9040149736	-3.9040622862	-3.9041055614	-3.9041811038	-3.9042139882	-3.9042439979
45	-3.9042104685	-3.9042404300	-3.9042678412	-3.9043156083	-3.9043362771	-3.9043550727
50	-3.9043390911	-3.9043574543	-3.9043741449	-3.9044030544	-3.9044155238	-3.9044268056
55	-3.9044197196	-3.9044305704	-3.9044403795	-3.9044572060	-3.9044643762	-3.9044708091
60	-3.9044678879	-3.9044740382	-3.9044795443	-3.9044888342	-3.9044927103	-3.9044961262
65	-3.9044953495	-3.9044986101	-3.9045014801	-3.9045062029	-3.9045081323	-3.9045098088
70	-3.9045103619	-3.9045119223	-3.9045132465	-3.9045152783	-3.9045160248	-3.9045166156
75	-3.9045181184	-3.9045186769	-3.9045190931	-3.9045195511	-3.9045196182	-3.9045195937
80	-3.9045218182	-3.9045218182	-3.9045217256	-3.9045213105	-3.9045210054	-3.9045206468
85	-3.9045234550	-3.9045231648	-3.9045228141	-3.9045219616	-3.9045214739	-3.9045209547
90	**-3.9045239575**	**-3.9045235799**	**-3.9045231519**	**-3.9045221728**	**-3.9045216342**	**-3.9045210700**

Table A.7 (cont'd).

	R (in a.u.)					
θ (deg)	6.95	7.00	7.05	7.10	7.15	7.20
0	**-3.9027257167**	**-3.9028906799**	**-3.9030412597**	**-3.9031787603**	**-3.9033042951**	**-3.9034188134**
5	-3.9027860736	-3.9029443607	-3.9030899262	-3.9032232951	-3.9033446976	-3.9034553998
10	-3.9029568988	-3.9031007297	-3.9032321972	-3.9033522425	-3.9034618011	-3.9035617395
15	-3.9032046373	-3.9033259543	-3.9034368767	-3.9035382000	-3.9036307251	-3.9037151713
20	-3.9034815335	-3.9035780756	-3.9036662944	-3.9037469005	-3.9038204427	-3.9038875467
25	-3.9037491461	-3.9038216624	-3.9038879067	-3.9039483721	-3.9040035258	-3.9040538021
30	-3.9039800847	-3.9040317559	-3.9040789103	-3.9041219122	-3.9041611016	-3.9041967979
35	-3.9041623487	-3.9041974058	-3.9042294236	-3.9042584295	-3.9042849120	-3.9043089936
40	-3.9042963413	-3.9043190646	-3.9043396819	-3.9043583615	-3.9043752887	-3.9043906165
45	-3.9043876338	-3.9044016588	-3.9044143442	-3.9044257969	-3.9044361195	-3.9044454115
50	-3.9044461831	-3.9044544514	-3.9044618807	-3.9044685412	-3.9044744979	-3.9044798132
55	-3.9044817041	-3.9044862782	-3.9044903367	-3.9044939252	-3.9044970867	-3.9044998630
60	-3.9045017483	-3.9045041136	-3.9045062029	-3.9045079633	-3.9045094503	-3.9045107062
65	-3.9045124286	-3.9045134162	-3.9045142209	-3.9045148609	-3.9045153528	-3.9045157129
70	-3.9045173839	-3.9045175890	-3.9045176897	-3.9045176963	-3.9045176207	-3.9045174728
75	-3.9045193129	-3.9045190752	-3.9045187831	**-3.9045184434**	**-3.9045180622**	**-3.9045176454**
80	-3.9045198023	**-3.9045193287**	**-3.9045188281**	-3.9045183057	-3.9045177656	-3.9045172128
85	-3.9045198319	-3.9045192380	-3.9045186301	-3.9045180202	-3.9045174217	-3.9045168323
90	**-3.9045198846**	-3.9045192718	-3.9045186501	-3.9045180223	-3.9045173910	-3.9045167587

Table A.7 (cont'd).

	R (in a.u.)					
θ (deg)	7.25	7.30	7.35	7.40	7.45	7.50
0	**-3.9035232579**	**-3.9036184679**	**-3.9037051932**	**-3.9037841620**	**-3.9038560390**	**-3.9039213981**
5	-3.9035563592	-3.9036484026	-3.9037322755	-3.9038086651	-3.9038782018	-3.9039414620
10	-3.9036528876	-3.9037359790	-3.9038116882	-3.9038806160	-3.9039433837	-3.9040004272
15	-3.9037922022	-3.9038624004	-3.9039263440	-3.9039845826	-3.9040375497	-3.9040856476
20	-3.9039487443	-3.9040044994	-3.9040551910	-3.9041012741	-3.9041431594	-3.9041812009
25	-3.9040996025	-3.9041412830	-3.9041791630	-3.9042135587	-3.9042447731	-3.9042730793
30	-3.9042292939	-3.9042588280	-3.9042855948	-3.9043098189	-3.9043317038	-3.9043514485
35	-3.9043308170	-3.9043505621	-3.9043684320	-3.9043845935	-3.9043991950	-3.9044123672
40	-3.9044044802	-3.9044170020	-3.9044282940	-3.9044384594	-3.9044475931	-3.9044557916
45	-3.9044537775	-3.9044612915	-3.9044680190	-3.9044740295	-3.9044793886	-3.9044841559
50	-3.9044845449	-3.9044887509	-3.9044924726	-3.9044957478	-3.9044986283	-3.9045011511
55	-3.9045022992	-3.9045044399	-3.9045063016	-3.9045078863	-3.9045092257	-3.9045103596
60	-3.9045117557	-3.9045126191	-3.9045133155	-3.9045138592	-3.9045142693	-3.9045145981
65	-3.9045159562	-3.9045160965	-3.9045161456	-3.9045161132	-3.9045160094	**-3.9045158421**
70	**-3.9045172620**	**-3.9045169968**	**-3.9045166847**	**-3.9045163327**	**-3.9045159466**	-3.9045155317
75	-3.9045171978	-3.9045167258	-3.9045162334	-3.9045157249	-3.9045152038	-3.9045146740
80	-3.9045166491	-3.9045160795	-3.9045155080	-3.9045149386	-3.9045143738	-3.9045138132
85	-3.9045162392	-3.9045156388	-3.9045150347	-3.9045144311	-3.9045138307	-3.9045132358
90	-3.9045161275	-3.9045154992	-3.9045148754	-3.9045142577	-3.9045136472	-3.9045130447

Table A.7 (cont'd).

	R (in a.u.)					
θ (deg)	7.55	7.60	7.65	7.70	7.75	7.80
0	**-3.9039808105**	**-3.9040347930**	**-3.9040837916**	**-3.9041282248**	**-3.9041684889**	**-3.9042049425**
5	-3.9039989736	-3.9040511911	-3.9040986309	-3.9041416215	-3.9041805313	-3.9042157558
10	-3.9040523165	-3.9040994039	-3.9041421141	-3.9041807895	-3.9042158208	-3.9042475509
15	-3.9041293228	-3.9041689532	-3.9042048725	-3.9042374199	-3.9042668875	-3.9042935434
20	-3.9042157150	-3.9042470119	-3.9042753647	-3.9043010257	-3.9043242266	-3.9043451777
25	-3.9042987242	-3.9043219344	-3.9043429176	-3.9043618696	-3.9043789636	-3.9043943643
30	-3.9043693238	-3.9043855227	-3.9044001603	-3.9044133529	-3.9044252195	-3.9044358725
35	-3.9044242319	-3.9044349019	-3.9044444822	-3.9044530687	-3.9044607515	-3.9044676129
40	-3.9044631285	-3.9044696796	-3.9044755207	-3.9044807282	-3.9044853615	-3.9044894641
45	-3.9044883854	-3.9044921272	-3.9044954259	-3.9044983221	-3.9045008523	-3.9045030505
50	-3.9045033499	-3.9045052548	-3.9045068928	-3.9045082886	-3.9045094659	-3.9045104476
55	-3.9045113128	-3.9045120828	-3.9045127461	-3.9045132330	-3.9045135858	-3.9045138244
60	-3.9045148060	-3.9045149119	-3.9045149307	**-3.9045148733**	**-3.9045147483**	**-3.9045145640**
65	**-3.9045156188**	**-3.9045153469**	**-3.9045150329**	-3.9045146830	-3.9045143025	-3.9045138959
70	-3.9045150929	-3.9045146344	-3.9045141607	-3.9045136766	-3.9045131830	-3.9045126825
75	-3.9045141375	-3.9045135979	-3.9045130593	-3.9045125264	-3.9045120028	-3.9045114852
80	-3.9045132539	-3.9045126941	-3.9045121353	-3.9045115797	-3.9045110296	-3.9045104866
85	-3.9045126478	-3.9045120677	-3.9045114965	-3.9045109347	-3.9045103829	-3.9045098417
90	-3.9045124512	-3.9045118672	-3.9045112934	-3.9045107303	-3.9045101781	-3.9045096374

Table A.7 (cont'd).

	R (in a.u.)					
θ (deg)	7.85	7.90	7.95	8.00	8.50	9.00
0	**-3.9042379198**	**-3.9042677277**	**-3.9042946366**	**-3.9043189048**	**-3.9044599009**	**-3.9045031646**
5	-3.9042476185	-3.9042764041	-3.9043023976	-3.9043258402	-3.9044620390	-3.9045036370
10	-3.9042762463	-3.9043021575	-3.9043255322	-3.9043465930	-3.9044685991	-3.9045052343
15	-3.9043176301	-3.9043393683	-3.9043589687	-3.9043766181	-3.9044779842	-3.9045074316
20	-3.9043640796	-3.9043811119	-3.9043964385	-3.9044102137	-3.9044882807	-3.9045096266
25	-3.9044082211	-3.9044206738	-3.9044318493	-3.9044418642	-3.9044976644	-3.9045112632
30	-3.9044454082	-3.9044539315	-3.9044615700	-3.9044683816	-3.9045049672	**-3.9045120332**
35	-3.9044737273	-3.9044791637	-3.9044839847	-3.9044882478	-3.9045097176	-3.9045118956
40	-3.9044930798	-3.9044962539	-3.9044990286	-3.9045014427	-3.9045121170	-3.9045110150
45	-3.9045049481	-3.9045065743	-3.9045079560	-3.9045091179	**-3.9045127156**	-3.9045096229
50	-3.9045112542	-3.9045119031	-3.9045124102	-3.9045127900	-3.9045120708	-3.9045079957
55	-3.9045139625	-3.9045140122	**-3.9045139837**	**-3.9045138880**	-3.9045106988	-3.9045063124
60	**-3.9045143277**	**-3.9045140463**	-3.9045137265	-3.9045133742	-3.9045090381	-3.9045047187
65	-3.9045134679	-3.9045130233	-3.9045125684	-3.9045121044	-3.9045074144	-3.9045033207
70	-3.9045121779	-3.9045116735	-3.9045111775	-3.9045106966	-3.9045059795	-3.9045021678
75	-3.9045109664	-3.9045104453	-3.9045099259	-3.9045094121	-3.9045048148	-3.9045012712
80	-3.9045099520	-3.9045094269	-3.9045089119	-3.9045084075	-3.9045039809	-3.9045006448
85	-3.9045093113	-3.9045087922	-3.9045082846	-3.9045077888	-3.9045034889	-3.9045002859
90	-3.9045091083	-3.9045085912	-3.9045080862	-3.9045075934	-3.9045033375	-3.9045001736

Table A.7 (cont'd).

	R (in a.u.)			
θ (deg)	9.50	10.00	10.50	11.00
0	**-3.9045119228**	**-3.9045099033**	**-3.9045057111**	**-3.9045019127**
5	-3.9045118490	-3.9045097668	-3.9045055827	-3.9045018147
10	-3.9045118290	-3.9045093849	-3.9045052135	-3.9045015294
15	-3.9045117259	-3.9045087799	-3.9045046315	-3.9045010803
20	-3.9045114455	-3.9045079653	-3.9045038734	-3.9045005016
25	-3.9045108328	-3.9045069490	-3.9045029849	-3.9044998322
30	-3.9045098418	-3.9045057607	-3.9045020150	-3.9044991231
35	-3.9045085283	-3.9045044336	-3.9045009809	-3.9044984100
40	-3.9045070240	-3.9045031048	-3.9044999793	-3.9044976800
45	-3.9045054599	-3.9045018211	-3.9044990256	-3.9044969838
50	-3.9045039257	-3.9045006225	-3.9044981527	-3.9044963478
55	-3.9045024974	-3.9044995479	-3.9044973777	-3.9044957827
60	-3.9045012332	-3.9044986228	-3.9044967067	-3.9044952968
65	-3.9045001678	-3.9044978508	-3.9044961455	-3.9044948903
70	-3.9044993135	-3.9044972280	-3.9044956916	-3.9044945655
75	-3.9044986597	-3.9044967536	-3.9044953456	-3.9044943197
80	-3.9044982031	-3.9044964193	-3.9044951057	-3.9044941488
85	-3.9044979442	-3.9044962313	-3.9044949677	-3.9044940483
90	**-3.9044978638**	**-3.9044961721**	**-3.9044949233**	**-3.9044940154**

Table A.7 (cont'd).

	R (in a.u.)			
θ (deg)	12.00	14.00	17.00	20.00
0	**-3.9044968687**	**-3.9044929022**	**-3.9044915540**	**-3.9044912643**
5	-3.9044968196	-3.9044928937	-3.9044915519	-3.9044912638
10	-3.9044966769	-3.9044928565	-3.9044915459	-3.9044912623
15	-3.9044964526	-3.9044927988	-3.9044915363	-3.9044912600
20	-3.9044961633	-3.9044927241	-3.9044915236	-3.9044912569
25	-3.9044958284	-3.9044926368	-3.9044915080	-3.9044912532
30	-3.9044954670	-3.9044925418	-3.9044914907	-3.9044912491
35	-3.9044950955	-3.9044924434	-3.9044914726	-3.9044912446
40	-3.9044947297	-3.9044923459	-3.9044914541	-3.9044912400
45	-3.9044943775	-3.9044922528	-3.9044914361	-3.9044912354
50	-3.9044940527	-3.9044921661	-3.9044914189	-3.9044912311
55	-3.9044937640	-3.9044920868	-3.9044914030	-3.9044912269
60	-3.9044935160	-3.9044920171	-3.9044913888	-3.9044912232
65	-3.9044933098	-3.9044919577	-3.9044913766	-3.9044912200
70	-3.9044931442	-3.9044919089	-3.9044913664	-3.9044912173
75	-3.9044930175	-3.9044918708	-3.9044913584	-3.9044912152
80	-3.9044929281	-3.9044918439	-3.9044913525	-3.9044912137
85	-3.9044928750	-3.9044918278	-3.9044913493	-3.9044912128
90	**-3.9044928579**	**-3.9044918230**	**-3.9044913489**	**-3.9044912131**

REFERENCES

REFERENCES

1. E. Miliordos and K. L. C. Hunt, *J. Chem. Phys*., accepted for publication 11/17/2018.
2. D. M. Bishop and J. Pipin, *Int. J. Quantum Chem*. 45, 349 (1993).
3. B. W. Bakr, D. G. A. Smith, and K. Patkowski, *J. Chem. Phys*. **139**, 144305 (2013).

CHAPTER 6: Conclusions and Future Work

In this thesis I have computed the energies of the ground and first excited singlet state of the $He–H_2$ system using the coupled-cluster[1] (CC) methods at over ~ 20,000 nuclear geometries. A total of approximately ~ 68,000 calculations have been carried out. The geometries included cover H–H bond lengths, r, ranging from 0.942 to 5.70 a_0 (at 14 values), intermolecular separations R from 0.25 to 20.0 a_0 (generally, at 74 values for each r value), and an angle between r and R, θ, from 0° to 90° degrees in increments of 5° (yielding 19 angular points for a given r and R). The ground state was treated with the CR-CC(2,3)[2] approach and the excited state with the CR-EOMCCSD(T)[3] method, with all calculations employing the aug-cc-pVXZ basis sets of Dunning and co-workers.[4] All calculations for the first-excited singlet state I have finished, and the results have been tabulated, however, a complete analysis of the data is ongoing, as is the analysis of the results obtained for the intersection between the ground and first-excited singlet electronic state.

The calculations reported in this thesis cover parts of the $H_2–He$ potential energy surfaces that have not been explored in previous work and should be useful in modeling spectra at higher temperatures than previously accessible. For example, *ab initio* results have been provided that may be used to study transitions of H_2 up to vibrational quantum number n = 8. These results are needed to model the radiative profiles of cool white dwarf stars, with temperatures between 3500 K and 7000 K. In addition, the results in this thesis have a smaller angular step size (for a given r and R) than done in any previous study that covered a wide range of the nuclear configuration space and yielded highly accurate ground-state energies. The inclusion of more angles allowed us to obtain higher anisotropies in the potential than earlier studies have reported. Calculations have been performed for all the nuclear geometries outlined above with both the aug-cc-pVQZ and aug-cc-pV5Z basis sets (for both the ground and first-excited singlet state) so that an extrapolation to the complete basis set limit via a two-point scheme may be performed with the results obtained in this thesis.

The numerical results in this thesis are only a portion of the total results that have been computed in this work. Points on the potential energy surface for H_2−He (not reported in this thesis) have been calculated for bond lengths r of H_2 (in a.u.) 1.280, 1.787, 2.125, 2.43, 2.463, 2.801, 3.730, and 5.700, plus 1.100, 1.448736, and 1.75 a.u. at the geometries not used for comparison with the results of Patkowski and co-workers[5] in Chapter 3 of this thesis. I am currently working on computing the spherical expansion coefficients $c_j(R)$ for these r values from the tables of computed ground-state energies. The isotropic potentials and the anisotropies for these r values are also being determined as is an analysis similar to that given in Chapter 5 for r = 1.110, 1.449, and 2.463 a.u.

Using perturbation theory, we have estimated the effect of the anisotropy on the energy of the J = 0 state of H_2 in the complex. The value at the minimum of the isotropic potential was found to be relatively small, but because the ground-state energy is so close to zero, the effect may be significant for other regions of the potential. This will be a focus of future work. Modification of the isotropic potential based on a perturbative treatment of the effect of the anisotropies may show that bound states with L = 1 exist for T_2–^{3}He, HT–^{4}He, and D_2–^{4}He.

The contribution of quadrupolar induction to the isotropic potential for r = 1.449 a.u. has been calculated and reported in this thesis. The contribution to the leading anisotropic potential will be determined in future work.

Since the bound state energy levels of a Lennard-Jones potential are known and have been given by Sesma,[6] we are planning to perform the integrations in the complex plane that are required in order to determine the Wronskians for our version of the Lennard-Jones potential so that we can report a value for the binding energy. Modification of the isotropic potential based on a perturbative treatment of the effect of the anisotropies may show that bound states with L = 1 exist for T_2–^{3}He, HT–^{4}He, and D_2–^{4}He. This is an additional focus of work that we are planning to conduct in the near future.

REFERENCES

REFERENCES

1. F. Coester, *Nucl. Phys*. **7**, 421 (1958); F. Coester and H. Kümmel, *Nucl. Phys*. **17**, 477 (1960); J. Čížek, *J. Chem. Phys*. **45**, 4256 (1966); *ibid*. *Adv. Chem. Phys*. **14**, 35 (1969).

2. K. Kowalski and P. Piecuch, *J. Chem. Phys*. **113**, 18 (2000); *ibid*. **122**, 074107 (2005); *ibid*. **115**, 643 (2001); K. Kowalski and P. Piecuch, *Chem. Phys. Lett*. **347**, 237 (2001).

3. K. Kowalski and P. Piecuch, *J. Chem. Phys*. **120**, 1715 (2004).

4. T. H. Dunning, Jr., *J. Chem. Phys*. **90**, 1007 (1989); R. A. Kendall, T. H. Dunning, Jr., and R. J. Harrison, *J. Chem. Phys*. **96**, 6769 (1992); D. E. Woon and T. H. Dunning, Jr., *J. Chem. Phys*. **100**, 2975 (1994).

5. B. W. Bakr, D. G. A. Smith, and K. Patkowski, *J. Chem. Phys*. **139**, 144305 (2013).

6. J. Sesma, *J. Math. Chem*. **51**, 1881 (2013).